

2011-01-01

# An Integrated Geographic Information Systems (IGIS) Analysis and Definition of the Tectonic Framework of Northern Mexico

Carlos Manuel Martinez

University of Texas at El Paso, [geologis.cm@live.com](mailto:geologis.cm@live.com)

Follow this and additional works at: [https://digitalcommons.utep.edu/open\\_etd](https://digitalcommons.utep.edu/open_etd)



Part of the [Geographic Information Sciences Commons](#), [Geology Commons](#), and the [Remote Sensing Commons](#)

---

## Recommended Citation

Martinez, Carlos Manuel, "An Integrated Geographic Information Systems (IGIS) Analysis and Definition of the Tectonic Framework of Northern Mexico" (2011). *Open Access Theses & Dissertations*. 2336.  
[https://digitalcommons.utep.edu/open\\_etd/2336](https://digitalcommons.utep.edu/open_etd/2336)

This is brought to you for free and open access by DigitalCommons@UTEP. It has been accepted for inclusion in Open Access Theses & Dissertations by an authorized administrator of DigitalCommons@UTEP. For more information, please contact [lweber@utep.edu](mailto:lweber@utep.edu).

AN INTEGRATED GEOGRAPHIC INFORMATION SYSTEMS (IGIS) ANALYSIS AND  
DEFINITION OF THE TECTONIC FRAMEWORK  
OF NORTHERN MEXICO

CARLOS MANUEL MARTINEZ PIÑA

Department of Geological Sciences

APPROVED:

---

Philip C. Goodell, Ph.D., Chair

---

José M. Hurtado Jr., PhD.

---

Raed Aldouri, Ph.D.

---

Bridget Konter, Ph.D.

---

Jasper Konter, Ph.D.

---

Benjamin C. Flores, Ph.D.  
Acting Dean of the Graduate School

Copyright ©

by

CARLOS MANUEL MARTINEZ PIÑA

2011

## **Dedication**

The dedication and love from my dad Carlos Martinez V (R.I.P), my mom Consuelo P. Martinez (R.I.P.) and my bro Saul E. Piña Martinez (R.I.P) gave me the strength to keep going and become for my wife Nidia and my daughter Damaris, a better husband and better father.

**Eternally grateful**

INTEGRATED GEOGRAPHIC INFORMATION SYSTEMS (IGIS) ANALYSIS AND  
DEFINITION OF THE TECTONIC FRAMEWORK  
OF NORTHERN MEXICO

by

CARLOS MANUEL MARTINEZ PIÑA

DISSERTATION

Presented to the Faculty of the Graduate School of  
The University of Texas at El Paso  
in Partial Fulfillment  
of the Requirements  
for the Degree of

DOCTOR OF PHILOSOPHY

Department of Geological Sciences  
THE UNIVERSITY OF TEXAS AT EL PASO  
December 2011

## **Acknowledgements**

I wish to thank M.S. Adrian Vazquez and Dr. Oscar Ibáñez for giving me the opportunity of coming back to school. Also to the unseen people, that is always supporting students: Pam Hart, Tina Carrick, Carlos Montana, because of them, problems never exist. I also want to thank Dr. Kenneth Clark, and Dr. Terry Pavlis for their help and discussion of relevant topics. Thanks to Dr. Raed Aldouri for helping me during the summers. Thanks to the members of my Committee Dra. Bridget Konter, Dr. Jasper Konter and Dr. José M. Hurtado Jr. for their time, help and patience; but most of all I want to express my everlasting gratitude to Dr. Philip Goodell, an exceptional man, who for the last five years has been more than my mentor; without him I could have never fulfill my dream. Of course my wife and my daughter, for their support, love and understanding. Thanks to my friends, Dr. Oscar Romero, M.S. Ivan Alvarado, M.S. Hugo Rojas, M.S. Abdiel Quezada, Dr. Miguel Dominguez and M.S. Victor Avila, for being there, and to all who in any way, helped me get through this stage of my life.

## **Abstract**

Crustal rupture structures reactivated in the course of the tectonic history of northern Mexico are the surface expressions of planes of weakness, in the form of simple or composite rectilinear features or slightly curved, defined as lineaments. Unless otherwise defined as strike-slip faults, lineaments are part of parallel and sub-parallel oblique convergent or oblique divergent tectonic zones cross cutting the Sierra Madre Occidental and northern Mexico, in a NW trend. These shear zones are the response to the oblique subduction of the Farallon plate beneath North America.

Kinematic analysis of five selected sites in northern Mexico, three basins and two compressional shear zones, proved possible a combination of shear mechanism diagram and models from analogue materials, with satellite imagery and geographic information systems, as an aid to define strike-slip fault motion. This was done using a reverse engineering process by comparing geometries. One of the sites assessed, involving the Parras Basin, Coahuila Block (CB), San Marcos fault, a postulated PBF-1 fault, allowed for palimpsestic reconstruction of the CB that corroborated the results of the vector motion defined, in addition to an extension of ~25% in a northwest southeast direction.

A GIS-based compilation and georeferenced regional structural studies by several researchers were used as ground control areas (GCA); their interpolation and interpretation, resulted in a tectonic framework map of northern Mexico. In addition, shaded relief models overlaid by the lineaments / fault layer allowed structural analyses of basins related to these major structures. Two important results were obtained from this study: the Tepehuanes-San Luis-fault (TSL) and the Guadalupe fault, named herein, displaces the Villa de Reyes graben, and the Aguascalientes graben, respectively, to the SE, confirming their left lateral vector motion; afterwards TSL was displaced south by the right lateral strike slip Taxco-San Miguel de Allende fault. The second result refers to the hypothesis that the Mesa Central was brought to its present location by a subduction zone located to the north. This subduction zone coincides with several researchers who postulated the idea. The compressional zones refer to segments of the Sinforosa and a postulated Aquinuari fault located in the stratotectonic Guerrero Terrane regarded as a highly mineralized zone.

Negative anomalies near -200 milligals are strongly suggestive of a cratonic block identified in western Chihuahua, it being named the Western Chihuahua Cratonic Block (WCCB). In the

southwestern portion of the North American craton the age provinces are well documented, but the block versus mobile belt idea has not been put forth or emphasized. The present study combines data of several types, sedimentological, structural, igneous geochemistry, and geochronologic data to evaluate this behavior in SW NA, and the proposed block is tested against these data. The presence of the WCCB is supported by a wide variety of data.

Basins, troughs, aulacogens, bimodal volcanism, and other rift and rift shoulder features, characterize the spatially constrained mobile belts. Mobile belts surrounding the WCCB contain geologic records of the events going back to 1.4 Ga, with different aspects being dominant over geologic time. Mobile belts will participate in compression,(subduction), extension (rifting), and transform (lateral) faulting. The WCCB may have been derived from closely, adjacent, North American craton by mobile belt action.

This study has shown that integration of data is essential, because allows detection of differences in hypotheses for the same event in the same area. This integration capability is what makes integrated geographic information systems a powerful tool, not only for their synergy, but because they can be combined with specific techniques that provide data before going to conduct fieldwork.

Whether the issue of defining the tectonic framework of northern Mexico can be resolved or not, depends on the viability of integrating volumes of data from research, hypotheses, or maps, and put together under the same geographic frame.

## List of Tables

Table 1.1: Comparison of theoretical angle values between the diagram of Riedels and those measured in PBF-1 .....	26
Table 1.2: Angle values of rotation applied to blocks for reconstruction of a solid Coahuila Block body . ....	26
Table 1.3: Comparison of theoretical values from Riedel shear mechanism diagram and those of PBF-2 fault system located in the northwestern portion of the Parras .....	27
Table 1.4: Comparison of the theoretical values from Riedel Shear mechanism diagram and those of SMF-1 system located in the northern portion of Sierra del Nido .....	27
Table 1.5: Comparison of theoretical angle values between Riedel diagram and those measured for Sinforosa .....	28
Table 1.6: Comparison of theoretical angle values between the diagram Riedel and those measured in Aquinuari .....	28
Table 1.7: Table of results of the studied strike slip basins.....	29
Table 2.1: Structural domains of northern Mexico and related faults .....	99
Table 2.1: Structural domains of northern Mexico and related faults (Cont.).....	100

## Table of Contents

Acknowledgements.....	v
Abstract.....	vi
List of Tables .....	viii
Table of Contents.....	ix
List of Figures.....	xiii
List of Charts .....	xvi
Chapter 1: Defining the kinematics of strike-slip systems in northern Mexico by Integrated Geographic Systems .....	1
1.1 Abstract.....	1
1.2 Introduction.....	2
1.2.1 Strike- Slip basins .....	3
1.2.2 Strike-Slip faults.....	4
1.2.3 Lineaments .....	5
1.2.4 Structural Analysis.....	5
1.2.5 Riedel shear mechanism ad analog models.....	6
1.2.6 Background .....	8
1.2.7 Study Areas .....	9
1.2.8 Hypothesis.....	9
1.3 Methodology.....	10
1.3.1 Data .....	10
1.3.2 Technique .....	11
1.4 Results.....	12
1.4.1 Kinematic Analysis .....	12
1.4.2 Parras Basin.....	12
1.4.2.1 Geometry .....	13
1.4.2.2 Parras Basin Fault -1 .....	13
1.4.2.3 Parras Basin Fault -2 .....	14
1.4.3 MSM-3 fault system.....	15
1.4.4 Tepehuanes-San Luis fault system.....	17

1.4.5 Tepehuanes Basins .....	18
1.4.6. San Marcos Fault -1 .....	19
1.4.7 Sinforosa Lineament .....	20
1.4.7.1 Sinforosa .....	21
1.4.7.2 Aquinquari.....	22
1.5 Discussion.....	23
1.5.1 Conclusion.....	24
Chapter 2: An IGIS-based characterization of the structural framework of Northern Mexico ..	58
2.1 Abstract.....	58
2.2 Introduction.....	59
2.2.1 Lineaments: definition and classification .....	61
2.2.2 Background.....	62
2.2.2.1 Mojave-Sonora-Megashear (Fig.10).....	63
2.2.2.2 Sawmill Canyon (SC) (Fig. 11) .....	65
2.2.2.3 Pitáycahi Fault (PF) (Fig, 12) .....	65
2.2.2.4 Tepehuanes-San Luis fault system (TSL) (Fig. 13,14,15).....	66
2.2.2.5 El Bajío Fault (EB) (Fig. 13,15) .....	68
2.2.2.6 Taxco-San Miguel de Allende fault system (TSMAFS) (Fig. 1,15) .....	68
2.2.2.7 Texas Lineament (TL) (Fig. 16) .....	69
2.2.2.8 La Babia (LB) and San Marcos (SMF) faults (Fig.17).....	70
2.2.2.9 Juarez (JF), Almagre (AF) and El Caballo (EC) (Fig. 18) .....	72
2.2.2.10 Rio Bravo Fault (RBF) (Fig. 19) .....	73
2.2.2.11 Strike Slip faults in the Mesozoic cover .....	73
2.2.2.12 West Chihuahua Cratonic Block .....	74
2.2.3 Study Area .....	75
2.2.4 Statement of the Problem.....	75
2.2.5 Hypothesis .....	76
2.3 Methodology.....	76
2.4 Results.....	78
2.4.1 Categorization of lineaments/faults .....	80
2.4.2 Weak faults or low strength shear zones .....	81
2.4.2.1 Parras Basin Fault, PBF-1 and PBF-2 .....	81

2.4.3 Strong faults or high strength shear zones .....	84
2.4.3.1 Tepehuanes-San Luis Fault system (TSL).....	84
2.4.3.2 Texas-La Babia-Rio Bravo fault system (TLBB).....	86
2.4.3.3 Mojave-Sonora Megashear .....	87
2.4.3.4 San Marcos Fault-1(SMF-1).....	88
2.4.3.5 Sinforosa (SL)and Aquinquiri (AF).....	89
2.4.3.6 Pitáycachi fault zone (PFZ) .....	90
2.4.4 Structural Domains .....	91
2.4.5 Convergent transcurrent tectonic domain NW .....	92
2.4.6 Divergent transcurrent tectonic domain NW .....	92
2.4.7 Extensional tectonic domain NNS and NNE.....	92
2.4.8 Compressional tectonic domain NNW .....	92
2.4.9 Oblique subduction and R-shears based on Holohan (2007) analog model .....	93
2.5 Discussion.....	94
2.5.1 Conclusion .....	97
Chapter 3 Do stable blocks and mobile belts exist in the southwestern North American Proterozoic craton?.....	130
3.1 Abstract.....	130
3.2. Introduction.....	131
3.2.1 Hypothesis .....	132
3.4. Regional Precambrian Provinces .....	133
3.5. Coherence of crustal material .....	135
3.6 Gravity .....	135
4. Geologic Character of the WCCB and adjacent regions .....	139
4.1 Precambrian rocks near the WCCB.....	142
4.1.1 Sierra Mojina .....	142
4.1.2 Los Filtros.....	143
5. Initial Sr isotope ratios.....	144
6. Linear Boundaries.....	144
6.1 Texas Lineament.....	145
6.2 Transition Zone, AZ .....	146
6.3 East and West boundaries of the WCCB .....	146

7. Basins/ mobile belts .....	146
7.1 Precambrian.....	147
7.2 Paleozoic.....	148
7.3 Mesozoic.....	150
7.4 Cenozoic.....	153
8. Terrane Tectonics .....	157
8.1 Caborca Block.....	157
8.2 Mojave-Sonora-Megashear.....	157
9. Discussion.....	158
9.1 Conclusions.....	158
References.....	170
Vita.....	180

## List of Figures

Figure 1.1: Shaded relief raster with elevation data showing the 5 study areas.....	30
Figure 1.2: Basement configuration of the three mechanisms.....	31
Figure 1.3: Analog models showing formation of lateral motion faults.....	32
Figure 1.4: Riedel shear stress mechanism .....	33
Figure 1.5: Shaded relief showing the Tepehuanes-San Luis fault system.....	34
Figure 1.6: Structural map of Mexico .....	35
Figure 1.7: Image-map of Mexico (IMM) composed of eight satellite mosaics .....	36
Figure 1.8: Shaded relief with elevation data showing paths of postulated faults PBF-1, PBF-2 and MSM-3 .....	37
Figure 1.9: Comparison of geometries between Parras Basin and intersecting faults .....	38
Figure 1.10: Shaded relief raster with elevation data shows outline the Coahuila Block.....	39
Figure 1.11: Palinpastic reconstruction of segments of the Coahuila Block .....	40
Figure 1.12: Shaded relief showing the postulated faults PBF-1, PBF-2 and MSM-3, and regional structures.....	41
Figure 1.13: Riedel shear system diagram on top, and the set of faults of the northwestern part of the Parras Basin.....	42
Figure 1.14: Structures associated with an idealized right slip fault. ....	43
Figure 1.15: Structural features of a part of the standard experiment.....	43
Figure 1.16: Simulation of strike-slip deformation in brittle crust.....	43
Figure 1.17 Map of area that includes from Parras Basin to the Tepehuanes San Luis fault.....	44
Figure 1.18: Shaded relief showing the Durango faulted basins. ....	45
Figure 1.19: Palinpastic reconstruction of five basins.....	46
Figure 1.20: Shaded relief raster shows the structural relationships between TSL, Guadalupe fault, Guadalupe graben (GG), Aguascalientes graben (AG).....	47
Figure 1.21: Image shows a curvilinear magnetic lineament oriented northwest southeast that corresponds with the SMF-1.....	48
Figure 1.22: Sierra del Nido Basin and faults outlined and compared to Riedel shear mechanism.....	49
Figure 1.23: Digital elevation model showing the Sinforosa and Aquinquari lineaments.....	50
Figure 1.24: MrSID images of southwestern portion of the state of Chihuahua and northeastern portion of Sinaloa.....	51

Figure 1.25: Enlarged Image of site A from figure 24, Sinforosa fault.....	52
Figure 1.26: Comparison of geometric elements of the Sinforosa Fault and Riedel shear mechanism .....	53
Figure 1.27: Enlarged image of site B from figure 24, Aquinquari fault.....	54
Figure 1.28: Comparison of geometric elements of the Aquinquari Fault and Riedel shear mechanism.....	55
Figure 1.29-1: Directional filter applied to Landsat image P 33 R 41.....	56
Figure 1.29-2: Four sets of lineaments used by Galvan (2006) for the state of Chihuahua.....	56
Figure 2.1: Study area including eleventh states of northern Mexico .....	101
Figure 2.2: Map shows versions of the Mojave -Sonora - Megashear in Northern Mexico by several authors .....	102
Figure 2.3: Known lineaments in northern Mexico. From north to south .....	103
Figure 2.4: Regional structures and lineaments in Northern Mexico .....	104
Figure 2.5: Map shows the West Chihuahua Cratonic Block location .....	105
Figure 2.6: Tectonostratigraphic terranes by Campa & Coney .....	106
Figure 2.7: Tectonostratigraphic terranes by Sedlock et al, (1993).....	106
Figure 2.8: Tectonostratigraphic terranes by Centeno et al, (2008).....	106
Figure 2.9: Tectonostratigraphic terranes by Dickinson and Lawton (2001).....	106
Figure 2.10: Map shows the Caborca Block, the Mojave-Sonora fault system, .....	107
Figure 2.11: Geologic map of Sierrita Mountains, showing Late Jurassic faults .....	108
Figure 2.12: Map shows the 1887 rupture segments of Pitáycachi, fault .....	109
Figure 2.13: Map shows the Mesa Central, the Tepehuanes-San Luis fault system .....	110
Figure 2.14 Digital elevation model showing the area where the TSL cuts and displace the Aguascalientes Graben .....	111
Figure 2.15: Map of Central Mexico showing the Trans-Volcanic Mexican Belt .....	112
Figure 2.16: Map shows the Texas Lineament .....	113
Figure 2.17: Map of La Babia & San Marcos fault systems .....	114
Figure 2.18: Map of El Caballo, Almagre and Juarez fault systems .....	115
Figure 2.19: Map shows the Vicksburg-Frio Oligocene depocenter displacement .....	116
Figure 2.20: Map of Mexico showing lineaments, faults sets, and domains of fault systems affecting the Mesozoic cover .....	117
Figure 2.21a and 2.1b: shows the Bouguer map and the residual map of northern Chihuahua.....	118

Figure 2.22: Digital elevation model of northern Mexico .....	119
Figure 2.23: Tectonic framework map of northern Mexico .....	120
Figure 2.24: Map depicting the three major parallel shear stress systems .....	121
Figure 2.25: Map showing strike slip basins .....	122
Figure 2.26: Shaded relief shows palinspastic restoration of PBF-1, PBF-2 .....	123
Figure 2.27: Composite map shows the location of the Potosi Fan, Mesa Central and the West Cratonic Chihuahua Block. ....	124
Figure 2.28: Shaded relief shows the Tepehuanes-San Luis and the Guadalupe faults .....	125
Figure 2.29: Shows the solid body of the silicic province of SMO .....	126
Figure 2.30: Enlargement of inset in figure 23, shows basalt outcrops .....	127
Figure 2.31: First segment of the fault SMF-1 is right lateral strike-slip .....	128
Figure 2.32: Upper map shows versions of the Mojave -Sonora - Megashear in Northern Mexico by several authors and the oblique geometry .....	129
Figure 3.1: Location map of the area of interest .....	160
Figure 3.2: Precambrian Provinces in southwestern Laurentia .....	161
Figure 3.3: Bouguer gravity map of area .....	162
Figure 3.4: Western Chihuahua Cratonic Block (WCCB) designated as within the -190 milligal gravity contour .....	163
Figure 3.5: Detailed vertical profile across the southwest boundary of the WCCB .....	164
Figure 3.6: Precambrian positive (blocks) and negative (basins) regions, and the WCCB .....	165
Figure 3.7: Paleozoic positive (blocks) and negative (basins) regions, and the WCCB.....	166
Figure 3.8: Mesozoic positive (blocks) and negative (basins) region, and the WCCB.....	167
Figure 3.9: Cenozoic positive (blocks) and negative (basins) regions, and the WCCB .....	168
Figure 3.10: Summary diagram .....	169

## **List of Charts**

Chart 1.1	Statistical data of 637 lineaments traced in Northern Mexico.....	57
-----------	---	----

# **Chapter 1: Defining the kinematics of strike-slip systems in northern Mexico by Integrated Geographic Systems**

## **1.1 Abstract**

Kinematic analysis of five selected sites in northern Mexico, three basins and two compressional shear zones, tested a combination of shear mechanism diagram and models from analogue materials, with satellite imagery and geographic information systems, as an aid to define strike-slip fault motion. This was done using a reverse engineering process by comparing geometries. One of the sites assessed, involving the Parras Basin, Coahuila Block (CB), San Marcos fault, a postulated PBF-1 fault, allowed for palimpsestic reconstruction of the CB that corroborated the results of the vector motion defined, in addition to an extension of ~25% in a northwest southeast direction. A second site assessed involved the Marcos Basin, and a postulated northwestern extension of the San Marcos fault (SMF-1), show reactivation of Paleozoic faults. A third basin, the Durango Basin (DB) was not assessed because its original geometric elements were distorted by recent faulting. However, after palimpsestic reconstruction the DB is inferred as a strike-slip basin belonging to the Tepehuanes-San Luis fault system. The compressional zones refer to segments of the Sinforosa and a postulated Aquinquiri fault located in the tectonostratigraphic Guerrero Terrane regarded as a highly mineralized zone. Both of the sites show mineral occurrences related to high-density clusters of extensional fractures (T- and R' shears). This study has shown that integration of data is essential, because it allows detection of differences in hypotheses for the same event in the same area. This integration capability is what makes integrated geographic information systems a powerful tool, not only for their synergy, but because they can be combined with specific techniques that provide data before going to conduct fieldwork.

## 1.2 Introduction

In North American Cordilleran evolution, the role of strike-slip faults and associated negative topographic features have been recognized for many decades, however there are also positive topographic features related to slip faults, which have been poorly studied. The magnitude and importance of such deformations seem to be underestimated (Christie-Blick & Biddle, 1985; Busby *et al.*, 2005; Busby & Bassett, 2007).

Large tectonic events have occurred in northern Mexico, but the only visible evidence left are geomorphic features that weathering, erosion, and /or volcanic processes, have reshaped, buried, or filled, with several meters or kilometers of sediments. Of these geomorphic features, the most outstanding and controversial are the lineaments; the less known and understood are strike-slip basins and exhumed lithological blocks.

Using a digital elevation model it is possible to pinpoint the most conspicuous basins in northern Mexico: A) the Parras Basin located in the State of Coahuila, B) the basins neighboring the city of Durango, in the State of Durango and C) the basin in the northern portion of the Sierra del Nido in the State of Chihuahua (Fig. 1). On the other hand, it is not possible to pinpoint exhumed lithological blocks because of their positive topographic relief, unless defined by fieldwork. For this reason, there is little record of any. Since ground level observation of lineaments/strike-slip faults and strike-slip basins is difficult, indirect methods such as satellite imagery and geophysical maps (magnetic) are commonly used to identify those (Richards, 2000).

This study focuses mainly on the kinematic knowledge of the strike-slip faults defined through analysis of releasing bends, restraining bends or compressive shear zones, providing a

better understanding of their formation and the role played in the geologic, volcanic, tectonic, and metallogenic history of the Sierra Madre Occidental and the northeast of Mexico.

Because of the size of the areas of interest, data integration requires the use of innovative technologies such as remote sensing (RS) and geographic information systems (GIS) (Srivastav *et al.*, 2000, Chang, 2008). Synergy between these two technologies constitutes what Estes and Star (1993) define as Integrated Geographic Information systems (IGIS). In addition, this work uses ideas, methods, and terminology from Riedel (1929); results from analogue material experiments (Holohan *et al.*, 2008, Atmaoui *et al.*, 2005,); structural analysis terminology and definitions from Mann *et al.*, (1983), Marrett & Peacock, (1999), ten Brink *et al.*, (1996), and Ahlgren (2001), and length categorization for lineaments used by Galvan (2006). The different concepts this analysis combines are synthesized in the following paragraphs.

### **1.2.1 Strike-Slip Basins**

The term “strike-slip basin” coined by Mann *et al.* (1983), better defines these types of tectonic features since sedimentation is related to significant strike-slip movement. These tectonic features can form by three mechanisms: local extension between two en échelon basement strike-slip faults, (basement configuration in figure 2A, surface expression in figure 3A); a distributed (simple) strike-slip shear mechanism, (basement configuration in figure 2B, surface expression in figure 3B), and the Riedel shear mechanism (basement configuration in figure 2C, surface expression in figure 3C) (Atmaoui, 2005). Local extension (Fig. 3A) is accommodated in the sedimentary cover by normal faults at the bends and oversteps. (Atmaoui, (2005). The Riedel shear mechanism implies formation of strike-slip basins in the sedimentary cover in two ways: a wide strike-slip zone in the basement and above distributed shear in

overpressure shales or evaporites layers (Fig. 3B) and, a single principal displacement fault that forms pull-apart basins along Riedel faults connected by subparallel segments (Fig. 3C).

Lineaments/strike-slip faults, basins, and pop-up ridges are commonly associated with boundaries of stratotectonic terranes. However, the literature and maps of northern Mexico that were reviewed, show different terranes related to lineaments/strike-slip faults, but not with the other features.

### **1.2.2 Strike-slip faults**

Strike-slip faults can form in continental and oceanic plate boundaries; in intraplate settings as a response to plate collision; as transfer zones connecting faults; and common in obliquely convergent subduction settings (Cunningham & Mann, 2007). When lithospheric blocks move, planes of weakness of subparallel lineaments can intersect, providing channels for the ascent of deeply derived magmas and fluids (Richards, 2000). In the horizontal sense, when lithospheric blocks move laterally with respect to an adjacent block, simple strike-slip faults occur and a linear or curvilinear lineament appears as a surface expression; however, if an oblique slip component is present, strike-slip basins form in the surface (Christie-Blick & Biddle, 1985). Field observations and experimental settings state that strike-slip faults are commonly formed by en échelon faults. The term en échelon implies a stepped arrangement of overlapping or underlapping structural elements approximately subparallel to each other and oblique to the linear zone in which they occur (Christie-Blick & Biddle, 1985).

When strike-slip displacement occurs in en échelon faults, fault segments are linked; these linked areas along the lineaments define alternating areas of convergent and divergent bends. The bends defined as offset areas are linked by bounding strike-slip faults (ten Brink, Katzman, & Lin 1996, Ahlgren, 2001, Atmaoui, 2005, Atmaoui et al, 2008, Holohan et al, 2008). Bends that accommodate local contraction are restraining bends and those that accommodate extension are releasing bends (Cunningham & Mann, 2007). Rhomboidal shaped stepovers are

zones of slip transfer between separate and subparallel strike-slip faults (Cunningham & Mann, 2007). The main characteristic of releasing bends is oblique deformation (Atmaoui, 2005, Cunningham & Mann, 2007, Holohan et al, 2008, Atmaoui et al, 2008).

### **1.2.3 Lineaments**

A lineament according to O'Leary et al, (1976) is “a mappable, simple, or composite linear feature of a surface, whose parts are aligned in a rectilinear or slightly curvilinear relationship which differs distinctly from the patterns of adjacent features and presumably reflects a subsurface phenomenon.” Scanvic (1997) emphasizes “lineament” maps as one of the most important inputs for structural analysis and proposes the term “image lineament”. This terminology defines all linear and curvilinear features that have a structural origin in the “absence of precise ground truth reference”.

Three major terms proposed by Scanvic (1997) for classifying lineaments based on similar terms used in geophysics are: image lineaments (linear morphological or radiometric expression without a precise ground reference), specific tectonic phenomena (identified totally or partially in existing or new maps), and composite image lineaments (characterized by their association with geochemical, geophysical, metallogenetic etc. anomalies, excluding structural geological structures).

### **1.2.4 Structural Analysis**

Structural analysis examines the final state known of a specific structure, as opposed to numerical or experimental models that focus on process (Marrett & Peacock, 1999). Structural analysis of rock comprises geometric analysis, kinematic analysis and dynamic analysis (Marrett & Peacock, 1999).

The foundation of structural analysis is the geometric description of structures (shapes, sizes, locations and orientation); kinematic analyses which interpret the pattern of motions and/or

displacements (e.g rotation, translation, strain) that produce structures without regard to associated stress, and dynamic analyses that interprets kinematic descriptions (Marrett & Peacock, 1999).

Structural analysis involves specific expressions and Marrett & Peacock (1999) address an important issue regarding confusion in the terminology of strain and stress. Strain terms are fundamentally descriptive. Strain terms suggest kinematics are closely related to observations, and therefore are best appropriate to describe the movements related with natural structural development. Extension and contraction are strain terms. On the other hand, stress terms are fundamentally genetic. Tension and compression are stress terms. Stress terms are best suited for inferences about the genesis of natural structures (Marrett & Peacock, 1999).

### **1.2.5 Riedel shear mechanism and analog models**

The Riedel shear mechanism is often associated to the geometric pattern of strike-slip fault systems (Ahlgren 2001). The geometric design is a series of faults with certain angular relationships between them, that trend oriented to the basement fault (Fig. 4). The most important elements of this mechanism are the conjugate R and R' shear fractures, each forms depending on the internal friction angle of the host rock ( $\phi$ ) (Fig. 4). Values assign to R, P and  $\phi$  calculates as follows:

$$R' = 45^\circ \pm \phi/2, \quad R = 45^\circ - \phi/2, \quad P = -45^\circ + \phi/2, \quad T = 45^\circ \quad \phi = 30^\circ$$

The conjugate Riedel shears concentrate at the overstepping areas with initial angles of orientation of  $70^\circ$ - $75^\circ$  to the shear direction (Atmaoui, 2005, Atmaoui *et al*, 2008, Holohan *et al*, 2008). They show shear displacement and progressive rotation and serve to transfer the horizontal displacement from one Riedel shear to the adjacent one. The formation of the pull-

apart structures is not a consequence of the conjugate shears (Atmaoui, 2005). Y- and P-shears are synthetic shears that are roughly parallel to the principal displacement zone (PDZ). The Y-shears tend to form at the tips of the Riedel shears, and are the surficial segments parallel to the principal displacement zone (Atmaoui, 2005). They accommodate the continuing strike-slip deformation while pulling the sides of the now passive Riedel shears further apart, rarely cutting through them. Fully developed Y- and P-shears intersecting at angles less than  $30^\circ$  show the rhombic shape that characterizes the pull-apart basins (Atmaoui, 2005). On the other hand, experiments by Holohan *et al* (2008) show synthetic R and P- shears formed at low angle (about the PDZ), cutting earlier R-shears. These R and P shears form an anastomosing fault pattern including rhombic graben and/or half-graben and/or push-up ridges. Atmaoui (2005) states that push-up ridges form when a Y-shear fails to develop. Two or more neighboring structures, with further displacement, can coalesce to form a long, narrow, and deep complex or composite strike slip-basin basin (Atmaoui, 2005). According to Ahlgren (2001), most workers agree that R-shears are the first or one of the first shears to form. However, P-shears may also form first, especially in dilational systems. Another characteristic of conjugate shears is that while R' rotates counterclockwise, R rotates clockwise (Atmaoui, 2005, Twiss and Moore, 2007).

Holohan *et al.*, (2008) working with analogue materials on a plate, found that at low opening angles ( $< \sim 5^\circ$ ) R-shears with limited dip-slip displacement formed at  $\sim 17^\circ$  to the velocity discontinuity. Synthetic faults subsequently cutting R-shears formed an anastomosing fault pattern including rhombic graben, half graben and/or pop ups. At an angle of  $> \sim 7^\circ$  along the velocity discontinuity, an axial graben formed with R-shears mostly restricted to the graben margins.

In natural systems, a number of factors such as strain rate and stress state at the time of the fault, causes variations in the angular relationships between the individual cutting surfaces and the PDZ (Ahlgren 2001, Coehlo, Passchier, & Marques 2006). Synthetic and antithetic shears can be more steeply inclined with respect to the trend of the PDZ, if reorientation of the principal stress is influenced by preexisting highly pressurized fluids in the region where faulting is occurring. Atmaoui (2005) states, that “in experiments by Cloos (1928) and Riedel (1929), tension fractures were observed to form only when water was sprayed on the surface of clay models.”

### **1.2.6 Background**

The most recent antecedent of an integrated structural study involving satellite imagery, magnetometry, geologic data, and geographic information systems applying the Riedel shear mechanism to a series of Cenozoic faults in Sonora, Mexico, was done by Valenzuela *et al* (2005).

Other important work referring to the tectonics of northern Mexico: documentation of three strike slip faults by Eguiluz de Antuñano (1984); the recognition of a cratonic block in northwestern Chihuahua by Goodell *et al*, (1986); a tectonic map of Mexico depicting a series of strike-slip faults by Longoria (1994); the tectonic evolution of central by Centeno-Garcia & Silva-Romo, 1997); structural studies of the San Marcos fault in northeastern Mexico by Aranda-Gomez, *et al*, (2005) and Chávez-Cabello *et al.*, (2005); the evolution of the western margin of North America and its relation to the Sierra Madre Occidental by Ferrari *et al*, (2005); the mid to late Tertiary extension in northeastern Mexico, by Aranda-Gómez (2005); recognition of the Rio Bravo fault, a left lateral strike slip fault in north-northeastern Mexico by Flotte *et al*, (2008); description of the Plomosas ridge and its relationship to a left lateral strike-slip in northeastern

Chihuahua by Oviedo P., (2008); the Mesa Central: stratigraphy, structure and evolution by Nieto-Samaniego, Alaniz-Alvarez, & Camprubi (2007); the collision and subsequent rifting of the Guerrero Composite Terrane of western Mexico by Centeno-Garcia, *et al.*, (2008); the tectonic setting and provenance of the late Triassic stratigraphy by Barboza-Gudiño, *et al.*, (2010).

Each one of these studies has contributed to an overall sense of the kinematics in northern Mexico. The Riedel shear mechanism was not applied to them, however useful data was still obtained.

### **1.2.7 Study Areas**

Based on the digital elevation model (DEM) with elevation data in figure 5 and 20, five sites were selected for analysis and are shown in Fig.1

1. The Parras Basin developed in sedimentary cover includes the north (PBF-1) and south (PBF-2) bounding faults, and the relation of PBF-2 to the MSM-3 fault (Fig. 5)
2. Marcos basin developed along a fault that puts sedimentary and volcanic rocks in contact.
3. Durango basins developed in a volcanic environment.
4. The Sinforosa lineament developed in a volcanic environment; along its path a basin is depicted at the intersection of faults (not evaluated).
5. Aquinuari lineament developed in a volcanic environment that does not show basins along its path (Martinez-Piña & Goodell, in progress) (Fig. 5).

### **1.2.8 Hypothesis**

If a basin associated with a fault formed because of the Riedel shear mechanism, assessment of the parallelism between the Riedel shear mechanism and the strike-slip basin geometry must give the kinematics of the fault.

### 1.3 Methodology

The major advantage to integration of geographic information systems (GIS) and RS is their synergy: GIS has information extraction potential, whereas RS has the ability to provide and update spatial data/information (Estes and Star, 1993). Faults are instruments of formation of releasing and restraining bends, and are an important element in compressional shear zones. Faults can be analyzed by comparing geometric components with known shear mechanism diagrams, i.e. Riedel (1929), Twiss & Moores (2007), and results of analogue materials experiments done by Atmaoui (2005), and Holohan *et al* (2008) and others.

#### 1.3.1 Data

Kinematic analysis of selected faults and associated basins required the assembly of structural elements, geographic data, as well as satellite imagery. Operations performed for the GIS portion are vector maps produced from field data or digitized from scanned maps, slope analysis, directional filter, interpolation maps, clipping, and georeferencing of vector data. Shaded relief maps were constructed under this phase.

Data used consisted of 1:500, 000 scale Cartas Geológico Minero (maps) from eleven states (Sonora, Chihuahua, Coahuila, Sinaloa, Durango, Nuevo Leon, Nayarit, San Luis Potosi, Aguascalientes, Jalisco, Zacatecas) available at the Servicio Geológico Mexicano website converted to a shapefile format (Fig. 6). MrSID (*multi-resolution seamless image database*) mosaics (n-12-30; n-12-25; n-12-20; n-13-30; ; n-13-25; n-13-20; n-11-30; n-11-25; n-14-20; n-14-25) (Fig.7). Enlargement and georeferencing of Carta Magnetica de Mexico obtained from the Carta Geológica de la República Mexicana, (2007) scale 1: 2,000, 000 from Servicio Geológico Mexicano. Data in ASCII e00 format (Fig.20). Riedel shear mechanism diagram and

Twiss & Moores (2007) (Fig. 2,3 and 4), and diagrams from Atmaoui (2005) and Holohan *et al* (2008).

- (1 ) Coordinate System: WGS 1984 UTM Zone 13N  
Projection: Transverse Mercator  
Datum: WGS 1984  
False Easting: 500,000.0000  
False Northing: 0.0000  
Central Meridian: -105.0000  
Scale Factor: 0.9996  
Latitude Of Origin: 0.0000  
Units: Meter

### 1.3.2 Technique

The first step was to create a structural map of Mexico. These maps were converted from a PDF format and scale 1: 250,000 to a ArcMap10® shapefile, and assembled into one structural map of Mexico (SMM) (Fig. 6); the map consists of 84,000 linear and circular features. The second step consisted in creating an image-map of northern Mexico using MrSID mosaics. The outline of lineaments of the three orders was made with these mosaics, and then those lineaments with length 0-15 km, 15-45 km, 45-100 and over 100 km (Chart 1) were select creating an image-map of Mexico (IMM) depicting major lineaments (Fig. 7). The third step consisted in creating a digital elevation model (DEM) of northern Mexico with data elevation, and outlining the basins and compressional shear zones. The fourth step consisted of interchanging the DEM and MrSID mosaic, used as base-maps, with the structural maps. This operation allowed selecting lineaments that intersected the basins and the compressional shear zones at different angles. The selected lineaments where then compared to those of the right and left lateral Riedel diagram. By visual comparison, a set of lineaments is selected. A lineament identified either as T, R, R', P or PDZ fault is selected and used as base value. Angles and strike between the faults and the walls of the basins, or compressional zones were measured with the GeoTools software.

Once the base value is determined, the hypothetical strike of the rest of the right or left lines in the Riedel diagram is computed. Finally, the measured strikes of the faults outlined are compared to the hypothetical strikes. Similarity in values define whether it is a left or right strike slip fault, hence the vector motion.

## **1.4 Results**

The results of the kinematics of each basin and lineaments at different locations give a partial picture of the dynamics of northern Mexico. The use of the Riedel diagram technique has helped to prove to predict the motion vectors of the strike-slip faults, regardless of rheology, the age of the faults and stratigraphic relations. In addition, the sites studied in conjunction with other research, can be used to define the tectonic framework of northern Mexico. A summary of the results of this study is shown in Table 7, and are described in the following paragraphs.

### **1.4.1 Kinematic Analysis**

Kinematic analysis refers to solving a geometrical problem (Marrett and Peacock, 1999) by defining and comparing the geometric elements of a strike slip-basin, to that of the Riedel shear mechanism diagram and determine the vector motion of the shear zone axis (Holohan *et al.*, (2007).

### **1.4.2 Parras Basin (PB)**

The Parras Basin located between the Coahuila Block and the Sierra Madre Oriental in the southern portion of the State of Coahuila. It formed by two fault systems proposed by Martinez-Piña and Goodell (in progress): the Parras Basin Fault-1 (PBF-1) to the north, the Parras Basin Fault-2 (PBF-2) to the south (Figs. 5 and 8). North of the basin, significant geomorphic features of the Coahuila Block consist of a valley with a bow shape (brown colored,

between numbers 2 and 3 in figure 8). In addition, there are two small parallel ranges striking NNW, west of the bow shaped valley. On the opposite side of these (SE), appears an arrowhead range with a flat bottom. In general, the slope decreases towards the NE.

#### **1.4.2.1 Geometry**

The two proposed faults are parallel to each other with a ridge in the middle (an irregular magnetic anomaly nears the center of the PB) that divides the basin into two, one north and one south. Dimensions of the northern basin are: 45 km wide and 225 km long; the dimensions of the southern basin are: 31 km wide and 190 km long; both basins strike WNW-ESE (Fig. 5 and 8). After merging, the basins change strike from WNW to NW. The geographic location is shown in a shaded relief raster with data elevation in figures 5 and 8. White colored areas are the highest elevation, maroon, yellow ochre and green being the lowest elevation.

#### **1.4.2.2 Parras Basin Fault-1 (PBF-1)**

The trace of the Parras Basin Fault-1 constitutes the present north margin of the Parras Basin and the southern boundary of the Coahuila Block (Fig. 8). Sets of normal faults striking northwest cross the Parras Basin Fault-1 (PBF-1), and define horsts and grabens (1 through 5, in figure 8). The angles at which these normal faults cross the segment are  $90^{\circ}$  for graben 1, and  $\sim 25^{\circ}$  to  $\sim 50^{\circ}$  for graben 5, with different angles in between. After outlining PBF-1 and the second order lineaments, these were compared first to the left lateral and then to right lateral Riedel shear mechanism diagram. The values of the angles measured in figure 9 and shown in Table 1, are consistent with those of the Riedel shear diagram defining a strike-slip right lateral fault. All angles measured are true because the image is georeferenced; therefore, strike of lines is also true.

Because the Coahuila Block is bounded by the San Marcos Fault (considered a Jurassic right lateral strike slip fault), and by the proposed fault PBF-1 (a Jurassic strike slip-fault), this tectonic setting provides a unique opportunity to corroborate the results rendered by this technique. For this, the geomorphic features of the Coahuila Block in figure 10 were used to reconstruct the Block into a hypothetical solid body. Reconstruction of the block consisted in outlining the Coahuila Block and the ranges in the area, and displacing and rotating the blocks at random until obtained a fit, as shown in figure 11. No paleomagnetic data is considered in the reconstruction of the CB. Only blocks B through F were utilized. Values of counterclockwise angles of rotation were found in values between  $15^{\circ}$  and  $37^{\circ}$  (Table 2). Block A was discarded because of the high angle of rotation, and the small area. Counterclockwise rotation of blocks is possible for those located between San Marcos fault and PBF-1 fault, because of the right-lateral motion of both systems (Figs. 10 and 11). This supports the kinematics determined by geometric comparison, between the Riedel shear mechanism and that of PBF-1.

A discrepancy found in the trace of San Marcos fault, because of the reconstruction of the block, is that at the point where the San Marcos fault crosses the block D, as shown in Figure 10, the Coahuila Block had to move towards the southwest, according to the motion vector of the fault. In accordance with the geological map of the state of Coahuila by the Service Geológico Mexicano (1993) the point of intersection shows a series of overturned folds. This result suggests that the trace of the SMF should be moved north (north of the bow-shaped range), where a magnetic lineament coincides with its strike (Figs. 1.10 and 1.11).

#### **1.4.2.3 Parras Basin Fault-2 (PBF-2).**

The fault system PBF-2 constitutes the south boundary of the Parras Basin (PB) and is parallel to PBF-1 (Figs. 5 and 12). Because of faults parallel along the trace of PBF-2 the area

selected for analysis, is the northwest portion of the basin (dashed blue box). The faults were outlined from the SMM, and the outline of the basin from the shaded relief image-map. Along the northwestern margin of the Parras Basin, corresponding with the trace of the PBF-2, lineaments crossing the fault were compared to the corresponding geometries of a left and right Riedel shear mechanism diagram. Three sets of faults were characterized: ENE, N, and NNW. Several traces of set ENE matches antithetic shear R' faults, while the margin in at least three sites varies from synthetic P shear faults to PDZ (Fig. 12). Moreover, the trace of a Y- synthetic fault can be found within the basin (at the bottom of the figure). Comparison of the geometry of PBF-2 to that of a right lateral strike-slip fault diagram, is shown in figure 13 with angle values in Table 3. The fault is defined as a right-lateral strike-slip system. There are also strong similarities of this geometric arrangement with results from analogue models of Atmaoui (2005) and Holohan *et al*, 2008).

#### **1.4.3 MSM-3 fault system**

Strike-slip basins and pop-up ridges simultaneous development along strike-slip faults has been described at several length scales (Christie-Blick and Biddle, 1985, Atmaoui 2005). Several researchers (Christie-Blick and Biddle, 1985; McClay 2001; Atmaoui 2005; Atmaoui *et al.*, 2008, Holohan *et al*, 2008) consider scaled analogue modeling a powerful tool to understand the geometries and kinematics of complex structures and their evolution as structures squeezed up at restraining bends and stepovers.

In a geometric arrangement different from that of PBF-1 and 2, the lineaments do not cross the fault MSM-3 proposed by Martinez-Piña and Goodell (in progress); instead are aligned parallel to the strike of the fault. Since comparison of the Riedel shear mechanism to that of any fault is based in the intersection of shears, kinematic analysis of structures in figure 12 will

consider diagrams and results from analogue materials experiments by ten Brink (1996), Christie-Blick & Biddle (1985), McClay 2001, Atmaoui (2005) and Holohan *et al*, 2008) (Fig. 15).

The fault MSM-3 is located between PBF-2 and the Tepehuanes-San Luis fault (TSL) (Fig. 5 and 12). In between faults PBF-2 and MSM-3, there is a complex zone, formed by a chain of basins and antiforms and a series of Jurassic alternating outcrops (Barbosa-Gudiño *et al*, 2008) align parallel to the strike of both faults (Figs. 8 and 12). The experiments by Christie-Blick & Biddle (1985), Atmaoui (2005) and Holohan *et al*, (2008) (Figs. 14, 15, 16, respectively), showed that extensional and contractional structures can originate from the same Riedel shear mechanism, and that contraction at the overstepping areas can generate by a left-stepping arrangement of the Riedel shears, where the conjugate Riedel shears predominate (Fig. 15).

By comparing the geometry of the strike slip-fault and associated basin from figure 12 (white dotted line) to a diagram from Atmaoui, (2005) (Figs. 17-1), it is clear the geometry of a left-stepping sinistral fault. On the other hand, alternating pop-up ridges (Ri) and strike-slip basins (B) in Figure 12 are located on both sides of the fault, but the pop-up ridges (Ri) on the west side end where the fault bends (basin), giving way to another basin, while the ones in the east side continue to the southeast. The prevalence of third order lineaments coincides with the ridges to the northwest and the lack of these with the basins of the southeast.

This additional strike-slip zone of a chain of tectonic features similar to those developed in analogue materials experiments (Figs. 15 and 16), could have formed at a low opening angle as a narrow shear zone, with small strike-slip basins, and pop-ridges bounded by Riedel shears,

as a result of the differential motion between MSM-3 and PBF-2. Jurassic volcanic outcrops (black dots Fig. 17) considered as pop-up ridges, are part of a continental arc that overlies Paleozoic metamorphic rocks and Triassic redbeds (Barbosa-Gudiño et al, 2009). Formation of pop-up ridges between two contiguous shears is the result of a strike-slip discontinuity in the basement that generates right left-stepping or left right-stepping shear faults in the overlying cover (Atmaoui, 2005). The area between the adjoining shear is under contraction, therefore both shears have either right lateral or left lateral strike-slip motion (Fig.1-D).

Other comparison to the diagram from Christie-Blick and Biddle (1985) shows that the origin of the pop up-ridges and strike-slip basins, could be the thrust faults and extension created by counterclockwise rotation of blocks included between MSM-3 and the interior strike-slip fault. Given that PBF-2 is a right lateral strike-slip fault, and that the geometry of the strike-slip fault in between (white dotted line, figure 12) is consistent with that of a left-lateral strike-slip fault, the vector motion of MSM-3 is inferred as a left lateral slip (Fig. 17-2).

#### **1.4.4 Tepehuanes-San Luis (TSL) fault system**

The Tepehuanes-San Luis fault system is considered as the southern edge of the Mesa Central (Nieto-Samaniego, Alaniz-Alvarez, & Camprubí 2007; Loza-Aguirre, *et al*, 2008) (Figs. 5, 12, 17). It has a N 60 W direction and an estimated length of ~ 660 km, measured from the city of San Luis Potosi. The TSL is not a continuous structural feature, because it is displaced by the normal faults radiating from the Jalisco rift. South of the TSL at 39 km, there is a parallel fault with a length of 32 km, which has been considered to be part of the TSL (Loza-Aguirre et al, 2008) (Fig. 5 and 20). This fault will be known as the Guadalupe Fault system. There are two grabens described by Loza-Aguirre et al, (2008): the Guadalupe graben (GG) located west of Zacatecas, NNE trending and a width of 8 km, and the Aguascalientes graben (AG), located

north of the city of Aguascalientes, NNE trending and a width of 12 km. This graben, according to Loza-Aguirre et al, (2008), has been displaced toward the NW, motion consistent with that of a left lateral strike-slip fault. The Guadalupe graben (GG) is included between the TSL and the Guadalupe fault, figure 20 shows the location of the geologic features just mentioned, and the scarcity of lineaments, reason by which the Riedel shear mechanism was not applied. Vector motion of the TSL is based on the kinematic relations between PBF-2, the left stepping sinistral fault in between, and the MSM-3 (Fig 17). The Aguascalientes Graben does not seem to be part of the GG, because it shows continuity and evidence of left lateral displacement along the edges of the valley after the trace of the TSL fault. On the other hand, GG has no continuity towards the north or south, meaning that either it was faulted on both sides, or created within the constrained area, since an extensional regime can be part of a lateral regime (Ahlgren, 2001, Coehlo, Passchier, & Marques, 2006). What these grabens show is reactivation of the TSL segments (since they are displacing grabens of a younger age), and that Guadalupe fault and the TSL are two separate left lateral strike-slip systems. However, a right stepping dextral fault between the TSL and the MSM-3 has been inferred by comparison to a diagram from Atmaoui (2005) (Figs. 12 and 17-3). This fault connects Durango Basin and TSL (Fig. 18).

#### **1.4.5 Durango Basin (DB)**

Shaded relief raster image of the area of Durango shows four basins bounded by normal faults (Fig 18, A –D) and second and third order lineaments striking 1) NW 2) NNW 3) NNE 4) WNW, and 5) NE; it also depicts the right stepping dextral fault of figure 17-3. Even when the shape of these basins is irregular, basin A has an elongated shape oriented NW, which seems to be the original shape of the basin. This original basin, dislocated by normal faults from an extensional regime, displaced the blocks towards the south (Fig. 19-1). Due to this condition and

to the parallelism between the boundaries of the basins and the strike of the faults any comparison to the Riedel shear diagram would render uncertain results. However, reconstruction of the basin into a single basin (Fig. 19-2), allowed drawing an axis that was overlaid to figure 5. By extending the axis southward, this coincide with the trace of the fault Tepehuanes-San Luis (TSL) is evident, and goes from Tepehuanes, Durango, to just south of Sombrerete, Zacatecas. Between these two cities, the direction of the fault changes from  $\sim N30^{\circ} W$  to  $\sim N 60^{\circ} W$ , in an area where the normal faults, related to the Jalisco Block, intersects the TSL. Durango basin is part of the TSL system that was afterwards dislocated by northeastern normal faulting.

#### **1.4.6 San Marcos Fault-1 (San Marcos northwestern extension)**

Aranda-Gómez *et al.* (2005), Chávez-Cabello *et al.* (2005) and others have mapped and studied the San Marcos Fault system in the southern part of the state of Coahuila. All of them have suggested that the length of this lineament could be over 300 km, striking NW.

A composite image-map consisting of a DEM and a reduce to the pole magnetic map of the state of Chihuahua, shows a magnetic lineament oriented northwest southeast with a length of  $\sim 400$  km. The lineament corresponds on the surface with two faults: the SMF-1 (Martinez-Piña & Goodell, in progress) and the Plomosas fault (Oviedo, 2008) (Fig. 21). The trace of the San Marcos Fault is a composite fault that extends from the Coahuila Block (in the state of Coahuila) to the eastern boundary of the state of Sonora. Here, the SMF-1 constitutes the northern boundary of a physiographic subsection known as Babicora-Bustillos (Hawley, 1969), which is a transitional zone in terms of terrain and geological features between the SMO and the Basin and Range. This physiographic subsection resulted from an extensional regime by reactivation of the faults in the area (Fig. 21-A).

Because of the contrast in elevation and morphology produced by valleys trending north south crossing the lineament, outline of the basin required the magnetic map of the state of Chihuahua. An anomaly of low magnetic values (blue color) aligned along the trace of the SMF-1- Plomosas fault is consistent with characteristics of a deep basin fill with alluvium. Lineaments at the edge of the basin show geometric elements parallel to those of the Riedel diagram (Fig. 22). Using the same procedure as before, R, R' and P were identified, T faults are also present. Compared values with the shear diagram of Riedel are in Table 4. This kinematic analysis establishes that SMF-1 fault last event was as a right lateral strike slip motion, which is the same as that of SMF in the southeast. However, Oviedo (2008) defined a left lateral strike-slip motion for the Plomosas fault, which would seem to contradict the results from the comparison of geometries. There are three possible explanations: 1) SMF-1 and Plomosas are two *en echelon* faults; the latter reactivated separately by a recent tectonic event i.e. the Rio Grande Rift. 2) SMF-1 and Plomosas are two *en echelon* faults; the first one reactivated separately by a recent tectonic event, i.e. opening of the Gulf of California, and 3) SMF-1 and Plomosas are two *en echelon* faults, reactivated separately by combination of the two events. In any case, this study considers the original vector motion of the fault as left lateral. The physiography of basins and ranges, oriented north south is inferred as generated by reactivation of SMF-1 and the Chipahuiqui fault.

#### **1.4.7 Sinforosa lineament (SL) and Aquinquiri lineament (AL)**

Structural characteristics of the Sinforosa lineament (SL) and the Aquinquiri lineament (AL) are different from those mentioned above. These are arc-shaped and the strike, in average, is NW, but their more important characteristic is their geometry (Fig. 23). Some researchers (Sedlock *et al.*, 1993; Centeno *et al.*, 2008, Ferrari, 2005) classify Sinforosa and Aquinquiri

lineaments as interblock lineaments or tectonostratigraphic boundaries. Aquinquari lineament was suggested as an unnamed northwest lineament by Ferrari (2005). Sinforosa is conspicuous in Landsat images, regular maps (since Rio San Ignacio follows its path), DEMs and shaded relief rasters. The Aquinquari lineament, on the other hand, can be observed in shaded relief rasters by changing parameters (215° azimuth and 45° light source above horizon, figure 23). Both lineaments crosscut the SMO and continue until they intersect (?) the Tepehuanes–San Luis fault system. Overlaying the structure layer obtained from the SMM to the IMM, the area included between the Sinforosa and the Aquinquari lineaments has a low to medium density of lineaments striking NW forming an acute angle, i.e. La Plumosa fault, with SL and AL (Fig. 24). High density second order lineaments can be seen to the southeast and northwest. The importance that these two lineaments have lies in the fact that they are located in the Guerrero Terrane, constituted by volcanic rocks highly susceptible to mineralization. In accord with Wisser (1966), veins occupying fractures are the main type of ore deposits, often pre-mineral faults, although post-mineral faulting is common. On the other hand, Clark & de la Fuente, (1978), established northeast and northwest as the principal mineralized fracture trends with subsidiary directions of north south and east west. Of the main strikes, the northwest is the pre-mineral type of fault, matching the Riedel shear mechanism as tension faults. Based on the latter, definition of SL and AL PDZ, consisted in comparison of geometries between second and third order lineaments cutting across, to the Riedel shear mechanism diagram.

#### **1.4.7.1 Sinforosa**

Sinforosa lineament/fault consists of several segments that give the characteristic arc-shape (Fig. 24). An enlargement of the image in site A of figure 24, shows the two segments analyzed have a western striking NE and an eastern, striking NW. By comparison, to the Riedel

shear mechanism diagram, these segments are parallel to P and R synthetic shears, respectively, and so are the T faults. Angle values are shown in Table 5. A layer of mineral occurrences superimposed shows alignment of these, with R', and T (Fig. 25). An extensional basin is found at the intersection of Sinforosa fault with the Rio Urique lineament; but basin was not evaluated. The Sinforosa lineament/fault is defined as a right lateral strike-slip fault.

#### **1.4.7.2 Aquinquari**

The same procedure of comparing geometries between lineament/fault and the Riedel diagram was applied for the Aquinquari fault; but in this case, since there is no strike-slip basins, a segment of ~300 km of the fault and lineaments that intersect were used for comparison (Fig. 27 and 28). Faults crossing the AL with a NW strike at an acute angle are normal tensional faults (T in Fig. 24 A and B, e.g. Comedero, La Plumosa, Conitaca) that delimit grabens in the southern area of AL. On the other hand, the proposed connection SA-1 (Martinez-Piña & Goodell, in progress) also shows a high degree of parallelism with R' or antithetic fault. This R' type of shear is not conspicuous in the images due to the high density of the lineaments. For this matter, a directional filter, kernel 7 x 7 and angle of 120° was applied to a Landsat image (P 33, R 41) that covers the area. Three sets of lineaments resulted (Fig. 29-1), A) NNE, B) NE and C) NNW or N-S, that compared to those defined by Galvan-Gutierrez, (2006) for the area (Fig. 29-2) are : sets A-C matches set 3, and set B matches set 4).

Sinforosa and Aquinquari are consistent with characteristics of right-lateral strike-slip fault systems. A tectonic map of the Ocampo Mining District area by Thorton and Arik (2004) located ~130 km north from site A (figure 24), shows two main *en échelon* right lateral strike slip faults striking N66°W. These faults are parallel to the synthetic R-shear of the Sinforosa fault. Predicted angle values by the shear mechanism diagram for the Sinforosa fault in site A,

are within range for those estimated (from the map of the Ocampo mining district) for the mineralized veins.

From the satellite image, a northwest fabric is observed, in fact, north of Sinforosa and south of Aquinquari this fabric is very consistent, but is not dense between the two faults (Fig. 24). Although calderas are present in the area, the SL and AL fault systems shows no perceptible disturbance by the volcanic dynamics, suggesting post-caldera activity. Application of the shear mechanism diagram to the “unarranged” spatial distribution shown by mineral occurrences, aside from their metallogenesis, can establish a relationship between structural patterns and mineral deposits. Either lack of mapping or structural reasons could be the cause for the low-density lineaments between SL and AL.

### **1.5 Discussion**

This study has shown a practical and viable use of the Riedel shear mechanism diagram and models, which combined with satellite imagery and geographic information systems, allows and produces kinematic analysis of any lineament in any type of area. Extensional and contractional structures (Fig. 15) can originate from the same Riedel shear mechanism, in which case kinematic analysis could require a simple geometric comparison; however, length and width in both cases are essential to apply the geometric analysis.

The kinematic analysis of the complex contractional zone between parallel faults PBF-2 and MSM-3 and MSM-3 and TSL (Figs.12 and 17) , consisting of a chain of small-scale ridges and basins, required a different approach. Between the first two major faults, secondary strike-slip faults of transverse direction formed, and were identified by comparison to the models resulting from experiments with analogue materials by Christie-Blick and Biddle (1985) and Atmaoui (2005). This approach, while unconventional, required an evaluation of at least three

different models to meet, from east to west, the motion vectors of the major faults. This assessment allowed deduction of strike-slip motion of the MSM-3. The use of this technique also provided the suggestion of possible changes in the traces of faults; such is the case of the San Marcos Fault (Figs. 10 and 11). The results obtained by this technique (Riedel diagram and model comparison), categorizes these as preliminary and should be the subject of extensive field work..

### **1.5.1 Conclusions**

Definition of the vector motion of a strike-slip fault by comparing geometries between strike-slip basins using the Riedel shear mechanism using IGIS is a technique that can apply to every segment of a fault, as long as lineaments/faults are found either on the walls of the basins or on the pop-up ridges. If the faults related to the basins or pop-up ridges are of a different age than that of the geological feature, reactivation of the fault should be considered. In any case the vector motion defined will always be the last of the fault. Results from analog materials research combined with the Riedel shear mechanism has been the basis in designing the model with which this study has been completed. Constraints in map scale allow only the visualization of major lineaments and their relationship to basins; however fieldwork can provide more data that may substantiate the first results.

It is shown that the combination IGIS-Riedel shear mechanism successfully defined the vector motion for the Tepehuanes-San Luis fault and the southeastern extension of the MSM. This is done by analyzing a parallel sequence of strike slip faults that begins with the *en échelon* faults of the Parras Basin. The kinematics of this region compared with that of the north appears to be the result of two different shear stress systems that occurred at different times. The Jurassic

outcrops between and along the strike of the MSM-3 and the PBF-2 faults defines this zone as a pop-up ridge, though not in the strict sense because no strike-slip basins are found at the ends.

All results obtained from using this technique refer to the last vector motion of the strike-slip, and unless reactivation is observed in the area, this vector motion is to be considered as the original. Left or right lateral motion does not seem influenced by lithology since some of the major lineaments cuts across sedimentary as well as volcanic rocks without changing their vector.

Interpretation of the kinematics of an area in which restraining bends, flower structures, *en echelon* faults, dilational and contractional stepovers are found, should consider the existence of a concealed a strike-slip fault, to lead to a better understanding of the structural geology of the zone.

Table 1.1 Comparison of theoretical angle values between Riedel's diagram and those measured in PBF-1 using figure 19

<b>Base value: T faults with strike N 22° W (Riedel shear mechanism diagram)</b>				
<b>R</b>	<b>T</b>	<b>R'</b>	<b>P</b>	<b>Main fault</b>
<b>N 52° W</b>	<b>N 22° W</b>	<b>N 08° E</b>	<b>N 83° E</b>	<b>N 83° W</b>
<b>Base value : measured on the image-map</b>				
<b>R</b>	<b>T</b>	<b>R'</b>	<b>P</b>	<b>Main fault</b>
<b>N 71° W</b>	<b>N 22° W</b>	<b>N 17° W</b>	<b>N 70° E</b>	<b>N 75° W</b>

Table 1.2 Angle values of rotation applied to blocks for reconstruction of a solid Coahuila Block body. Values of block A discarded because of high value and small size of the block.

<b>Block</b>	<b>Counter-clockwise Rotation angle</b>	<b>Azimuth</b>
<b>A</b>	-51°	309°
<b>B</b>	0°	0°
<b>C</b>	0°	0°
<b>D</b>	0°	0°
<b>E</b>	-28°	332°
<b>F</b>	0°	0°
<b>G</b>	-24°	336°
<b>H</b>	?	?
<b>I</b>	?	?
<b>J</b>	?	?
<b>K</b>	?	?

Table 1.3 Comparison of theoretical values from Riedel shear mechanism diagram and those of PBF-2 fault system located in the northwestern portion of the Parras Basin using figure 1.13.

<b>Base value: R' faults with strike N 37° W (Riedel shear mechanism diagram)</b>				
<b>R</b>	<b>T</b>	<b>R'</b>	<b>P</b>	<b>Main fault</b>
N 22° W	N 1° E	N 38° E	N 52° W	N 37° W
<b>Base value : measured on the image-map</b>				
<b>R</b>	<b>T</b>	<b>R'</b>	<b>P</b>	<b>Main fault</b>
N 14° W	N 1° W	N 49° E	-	N 37° W

Table 1.4 Comparison of the theoretical values from Riedel Shear mechanism diagram and those of SMF-1 system located in the northern portion of Marcos basin, in the state of Chihuahua using figure 1. 22

<b>Base value: R' faults with strike N 01° E (Riedel shear mechanism diagram)</b>				
<b>R</b>	<b>T</b>	<b>R'</b>	<b>P</b>	<b>Main fault</b>
N 59° W	N 29° W	N 01° E	N 89° E	N 74° W
<b>Base value : measured on the image-map</b>				
<b>R</b>	<b>T</b>	<b>R'</b>	<b>P</b>	<b>Main fault</b>
N 40° W	N 31° W	N 01° E	-	N 68° W

Table 1.5 Comparison of theoretical angle values between Riedel diagram and those measured for Sinforosa using figure 1.26

<b>T faults with strike N 26° W (Riedel shear mechanism diagram)</b>				
<b>R</b>	<b>T</b>	<b>R'</b>	<b>P</b>	<b>Main fault</b>
<b>N 56° W</b>	<b>N 26° W</b>	<b>N 4° E</b>	<b>N 86° E</b>	<b>N 79° W</b>
<b>Base value : measured on the image-map</b>				
<b>R</b>	<b>T</b>	<b>R'</b>	<b>P</b>	<b>Main fault</b>
<b>N 67° W</b>	<b>N 26° W</b>	<b>N 1° W</b>	<b>N 81° E</b>	<b>N 83° W</b>

Table 1.6 Comparison of theoretical angle values between the diagram Riedel and those measured in Aquinquari using figures 1.24, 1.27, 1.28

<b>Base value: T faults with strike N 34° W (Riedel shear mechanism diagram)</b>				
<b>R</b>	<b>T</b>	<b>R'</b>	<b>P</b>	<b>Main fault</b>
<b>N 64° W</b>	<b>N 34° W</b>	<b>N 4° W</b>	<b>N 86° E</b>	<b>N 79° W</b>
<b>Base value : measured on the image-map</b>				
<b>R</b>	<b>T</b>	<b>R'</b>	<b>P</b>	<b>Main fault</b>
<b>-</b>	<b>N 34° W</b>	<b>N 6° W</b>	<b>W- E</b>	<b>N 81° W</b>

Table: 1.7 Table of results of the studied strike slip basins

Basin	Lineaments	Location	Figure No.	Analysis	Input	Reference	Last vector motion	Figure No.
<b>PBF-1 (Parras Basin Fault-1)</b>		South boundary of Coahuila Block	8	Riedel shear mecahinsm	Linear features	This study	Right lateral strike-slip fault	9
<b>PBF-2 (Parras Basin Fault-2)</b>		North boundary of Sierra Madre Oriental	12	Riedel shear mecahinsm	Linear features	This study	Right lateral strike-slip fault	13
	<b>MSM-3- (Mojave-Sonora-Megashear-3)</b>	North boundary of Mesa central	12	Riedel shear mecahinsm	Linear features	This study	Left lateral strike-slip fault	17
<b>Durango</b>		Durango City	18	NA	Linear features	This study	Extensional basins	19
<b>Marcos</b>		Northern boundary of Sierra del Nido	21	Riedel shear mecahinsm	Linear features	This study	Right lateral strike-slip fault	22
	<b>Sinforosa</b>	Western Sierra Madre Occidental	24-A	Riedel shear mecahinsm	Linear features	This study	Right lateral strike-slip fault	25-26
	<b>Aquinhuari</b>	Western Sierra Madre Occidental	24-B	Riedel shear mecahinsm	Linear features	This study	Right lateral strike-slip fault	27-28

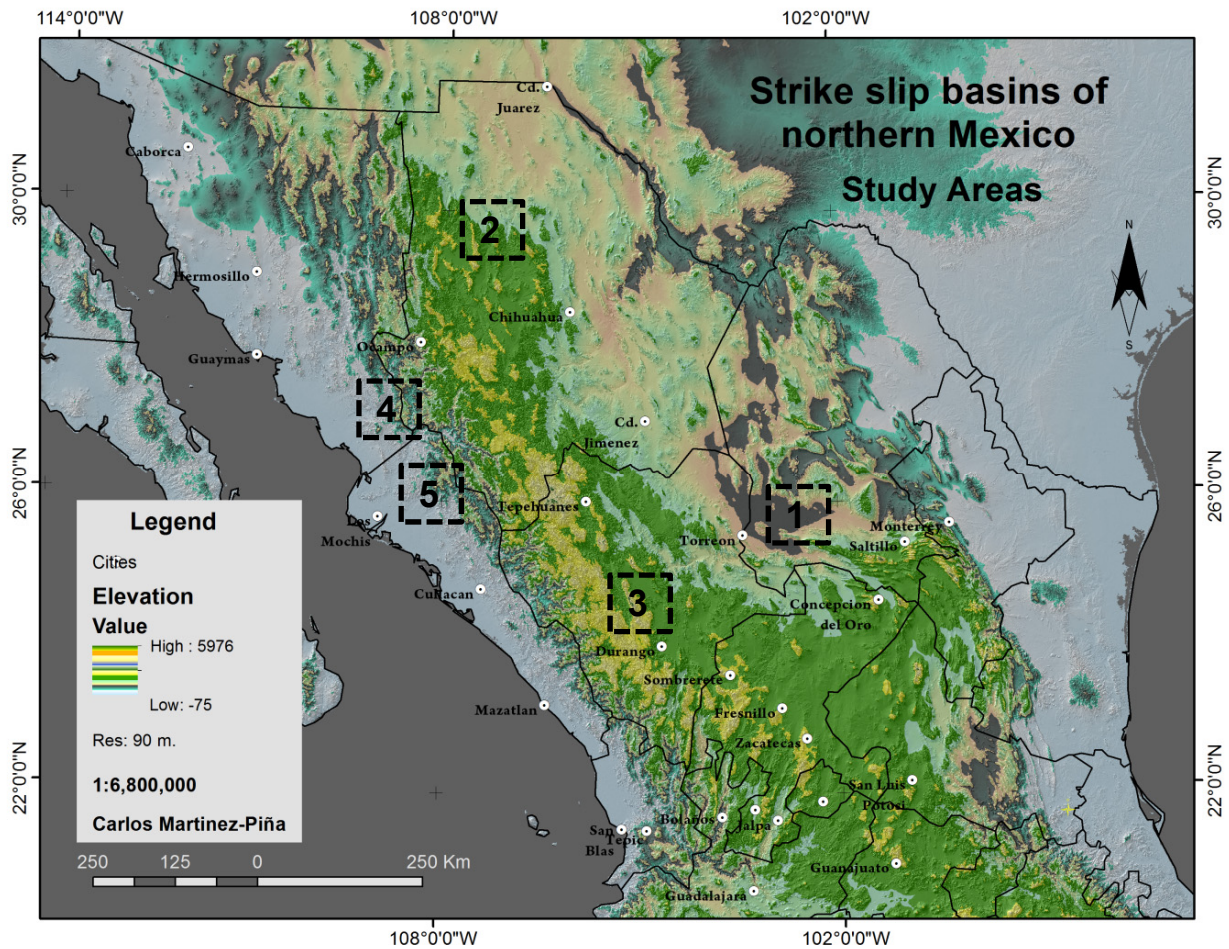


Figure 1.1: Shaded relief raster with elevation data showing the 5 study areas. Faults and basins are postulated Martinez-Piña & Goodell, (in progress). Site 1) Parras Basin and MSM3; 2) Marcos Basin 3) Durango basin 4) Sinforosa lineament 5) Aquinquiri lineament. SRTM Shaded Relief (North West, one of six data sets) represents a shaded relief map (between 60 degrees North and 56 degrees South latitude) of the world derived from the Global Digital Elevation Model (SRTM) data sets from the U.S. Geological Survey's EROS Data Center. The resolution is 3 arc seconds (90 meters). The version of the SRTM 3-arc-second data that served as the basis for the SRTM Global Digital Elevation Model data is the Version 2 "Finished" data in DTED Level 1 format that was created by NGA by subsampling SRTM 1-arc-second data.

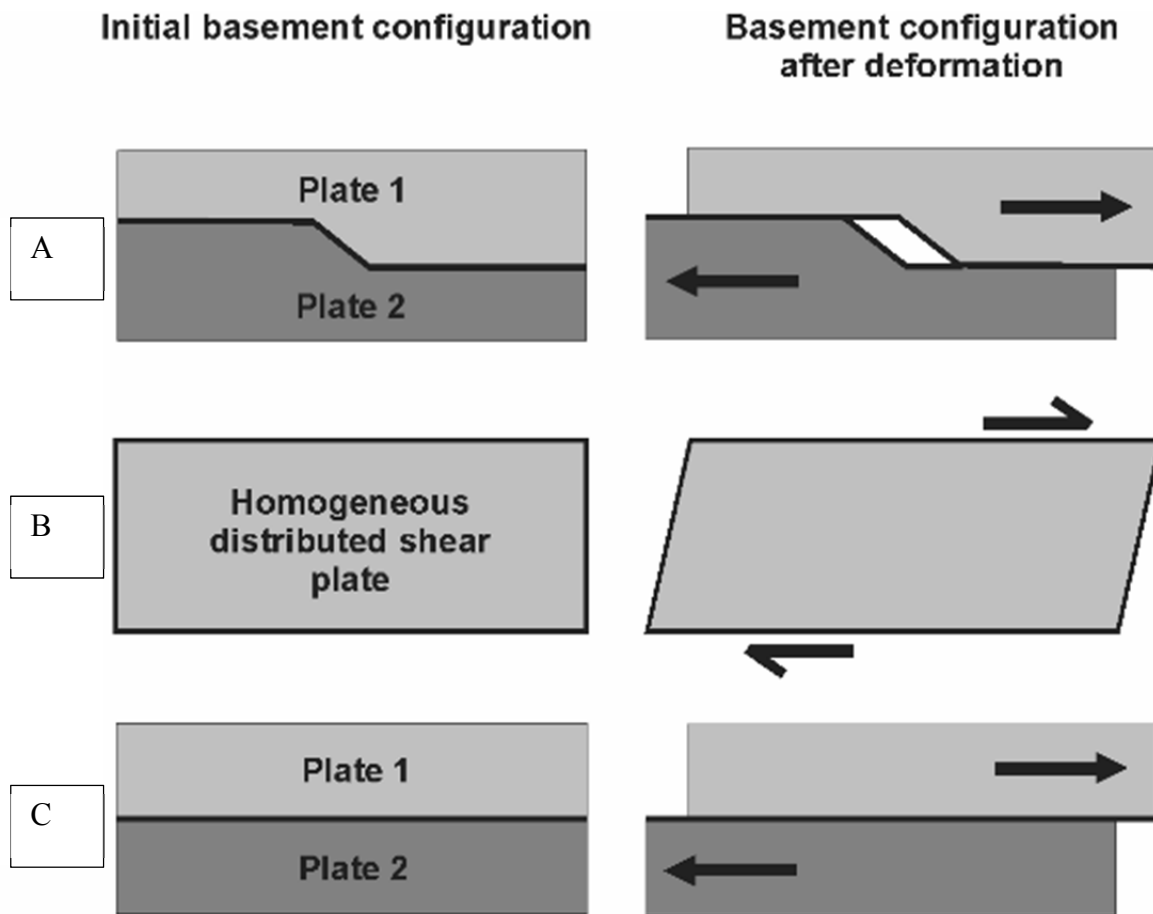


Figure 1.2: Basement configuration of the three mechanisms in Figure 1: before and after deformation. Analogue experiments on pull-apart basin formation. Modified from Atmaoui, (2005)

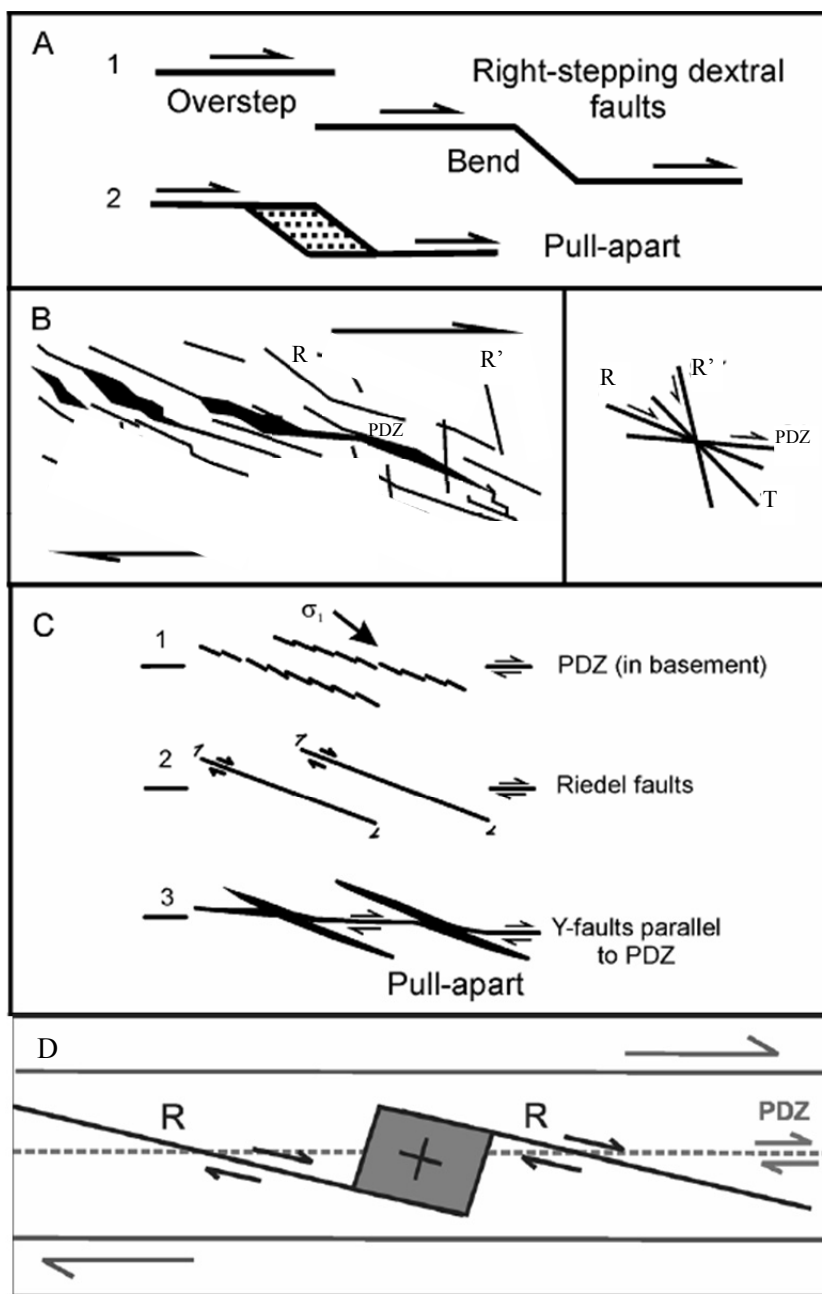


Figure 1.3: Figures and descriptions modified from Atmaoui, (2005)

A) En echelon right-stepping dextral strike-slip faults. Pull-apart basins form at the overstep or bend (Mirror image for the left-stepping sinistral faults)

B) Distributed shear. Pull-apart basins form during linking and coalescence of main faults (simplified from An and Sammis, 1996).

C) Riedel shear 1) Initiation and coalescence of first generation shears into Riedel faults 2) Strike-slip displacement and rotation of Riedel shears 3) Development of Y-faults, parallel to the principal displacement zone (PDZ). Pull-apart basins form at the passive Riedel faults (modified from Hagglauser-Ruppel, (1999). contraction.

D) Formation of a push-up ridge (grey colored box) between two contiguous Riedel shears (R). The dextral motion along the strike-slip discontinuity in the basement (PDZ) generates dextral left-stepping Riedel shear fractures in the overlying slab. The area between the neighboring shears is under



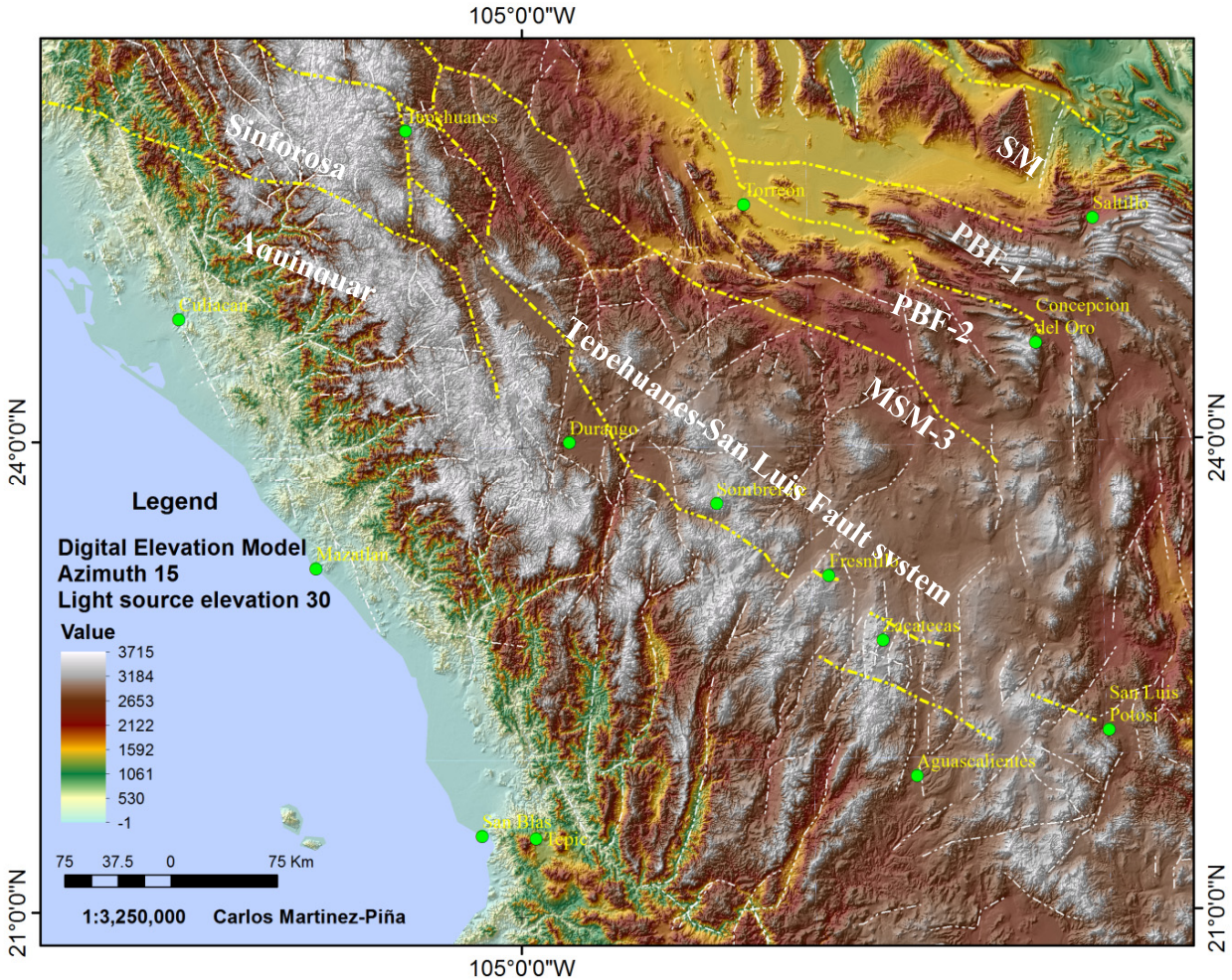


Figure 1.5: Shaded relief raster with elevation data showing the Tepehuanes-San Luis fault system, and the San Marcos fault and parallelism of major faults PBF-1, PBF-2 and MSM-3 postulated by Martinez-Piña & Goodell, (in progress). Durango basin near the city of Durango (approximately in center of image); Parras Basin in the upper right corner. At the bottom the Jalisco Block. Resolution of raster : 90m.

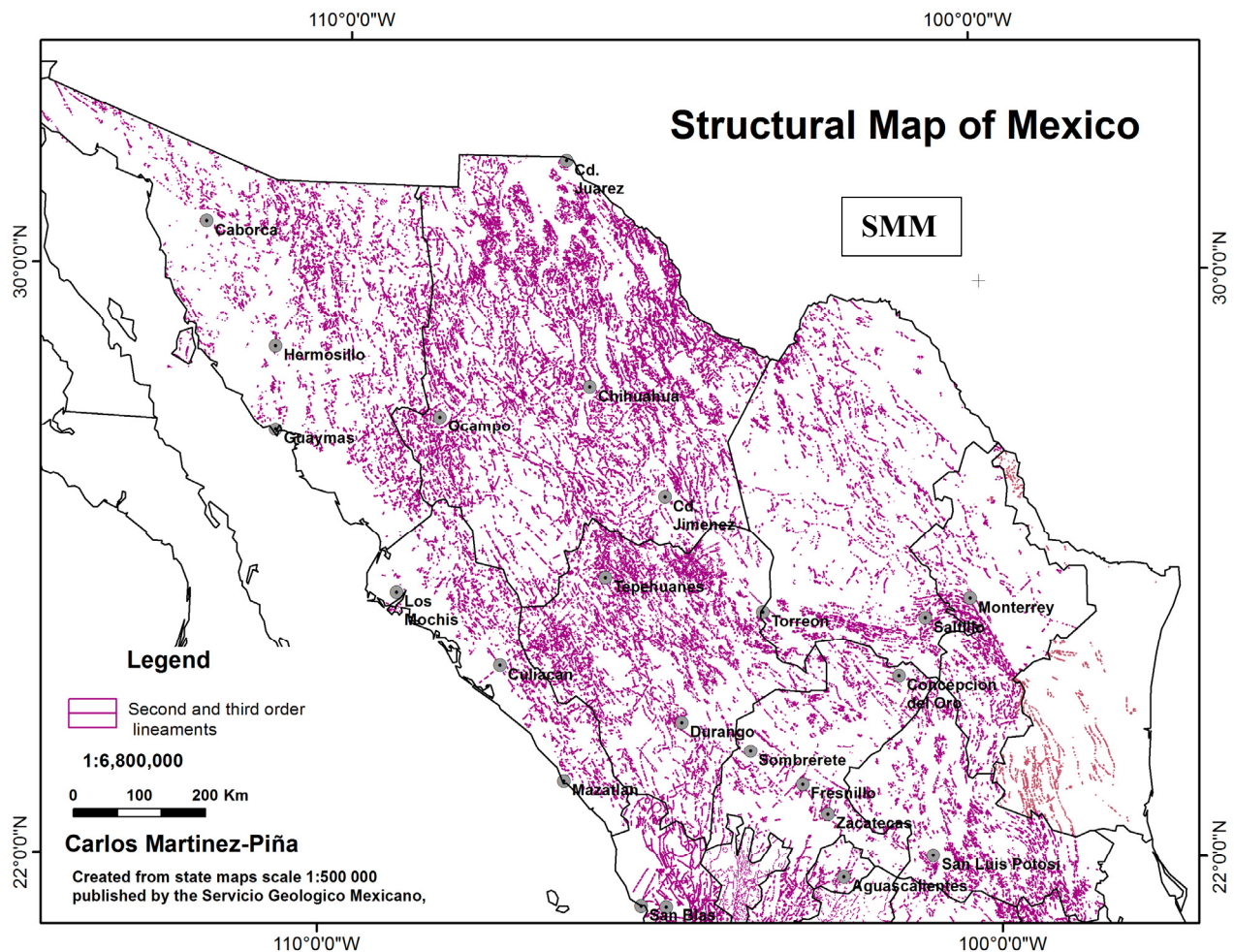


Figure 1.6: Structural map of Mexico (SMM) consisting of 84,000 structural features, (arc, circles and linear) created from Servicio Geológico Mexicano geological state maps scale 1:500, 000 in PDF format. Original maps available at their website. Structural data added to the state of Chihuahua from Martinez-Piña (2006).

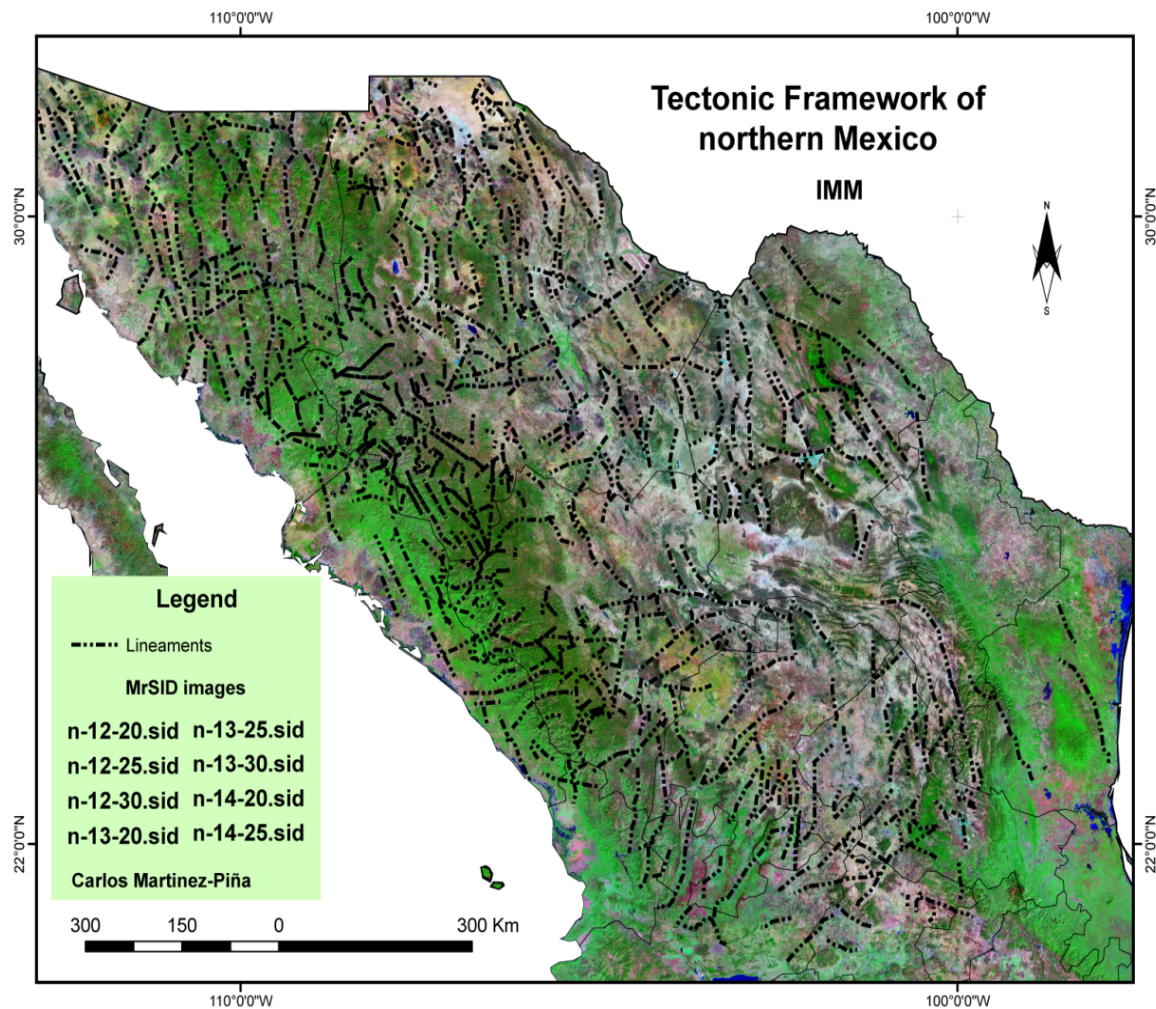


Figure 1.7: Image-map of Mexico (IMM) composed of eight satellite mosaics. Image depicts major lineaments showing 637 first, second and third order lineaments in northern Mexico. The outlining of these lineaments required a digital elevation model at different azimuth and source elevations. These lineaments were used for length categorization.

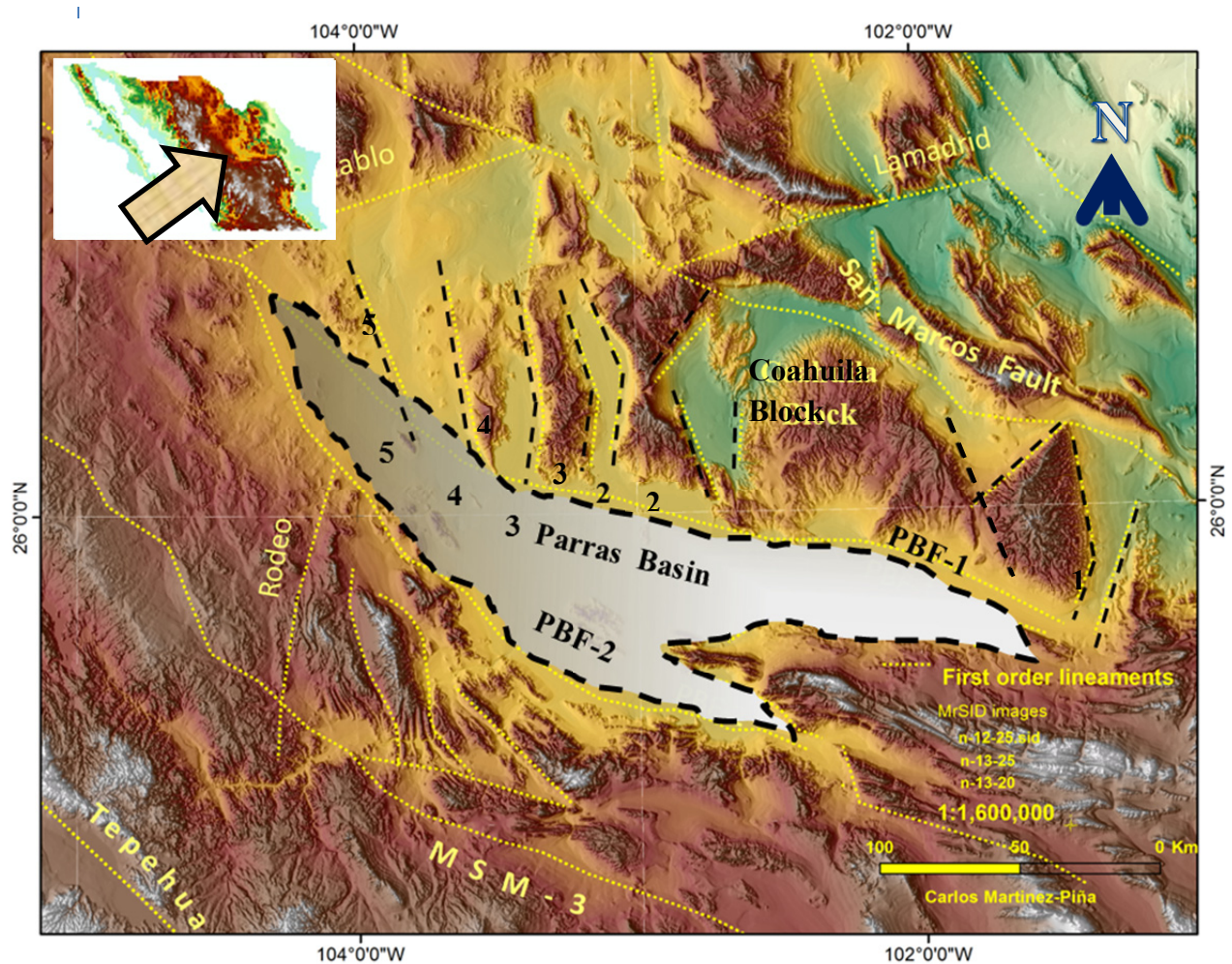


Figure 1.8: Shaded relief with elevation data showing paths of postulated faults PBF-1, PBF-2 and MSM-3 by Martinez-Piña & Goodell,(in progress). Notice the series of parallel grabens (1 thru 5) intersecting PBF-1. Trace of the SMF from Chavez-Cabello et al, (2005). Slope decreases towards the right upper corner. Map and arrow in upper left corner point to geographic location. Resolution of raster: 90m.

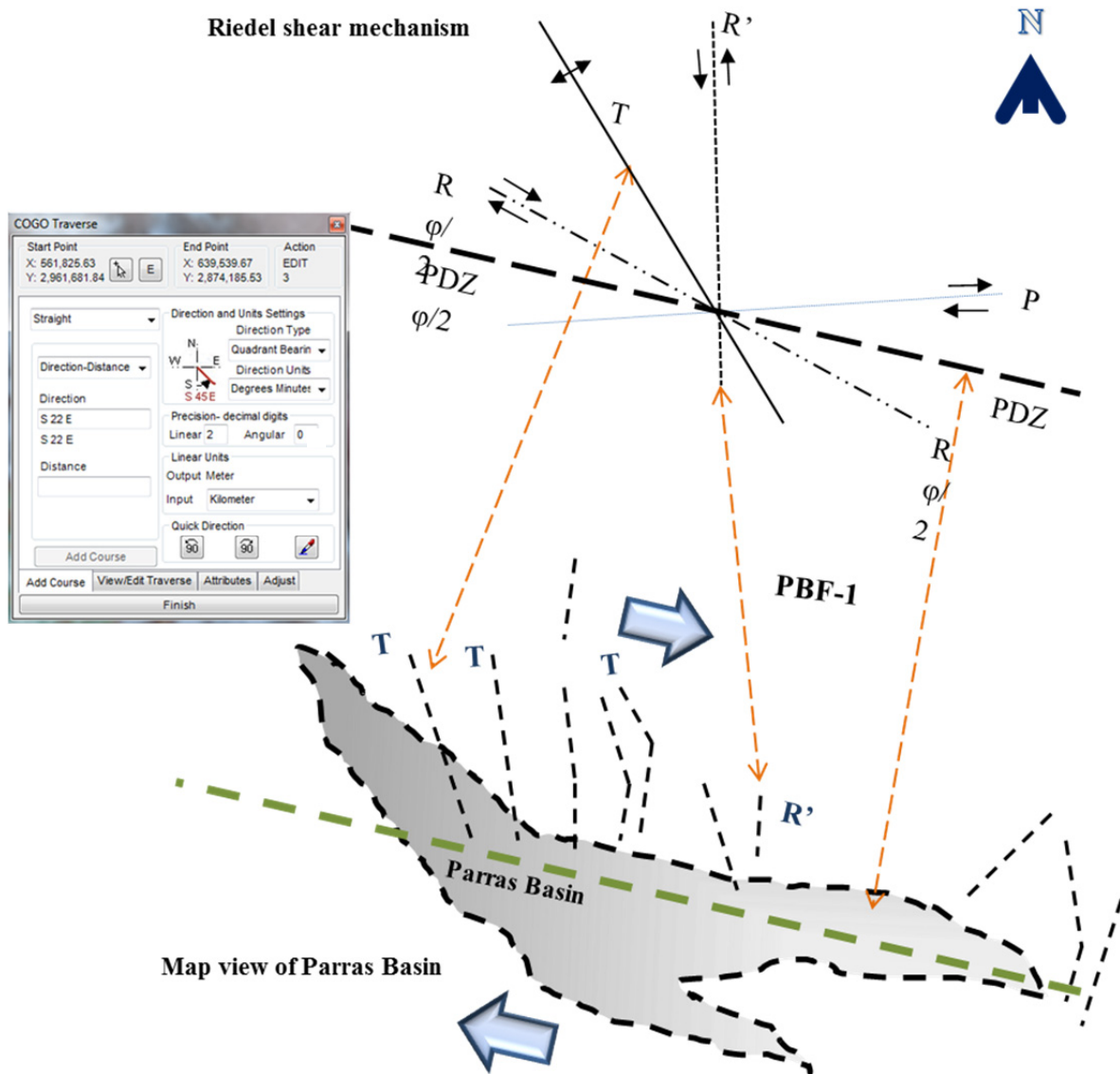


Figure 1.9: Comparison of geometries between Parras Basin and intersecting faults, to the Riedel shear mechanism diagram. Black line dashed is the outline of the Parras Basin and black shorter lines dashed are faults that bound tectonic grabens and horsts. Red lines dashed point to parallel elements in the Riedel diagram and indicate the correspondence with geometric elements from the basin. ET GeoTools<sup>®</sup> window shows measured base angle, compared angles are depicted in Table 1.1

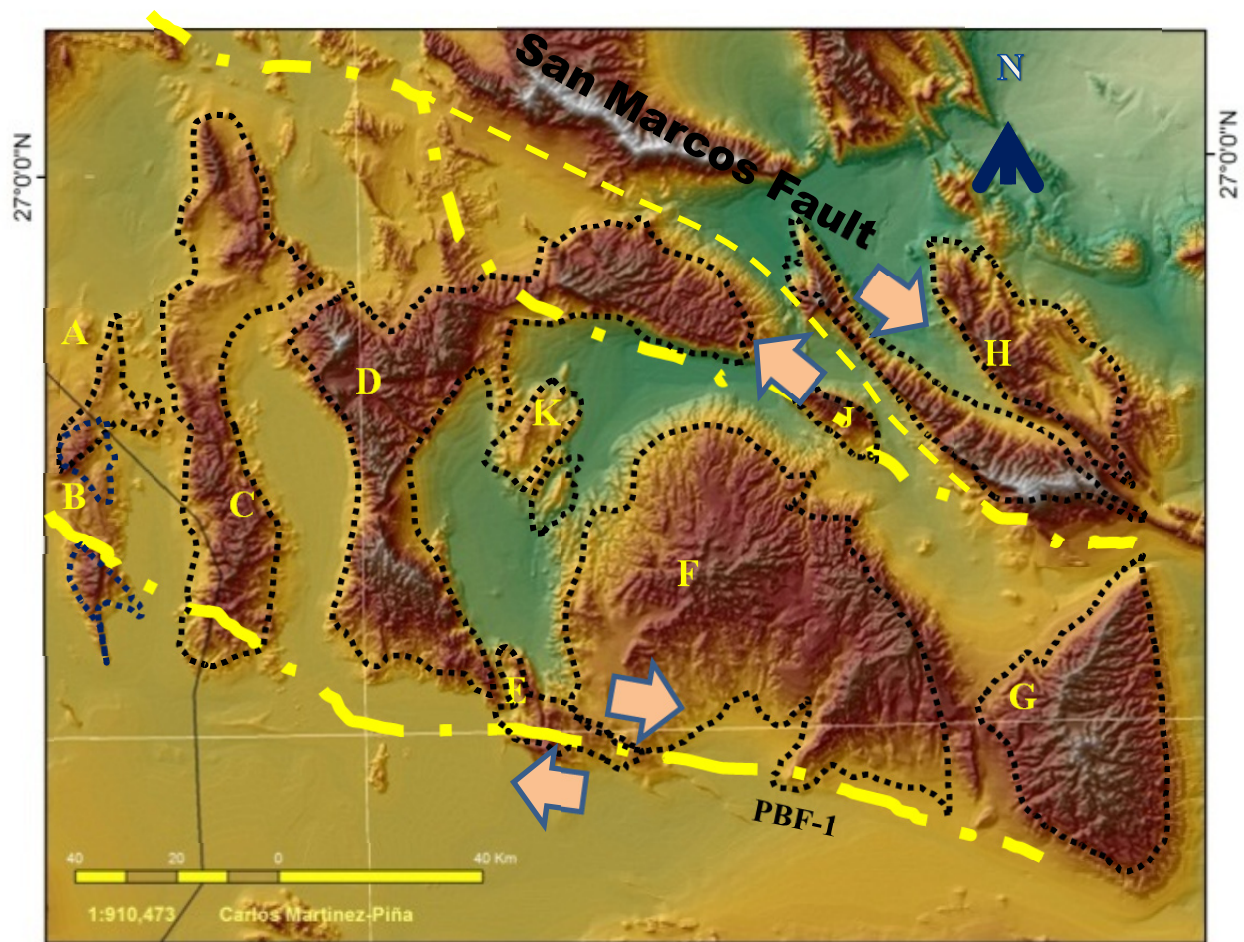


Figure 1.10: Shaded relief raster with elevation data shows outline of the Coahuila Block and ranges around it. Also shows location of the SMF and PBF-1 faults. Vector motion of the SMF fault defined by Chavez-Cabello and vector motion of PBF-1 by this research. Dashed line depict the proposed trace for the San Marcos fault. Resolution of raster : 90 m.

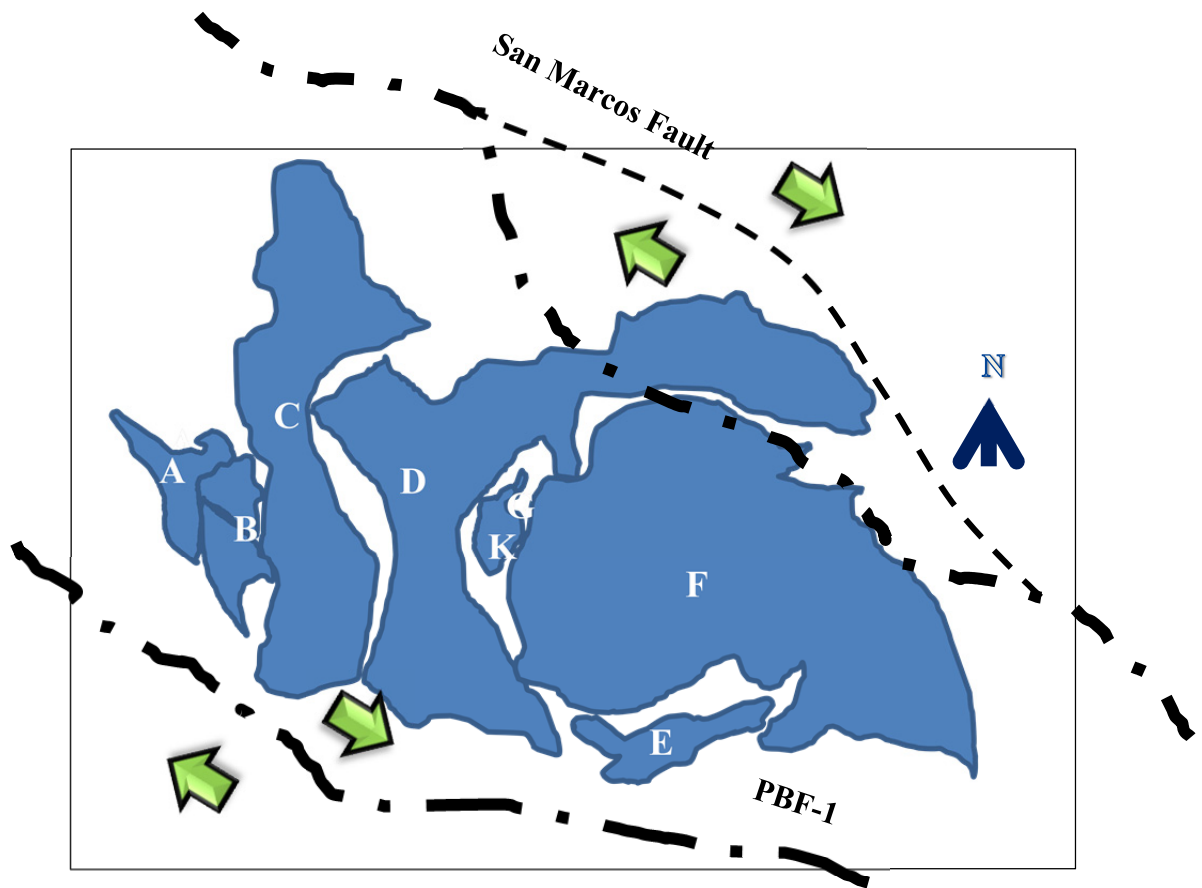


Figure 1.11: Palinaptic reconstruction of segments of the Coahuila Block. Blocks displaced and/or rotated randomly to reconstruct a theoretical solid body. Final angles of rotation for each block are shown in Table 2. Dashed line depict the proposed trace for the San Marcos fault.

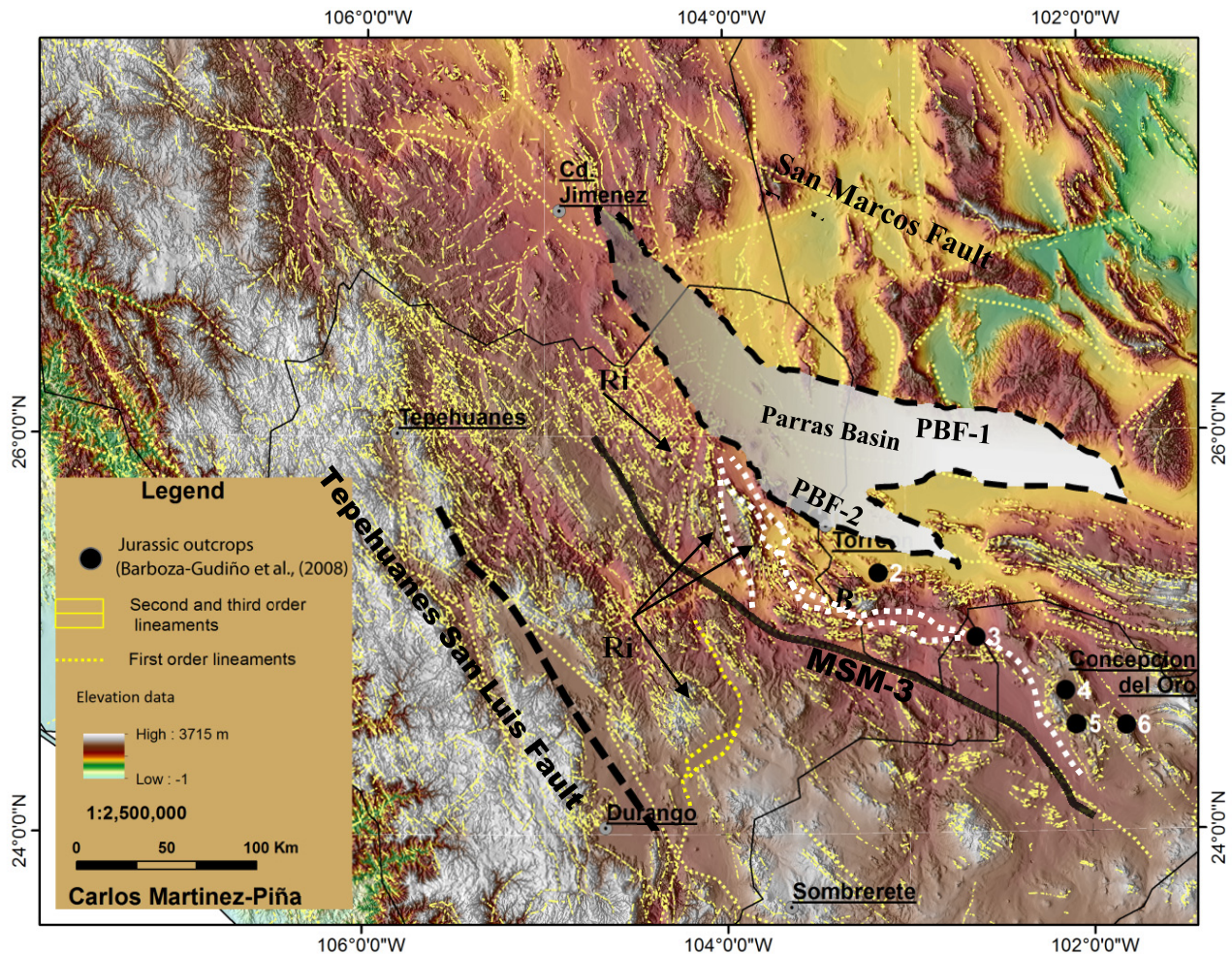


Figure 1.12: Shaded relief raster with elevation data, showing the postulated faults PBF-1, PBF-2 and MSM-3. Of these, PBF-1 is right-lateral strike-slip fault and PBF-2 is a left-lateral strike-slip fault. Second and third order lineaments (yellow lines) from SMM. Trace of faults in dotted thick yellow lines, by this study. Blue dotted box depicts study area of PBF-2 presented in figure 14. Zone between PBF-2 and MSM-3 (black continuous lines) show a complex series of restraining and releasing bends (white dotted, Ri=ridges, B= basins). Black dots numbered depict Jurassiac outcrops studied by Barboza-Gudiño et al (2008). See figure 17 for more information. Black dash line Tepehuanes-San Luis fault (TSL). Resolution of raster: 90 m.

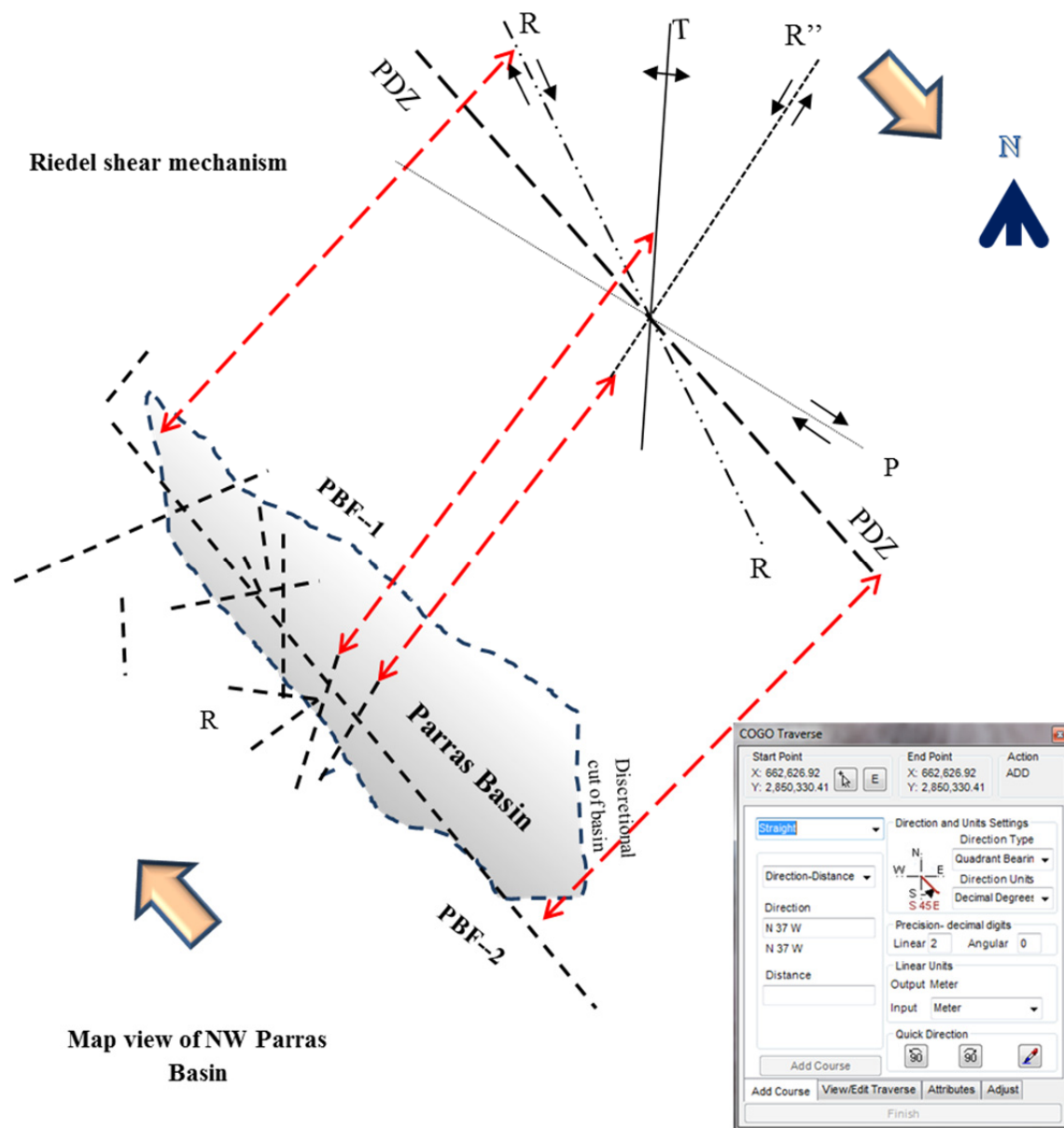


Figure 1.13: Riedel shear system diagram on top, and the set of faults of the northwestern part of the Parras Basin (blue dotted box corresponds with figure 13), mapped by the Servicio Geológico Mexicano and taken from the geology map of Durango. Boundaries of the basin are Y and P faults. Several R' types of faults are present. PBF-2 consistent with a right-lateral strike-slip fault. ET GeoTools® window shows measured base angle, compared angles are depicted in Table 1.3

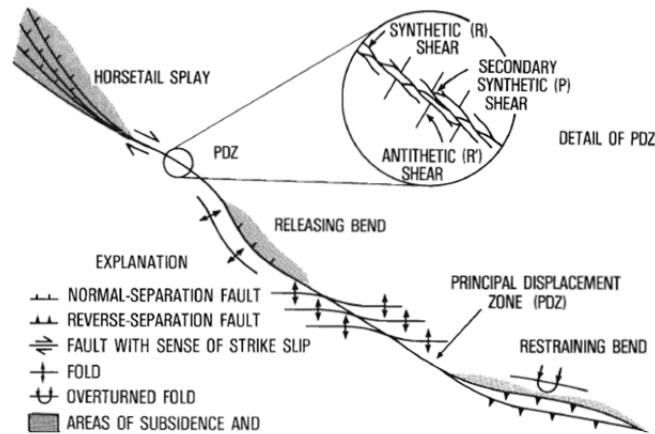


Figure 1.14: Image and description taken from Christie-Blick and Biddle,(1985). The spatial arrangement in map view of structures associated with an idealized right slip fault.

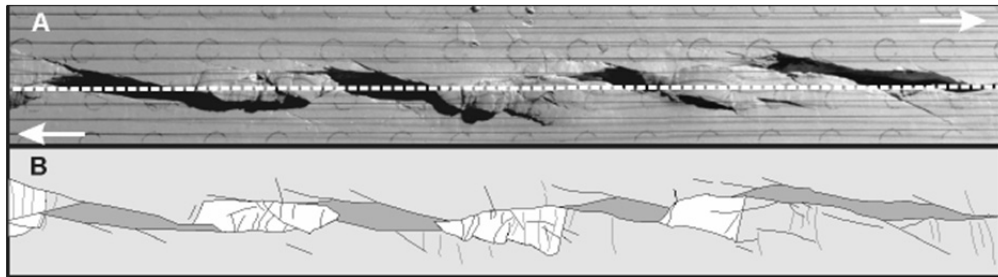


Figure 1.15: Image and description taken from Atmaoui (2005). Structural features of a part of the standard experiment NA4 after a NBD of 2 (basal displacement is twice the thickness of the slab). A) The raw image shows the strike-slip zone formed of alternating pull-apart structures with push-up ridges. The dashed line indicates the location of the PDZ at depth, and the arrows the dextral motion of the plates. B) Drawing of the image emphasizing the structural features. Push-up ridges and pull-apart structures are white and dark grey respectively.

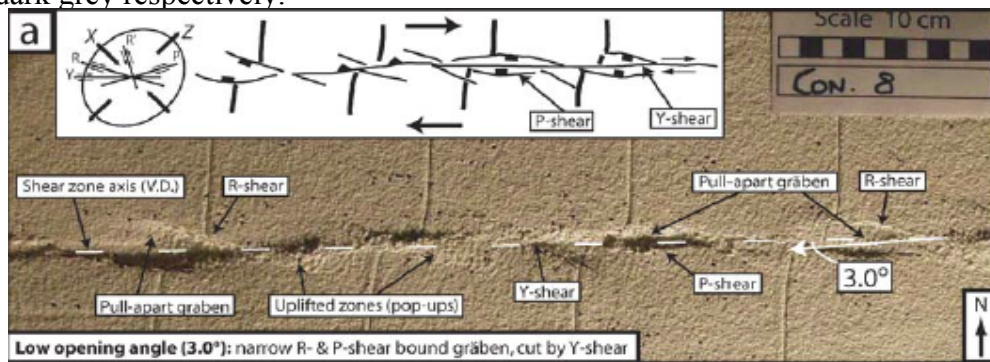


Figure 1.16: Image and description taken from Holohan, Wyk de Vries and Troll (2008). Simulation of strike-slip deformation in brittle crust (light from S). a) At low opening angles ( $3^\circ$ ), a narrow shear zone forms with small, Riedel shear bound, pull-apart-type graben and occasional pop-ups. B) At higher opening angles ( $8.5^\circ$ ), a series of rhombic pull-apart-type graben forms along a broader shear zone. These graben rapidly coalesce to form a single graben system. Insets show sketches of structures and their theoretical orientation with respect to the incremental strain ellipse (Woodcock and Schubert 1994)

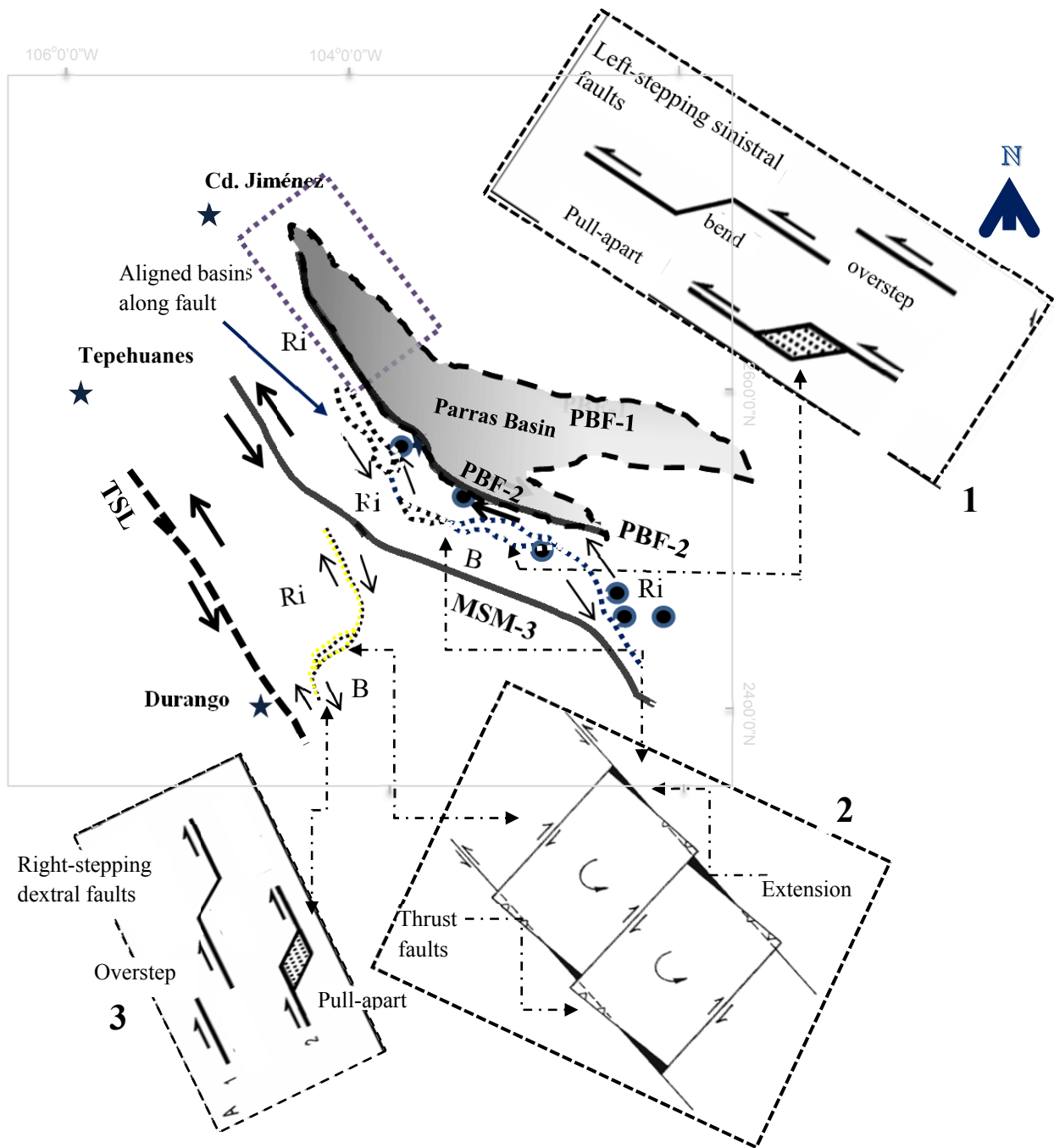


Figure 1.17 Map of area that includes from Parras Basin to the Tepehuanes San Luis fault, drawn from figure 12. Diagram shows outline and kinematics of faults MSM-3, PBF-2, and TSL based in figure 14; PBF-2 is a right lateral strike-slip fault and MSM-3 is a left lateral strike-slip fault; both constrain a zone in which left-stepping sinistral fault and strike slip basin (dotted line) are parallel to the main faults. Push-up ridges (Ri) and strike-slip basins (B); black circles are Jurassic outcrops (Barboza-Gudiño et al, 2008). Kinematics of PBF-2 compared to diagram from Atmaoui, (2005) (1). Kinematics of strike-slip fault between the MSM-3 and TSL compared with the diagram of Christie-Blick and Biddle, (1985) and Atmaoui (2005) (1 and 2). The zone constrained by MSM-3 and TSL, shows a connecting (?) right stepping dextral fault. Map compared with the diagram of Atmaoui, (2005) (3)

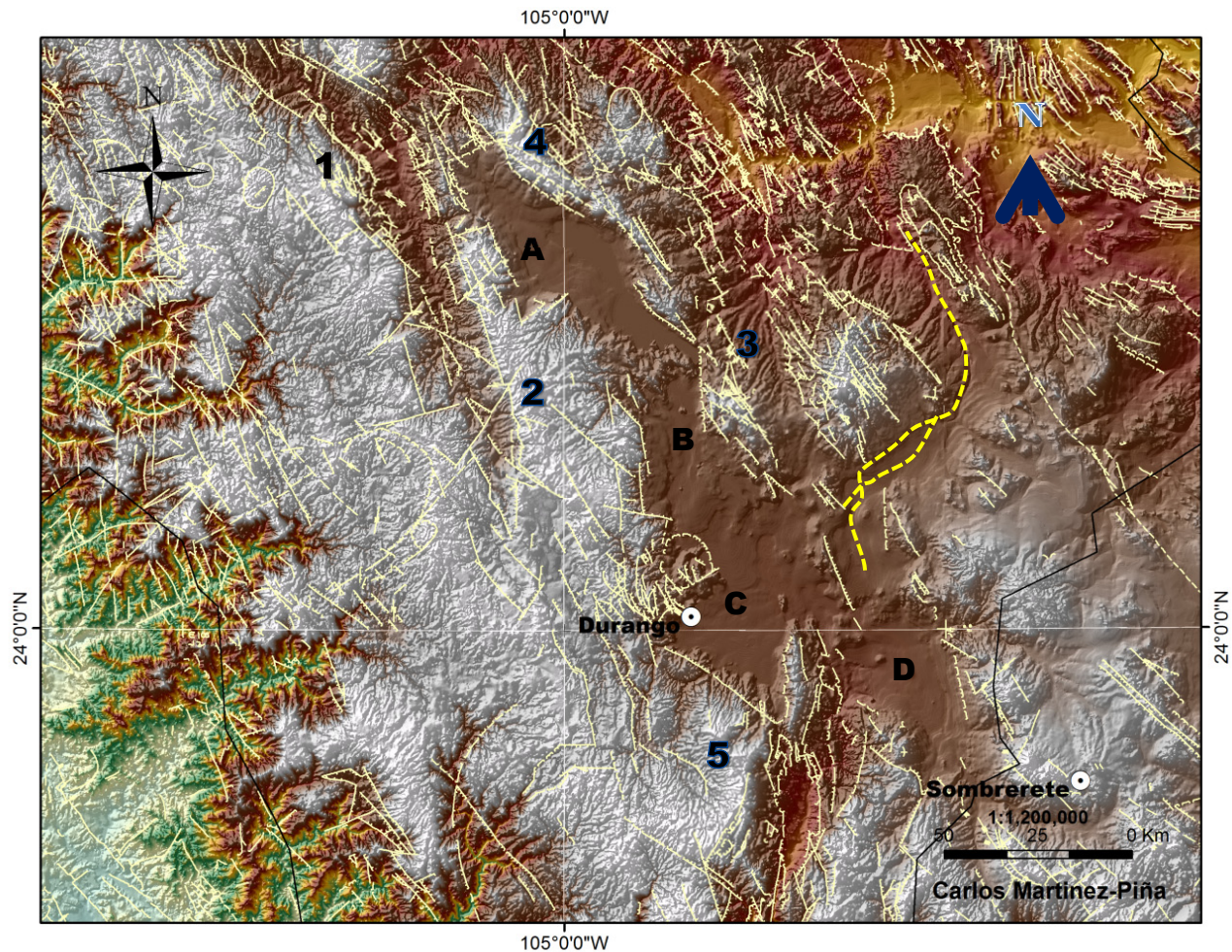


Figure 1.18: Shaded relief showing lineaments and their relationship to the Durango faulted basins (A-D) located in the area of Durango city and in the north westernmost portion of the Tepehuanes-San Luis fault system. Yellow dotted line is a right lateral strike-slip fault shown in figure 15. Numbers correspond to fault strikes 1) NW 2) NNW 3) NNE 4) WNW, and 5) NE. Circular features observed near Durango City. Lineaments from the SMM. Resolution of raster: 90 m.

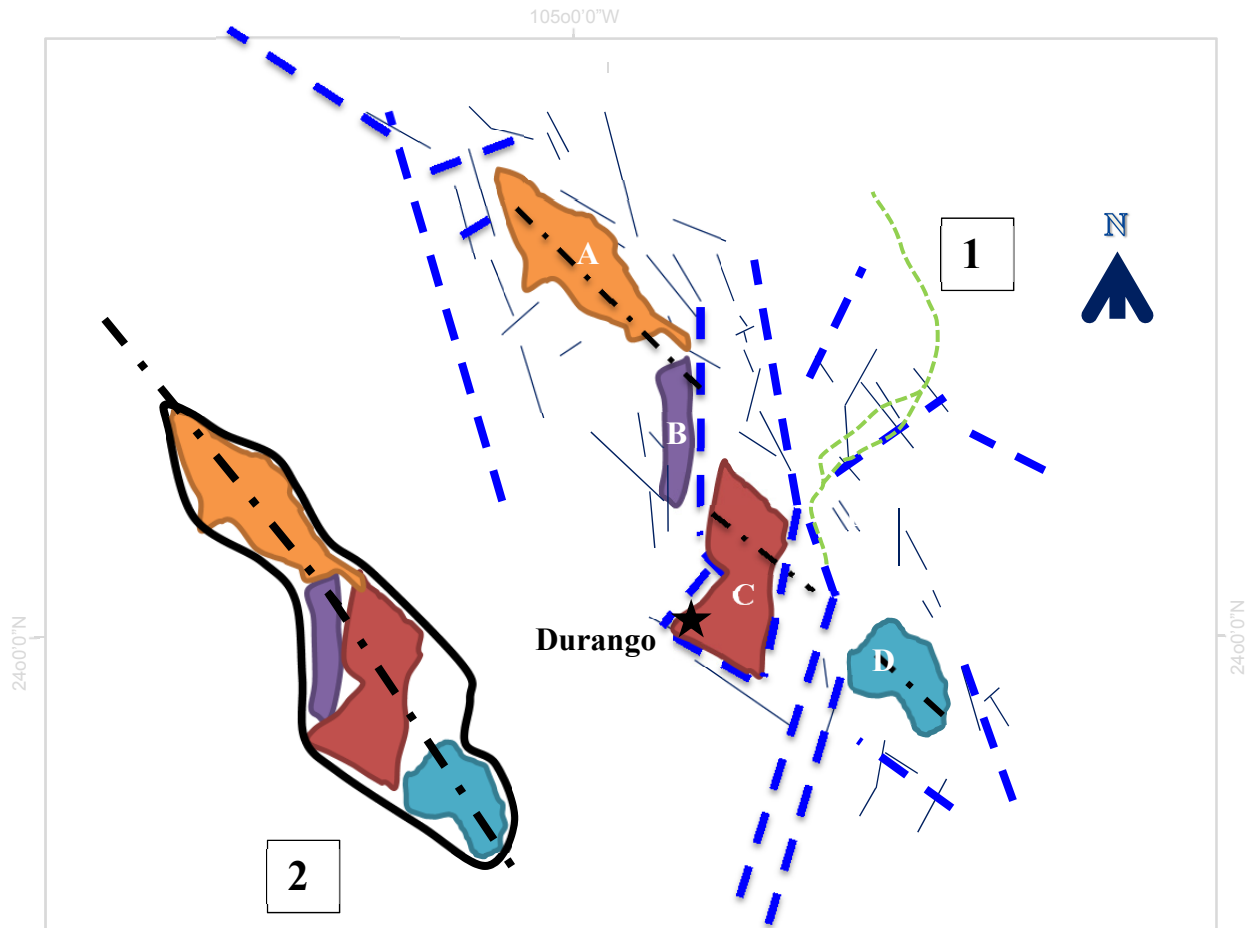


Figure 1.19: The five basins (outlined from figure 18) located in north westernmost portion of the Tepehuanes-San Luis fault system (1). Hypothesized PDZ for each basin segment (lines in black). Subsequent northeast faults dislocated the basin (lines in blue). Palimpsestic reconstruction of basin and outline of axis (2). Third order lineaments parallel to the borders of each basin. Orange dashed line depicts the same basin and faults as in figures 17 and 18.

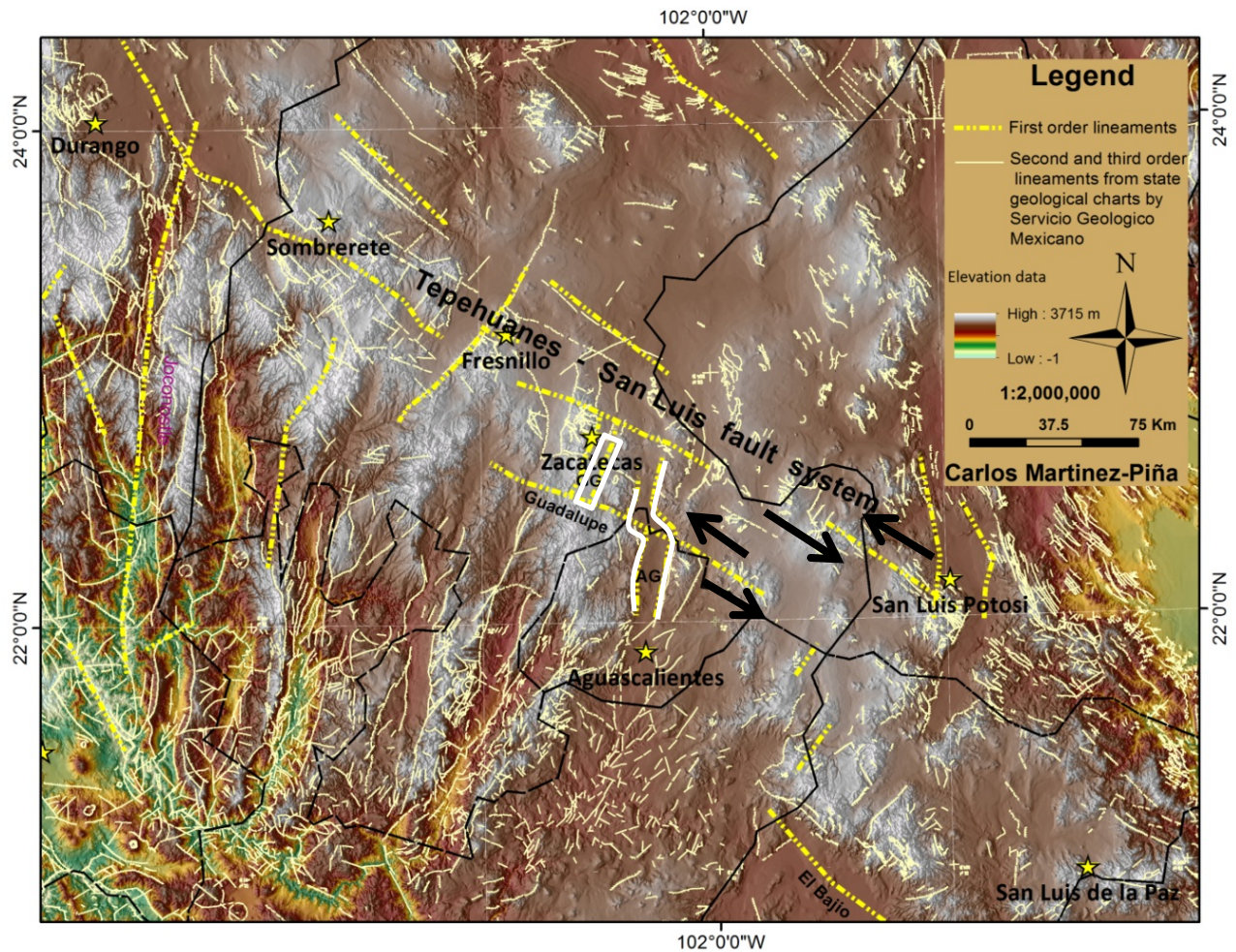


Figure 1.20: Shaded relief raster shows the structural relationships between TSL, Guadalupe fault, Guadalupe graben (GG), Aguascalientes graben (AG) (white lines) and the normal faults irradiating from the Jalisco Rift. TSL and the Guadalupe fault are two separate left lateral strike-slip systems. Total length of the TSL is not shown. Resolution of raster: 90 m.

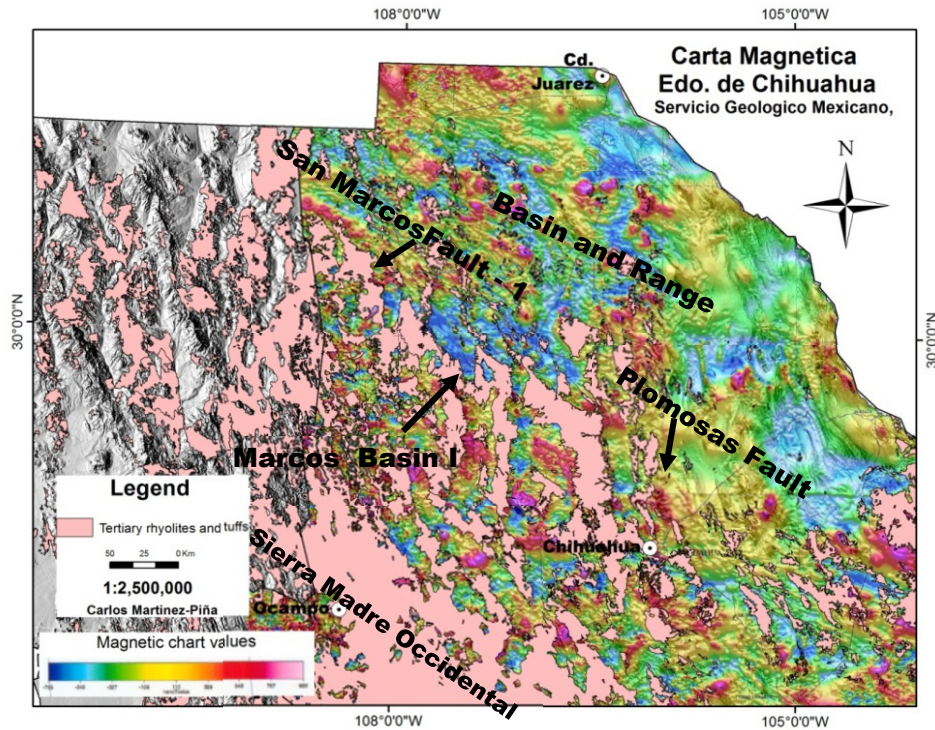
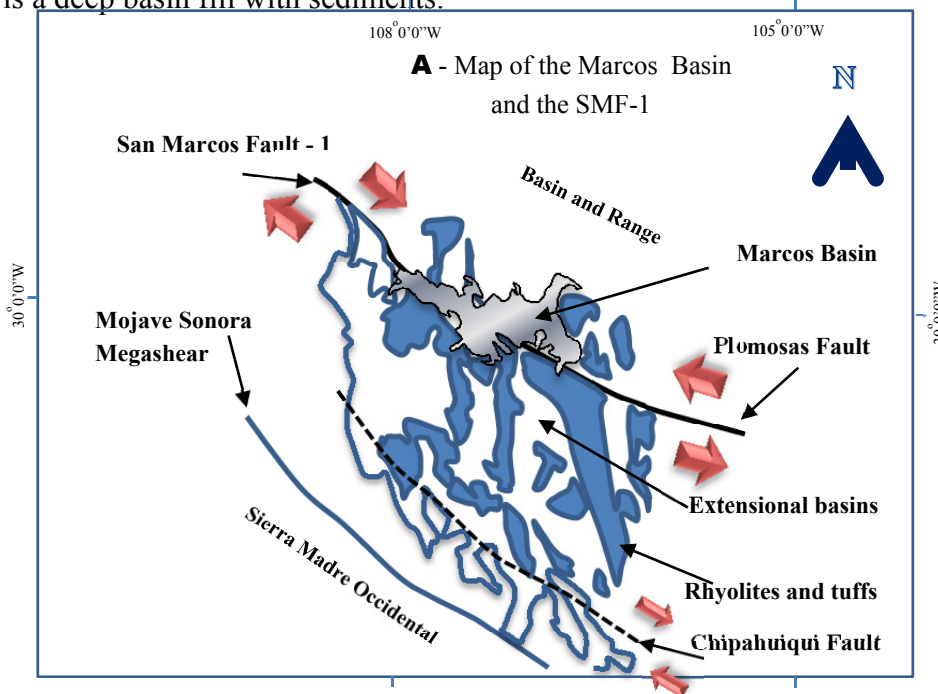


Figure 1.21: Digital elevation model overlaid by a reduced to the pole magnetic chart of the state of Chihuahua, produced by the Servicio Geológico Mexicano, and a layer of Tertiary rhyolites and tuffs. Image shows a curvilinear magnetic lineament oriented northwest southeast that corresponds with the SMF-1 (Martinez-Piña & Goodell, in progress) and to the Plomosas fault (Oviedo, 2008). At the bottom the trace of the MSM and Chipahuíqui fault. Reactivation of these faults displaced Tertiary rhyolites and tuffs, a topographic change in relief and the northernmost boundary of Sierra Madre Occidental. The irregular shape in blue, aligned with the SMF-1 is a deep basin fill with sediments.



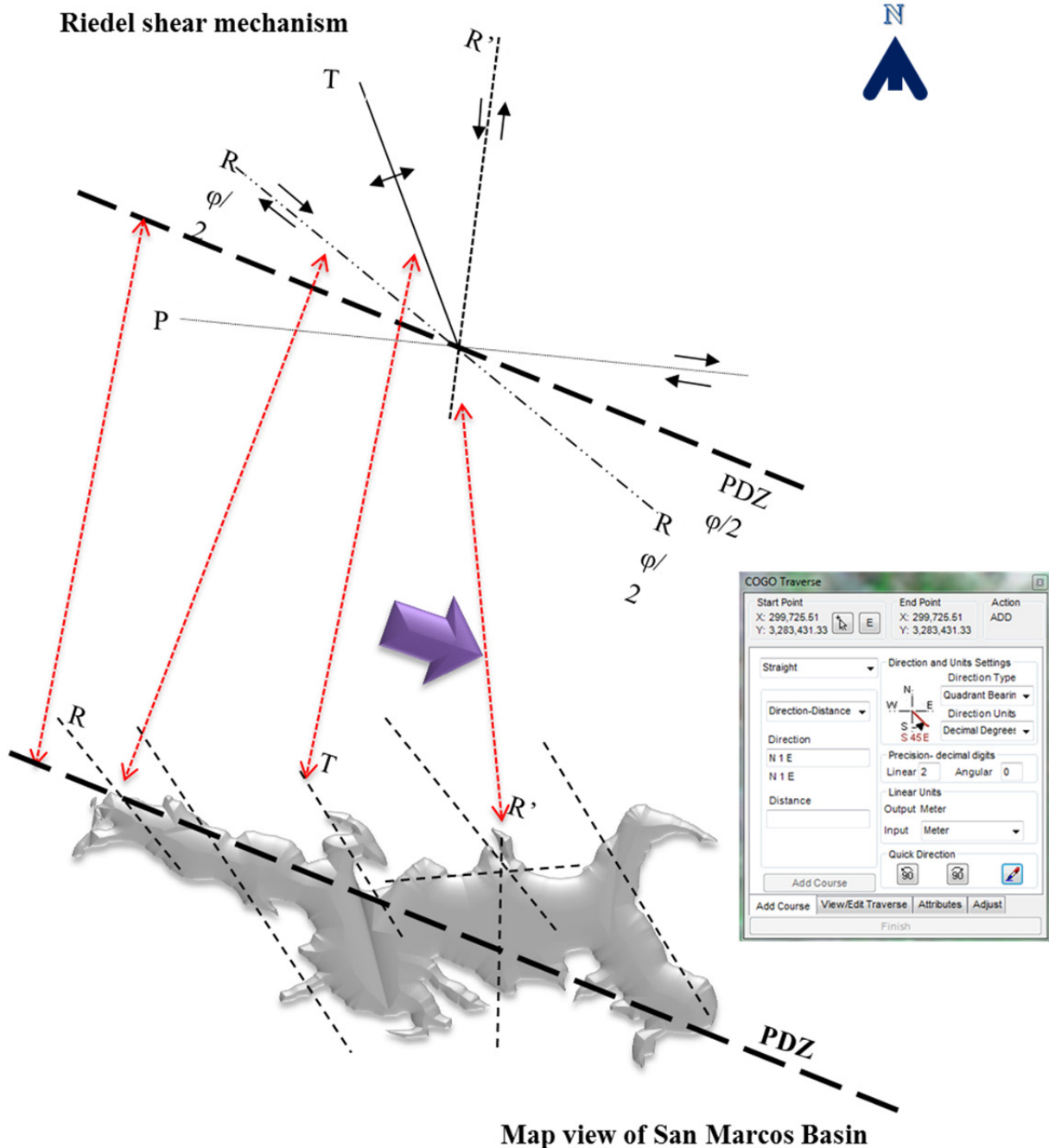


Figure 1.22: Marcos Basin and faults outlined and compared to Riedel shear mechanism diagram. Traces and orientation of lineaments show parallelism (red lines) dashed with the geometry of the Riedel shear mechanism diagram. San Marcos Fault in this area is defined as right-lateral strike-slip fault. ET GeoTools® window shows measured base angle, compared angles are depicted in Table 1.4

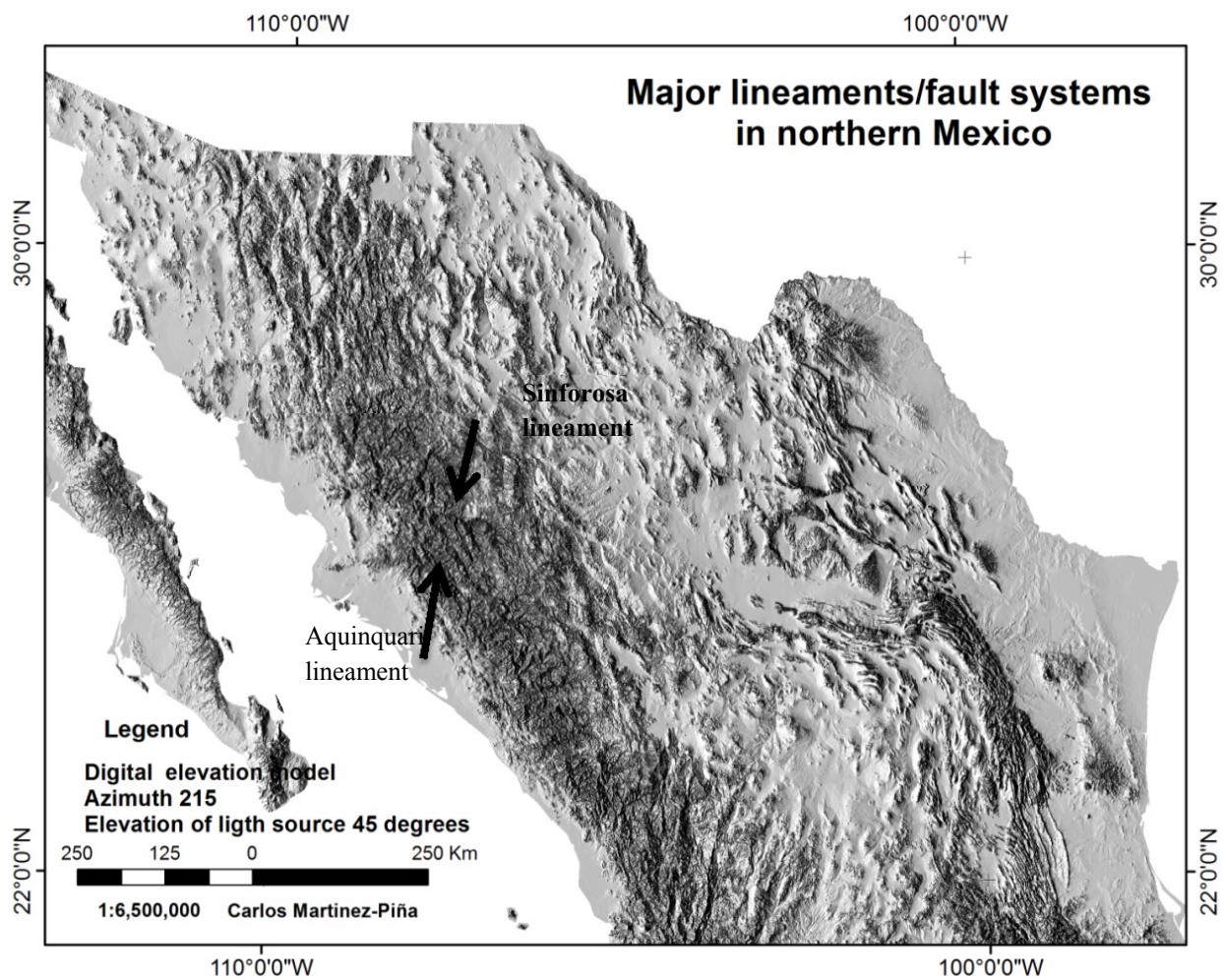


Figure 1.23: Digital elevation model with azimuth 215 and source light elevation of 30 deg, showing the Sinforosa and Aquinquari lineaments. Both crosscut the SMO and are parallel. Aquinquari gives the impression of going all the way across to intersect the Sierra Madre Oriental. Raster resolution: 90 m.

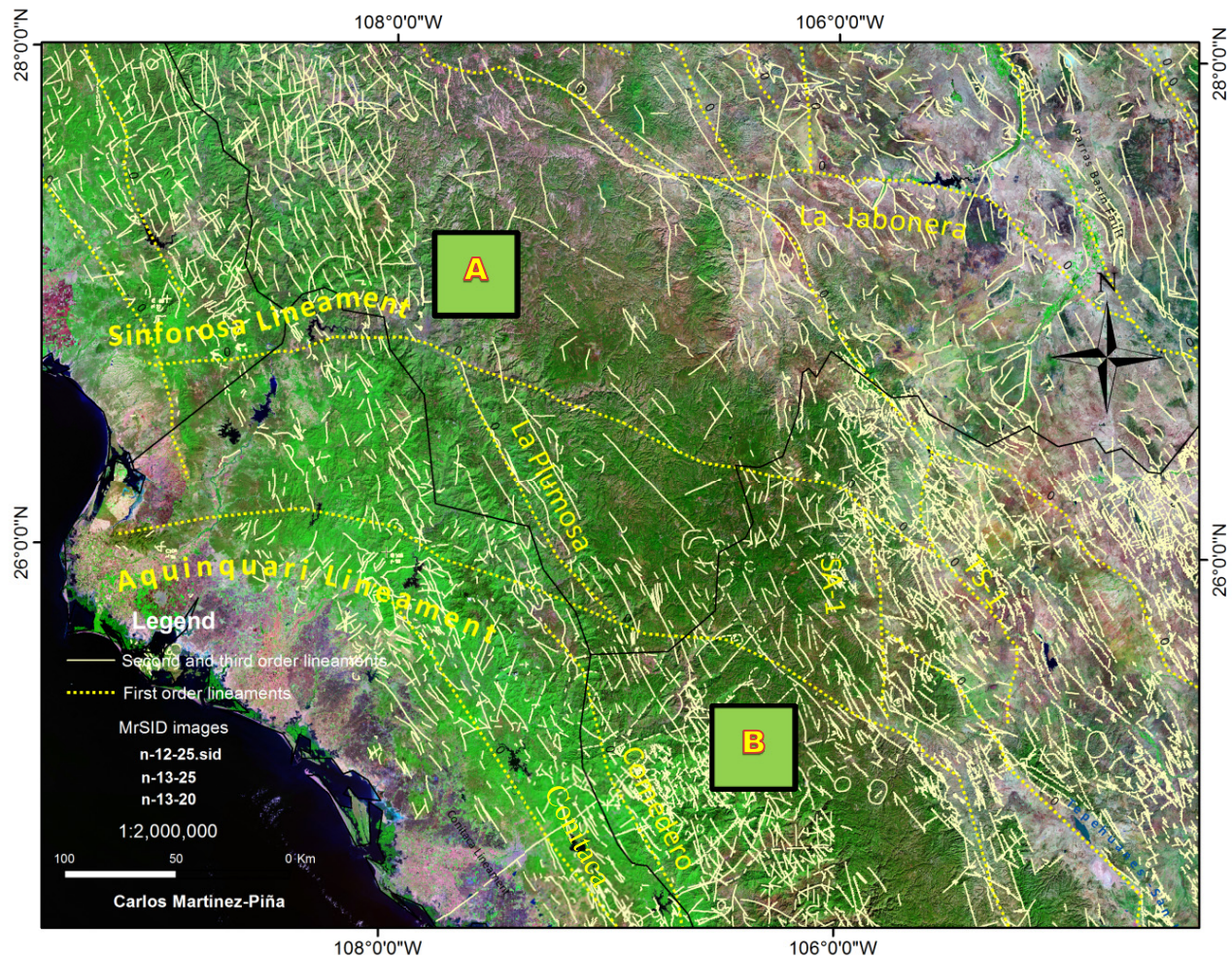


Figure 1.24: MrSID images of southwestern portion of the state of Chihuahua and northeastern portion of Sinaloa, overlaid by a layer of first and third order lineaments trending WNW and NW, respectively. Notice the arc-shape of the two faults and the acute angles formed by second and third order lineaments between Aquinquiri and Sinforosa lineaments in sites A and B. Some NE observed in its southeastern portion. High density extension fractures zones to the south and east of AL. Resolution of raster: 90 m.

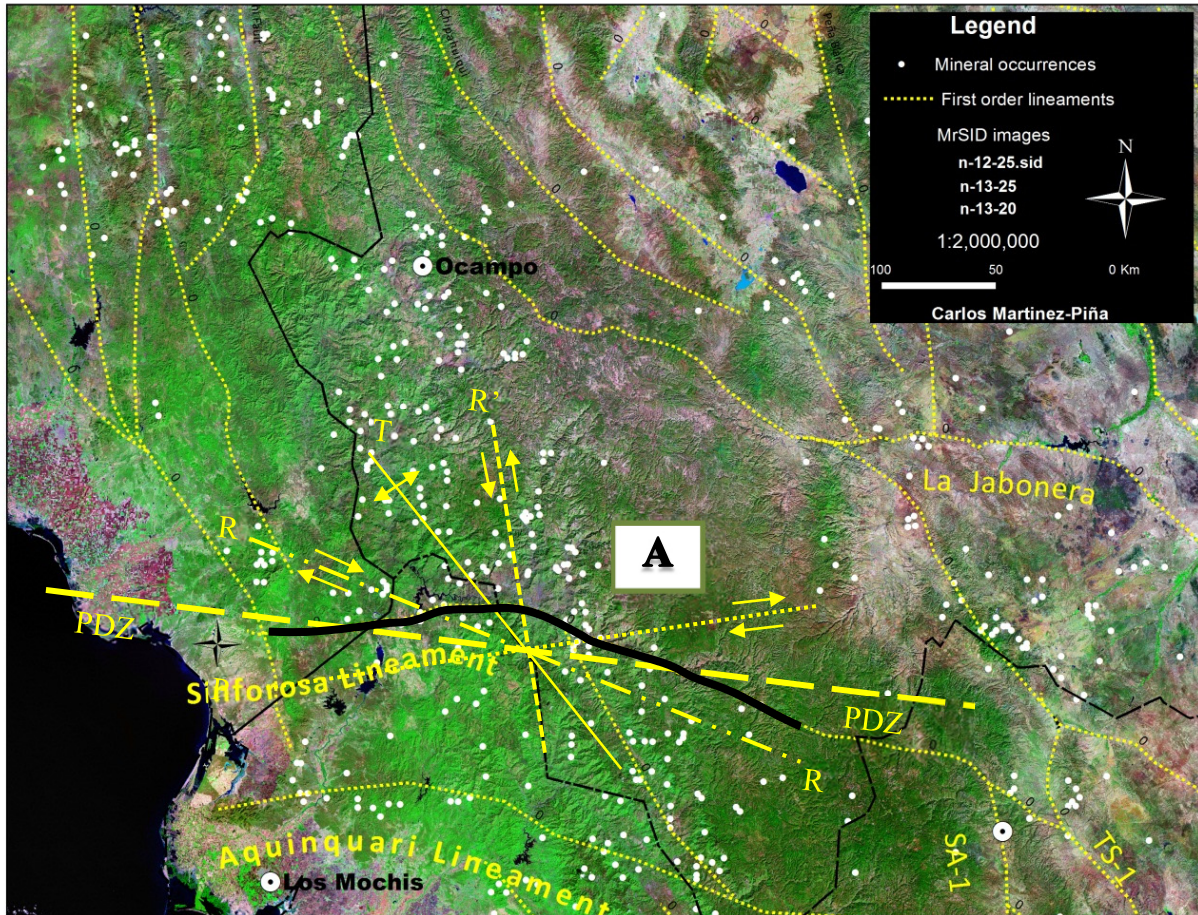
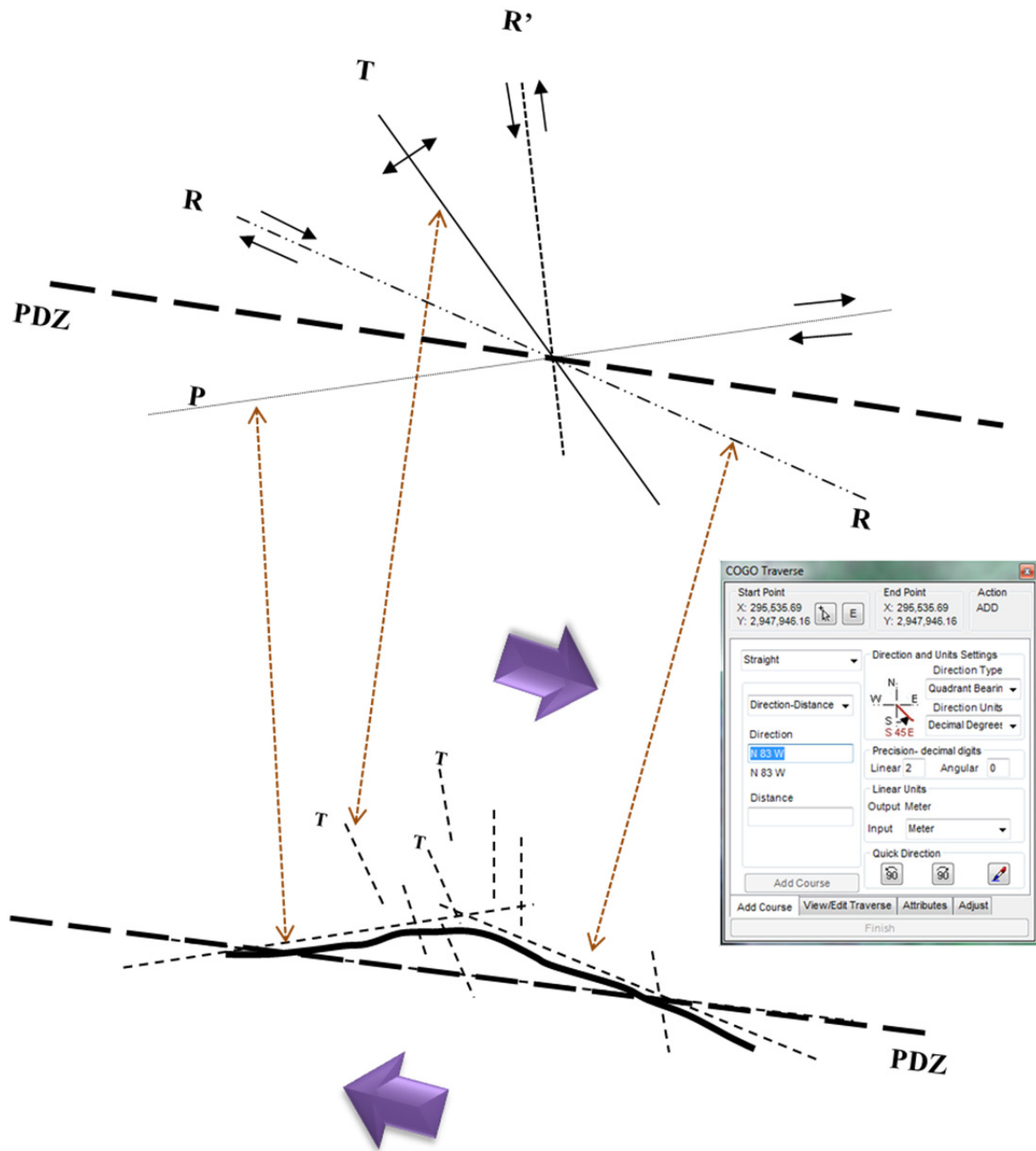


Figure 1.25: Enlarged Image of site A from figure 24, Sinforosa fault. Segments of the Sinforosa fault (black line) compared to the Riedel shear mechanism. P and R synthetic shears shows a high degree of parallelism to these segments of the fault. T shear is also parallel to Plumasas fault (dotted yellow line to the southeast end of T shear). R' antithetic shear also related to mineral occurrences. Resolution of raster: 90 m.



**Map view of Sinforosa Fault**

Figure 1.26: Comparison of geometric elements of the Sinforosa Fault and Riedel shear mechanism diagram in site A from figure 24. Parallelism (red dashed lines) allows the identification of geometric elements from selected site A along the Sinforosa fault (T= tension, R synthetic, R' antithetic, PDZ principal displacement zone). ET GeoTools® window shows measured base angle; compared angles are depicted in Table 1. 5

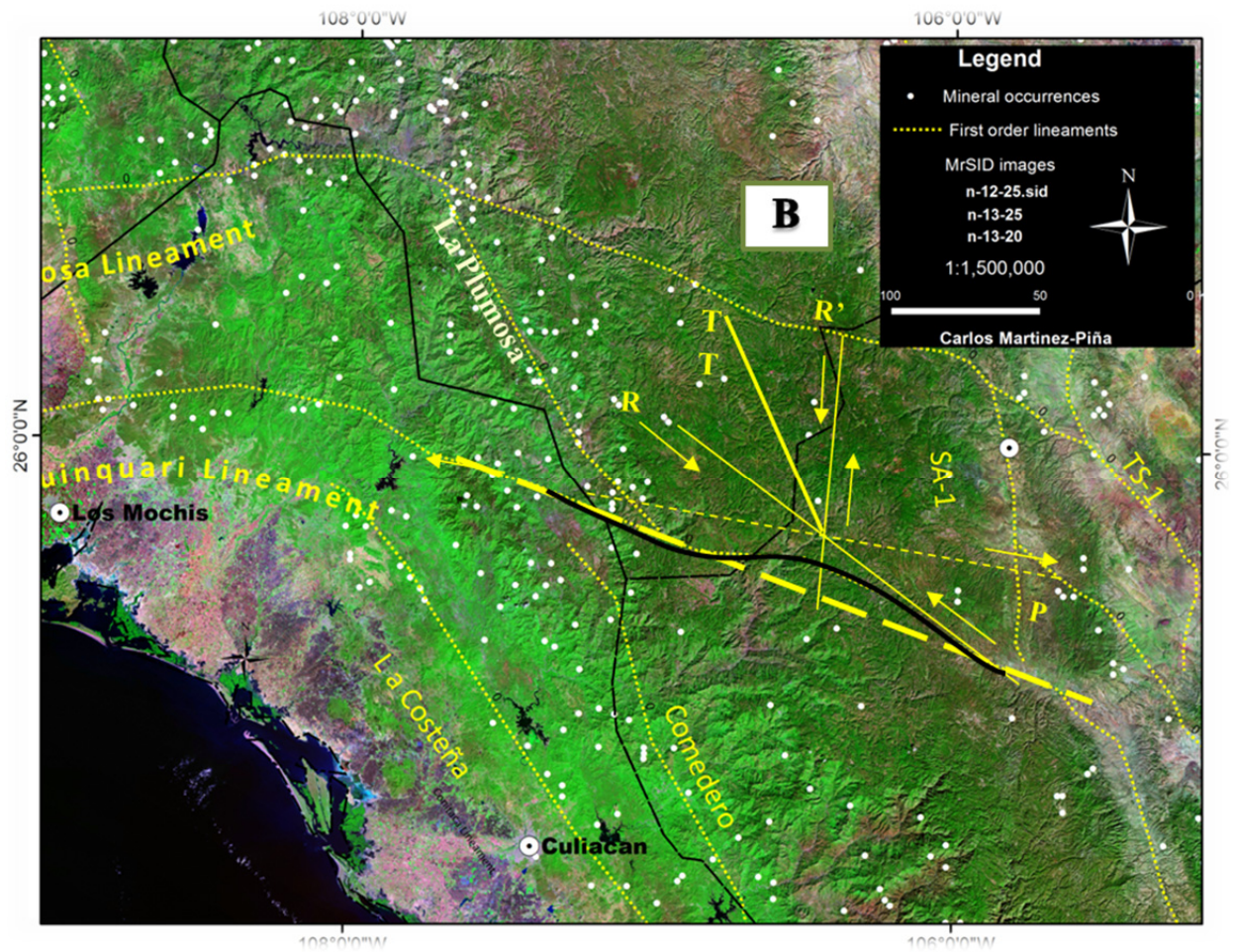


Figure 1.27: Enlarged image of site B from figure 24, Aquinuari fault. Geometry of shear mechanism diagram from Riedel compared to a ~300 km segment of the Aquinuari fault (black line). Tension fault La Plumosa parallel to the tension fault of the diagram and SA-1 parallel to R'. Faults south of the AL (Comedero and Conitaca/La Costeña strike NW and are parallel to the T shear. Mineral occurrences mainly aligned along T and R' faults. Resolution of raster: 90 m.

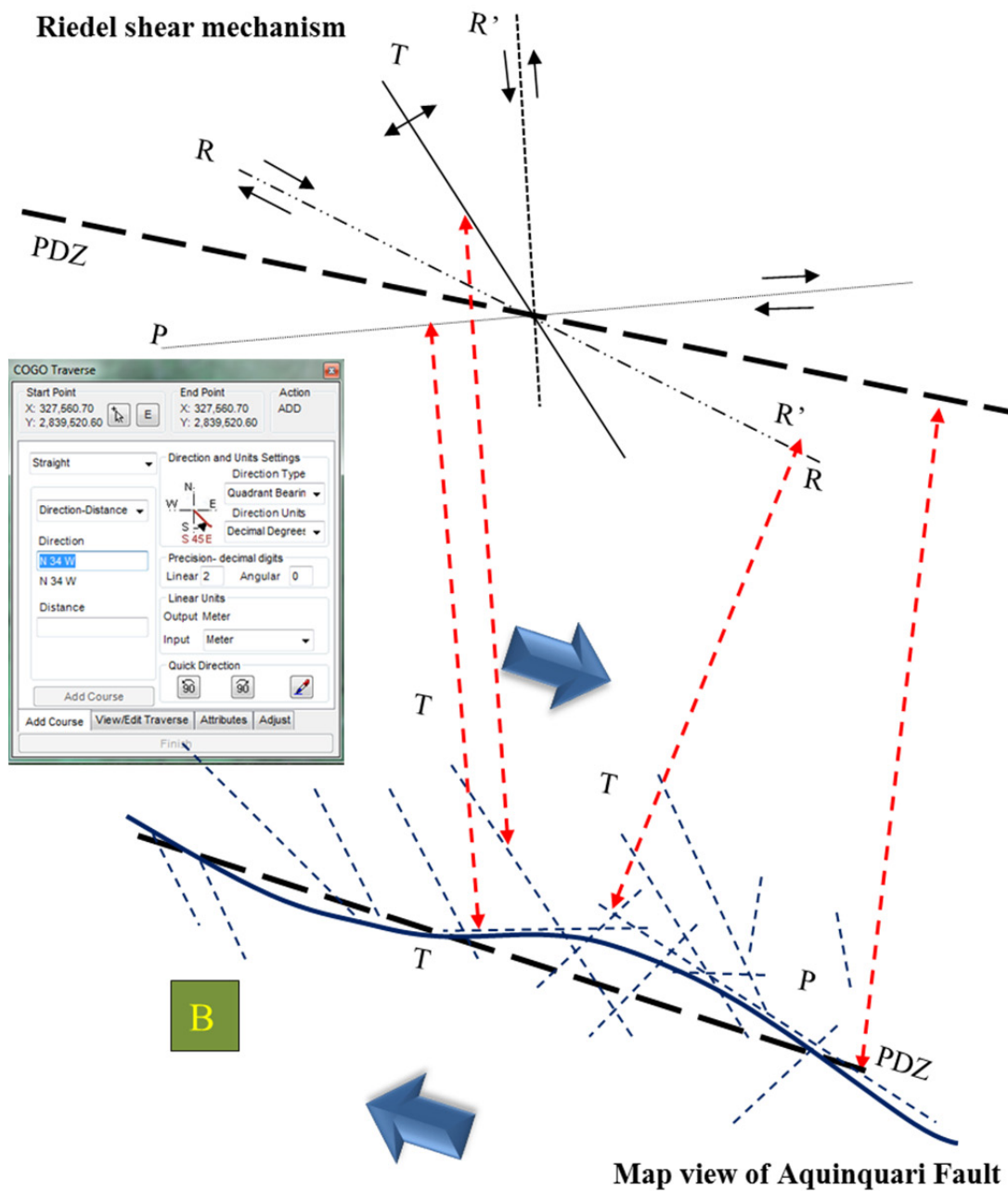


Figure 1.28 Comparison of geometric elements of the Aquinquari Fault and Riedel shear mechanism diagram in site B from figure 24. Parallelism (red dashed lines) allows the identification of geometric elements from selected segment along the fault (T= tension, R synthetic, R' antithetic, PDZ principal displacement zone). ET GeoTools<sup>®</sup> window shows measured base angle; compared angles are depicted in Table 1. 6

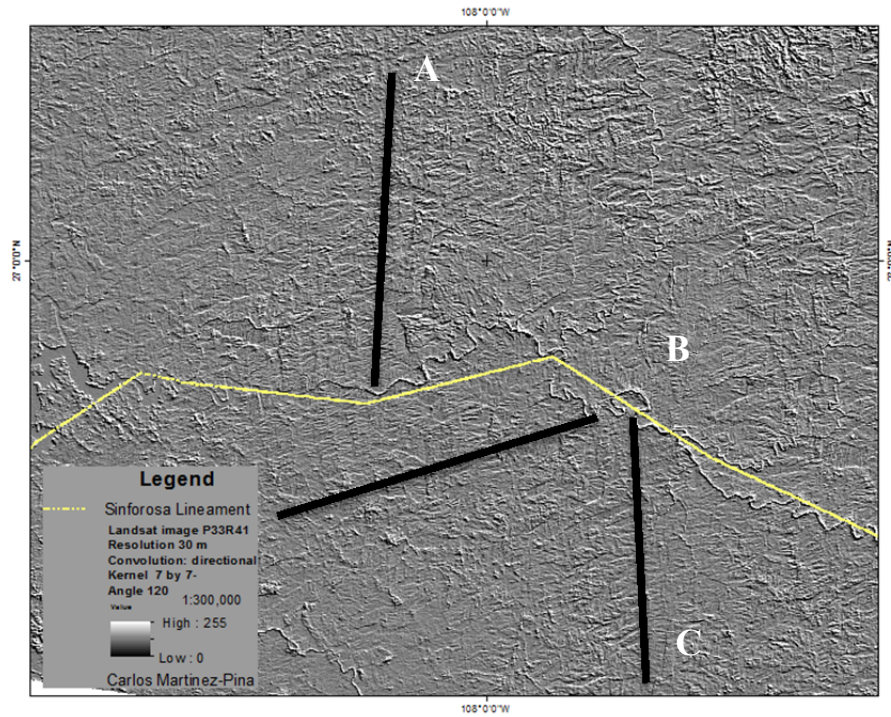


Figure 1.29-1 Directional filter applied to Landsat image P 33 R 41. Site B shows three sets of third order lineaments along the Sinforosa lineament. Res: 90 m.

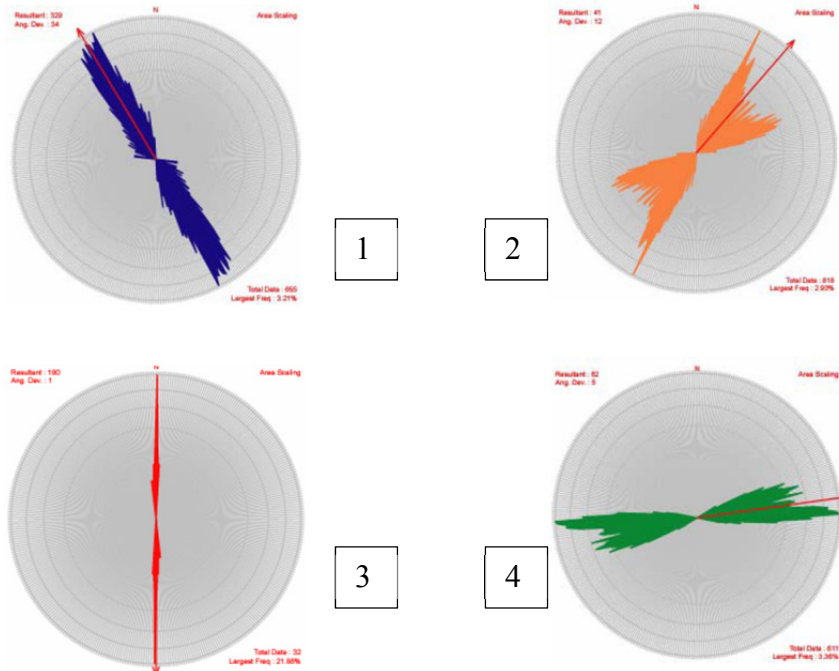
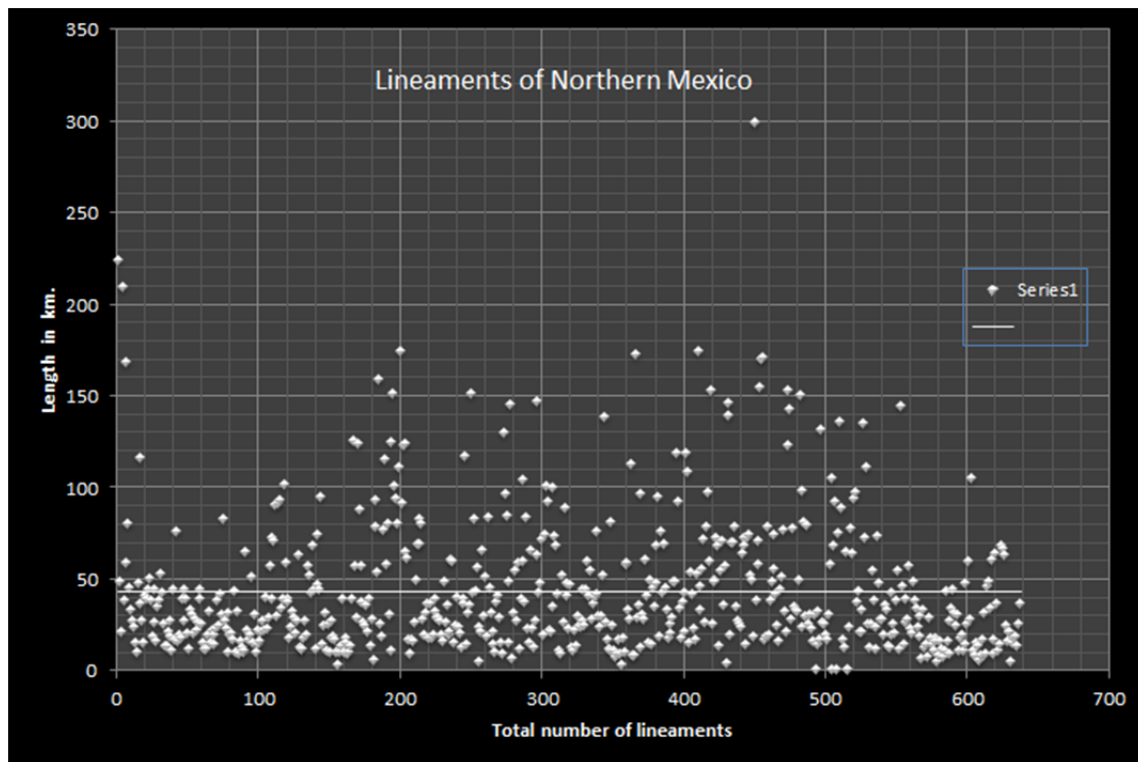


Figure 1.29-2 Four sets of lineaments used by Galvan (2006) for the state of Chihuahua. From the directional filter image set A and C matches set 3; set 1 matches T faults in the shear mechanism of Riedel (not shown), and set B matches 4

**Chart 1.1 Statistical data of 637 lineaments traced in Northern Mexico using data from IMM and ArcMap10™ statistical module**



Length (km) -- %	Range	Category
1. 12.8 -- 10.9	0- 15 km.	3 <sup>rd</sup> Order
2. 24.8-- 25.5%		
3. 36.7 -- 19.7		
4. 48.7 -- 13.6	15- 45 km.	2 <sup>nd</sup> Order
5. 60.7 -- 8.8		
6. 72.6 -- 5.5		
7. 84.6 -- 5.2		
8. 96.6 -- 2.5	100 km.-- over	1 <sup>st</sup> Order
9. 108.5- 1.9		

## **Chapter 2: An IGIS-based characterization of the structural framework of Northern Mexico**

### **2.1 Abstract**

Crustal rupture structures reactivated in the course of the tectonic history of northern Mexico are the surface expressions of planes of weakness, in the form of simple or composite rectilinear features or slightly curved, defined as lineaments. Unless otherwise defined as strike-slip faults, lineaments are part of parallel and sub-parallel oblique convergent or oblique divergent tectonic zones cross cutting the Sierra Madre Occidental and northern Mexico, in a NW trend. These shear zones are the response to the oblique subduction of the Farallon plate beneath North America. The importance of lineaments goes from tectonostratigraphic studies to mineral exploration. There are several maps of Mexico dealing with lineaments, but only the most recent includes motion vectors. A GIS-based compilation and georeferenced regional structural studies by renowned researchers were used as ground control areas (GCA); their interpolation and interpretation, resulted in a tectonic framework map of northern Mexico. In addition, shaded relief models overlaid by the lineaments / fault layer allowed structural analyses of basins related to these major structures. Two important results were obtained from this study: the Tepehuanes-San Luis-fault (TSL) and the Guadalupe fault, named herein, displaces the Villa de Reyes graben, and the Aguascalientes graben, respectively, to the SE, confirming their left lateral vector motion; afterwards TSL was displaced south by the right lateral strike slip Taxco-San Miguel de Allende fault. The second result refers to the hypothesis that the Mesa Central was brought to its present location by a subduction zone located to the north. This subduction zone coincides with several researchers who postulated the idea. The proposed hypothesis, about all NW lineaments are left lateral strike-slip has proven to be false.

## 2.2 Introduction

Six provinces characterize Northern Mexico, according to the physiographic map of the Instituto Nacional de Geografía e Informática: Plains of Sonora, Pacific Coastal Plain, Sierra Madre Occidental, Basin and Range, Sierra Madre Oriental and Mesa Central. Sierra Madre Occidental (SMO) is considered the largest silicic province in North America (Bryan, 2002), but is also one of the least accessible areas of Mexico. Detailed tectonic and geologic knowledge is restricted either by the lack of roads or limited to small accessible areas of interest. Ground mapping is usually constrained to large roads that traverse the rugged topography of the SMO.

Tectonic events that occurred in northern México require macro-scale studies for the understanding and interpretation of the remaining evidence: the lineaments, one of the most common. Since the recognition of lineaments debate has been constant because, while researchers like Richards (2000) argue about their economic importance (especially in the field of mineral exploration), others reject their existence, and for others the use of lineaments is trivial.

Salas (1975), De Cserna (1976), Lopez-Ramos (1979), and Longoria (1994) have addressed at regional level, the important issue of recognition of strike slip faults in northern Mexico. The knowledge acquired from mapping and classifying of lineaments, allows the understanding of their genesis and the role-played in the geological and economic history of the regions. It is impossible to ignore the relationship between metallogenesis and lineaments and tectonostratigraphic terranes and lineaments, because the evolution of one influenced the development of the other. However, as important as these relationships are, they will not be address in this work, but in subsequent studies.

The study of  $\sim 1.4$  million km<sup>2</sup> selected for this study (Fig. 1), which includes eleven states, demanded a strategy to extract the most of integrated geographic information systems (IGIS). To accomplish this, it was necessary to gather all relevant information regarding lineaments, faults, and fault zones, from different locations and put them in a single geographic frame. This procedure allows visual analysis of segments of lineaments, or complete lineaments that have the same geological characteristics. To achieve the objectives of this study, a selection of regional tectonic studies considered as representative of an area, were defined as ground control area (GCA) (Fig. 1). GCAs are study areas or key areas with extensive fieldwork and reliable data carried out by researchers. These key areas are found scattered in northern Mexico, at times, referring to the same structure but at hundreds of kilometers apart. To accomplish this study were needed the results of kinematic analysis of several strike slip basins in northern Mexico by Martinez-Piña and Goodell (in progress). Areas studied by the cited reference are shown in figure 1 A-F. Interpolation of lineaments/faults between GCA used geophysical, geomorphological, and topographic data as far as available. A brief description of each of the selected GCA follows in the next paragraphs, so that together with the description of the tectonics of the area, the corresponding figure number gives its location.

Literature review has shown several issues that this study intent to address. For instance, an undefined southeast connection of northeastern MSM segment; MSM is a fault thoroughly studied in the state of Sonora, but yet unknown in the Sierra Madre Occidental, hence in the state of Chihuahua. A southeast connection without a proposed lineament / fault, require more than a convenient trace (Fig. 2). The speculation about the MSM as the southwestern margin of cratonic North America as a curved line (Fig. 4), has turned more conservative, but still in disagreement (Fig. 2). A parallel pattern of important lineament/faults like the Texas Lineament (Muehlberger,

1980), La Babia (Charleston, 1981); San Marcos Fault (Charleston, 1981) and the Tepehuanes-San Luis fault (Nieto-Samaniego et al, 2005) to the Mojave Sonora Megashear, (Fig. 3). These lineaments reflect from east to west, a poorly known time framework. The significance and importance of an overlooked stratotectonic block in northwestern México: the West Chihuahua Cratonic Block: the West Chihuahua Cratonic Block (Goodell, 1985; Martinez-Piña & Goodell, in progress) (Fig. 5). The role of this tectonic block played in the tectonic setting of northern Mexico has not been considered, much less evaluated (as shown in Figures 6-9).

What to expect from this work? An integrated tectonic framework map based on interpretation and interpolation of tectonic works in northern Mexico that shows structural domains and possible kinematic with the highest possible degree of geographic referencing.

### **2.2.1 Lineaments: definition and classification**

The definition of a lineament by O’Leary *et al*, (1976) as “a mappable, simple, or composite linear feature of a surface, whose parts are aligned in a rectilinear or slightly curvilinear relationship which differs distinctly from the patterns of adjacent features and presumably reflects a subsurface phenomenon”, has evolved with the use of satellite imagery.

Scanvic (1997) emphasizes “lineament” maps as one of the most important inputs for structural analysis and proposes the term “image lineament”. This terminology defines all linear and curvilinear features that have a structural origin in the “absence of precise ground truth reference”. Three subdivisions are proposed: *image lineaments* (linear morphological or radiometric expression without a precise ground reference), *specific tectonic phenomena* (identified totally or partially in existing or new maps), and *composite image lineaments*

(characterized by their association with geochemical, geophysical, metallogenetic etc. anomalies, excluding structural geological structures).

In addition to the classification by Scanvic (1997), there are others that categorize lineaments/faults, considering physical characteristics (length, width), and structural or metallogeny relationships. Because some of the fault names preserve the lineament word in their description, the use of the word lineament in this study includes the above definitions and the indiscriminate use of the term.

### **2.2.2 Background**

As background, a relevant look will be given, to prior studies and use of data which are used for this study and considered as GCAs, starting with some general concepts shown in maps 3 to 8. Work by Campa & Cony (1983) (Fig. 6), shows the tracing of the Mojave-Sonora-Megashear and the relationship between Chihuahua, Coahuila and Guerrero terranes; Sedlock *et al*, (1993) (Fig. 7), defined the tectonostratigraphic terranes by lineaments mainly striking northwest with a different configuration; Centeno-Garcia *et al*, (2008) (Fig. 8) definition of the Oaxaquia, Caborca, Cortes, Central and Guerrero terranes, and a subduction zone and an accretional prism southwest of the Central Terrane; Dickinson and Lawton (2001) (Fig. 9), the California-Coahuila Transform with the same path as the MSM, and a suture zone related to the Guerrero terrane. The lineaments studied by Anderson and Nourse (2005) in a shapefile format are shown in figure 8. The tectonic collage zone proposed by Murray (1989) (Fig. 4), includes eight major faults embedded in a “crustal fracture zone characterized by continuous weakness and deformation since Precambrian” located in northern Mexico (Fig.1). Murray (1989) argues that this geodiscontinuity is a zone of hundreds of kilometers wide, extending from California

to the Gulf of Mexico (~ 2500 km.). Literature review does not show specific studies or follow ups on any of Caltham, Pilger's (1978) unnamed lineament or the Torreon-Monterrey lineament. Use of figures 6 to 9 was to analyze the trace of the MSM and help the criteria of interpolation between CGAs.

#### **2.2.2.1 Mojave-Sonora-Megashear- MSM (Fig. 10)**

Anderson & Silver (1974) postulated the Mojave Sonora Megashear hypothesis (Fig 10) as a major left-lateral strike-slip fault. It is considered one of the largest NW lineaments crossing northern Mexico (Anderson and Silver, 2005; Sedlock, *et al.*, 1993; Dickinson, *et al.*, 2001; Nourse, *et al.*, 2005; Molina, *et al.*, 2005; Iriondo, *et al.*, 2005; Centeno-Garcia, 2005), even when certainty of this only includes the state of Sonora. Anderson and Nourse (2005) contend that the southeasternmost segment of the MSM lays within the zone of tectonic collage (Murray (1989) known as the California-Tamaulipas geodiscontinuity, but such a statement has not been proved. Researchers such as Aranda-Gomez *et al.*, (2005) agrees on the fact that MSM helps the explanation of several events, the most important ones being among the different styles in Laramide folding in the Sierra Madre Oriental of northeastern Mexico. However, such statements will remain partially true, at least until the southeastern extension of the MSM, through the state of Chihuahua is known.

Coney and Campa (1983) (Fig. 6), Sedlock *et al.*, (1993) (Fig. 7), Centeno-Garcia & Silva Romo (1997), Longoria (1984) (Fig. 20), Dickinson (2001) (Fig. 9), Anderson and Nourse (2005) and Centeno-Garcia *et al.*, (2008) (Fig.8) have suggested that the trace of MSM not only extends into the State of Chihuahua but beyond. Five different versions of the MSM compiled in one layer (Fig. 2) shows discrepancies in the interpretation of the data that each author had

available. The layer shows more agreement in the northwestern portion of Mexico (Sonora, Chihuahua, Durango), while (Coney and Campa, 1984; Sedlock *et al.*, 1993; Anderson, and Nourse, 2005; Centeno-Garcia, 2008) showing significant differences in southeastern Mexico (Nuevo León, Coahuila, Tamaulipas). What is noticeable about all MSM traces is that all start more or less at the same point and all end more or less at the same point (Fig. 2). The majority of these fault systems are lower Mesozoic in age (MSM, LB, SM.), but Cenozoic reactivation, which has not been thoroughly address, seems to be a factor overprinting the tectonic history of the lineaments in northern Mexico (MSM, SM). Some studies have inferred from scarce outcrops of rocks of Pre-Oxfordian age found in Central Mexico, the southwestern extension of the MSM, to be one of the bounding faults of the Parras Basin. Attempts to define the southeastern portion of the MSM are not as profuse as those of the northwestern part are.

In any case, Mojave-Sonora-Megashear is a fundamental geologic model in the tectonic reconstruction of Mexico. Alternative models have been proposed by Dickinson and Lawton (2001) and Iriondo *et al.*, (2004), but those also require shear zones and lateral displacement (Ferrari & Valencia-Moreno, 2005).

According to Molina-Garza and Iriondo (2007) the Mojave Sonora Megashear, parallel to several strike-slip faults in northeastern Mexico, such as the Texas Lineament (TL), La Babia (LB), San Marcos (SM), and Tepehuanes- San Luis (TS) may or may not be linked to the MSM hypothesis.

#### **2.2.2.2 Sawmill Canyon (SC) (Fig.11)**

Sawmill Canyon fault zone is located on the borderline between the state of Arizona, USA and the state of Sonora, Mexico. It is the widest and longest fault zone in the Bisbee basin (Busby *et al.*, 2005). Hypothetical changes in plate motions inducing North America northward drift, were responsible for forming the Sawmill Canyon strike-slip basins in the Upper Jurassic arc, causing sinistral deformation of the Paleo-Pacific margin (Busby *et al.*, 2005). This fault zone and steeply dipping faults trending NW were inherited from a Precambrian basement regional lineament and reactivated in Mesozoic and Cenozoic times. Their final conclusion is that northward drift of NA, changed the tectonic style within the arc from dominantly extensional, in Early to Middle Jurassic to sinistral oblique convergent in Late Middle to Late Jurassic.

#### **2.2.2.3 Pitáycachi Fault (PF) (Fig.12)**

Suter and Contreras (2002) stated that the Pitáycachi fault belongs to a macro-scale pattern of roughly normal high angle north south striking faults, associated to half-grabens and located in the southern Basin and Range province, in the state of Sonora (Fig. 11). They estimated that faults and grabens extend for more than 300 km between the San Bernardino basin in the north and the Sahuaripa basin in the south. A series of earthquakes since 1887 until 1931 indicates that this deformation is still active (Sutter and Contreras, 2002, and references). The elongation inferred, from boreholes is horizontal and approximately east west, which is perpendicular to the fault traces in the Basin and Range. The 1887 rupture dips  $\sim 74^\circ$  W and is composed of A) Pitáycachi, B) Teras and C) Otates segments. East-west extension rate is unknown for the Mexican Basin and Range because knowledge base is limited to a few regional

studies of Late Cenozoic (Suter & Contreras, 2002). Throw estimates for the Otates fault is at least 1360 m, for the Teras fault at least 1640 m and over 4000 m for the Pitáycachi. According to Suter & Contreras, (2002) a minor right-lateral strike-slip motion took place during the 1907 second-largest earthquake of this region. The focal mechanism for the 1989 event suggests, “dip-slip with a minor left-lateral strike-slip component” (Sutter and Contreras, 2002, and references within). Age estimated by the above reference based on the age of the basalts flows intercalated with the lowermost fill of nearby basins, is at 23 Ma (Miocene) but they also suggests based on their data, that failure of the western edge of the Sierra Madre Occidental plateau happen in the past, in segment combinations different to the 1887 rupture.

A study area of Rodríguez-Castañeda (1997), south of Cananea and 150 km northeast of Hermosillo, Sonora, is located within the Pitáycachi fault zone. The author speculates about this zone being a heterogeneous deformation style associated to a vertical uplift that occurred from Late Jurassic to Early Cretaceous. The author recognized three events: 1) a vertical faulting of Late Cretaceous age, 2) a thermal uplift, and 3) detachment by faulting during Tertiary.

#### **2.2.2.4 Tepehuanes-San Luis Fault System (TSL) (Figs. 13,14,15)**

Mesa Central (MC) is delimited by three important fault systems (Nieto-Samaniego *et al.*, 2007) (Figs. 8 and 13):

1. El Bajío Fault System
2. Taxco-San Miguel de Allende Fault System and,
3. Tepehuanes-San Luis Fault System

Nieto-Samaniego *et al.*, (2007), describes the Tepehuanes-San Luis fault system as a major NW-SE striking lineament that extends from San Luis de La Paz (SLDP) in the State of

Guanajuato, to Tepehuanes (upper left corner) in the State of Durango. A rough coincidence of the lineament, with the boundary between Cenozoic volcanic rocks and Mesozoic volcanosedimentary sequences, and the northern edge of the N-S grabens is considered by them.

San Luis –Tepehuanes fault system was divided for study into two segments (Nieto-Samaniego *et al.*, 2007):

1. From San Luis de La Paz (SLDP) to Salinas Hidalgo, an eastern segment constitutes the boundary between southern and northern regions of the MC. This system comprises NW-SE trending normal faults dipping to the SW. Faults form grabens cut early Oligocene rocks.
2. From San Luis de La Paz (SLDP) to Tepehuanes a western segment extends. This segment comprises Cenozoic normal faults striking N30-60W dipping NE .
3. The Tepehuanes-San Luis fault system in the Durango region consists of NNW normal faults, and grabens. It was estimated by Nieto-Samaniego *et al.*, (2007) that Tepehuanes-San Luis fault system is ~600 km. long and considered by Loza-Aguirre *et al.*, (2008) as the boundary between the geomorphic provinces of the SMO and the Mesa Central.

At least 13 fault systems were studied by Loza-Aguirre *et al.*, (2008) out of which, five consists of faults trending N60-80W and three cut Mesozoic basement. Only one NE system, near Cd. Cuauhtemoc Zacatecas, cuts the basement. All fault systems are consider to be normal and to have vertical displacements up to 250 m. Even though they do not consider any possibilities of sinistral lateral movement for the study area, in one digital elevation model shown in Loza-Aguirre *et al.*, (2008, p. 535), it is mentioned the Aguascalientes Graben (GA) as being displaced at least 15 km to the NW by the Tepehuanes-San Luis fault system, this would be consistent with a strike-slip left lateral motion (Fig. 14).

Megaw (2010) states that the “Fresnillo silver trend is underlain by a regional traceable northwest-trending sinistral shear zone that is locally cut by younger northeast-southwest faults”.

#### **2.2.2.5 El Bajío Fault (BF) (Fig. 13,15)**

According to Nieto-Samaniego *et al.*, (1999) and Alanis-Alvarez and Nieto-Samaniego (2005) (Fig. 13), El Bajío fault constitutes the southern edge of Mesa Central as a dominantly normal fault. Consists of two segments, an eastern striking east, shows an offset of ~700 m west of Celaya. The western half strikes N50°W and bounds Mesozoic basement and Paleogene plutons. The cumulative offset of the fault reaches ~ 2850 m. El Bajío intersects the north trending Penjamillo graben where it vanishes. The southern boundary of the Mesa Central is not well defined because most of the area is covered by late Tertiary sediments and by extensive late Miocene basalts.

Xu *et al.*, (2008) (Fig.15) concludes from his work in the Mesa Central, that fault block rotation took place as the fault slip increased. According to Alanis-Alvarez and Nieto-Samaniego (2005), El Bajío fault (BF) is a normal fault with its down-thrown block to the north (Mesa Central) and the up-thrown block to the south (Mexican Trans-Volcanic Belt) (Fig.15). Also represents the frontier between the Oligocene silicic volcanism, and the Miocene-Recent mafic volcanism and characterizes a topographic low from San Francisco del Rincon to Queretaro City. The strike of the fault is N45°W changing to E-W in its southeasternmost portion.

#### **2.2.2.6 Taxco-San Miguel de Allende fault systems (TSMAFS) (Fig. 13, 15)**

According to Nieto-Samaniego *et al.*, (1997) and Alanis-Alvarez and Nieto-Samaniego (2005), the Taxco-San Miguel de Allende fault system (TSMAFS), constitutes the western

boundary of the Mesa Central. This fault system had a right lateral fault system during Miocene. The fault trace after being interrupted in the Sierra del Cubo, appears at the Villa de Reyes graben as a northern extension. Alanis-Alvarez and Nieto-Samaniego (2005), also considers the TSMAFS as a line of separation between two crustal blocks with different geological characteristics, topography and crustal thickness. The trace of this fault system is located along the transition zone between a continental platform and a deeper one. This discontinuity explains the persistence of faults striking NNW, and other systems with different orientations; the gravimetric anomaly observed on both sides of the TSMAFS, and the widening of the fault zone between San Miguel de Allende and Queretaro, among others (Fig.15)

#### **2.2.2.7 Texas lineament/fault (TL) (Fig. 16)**

Muehlberger (1980) characterized the TL (Figs.8 and 16) as a separation zone of recurrent movement between the more stable crust to the north, and a less stable to the south. This major discontinuity trending N60W separates the Diablo Platform (DP) from the Chihuahua Trough (Cht). Haenggi (2002) includes, within this broad separation zone the Marfa Basin and considers, that the southern limit along La Babia zone includes the northeastern projection. Haenggi (2002) also suggests a pre-Wolfcampian left-lateral-regime for the Texas Lineament and La Babia, based on interpretation of subsurface data and reversal movement of east-trending faults. Beck and Chapin (cited by Haenggi, 2002) interpret a left-lateral late Paleozoic wrench zone that embraces the Oro-Grande and Lucero basins in New Mexico, and is considered by Haenggi (2002) a strong support for the existence of wide spread left-lateral regimes. Hills (cited by Haenggi, 2002), suggests left-lateral movement along a deep-seated zone along the Pecos Valley fault (trending N60W), and relates it to the Babb and Victorio flexures. Extensive work by Wood (1981) also shows existence of left lateral strike slip faults along the TL zone.

Anderson & Nourse (2005) also indicate that maps from the Diablo Plateau (east of the Rio Grande) shows three sets of faults: 1) NW-trending, left-lateral strike slip 2) NE-trending, right lateral and 3) E-trending normal slip, cutting Precambrian and Paleozoic rocks. The coincidence in orientation and sense displacement between these sets of faults and those of the Mojave-Sonora system is pointed out by Anderson & Nourse (2005). According to Haenggi (2002) the Marfa Basin (north of Persidio, TX) is within the broad zone of The Texas Lineament.

#### **2.2.2.8 La Babia (LBF) and San Marcos (SMF) Faults (Fig. 17)**

McKee and Jones (1979) described two structures located in the northern part of the state of Coahuila; these intersect the Coahuila Block and are defined as left-lateral strike-slip faults striking NW (McKee & Jones, 1979; Charleston, 1981; McKee & Jones, 1984; McKee, Jones, & Anderson, 1999). Charleston (1981) named the fault to the north of the block, La Babia Fault (LBF). La Babia Fault (Fig. 8 and 17) is a large lineament located in the states of Nuevo León and Coahuila (Charleston, 1981; McKee, 1990; Goldhammer, 1999; Aranda- Gomez., 2005; Chavez-Cabello, 2005, Gonzalez, 2008). The fault to the south (parallel to LBF also named by Charleston), the San Marcos Fault (SMF) is considered a transcurrent fault. Charleston (1981) argues that the Coahuila Folded Belt formed by northwest-southeast shearing between the Coahuila-Texas Craton (CTC) and the Coahuila Platform (CP). Charleston (1981) also considers that a southwest-northeast compression produced a mechanism that accounts for the LBF and SMF left-lateral wrench condition. Although Charleston (1981) did not set the age of the faulting, he related the Sierra de San Marcos to the Upper Jurassic paleogeography of the Tamaulipas Peninsula.

According to Anderson & Nourse (2005), the segments northwest and west-northwest of the SMF, delimit ~280 km the Coahuila platform, and the gentle westward curve of the SMF, north of the Coahuila Block, may be accounted for the releasing bends and pull-apart basins observed. Aranda-Gómez *et al.*, (2005), considered that San Marcos fault, La Babia fault and the Mojave-Sonora-Megashear constitute a system of left lateral mega-faults that help explain the distribution of Precambrian and Paleozoic rocks, the stratigraphy of Jurassic -Lower Cretaceous rocks in Chihuahua and Coahuila, and changes in styles of Laramide folding in the Sierra Madre Oriental in northeastern Mexico. This mega-fault system was active during late Jurassic and early Cretaceous time and some authors relate it to the opening of the Gulf of Mexico (Aranda-Gómez *et al.*, 2005; Flotte *et al.* 2008).

San Marcos Fault activity started before Tithonian, and reactivation of these fault system occurred during the early Tertiary Laramide Orogeny (Chávez-Cabello *et al.*, 2005). These authors also considered SMF to be a regional structural lineament with over 300 km long, striking WNW and dipping NNE. The SMF is a multi-reactivated basement structure that on the surface shows stratigraphic and structural evidences of intermittent activity from Late Jurassic to Pliocene-Quaternary. Four reactivation events have been identified by Chávez-Cabello *et al.*, (2005): first reactivation event with a normal component during Neocomian. Second reactivation event involved a reverse slip component during Paleogene. Third reactivation event is normal to a left-lateral component during Late Miocene-Early Pliocene. Fourth reactivation event is dominantly normal, during Pliocene- Quaternary. Molina-Garza *et al.*, (2008) suggests that the last manifestation of shortening produced by Laramide orogenesis is the San Marcos fault reactivation. During this period, several different structural patterns developed that are consistently parallel and perpendicular to the axis of the SMO.

#### **2.2.2.9 Juarez (JF), Almagre (AF), and El Caballo (CF) faults (Fig. 18)**

Unpublished reports of Petroleos Mexicanos (PEMEX) by de Antuñano (1984) define three fault systems were reported on the northeastern part of Mexico striking NNW. El Caballo and Juarez faults are considered as left-lateral strike-slip, while the Almagre system, in the middle, is consider a right-lateral strike-slip. De Antuñano (1984) argues that these systems modified Jurassic basement, since El Caballo and Almagre exposed permo-triassic rocks in Sierra del Carmen, La Mula, and Acatita, in the state of Coahuila and in San Julian in Zacatecas. Cenozoic granites and diorites lined up along the borders of the fault El Caballo or inside its weak zone, and granodiorite intrusives aligned along the fault El Almagre , are reported by de Antuñano (1984).

A 10 km. left lateral strike-slip displacement is reported between pre-existing Laramide structures Sierras El Caballo and Cañada Oscura; and 5 to 8 km right-lateral strike-slip displacement is for the Almagre system (in figure 15 appears as a left-lateral displacement). Bouguer anomalies studied by de Antuñano (1984) “shows a minimum persistent alignment that coincides with the location and trend of this megafault” referring to the Juarez fault system. Inferred by the author, origin of these systems is deep within the crust; also, the author infers that these faults were reactivated during Late Oligocene or early Miocene.

I should be recognized that this is proprietary data, which only one author has been given access, whereas other researcher has spent years in the field studying this area. No independent verification of all his results. Certain segments of his results can be substantiated.

#### **2.2.2.10 Rio Bravo fault (RBF) (Fig.19)**

Rifting of the Gulf of Mexico during early Jurassic was favorable to the development of the Chihuahua Trough and the Sabinas Basin (Muehlberger, 1980; Haenggi, 2002; Flotte, 2008; others). Movement of South America away from North America probably reflected extensional and transtensional processes during Mesozoic era. Flotté *et al.*, (2008) studied what they called the Rio Bravo Fault Zone (RBF). This zone trends SE-NW and links the Burgos Basin (boundary between USA, Mexico and the Gulf of Mexico coastline) and the Trans-Pecos area (Ojinaga, Chih,-Presidio, Texas) (Fig. 16). The northern boundary of the RGFZ coincides with the La Babia Fault and the southern with the San Marcos Fault. Flotté *et al.*, (2008) argued that this is an inherited fault zone from the Jurassic opening of the Gulf of Mexico. The authors also stated that tight folding of the Upper Cretaceous before 30 Ma, is associated with a major left-lateral fault, and that sigmoidal fabric of the Chihuahua fold belt (structures swinging from N-S to NNE, NNW and locally to NW) has controlled the northern trace of the Rio Bravo. A 55-50 km NW displacement of the NE trending Oligocene Vicksburg-Frio depocenter of Burgos Basin, was determined by Flotte *et al.*, (2008), using gravimetric maps, surficial mapping, and microtectonic observations.

#### **2.2.2.11 Strike slip faults in the Mesozoic cover (Fig.20)**

The analysis by Longoria (1994) of Landsat and SIR-A imagery of Mexico resulted in a morphotectonic map of the Mesozoic cover (Fig. 20). Longoria, (1994) finds that a lack of information is partly liable for strike-slip faults being difficult to identify in the field, and commonly mapped as normal, reverse or thrust faults. Another reason is the Quaternary deposits concealing the faults, which impedes surface exposure.

Longoria (1994) postulates 34 strike-slip faults for all of Mexico, and suggests basement faults to be the cause of Mexico's Mesozoic cover deformation. Four main structural domains of fault sets define this structural system, according to the cited reference: 1) West-northwest (left lateral, average N60W) set; this fault set developed in late Triassic and formed by plate interaction and subduction of the Kula-Farallon plate underneath North American plate. 2) North-northwest (left lateral, average N40W) set; this set of faults developed during the late Jurassic-early Cretaceous subduction/spreading phases. 3) North-northeast (right lateral, average N51E) set; this set of faults resulted from an early Cretaceous diastrophic event, and 4) West (left lateral, N85W) set; this fault set relates to a more recent tectonic reactivation of the basement; their strike reflects a relation to oblique subduction of the Cocos plate. Longoria (1994) identifies three tectonic regimes affecting the sedimentary cover of Mexico: transpressional tectonics, compressional tectonics and, transtensional tectonics. The author concludes that the Mesozoic paleogeography of Mexico was ruled by four events: 1) oblique subduction along western margin of Pangea. 2) changes in the direction of convergence of the Farallon and the North America Plates 3) drifting phase accompanying the separation of South America from North America and, 4) sea floor spreading in the Gulf of Mexico and the migration of Yucatan. Longoria, (1994) finds that NW to WNW are left-lateral strike-slip faults cutting Jurassic basement or older, and that NNE faults are right lateral-strike-slip faults cutting Cretaceous basement, also that W faults are left lateral strike-slip faults due to reactivation events.

#### **2.2.2.12 West Chihuahua Cratonic Block (WCCB) (Figs. 21a and 21b)**

Martinez-Piña and Goodell (in progress) proposes the concept of the “stable block/mobile belt” model to northern Mexico and the southwestern US, in order to better

understand and define the North American craton and its history. The location and geologic history of the southwestern boundary of the North American craton is a subject of considerable controversy and interest. The Bouguer gravity map and residual gravity map of northern Chihuahua and adjacent regions is given in Figures 21a and 21b. Martinez and Goodell (in progress) defined the gravity characteristics which help define the WCCB 1) large negative values (-200 milligals), 2) uniformity (smoothness) of values, 3) contrast with adjacent regions. The -190 milligal contour was chosen to define by gravity the boundary of the WCCB. Conclusions reached by Martinez-Piña and Goodell (in progress) is that cratonic blocks have “a significantly greater long term stability than adjacent areas and can be identified within Precambrian provinces” and that a “new such block is identified here located in western Chihuahua, the WCCB.”

### **2.2.3 Study area**

Study area (Fig. 1) includes eleventh states of northern Mexico covering approximately 1.4 million Km<sup>2</sup>. The limits of the area are the international borderline between the USA and Mexico to the north, and the Mexican Trans Volcanic Belt to the south. The area includes the domain of major lineament/fault systems and the states of Sonora, Chihuahua, Coahuila, Nuevo Leon, Sinaloa, Nayarit, Durango, Zacatecas, San Luis Potosi, Aguascalientes, and Jalisco.

### **2.2.4 Statement of the Problem**

Definition of the vector motion of major faults in northern Mexico has been partially done. There are two hypotheses that try to define the vector motion of major faults: by the age of the basement they cut, and/or by changes in orientation that goes from slight within a NE quadrant to radical, from a NW quadrant to a NE one. One of the hypotheses generates from studying a mid-

size area (northern Sonora) and formulates a proposal for distinguishing Jurassic structures from Cretaceous, based on the age of the fault and its orientation, despite reactivation. The other one has a regional coverage; however, the lack of georeferencing does not allow the certainty of their location, or that of its vector motion. Definition of the vector motion of a fault using stratigraphic models can be achieved at certain regional levels, but not always. None of these hypotheses is linked to topographic maps, digital elevation models, satellite imagery, or geographic information systems.

### **2.2.5 Hypothesis**

Development of multilayer data, synthesis and interpretation, may lead to proper definition of the vector motion of faults, and the interrelation between multiple fault families.

Construction of layers from different data sets, including the georeferencing of GCAs, will provide elements and a wider scope for interpretation and association of fault families and definition of their motion.

## **2.3 Methodology**

The present study is based totally on integrated geographic information systems which included remote sensing. Integrated Geographic Information Systems (IGIS) is a term used to define systems, which can process remotely sensed imagery as well as raster and vector data sets in a consistent fashion (Estes and Star, 1993). The major advantage to integration of GIS and RS is their synergy: GIS has information extraction potential, whereas RS has the ability to provide and update spatial data/information (Estes and Star, 1993). Three phases constitutes the first branch of this methodology presented in chart 1. Phase I refers to acquisition and preparation of GIS and RS data. Phase II constitutes the interpretation and production of maps and the

processing of images and the integration of GIS and RS products. Phase III consists of IGIS maps characterized by overlaying draping and merging of thematic maps. Level 1 and level 2 areas will be studied by GIS and RS using ArcMap10® and ENVI® 4.5 software. Complimentary software: Illustrator®, Photoshop®, and Photoimpact®

#### Phase 1 (GIS and RS)

This phase involved acquisition, preparation, and conversion of GIS and RS data. All data complies with WGS84, UTM zone 13 coordinate system (1). Data was georeferenced whether paper or digital, scanned maps or maps in PDF format, digital or paper topographic maps, or data in ASCII e00 format. Data processes to create vector and image-maps from GIS and RS took place under this phase. Operations performed for the GIS portion, are vector maps produced from field data or digitized from scanned maps, slope analysis, directional filter, interpolation maps, clipping, and georeferencing of vector data. Shaded relief maps also constructed under this phase.

- (1 ) Coordinate System: WGS 1984 UTM Zone 13N
  - Projection: Transverse Mercator
  - Datum: WGS 1984
  - False Easting: 500,000.0000
  - False Northing: 0.0000
  - Central Meridian: -105.0000
  - Scale Factor: 0.9996
  - Latitude Of Origin: 0.0000
  - Units: Meter

#### Phase 2 (IGIS)

Data processes and creation of vector and image-maps from GIS and RS took place under this phase. In Phase II of IGIS, each of the images selected after georeferencing and place in their geographic context went under consideration as a ground control area (GCA). Subsequently from the GCA decision, all features of interest were digitized creating a shapefile for overlaying

it to a series of shapefiles and raster images. Shaded relief raster map based on ASCII format data, SRTM raster map (Shuttle Radar Topographic Mission) with elevation data, MrSID set of satellite images and the structural shapefile-map created using data from the Servicio Geológico Mexicano were the basis for the connection of the linear features between GCAs. Some of the geomorphic criteria used to trace the lineament connections between GCAs, are abrupt linear relief, linear drainage, anomalous linear vegetation cover, linear alignment of valleys, abrupt linear termination of structural features. Each one of these criteria was weighted against the available map data.

### Phase 3 (GIS and RS)

Phase 3 refers to the final stage in map production. Preliminary GIS, RS and IGIS maps evaluation for accuracy will be undertaken. However, georeferencing scanned, maps were more often than not, less accurate. GPS location of mineral occurrences and points of interest added or modified. Final vector IGIS maps were stored in an inventory.

### Specific Processes

Construction of several digital elevation models (DEM) at different azimuths and elevation of the light source (azimuth at  $245^{\circ}$ , and light source at  $30^{\circ}$  from the NW and azimuth at  $215^{\circ}$  and light source at  $45^{\circ}$ , both from the NE) allowed an improvement of the image and the tracing of lineaments. Manipulation of azimuths, and elevations of source light used for the construction of the DEMs, enhanced the raster- image array of tones. Visual comparison between DEMs raster-images (Fig. 22), revealed a west-east striking lineament.

## 2.4 Results

Final map of northern Mexico depicts: 26 new named, 24 new unnamed, 10 known named and 19 known but unnamed for a total of 79 lineaments/faults of first, second and third order (Fig. 23). Lineaments in red were obtained from other sources. Description of the major faults and their characterization is shown in Table 1.

The tectonic framework of northern Mexico (Fig.24) can be described as follows:

- 1) Three major parallel shear stress systems (1-NW, 2NW and 3NW) striking NW and left lateral motion
- 2) Shear stress system 2-NW and 3-NW connected (?) in its northern portion at the Plomosas area by a shear stress system S-1 (green line) striking NNW and right lateral motion,; in the southern portion S-1 connects (?) with shear stress system 1-NW
- 3) Shear stress system S-1a (red dotted lines) connected (?) to W-1, by faults TS-1 and SA-1.
- 4) Shear stress systems E-1 and E-2 disrupts systems 1-NW and S-1a, respectively.
- 5) The main shear stress systems 1-NW and 3-NW are oblique contraction (Marrett and Peacock, 1999) or high strength shear zones, while shear system 2-NW and S-1 are considered as oblique extension (Marrett and Peacock, 1999), or low strength shear zones (ten Brink, 1996).
- 6) Shear stress system 2-NW and S-1 connect in an area where a pop-up ridge is formed (Oviedo *et al.*, 2008) (Fig. 30). Shear stress systems W-1 and S-1a, may be connected by faults TS-1 or SA-1, where a pop-up ridge is formed (Fig. 30) .

- 7) Shear systems E-1 and E-2 are extensional systems (grey dotted lines) located one in the state of Sonora (E-1), and the other in the state of Jalisco (E-2), this one related to the rifting of the Jalisco Block (Fig. 24).
- 8) Distance between main shear system 1-NW and 2-NW is 190 km while distance between 2 NW and 3 NW is 186 km. Distance between Sinforosa and Aquinquiri faults is  $\pm 80$  km. Length of lineament/faults are depicted in Table 1.

#### **2.4.1 Categorization of lineaments / faults**

Ten Brink *et al*, 1996 states that shear zone width is directly proportional to pull-apart elongation and inversely proportional to deformation near the tips of the fault. In addition to ten Brink *et al*, (1996), Atmaoui, *et al*, (2008) also argues that faults with wide shear zones are labeled as weak faults or low strength shear zones. Their explanation is that these faults hypothetically formed where upper crust detaches from the lower crust, especially near plate boundaries. This wide shear zone, by moving in all directions including vertical, tends to adjust itself (ten Brink *et al*, 1996). On the other hand, narrow shear zones or strong faults are structures hypothetically formed when pre-existing displacements or ruptures, located at the base of the upper crust, constitute a narrow fault zone that continues towards the lower crust (ten Brink *et al*, 1996). Scale models with analogue materials of similar shear strength and varying thickness values, showed length and continuity of lineaments /faults and scarcity of synthetic fractures (Atmaoui, *et al*, 2008). A model with opposite parameters showed shorter lineaments and more synthetic fractures.

Ten Brink *et al*, (1996) and Keary *et al*, (2009) point out the importance of the relationship of the basin-wide thickness of the layer (s), that is, the effect that the width of the shear zone has on the amount of rotation around the horizontal and vertical axis, and the surficial

extent and amplitude of the vertical and horizontal deformation. The effect of a shear zone developed at the base of the upper crust also has a strong effect of vertical contrasts in the upper crust rheology (Keary et al, 2009). Distribution of deformation along such faults occurs when uplift and subsidence distribute along the fault, beyond the fault tips; basins along the structure are, with increasing width of the shear zone, more elongated.

#### **2.4.2 Weak faults or low-strength shear zone in an oblique extension system**

(Parras Basin, Parras Basin 1, and Parras Basin 2 faults)

The width of the shear zones in weak faults has a significant effect on the amplitude of the horizontal and vertical deformation and its surficial extent; also for the amount of rotation around the vertical and horizontal axes (ten Brink, *et al.*, 1996). Both faults (Parras Basin 1 and 2) are hypothesized to have rotated towards the east northeast by a drag effect produced by a subduction zone located north of the Mesa Central (Fig. 27). Map in figure 25 shows the strike slip basins (1-3) defined by Martinez-Piña and Goodell aligned along 2-NW and S-1 (Fig. 24), related to low-strength shear zones.

##### **2.4.2.1 Parras Basin Fault, PBF-1, and PBF-2**

Martinez-Piña and Goodell (in progress) analyzed the Parras Basin (Fig. 22) defining it as a strike-slip basin, and postulated two major *en échelon* faults (PBF-1 and PBF-2) (Figs. 23), which formed the Basin. Even when these faults are considered to have been displaced from their original location, show sufficient geometric elements that can be compared to the Riedel shear mechanism diagram, after which, it was concluded that the right lateral slip was the last of the vector motion of each of the faults. An empirical palaeogeographic reconstruction of the Coahuila block substantiates this vector motion.

Faults PBF-1- and PBF-2 jointly with the Juarez and Parras Basin faults constitute a composite weak fault or low-strength shear zone (dashed green line in Fig. 24; white in Fig. 26). Hypothetically, these types of faults developed from an upper-lower detachment zone in or near layers of evaporites or overpressure shales, forming wide shear zones (Atmaoui, *et al*, 2008). Chavez-Cabello *et al.*, (2001) interpreted Sierra Madre Oriental fold thrust-belt as the result of regional *decollément* of Upper Mesozoic produced by accretion of the Guerrero Terrane.

Faults PBF-1 and PBF-2 prior to the accretion of the Guerrero Terrane, formed the Parras Basin. Because of the accretion of the Guerrero Terrane these faults rotated towards the NE (green dotted line in Fig. 24, white dashed in Fig. 26 and left lateral Juarez-Parras composite fault in Fig. 27, depicts palinoplastic restoration of PBF-1) by the drag effect of the compressional tectonics exerted on the Sierra Madre Oriental. This drag in addition to changing the orientation of the basin from NNW to WNW developed folds and overthrusts. For rotation of PBF-1 from a WNW to a NNW direction, the point of intersection between PBF-1 and PBF-2 was used as hinge; once rotated (angle of  $37^{\circ}$  shown in Fig. 26) the segment aligns with the fault Juarez-Parras Basin (Figs. 24 and 26, green and white, respectively).

Restoration of PBF-1 and 2 carries another paleogeographic question: did Mesa Central rotated with PBF-1 and 2? Where was Mesa Central before rotation started? Centeno-Garcia and Silva-Romo (1997) placed between the cities of Zacatecas and Villa Hidalgo (long.  $102^{\circ}$ , lat.  $23^{\circ}$ ) an approximate boundary of the Guerrero terrane and the Sierra Madre Oriental terrane trending approximately N $35^{\circ}$ W. Applying the same angle ( $37^{\circ}$ ) used to rotate PBF-1 and PBF-2, to the northern boundary of the Mesa Central, the trace of this boundary, after rotation, strikes approximately N  $30^{\circ}$ W, and tough is to the south, it could be the line between the Mesa Central and the Sierra Madre Oriental. This displacement of the MC, (as shown in figure 26, blue color)

also places it directly under the source of the Triassic turbidites (Potosi Fan) found over and around the MC (Fig. 27, Juarez-Parras composite fault) (Burckhart, 1906; Nieto-Samaniego 1997; Centeno-Garcia Silva-Romo 1997; Alanis *et al.*, 2005; Centeno-Garcia *et al.*, 2008; Barboza-Gudiño *et al.*, 2010; Dickinson *et al.*, 2010).

Ten Brink *et al.*, (1996) and Keary *et al.*, (2009) point out the importance of the relationship of the basin-wide thickness of the layer (s), that is, the effect that the width of the shear zone has on the amount of rotation around the horizontal and vertical axis, and the surficial extent and amplitude of the vertical and horizontal deformation. The effect of a shear zone developed at the base of the upper crust also has a strong effect of vertical contrasts in the upper crust rheology (Keary *et al.*, 2009). Distribution of deformation along such faults occurs when uplift and subsidence distribute along the fault, beyond the fault tips; basins along the structure are, with increasing width of the shear zone, more elongated.

By connecting the mid parts where the Sierra Madre Oriental bends, area located to the north of the Mesa Central, an N60°E direction of regional tectonic transport vector was drawn. Chavez-Cabello *et al.*, (2011) shows a N37°E direction for regional tectonic transport in a small region south of Monterrey. The angle between the northern limit of the restored MC (blue color) and the regional tectonic transport vector is 85°, almost orthogonal (Fig. 26).

Displacement of the Mesa Central from the hypothetical paleogeographic position to its current one is not possible if based on the regional tectonic transport vector; however based on a subduction zone, located north of the restored MC, dipping to the east, is possible. Models by several workers, analyzed by Centeno-Garcia-Silva-Romo (1997), were proposed to explain the tectonic evolution of western Mexico during Triassic-Jurassic time, in different ways support the

idea of subduction taking place in northeastern Mexico. Torres (1999) as an “east dipping subduction zone” described the southeastern continental margin that includes the Permo-Triassic granite belt. Barboza-Gudiño *et al.*, (2011) also supports this idea, and that of Centeno-Garcia (2008) about the Potosi Fan.

### **2.4.3 Strong faults or high strength shear zone in an oblique contraction system (MSM-MSM-3, Texas, La Babia, Rio Bravo, and the San Marcos faults)**

In strong faults (narrow shear zone) as fault strength increases, more deformation distributes around the fault and less deformation as strike-slip deformation happens. Deformation at the tip of the fault is more localized, and is partly distributed outside the fault (ten Brink, *et al.*, 1996).

#### **2.4.3.1 Tepehuanes-San Luis Fault system (TSL)**

The TSL has an estimated length of ~ 660 km measured from San Luis de la Paz to Tepehuanes. At a mid-point between the cities of Durango (D) and Sombrerete (Sm) (Fig. 28), this fault system changes direction from ~N30° W to ~N 60° W. This area is an area where the normal faults related to the Jalisco Block intersects the TSL. Parallel to the TSL and located to the south at 36 km, a fault with a length of ~140 km is considered the southern boundary of the TSL shear zone by Loza-Aguirre *et al.*, (2008) (Fig. 13 small dashed square, Fig. 14). This fault herein postulated as the Guadalupe Fault (GF), extends 66 km northwestward of the AG and ends at the Tlaltenango Graben while extends 48 km eastward.

The Guadalupe graben (GG) and the Aguascalientes graben (AG) (Nieto-Samaniego *et al.*, 2005 and Loza-Aguirre *et al.*, 2008), are located east of Zacatecas, and west of Aguascalientes, trending NNE and NNW with lengths of 38 and 100 km, and widths of 8 km and 12 km, respectively. The AG is included between the TSL and the GF, while the AG extends 67

km south of the GF. A layer with the Aguascalientes Graben, from figures 13 and 14, and the Villa de Reyes Graben from figures 13 and 15, were overlaid to the shaded relief image-map in figure 28 of the Mesa Central area. This composite map shows the first graben displaced toward the NW by the Guadalupe Fault, in a motion consistent with that of a left lateral slip as shown in figure 28-1. On the other hand, the Villa de Reyes Graben (VRG), which trends north south, is parallel to the AG; this graben was displaced by the TSL in the same manner as the AG is displaced by the GF. It can also be seen the southeast extension of TSL intersecting the VRG on its west boundary, and its continuation, on the east side of the VRG (Fig. 28-3), displaced southward as shown in figure 28-4. The VRG is part of the Taxco-San Miguel Fault system that had a right lateral-strike-slip vector motion. In between these two grabens, there is another structure forming a graben with the same geometric characteristics of the AG and the VRG (Fig. 28-2). This fault could be the northern extension of the El Bajío Fault. Displacement of these grabens towards the northwest in these cases is consistent with the reactivation of a left lateral strike-slip regime, since these faults displace grabens formed in younger rocks.

A layer of Triassic outcrops; the boundaries of the Mesa Central (green line); traces of the TSL and the GF overlaying the image-map of figure 28, confirms the statement of Nieto-Samaniego *et al.*, (2007) about Paleozoic rocks appearing at the edges of Mesa Central. What this image-map also shows are Triassic outcrops on both sides of the TSL; if the TSL is considered the western boundary of MC, and Triassic outcrops are on both sides, then TSL cannot be the western limit. This study considers the western limit of the MC further south of the GF.

#### **2.4.3.2 Texas-La Babia-Rio Bravo fault system (TLBB)**

Along the composite fault Texas-La Babia-Rio Bravo fault system, according to Flotté (2008), an Oligocene transpressive deformation in the Ojinaga region “was probably guided at depth by a left lateral strike-slip fault system” (Fig. 23). This system had a compressive stress axis oriented N40° E to N50 ° E (Flotté, 2008). A higher angle (N65°W) was estimated by this study. Haenggi (2002), summarizes interpretations along the Texas Lineament of several authors that describe left lateral wrench zones including the Oro Grande and Lucero Basins in New Mexico; Early Permian left lateral motion of the N60W Pecos Valley fault; the beginning of the left lateral faulting activity during latest Mississippian time throughout Pennsylvanian time and “preceded activity on a right lateral fault system”. Haenggi (2002) also argues that the Southern Diablo Platform and possibly the Ojinaga area are the resultant of left lateral motion on segments of the Texas Zone (Fig. 23).

From the map in figure 23, the TLBB left lateral composite fault seems displaced by faults striking northeast i.e. Alamitos fault, which is a northwest normal fault, the El Caballo that is a left lateral fault, and by the La Cuesta, near the area where the Rio Grande River changes course to the northeast. Around this area the Presidio Bolsón is located, and the Ouachita-Marathon belt is usually placed.

Muehlberger, (1965) stated that the Texs Lineament “strike-slip movement can be documented for episodes, but the amount of slip necessary to produce the observed effects is in miles rather than in hundreds of miles”. DeFord (1969) considered it as a “major geotectonic discontinuity”, while Lowman Jr. & Tiedemann (1971), described it as an “hypothetical shear zone of regional extent reaching from west Texas to southern California”. Wood (1981) proposed “ a transform coast, trending northwest, constituted the southern edge of North

American plate from Precambrian until Triassic”. The author concluded first by questioning the great distances of transport proposed for Laramide overthrusting in the Chihuahua Belt, and second, by agreeing with Anderson and Schmidt (1983) proposal of “a left lateral shear throughout this margin during Mesozoic” being more compatible with the preceding structures. Among these authors consensus is that the fault is a transcurrent left lateral strike slip fault.

#### **2.4.3.3 Mojave Sonora Megashear (MSM)**

Mojave Sonora Megashear in northwestern Sonora presents a more complicated kinematics according to Anderson and Nourse (2005). A northeast contraction reactivated older east-striking normal faults that acted as sinistral strike-faults, and northwest-striking sinistral faults reactivated as steep reverse faults (Anderson and Nourse (2005). One question arises from these reactivations: why after the north south striking faults of the Pitáycachi zone, Miocene in age with throws of up to 4 km after disrupting, displacing, and concealing the MSM under the Cenozoic conglomerates is still traceable? The answer is a recent reactivation of the MSM (Fig.29). Following the trace of the MSM across the Pitáycachi fault zone, there is an apparent displacement to the north of a segment of the fault over a distance of  $\pm 250$  km.

Reactivation of Mojave Sonora Megashear and SMF-1 played a significant role in the extensional regime of the Sierra del Nido (Fig. 29 and 30). Elongated blocks with a centerline parallel to both faults, and elongated blocks with a centerline north south, parallel to the Juarez fault predominate as geometry of strike-slip basins and extensional basins.

After evaluating three options (PBF-1, PBF-2 and MSM-3) as the southward extension of the MSM more likely to be MSM-3, as shown by Martinez-Piña and Goodell (in progress) (Fig. 23). The structure shows a single lineament/fault narrow shear zone with no noticeable strike-slip

basins along its trace, and was defined as left lateral strike-slip fault. Mojave Sonora Megashear possibly connects to the Tepehuanes-San Luis fault system by likely tension faults of the subsystem SE-1 (orange dotted lines in figure 24).

#### **2.4.3.4 San Marcos Fault -1 (SMF-1), northwestern extension**

Kinematics of four events during San Marcos Cenozoic reactivation have been identified: one normal, one reverse slip, one that shifts from normal to left-lateral, and a fourth, which is predominantly normal (Chavez-Cabello *et al.*, 2005). Similarly, SMF-1 has had several reactivations, as seen in figures 29 and 30; these maps depict the relationship between the faults to the silicic and mafic cover from the Upper Volcanic Series. In addition, north of the SMF-1, topographic maps show a strong change in slope and scattered low ranges. Martinez-Piña and Goodell (in progress) characterized this segment of the SMF fault as a right lateral strike-slip, though considering that, the original vector of motion was left lateral (Fig.1–A). Ovideo *et al* (2010) hypothesized that the Laramide Orogeny inverted the original vector motion of strike-slip faults during a Paleogene extensional regime.

SMF-1 oriented northwest and a series of north oriented faults considered as normal faults and parallel to the Juarez fault, delimits and controls the morphology of basin and ranges, conglomerates and alluvial sediments that fill the basins to the north and west of Sierra del Nido. Comparison of these geometric elements to those of the shear mechanism diagram shows that north south faults match R'-antithetic shear and northwest R-synthetic shear resemble subsidiary synthetic faults. Shear stress mechanisms are evident because of the faults that delimit the blocks in a rhombic shape or by the strike-slip basins, inside the WCCB.

The composite SMF-1-San Marcos Fault characterized as a right stepping left-lateral strike slip fault (Fig. 31) as result of Cenozoic reactivation. The area bounded by the Plomosas, Acebuches, El Minero and Juarez faults, corresponds to a restraining bend (rhombohedral shape) or pop-up ridge, where Precambrian and Paleozoic rocks are described, and contraction and left lateral strike-slip motion is recognized (Oviedo *et al*, 2010) (Fig. 31).

#### **2.4.3.5 Sinforosa (SL) and Aquinquari (A) faults**

Sinforosa and Aquinquari fault systems developed in an island volcanic arc that accreted to continental Mexico during Late Cretaceous to Early Tertiary (Campa and Coney, 1983). Though parallel, these tectonic features did not behave as *en echelon* faults, rather they formed by oblique contraction as the Guerrero Terrane was being accreted (Martinez-Piña and Goodell, in progress, Fig.1- B and C). There is poor evidence from satellite images of reactivation of the Sinforosa lineament; however, its right lateral strike slip motion could be due to the relaxation of the compressional regime. On the other hand, Aquinquari outstanding characteristic is that it dies out northwest of Durango city. Sinforosa and Aquinquari faults are connected by transverse normal faults (Plumosas, Conitaca and Comedero). Characteristics of these fault systems involve parallelism, arch shape traces, and interconnection by segments developed at different stages.

There are similarities between the Sinforosa Lineament and the Tepehuanes –San Luis (TSL) fault and those of SMF-1 and SMF: opposite directions and a restraining bend (rhombohedral shape) linking them (Fig. 31, black and dotted lines). This geometry and the vector motion of this tectonic structure, defines it as a right stepping left lateral strike-slip fault. The restraining bend consists of two blocks separated by a normal fault. The south block is probably the second place with the highest elevation in SMO with 3100 m a s l.; the nearest point with the same elevation is 150 km to the northwest.

The Aquinuari fault is a single structure with a last motion as right lateral strike-slip fault. Does not seem to connect to the TSL, but it connects to the Sinforosa fault by the northwest Plumosas and the SA-1, two normal extensional faults.

#### **2.4.3.6 Pitáycachi Fault zone (PFZ)**

The Pitáycachi fault is a north south oriented fault located near the state limits of Chihuahua and Sonora. West of the Pitáycachi fault a series of parallel structures dipping west, constitutes the Pitáycachi fault zone (Fig. 23, and 24E-1). This fault zone bounds Triassic lithology (Lopez-Ramos, (1981) which overlies Precambrian rocks (Pinal Schist) (Anderson and Silver (1974). According to Suter and Contreras (2002), the zone extends at various rates in an east-west direction and defines as Miocene the age of faulting.

Suter and Contreras (2002) on the eastern limit of the Pitáycachi fault zone, found normal high angle north south striking faults of Miocene age associated to half-grabens. Within this zone, Rodríguez-Castañeda (1997) just north of the MSM and west of Suter and Contreras (2002), found vertical faulting, but of different age, Late Jurassic to late Cretaceous; also found thermal uplift and detachment by faulting during Tertiary. On the western limit, Busby *et al.*, (2005) at Sawmill Canyon (international boundary between Sonora and Arizona) argues that this zone and faults striking NW were inherited from a Precambrian regional lineament that was reactivated during Mesozoic and Cenozoic times (Fig. 11).

The relative dating by Busby *et al.*, (2005), the stratigraphic dating by Rodríguez-Castañeda (1997), and relative dating of the Pitáycachi fault by Suter and Contreras (2002) sets a timeline, from west to east, ranging from Precambrian (?) Late Jurassic-Early Cretaceous to Miocene. Valenzuela *et al.*, (2005), after comparing the N-S faults of the Pitáycachi fault zone to the Riedel

shear mechanism diagram, concludes that these T-synthetical faults belong to the youngest of three fault systems with Y-fault at N45 W. The other two systems also show T faults at much different strikes, NNW-SSE and E-W. Valenzuela (2005) concludes that reactivation is the cause of such variations.

#### **2.4.4 Structural domains**

Transcurrent faults, strike slip faults, and megashears are usually part of hypothetical tectonic reconstruction models. As stated by Longoria (1994), in 1992 only five strike-slip faults had been recognized throughout Mexico; after numbering the difficulties that represent recognition of these tectonic features, he postulated 34. However, the author links these morphotectonic features and its genesis to the movements / rupture in the basement, validated by experimental work with analogue materials.

It is clear that oblique compressional and extensional regimes (Longoria, 1994; Keary *et al.*, 2009) are present in northern Mexico and genetically related to convergence or divergence of the tectonic plates, resulting in intraplate (basement) or interplate (boundaries) tectonic kinematics. Atwater (1988) argues that dilational components were consistently included because of the oblique Pacific-North American plate motion vector.

The tectonic framework of northern Mexico characterized by this work recognized four structural domains (Fig. 24): NW (1, 2, 3 NW), N-S (E-1), NNE (E-2), WNW (W-1), and SE (S-1 and S-1a). Of these, the SE domain includes four intermediate parallel transcurrent shear zones, at an acute angle with respect to the major lineaments. Of the two parallel lineaments to the north (S-1), one is a divergent transcurrent (green line) while the other is a convergent transcurrent. Both connect with a major lineament, while the one on the south (S-1) relates to

extensional tectonics, the other to compressional tectonics, both are related to the accretion of the volcanic arc.

#### **2.4.5 Convergent transcurrent tectonic domain NW**

Two major parallel shear zones because of convergence transcurrence are included in this domain (Fig. 24):

1-NW includes: 1) Mojave-Sonora-Megashear (MSM)- MSM-3 and

3-NW includes: 1) Texas Lineament 2) La Babia, 3) Rio Bravo, 4) El Caballo

#### **2.4.6 Divergent transcurrent tectonic domain NW**

2-NW includes 1) SMF-1, 2) San Marcos, 3) PBF-1, PBF-2

#### **2.4.7 Extensional tectonic domains NNS and NNE**

Includes 1) Pitáycachi fault zone, Xoconostle and faults related to the Jalisco Block.

Within this extensional tectonic domain with a NW strike are included 2) Conitaca, 3)

La Plumosa, and 4) Comedero

#### **2.4.8 Compressional tectonic domain NNW**

Includes 1) Tepehuanes-San Luis and, TS-1, 2) SA-1 3) Sinforosa 4 ) Aquinquari and 5)

Taxco-San Miguel de Allende fault system.

#### **2.4.9 Oblique subduction and R-shears based on Holohan analog model**

Ward (1991) argues that between late Oligocene early Miocene (36 Ma and 20 Ma) the vector motion between the North American Plate and the Pacific Plate was at N64W and the strike of the trench at N37W. Atwater (1988) with a slight difference estimated the vector motion at N60W during the Miocene changing to N37W at about 8 Ma, since then plate motion has been

closer to coast-parallel. Umhoefer (2003) suggests for the Lower Cretaceous that relative plate motion between Farallon plate and North America had a component of southward oblique convergence, that is, a southeast direction. Antonelis *et al*, (1999) estimated the current vector motion at N59W while Plattner *et al*, (2007) estimated it at N55W. On the other hand, is a known fact that transform faults such as the MSM developed during Jurassic time (Anderson and Silver (1974) and as result of oblique convergence.

A map drawn in figure 32 with the above data, includes the angle of  $\sim 17^\circ$  (angle at which R shears are formed, data from experiments with analogue materials by Holohan, 2007), overlaid on the map of versions of the Mojave-Sonora-Megashear (Fig. 2), allow some conclusions to be drawn from this. The angle between the line representing the trench at N37W (Ward, 1991) and a mean line of the different versions of the MSM, form an acute angle of  $\sim 22^\circ$  for a  $+5^\circ$  difference from that found by Holohan (2007) of  $17^\circ$ . On the other hand, even when the map of Umhoefer (2003) shows no direction for the vector motion of the Farallon plate for half of Early Cretaceous, it is possible to assume that this vector motion comes from late Jurassic

In fact, Umhoefer (2003) states that his map (in figure 32, bottom figure) combines the “sinistral oblique convergence in the northern Cordillera with the palaeogeography proposed by Dickinson and Lawton (2001) for Mexico”.

## **2.5 Discussion**

It is clear that there is no update of the tectonic framework of Mexico. Salas (1975), De Cserna (1976), Lopez-Ramos (1979), and Longoria (1994) pioneered this task, but literature review shows that since 1994 (Longoria, 1994) no recent work on this subject has been done, probably because of the area that this type of work needs to cover. Structural studies tend to be more regional-scale and repetitive, i.e. Mojave-Sonora Megashear has had more studies than any

other has, maybe the Texas Lineament is the only competing. The lack of geological data for the region Mexico-USA international boundary only reflects in the diversity of hypotheses regarding the southwestern margin of cratonic North America, and of northern Mexico.

1. The hypothesis that all major lineaments striking northwest had a sinistral motion, while all major lineaments striking northeast had a dextral motion was put to the test by Martinez-Piña and Goodell (in progress) and found, among other factors, that reactivation is a major factor overprinting the original vector motion of the faults. Some faults have been typified as dextral or sinistral because they are considered to cut Jurassic or Mesozoic basement; however relative dating of faults has been done based on outcropping lithology. Longoria (1984) argues that changes in plate kinematics are a "major limitation in kinematic analysis of the fault system in Mexico whereby reactivation of the strike slip faults make take place in different slip senses at different times". If left lateral strike-slip was the prime vector motion of the shear zones that crosscut Mexico during the Pangea break up; subduction of Pacific plate, the opening of the Gulf of Mexico, the Laramide Orogeny, and the opening of the Gulf of California, have modified it substantially to a point of motion vector inversion.
2. Some workers have hypothesized about the direction of the MSM in northern Mexico being a curved line, and constituting the edge of the North American craton (Fig. 4). The figure itself shows an inconsistency: parallel lineaments constrained by a curve boundary. There are restraints to this idea such as the existence of the West Chihuahua Cratonic Block. Campa and Coney (1983), Sedlock *et al.*, (1993), Dickinson (2001) and Centeno-Garcia *et al.*, (2008) even when overlooking the WCCB, they always placed the MSM and the cratonic boundary of North America to the south end of this block. The block was

faulted from the NA craton and displaced to the current location through a left lateral movement, the WCCB is included between the MSM and the SMF-1, which are parallel faults. The geometry of this system can be the result of oblique subduction between the Farallon Plate and the North American Plate and the precedent to the parallelism as a characteristic of the tectonic framework. The equidistance between the axes, whether arched or straight, could reflect in more than one way a uniform condition of each basement they cut, that is, “homogeneous basement”. Centeno-Garcia *et al* (2008) considered that terranes of Gondwana affinity were already accreted to the southern part of the North American craton at the end of the Paleozoic. This homogeneity can account for parallelism of the faults systems. Arched lineaments and main parallel shear stress systems (Fig. 23) constitute the tectonic framework developed by four styles of stress regimes: extensional, compressive, convergent transcurrent and divergent transcurrent shear zones.

3. The Texas Lineament (Muehlberger, 1980), La Babia (Charleston, 1981), San Marcos Fault (Charleston, 1981) and the Tepehuanes-San Luis fault (Nieto-Samaniego et al, 2005) (Fig.22), are lineaments parallel to the Mojave Sonora Megashear forming an acute angle with the strike of the trench at  $N37^{\circ}$  that Ward (1991) places within the Gulf of California, (Fig. 32). Applying the analogue model of Holohan *et al.*, (2007) to this geometry, and angle average for the vector motion between the Pacific and North America plate of  $N61W$ , the result should be strike slip faults formed at an angle of  $17^{\circ}$  with respect the strike of the trench that is with a northwest strike. This model points out to oblique subduction with respect to the western margin of continental Mexico. Subsequent tectonic events formed the tectonic framework of northern Mexico that does

not consist of just a few major lineaments rather, consists of structural systems developed according to the rheology of the basement and overlaying lithology.

4. Overlooking the WCCB, tends to distort the hypotheses about the tectonostratigraphic history of northern Mexico casting doubt and uncertainty. If not well defined the role of WCCB in the development of the tectonic framework, the validity of any hypothesis must be questioned. A detailed study involving the WCCB, the MSM, San Marcos and La Bafia, will show a timeline from east to west, ranging from late Paleozoic to late Mesozoic, with reactivation during the Tertiary.
5. Basin analysis and their definition are an important issue because their definition helps understand or isolate the kinematics that operated in different regions of the structural framework. It is contrasting to observe distension basins located at higher elevations in the Sierra Madre Oriental, resulting from the relaxation of a compressive regime exerted on the Mesozoic cover by the Laramide Orogeny, to basins resulting from divergent transcurrent regimes (Parras Basin) of Jurassic age at lower elevations. Regional tectonic transport vector of the orogeny over the Mesozoic cover in a SW-NE direction, and the shear stress applied to the PFB faults, probably oblique to its path, show different events at different times.
6. Breaking up of Pangea; the southward migration of cratonic blocks (WCCB) (Goodell, 1985; Martinez-Piña and Goodell, in progress); the Triassic aulacogens in northern Mexico (Goetz and Dickinson 1989; Goodell, 1985) and in northwestern Mexico (Goodell, 1985; Martinez-Piña and Goodell, in progress); the mid-continent Jurassic-subduction zone (Centeno-Garcia and Silva-Romo 1997; Centeno-Garcia *et al.*, 2008;

Barboza-Gudiño, 2010); the Early Cretaceous-Late Tertiary subduction zone and emplacement of the coastal batholith; the accretion of the Guerrero Terrane (Campa and Coney, 1983), the opening of the Gulf of Mexico, and of the Gulf of California, subjected continental Mexico to alternating shear stress regimes that overprinted the original vector motion with several stages of strike slip motion.

### **2.5.1 Conclusions**

Accomplishment of the definition of the tectonic framework was done by use of the integrated geographic information system. Three major shear stress systems constitute the tectonic framework of northern Mexico. The analysis done by this study, tend to show, that the three initially could have been formed as left lateral strike slips by oblique subduction on cratonic terrane, but in the course of other events such as opening of the Gulf of Mexico and California the sense of the faults changed. The homogeneity of the terrane in which these lineaments developed is probable responsible for the parallel characteristic of the tectonic systems of northern Mexico, additionally the location of the WCCB, is another probable cause of this characteristic. Other factors such as terrane accretion and volcanism had some role in their development. Vector motion of faults, here study, refers to their last motion, which could reflect reactivation that occurred in recent time. Even under this consideration, and in a general way, it can be established that from the shear stress system 1-NW, to the north, there is a prevalence of straight faults striking NW showing left lateral motion; while south of this shear stress system, curvilinear faults striking NW have a right lateral motion. The major shear stress systems developed in continental Mexico, while subsystem W-1 developed in accreted terrane. Connecting faults that have opposite motion to the main fault must be antithetic faults that formed under the Riedel mechanism.

It was shown by applying IGIS, the importance that the WCCB had in the development of the tectonic framework in northern Mexico, and the need to re-evaluate the tectonostratigraphic history of northwestern Mexico.

Accretion of the Guerrero Terrane produced a regional transport tectonic vector, folding the Sierra Madre Oriental and dragging the Parras Basin to its current location. A key feature of sedimentological nature is the Triassic Potosi Fan. The presence of Triassic lithology on the MC establishes a relation of location between the PF and the MC. A hypothesis conceived during the course of this study refers to the rotation of the MC towards the west, placing it under the PF, and then been dragged by a Jurassic subduction, proposed by other researchers, located north of the MC.

Whether the issue of defining the strike slip motion of faults of different events at different times, can be resolved or not, depends on the viability of integrating volumes of data, from research, hypotheses, tectonic setting and tectonic framework maps, and put together under the same geographic frame.

Table 2.2 Structural domains of northern Mexico and related faults

Fault	Author	Length (km)	Measured length	Last Vector Motion	Strike	Dip	Age	Structural Domain	Shear Stress System
Mojave-Sonora-Megashear	Silver & Anderson, (1974)	ND	700	Left-Lateral strike-slip	NW-SE	ND	Jurassic	NW Convergent transcurrent tectonic domain	1-NW
MSM-3	Martinez-Piña & Goodell		467	Left-Lateral strike-slip	NW-SE	ND	Jurassic		
Texas Lineament	Albrithon & Smith (1957) DeFord (1969) (1). Haenggi (2002) (2)	ND	450	Left-Lateral strike-slip ?	NW-SE	ND	ND		
La Babia	Charleston, (1981) (1) Padilla & Sanchez, (1986) Gonzalez-Sanchez, (2008)	ND	412	Left-Lateral strike-slip	NW-SE	ND	Jurassic (?)		3-NW
Rio Bravo	Flotte <i>et al.</i> (2008)	ND	300	Left-Lateral strike-slip	ND	ND	Jurassic		
El Caballo	Eguilus-Antuñano, (1984)	ND	261	Left-lateral	NNW-SSE	ND	Jurassic (?)		
Tepehuanes-San Luis	Centeno-Garcia & Silva-Romo (1997) Nieto-Samaniego et al., (2007)	~ 600 km.	660	NW-SE (Normal faults)	SW	ND			S-1a

Table 2.1 continuation

Fault	Author	Length (km)	Measured length	Last Vector Motion	Strike	Dip	Age	Structural Domain	Shear Stress System
SMF-1	Martinez-Piña & Goodell		281	Right-lateral	NW-SE	ND	Triassic?-Jurassic	Divergent transcurrent tectonic domain NW	2-NW
San Marcos	Charleston, (1981) (1) McKee et al., (1990) Chavez-Cabello 2005)( 2) Aranda- Gomez (2005) (3)	~ 300	371	Left-Lateral strike-slip	NW-SE	ND	Jurassic		
Parras Basin - 1 & Basin 2	Martinez-Piña & Goodell		221 145	Right-lateral	WNW		Triassic-Jurassic (?)		
Pitáycachi	Suter & Contreras (2002)		336	Minor left lateral motion	N-S	Vertical	Tertiary		
Juarez-Parras Basin	Martinez-Piña & Goodell		447	ND	NW	ND	Tertiary	Extensional tectonic domain	S-1a
La Plumosa	Martinez-Piña & Goodell		140	ND	NW	W	Tertiary		
Comedero	Martinez-Piña & Goodell		288				Tertiary		
Sinforosa	Martinez-Piña & Goodell		415	Right lateral	WNW	ND	Tertiary	Compressional tectonic domain	W-1
Aquinquari	Martinez-Piña & Goodell		500	Right lateral	WNW	ND	Tertiary		

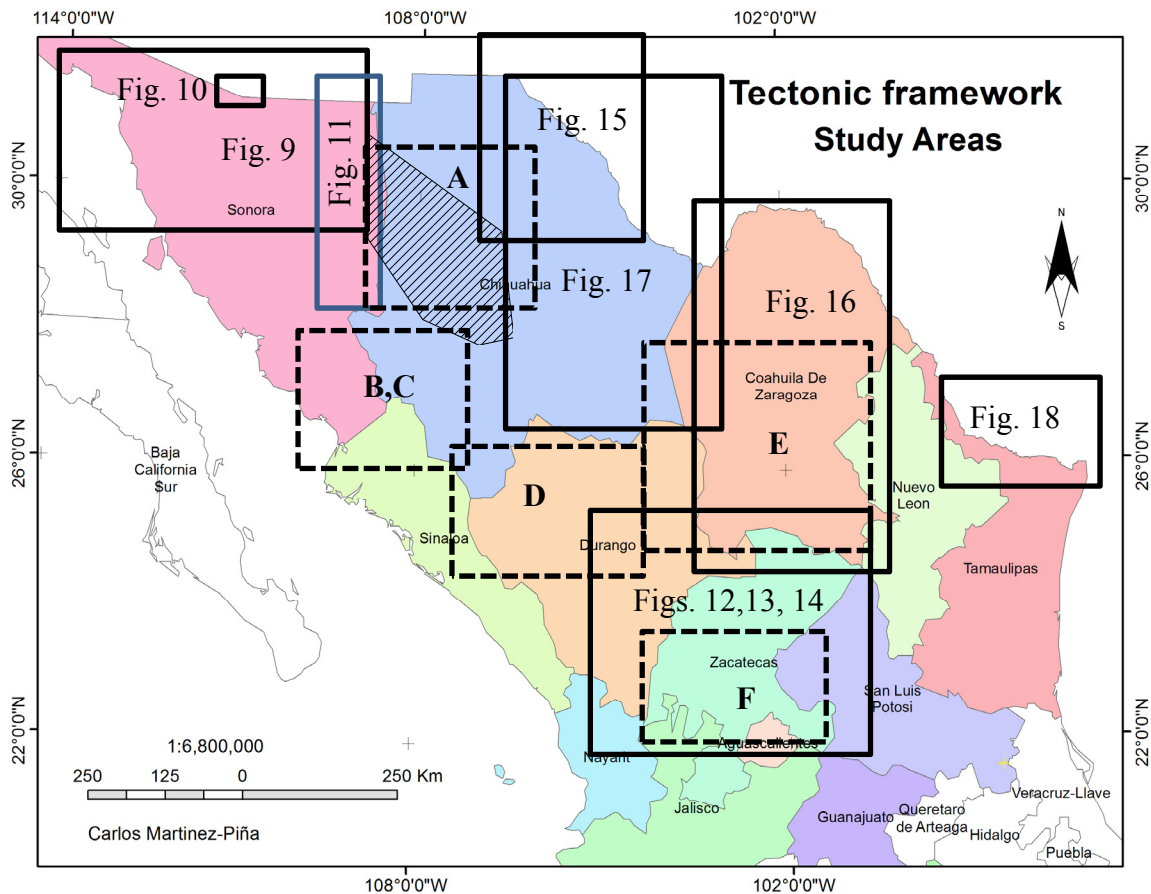


Figure 2.1 Study area including eleven states of northern Mexico covering ~1.4 million km<sup>2</sup>. Numbers refers to selected areas (CGAs): Mojave-Sonora-Megashear (Fig 9); Sawmill Canyon faults (Fig. 10); 3) Pitáycachi fault system (Fig. 11); 4) Tepehuanes-San Luis fault systems (Fig. 12, includes Figs. 13 and 14); 5 ) Texas Lineament/fault (Fig. 15); 6) La Babia- San Marcos faults (Fig. 16); ( 7) Juarez-Almagre-El Caballo faults (Fig. 17) and 8) Rio Bravo fault (Fig. 18). Dashed polygon depicts the West Chihuahua Cratonic Block (Fig.19). Dotted black line boxes with letters refer to areas studied by Martinez-Piña and Goodell (in progress ) A) San Marcos Fault -1 and Marcos Basin B and C) Sinforosa and Aquinuari faults D) Durango basin E) MSM-3 fault and E) Parras Basin and PBF-1 and PBF-2 faults and F) Tepehuanes –San Luis fault.

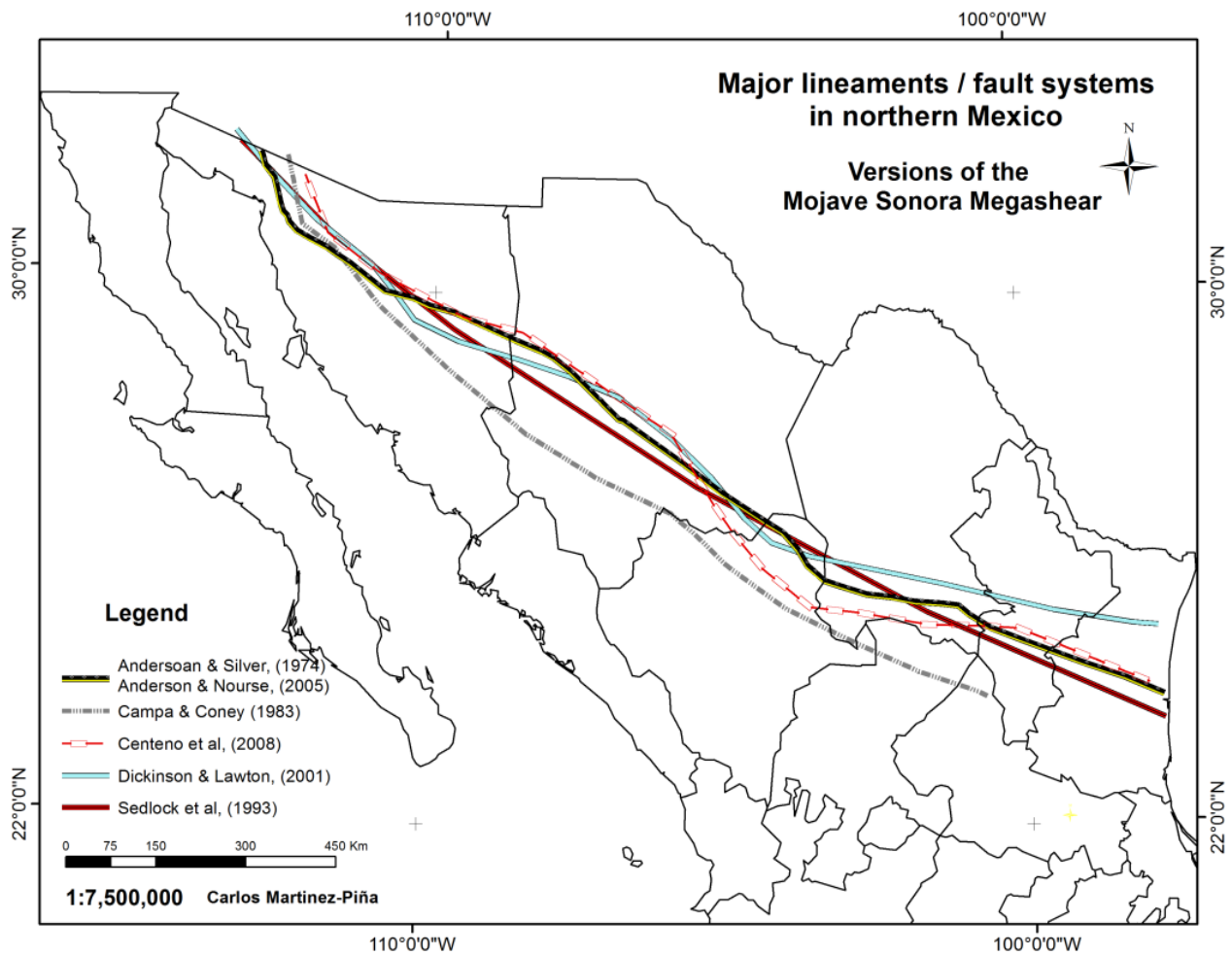


Figure 2.2 Map shows versions of the Mojave -Sonora - Megashear in Northern Mexico by several authors

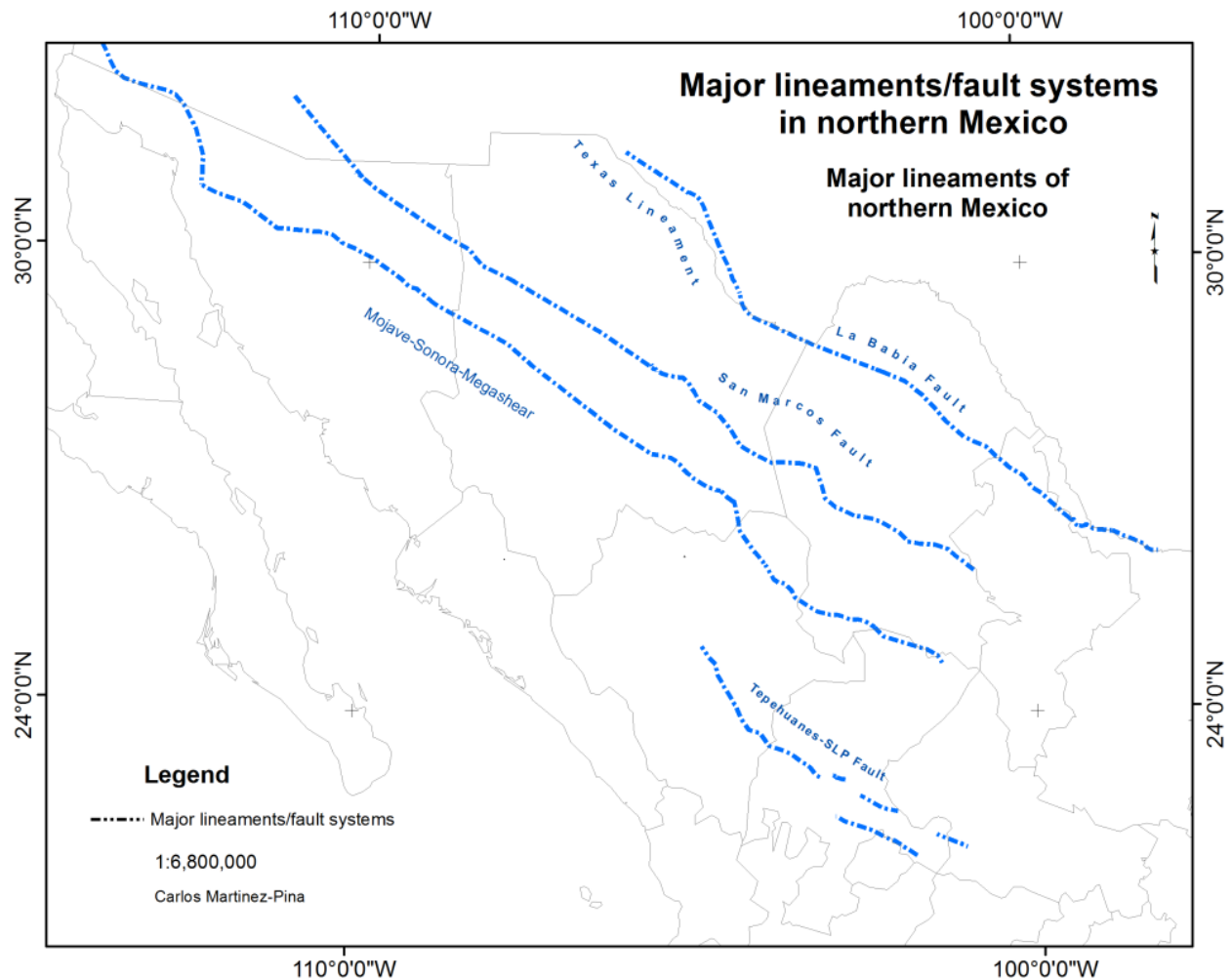


Figure 2.3 Known lineaments in northern Mexico. From north to south: Texas Lineament (Muehlberger, 1980) and La Babiá (Charleston, 1981); San Marcos Fault (Charleston, 1981); Mojave Sonora Megashear (Anderson and Silver, 1974) and the Tepehuanes-San Luis fault (Nieto-Samaniego *et al*, 2005).

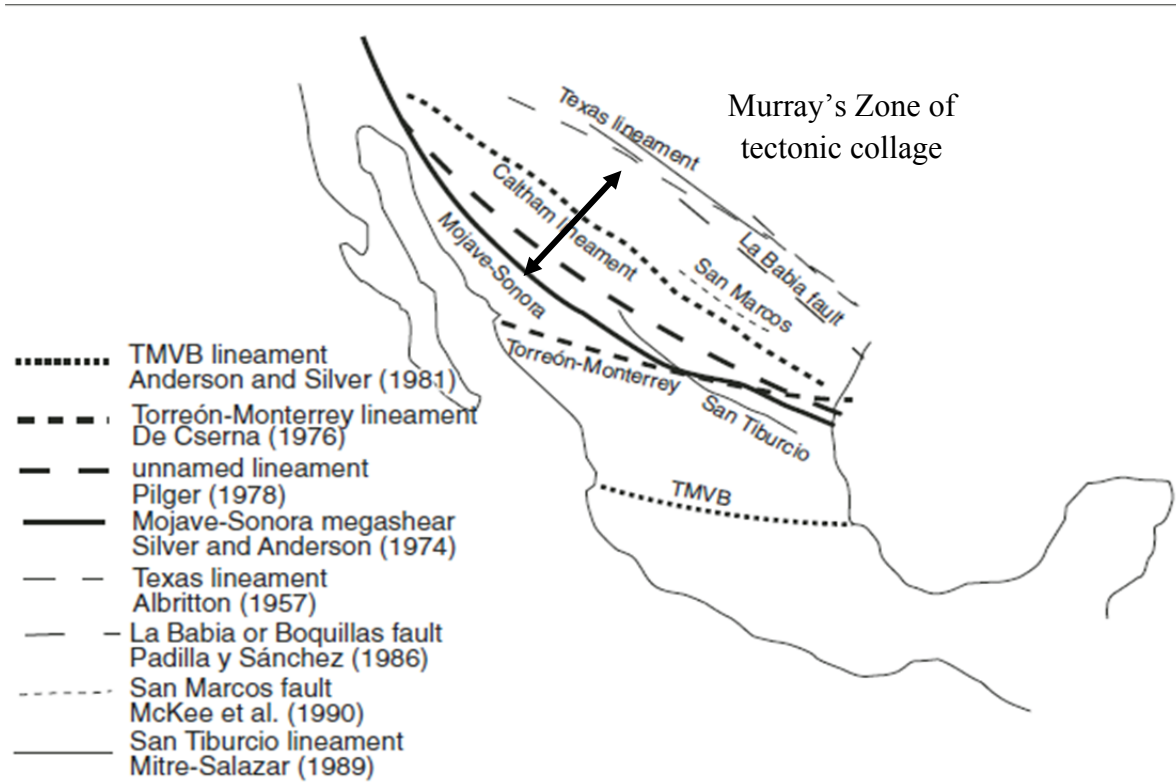


Figure 2.4 Regional structures and lineaments in Northern Mexico. Murray's (1989) zone of tectonic collage includes almost all lineaments except the Trans-Mexican Volcanic Belt. Taken from Molina & Iriondo (2007).

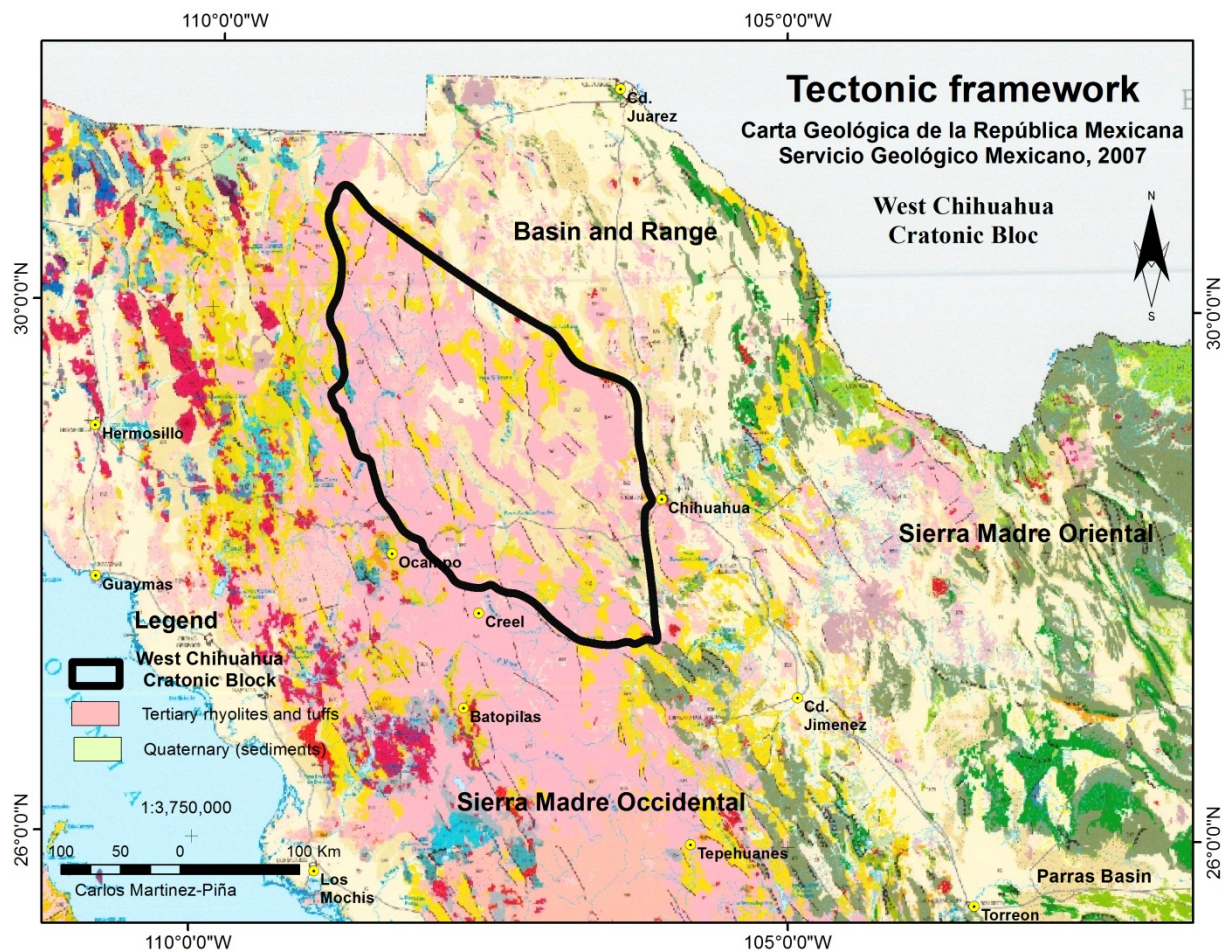


Figure 2.5 Map shows the West Chihuahua Cratonic Block location W of Chihuahua City. Extends westward from Highway 45 to the border with Sonora. The block has a rhombohedric shape with borders north and south striking NW, while borders west and east strike N-S. The WCCB block is topographically elevated. The eastern portion of the block is a high volcanic plateau, with large flat surfaces and isolated ranges.

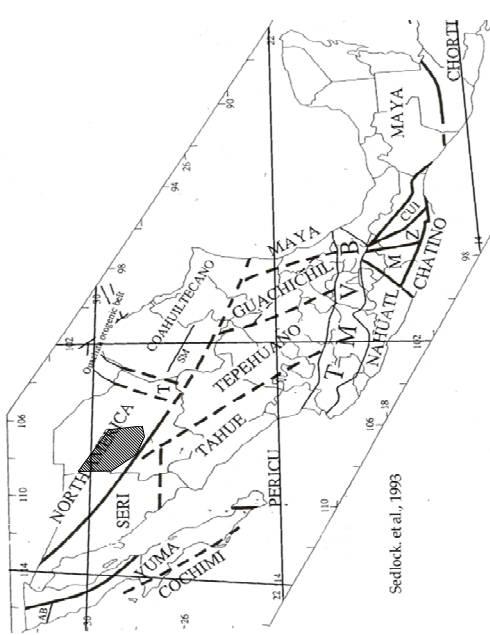


Figure 2.7 Tectonostratigraphic terranes by Sedlock *et al*, 1993 showing location of the WCCB

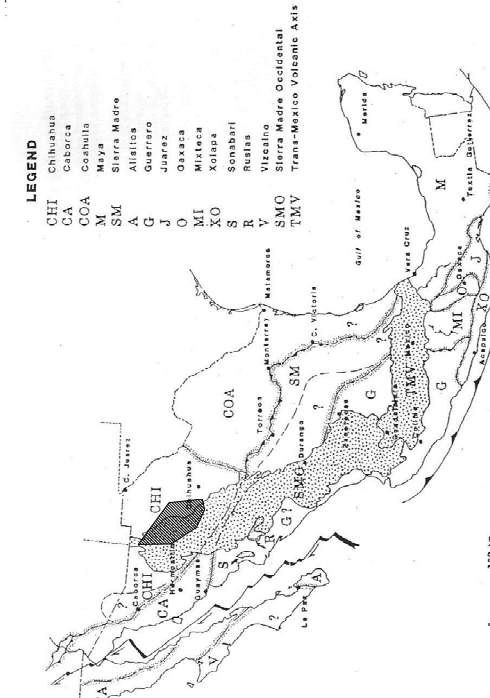


Figure 2.6 Tectonostratigraphic terranes by Campa & Coney (1983) showing location of the WCCB

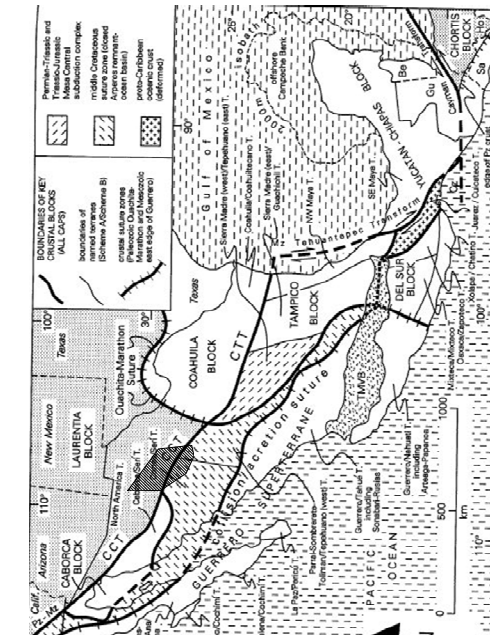


Figure 2.9 Tectonostratigraphic terranes by Dickinson and Lawton (2001) showing location of the WCCB

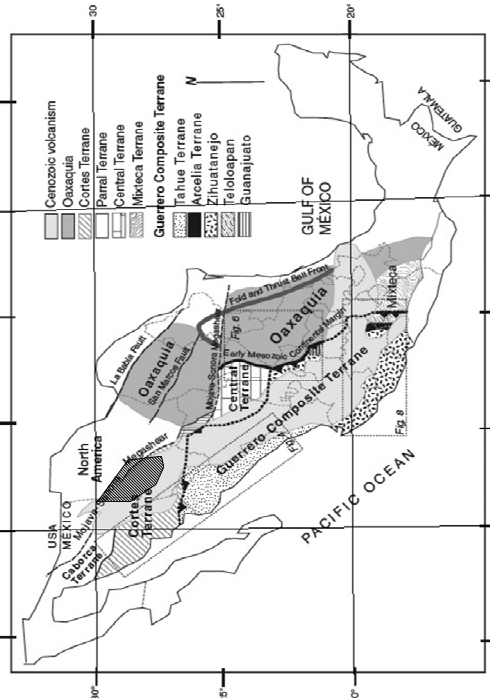


Figure 2.8 Tectonostratigraphic terranes by Centeno *et al*, (2008) showing location of the WCCB

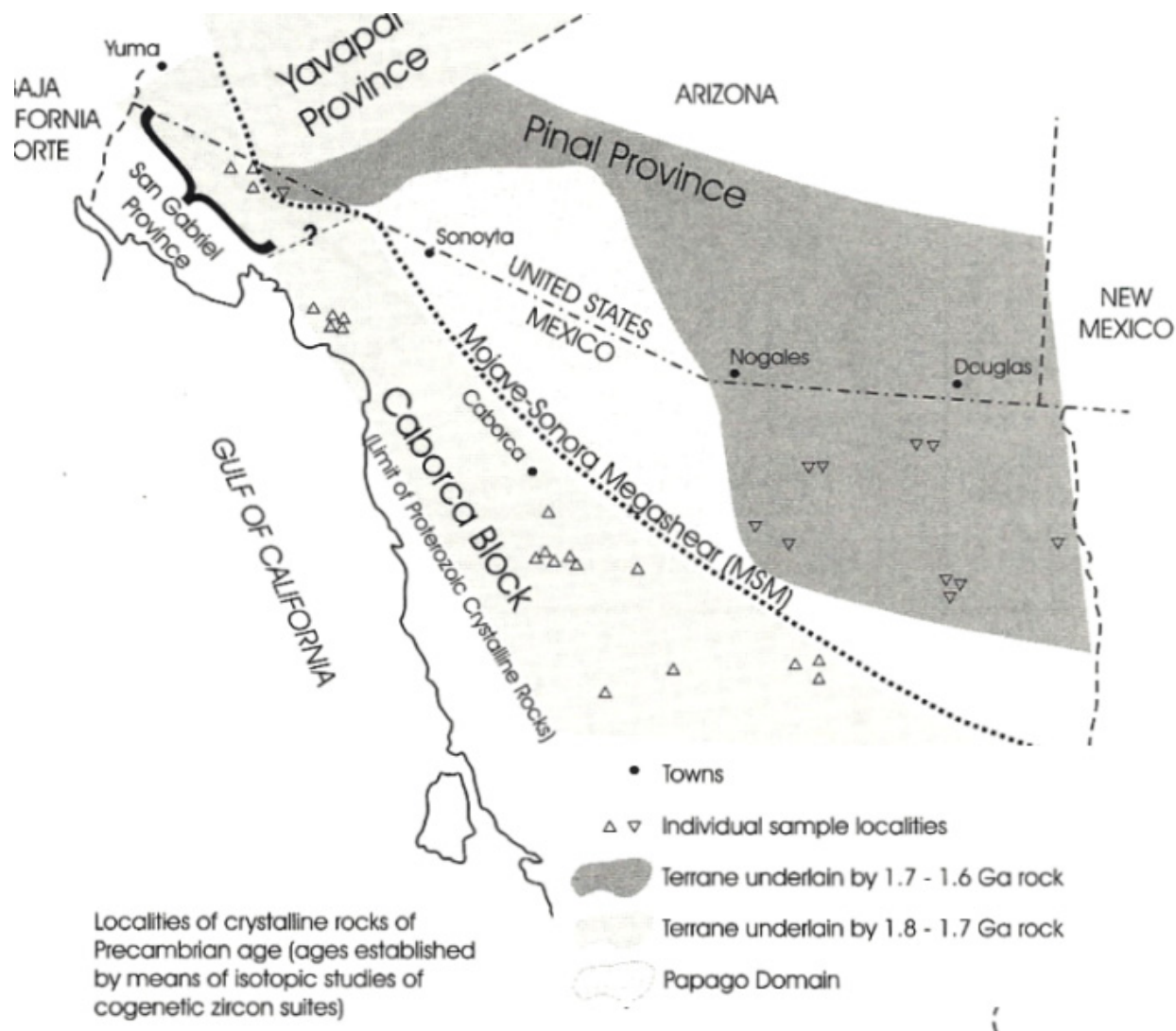


Figure 2.10 Map shows the Caborca Block, the Mojave-Sonora fault system, Yavapai, San Gabriel and Papago Provinces. Taken from Anderson & Silver (1974; 2005)

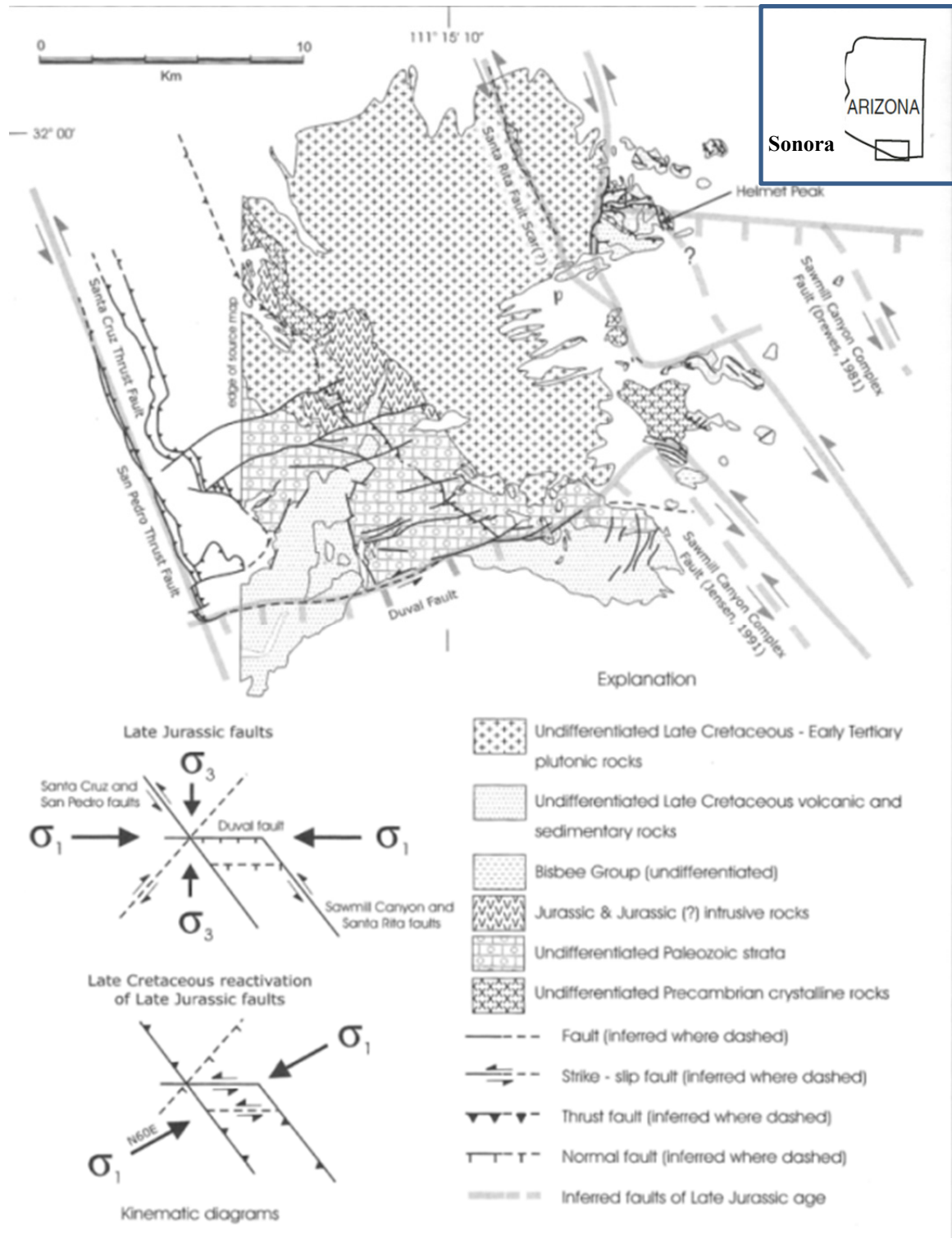


Figure 2.11 Geologic map of Sierrita Mountains, showing Late Jurassic faults reactivated during Cretaceous contraction and kinematic diagrams of transtensional stress and compressional regimes. Location of the area in the upper right corner. Taken from Busby *et al.*, (2005)

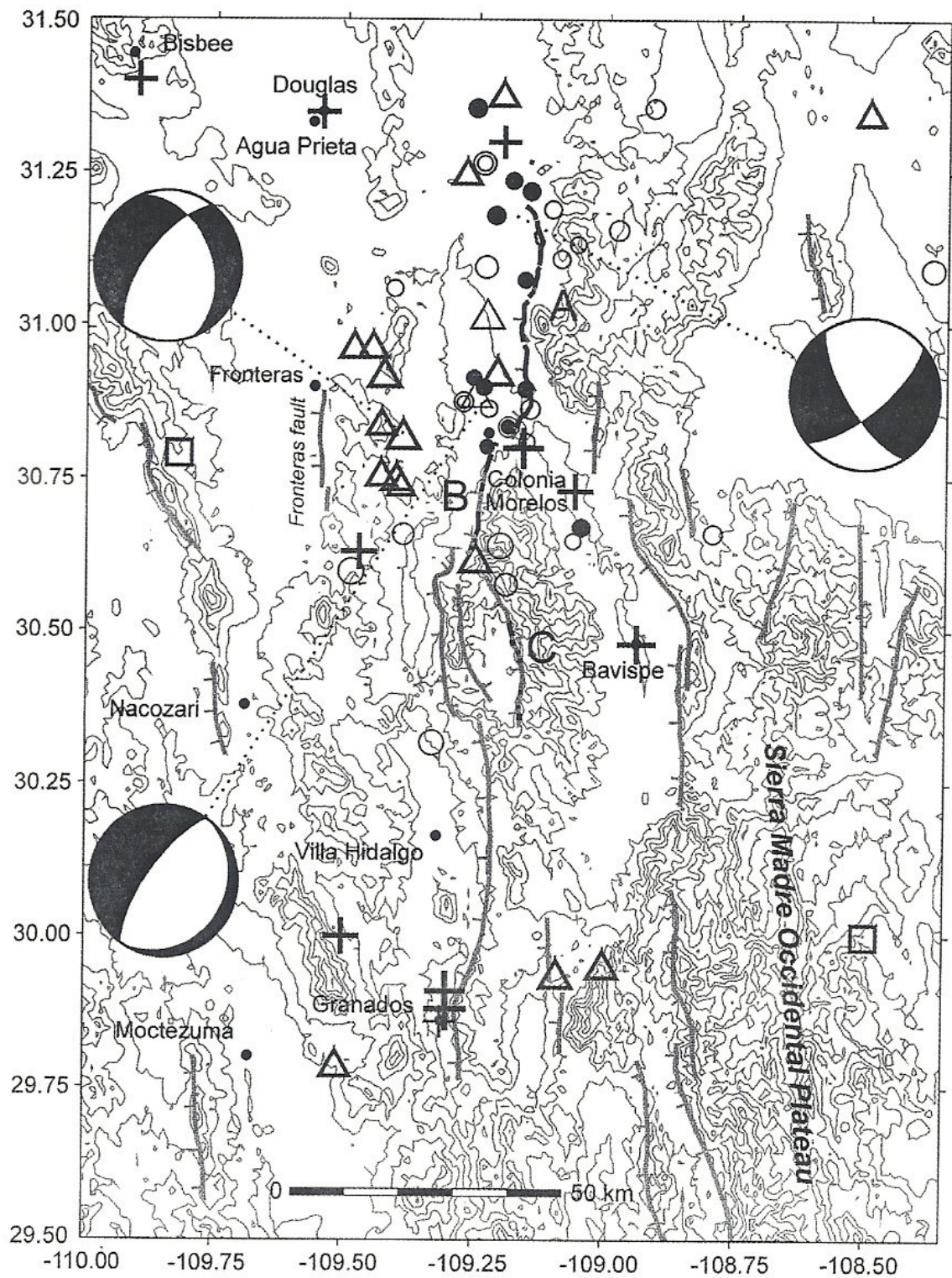


Figure 2.12 Map shows the 1887 rupture segments A Pitáycachi, B Teras, and C Otates, Region near the USA-Mexico international border. Taken from Sutter and Contreras, (2002).

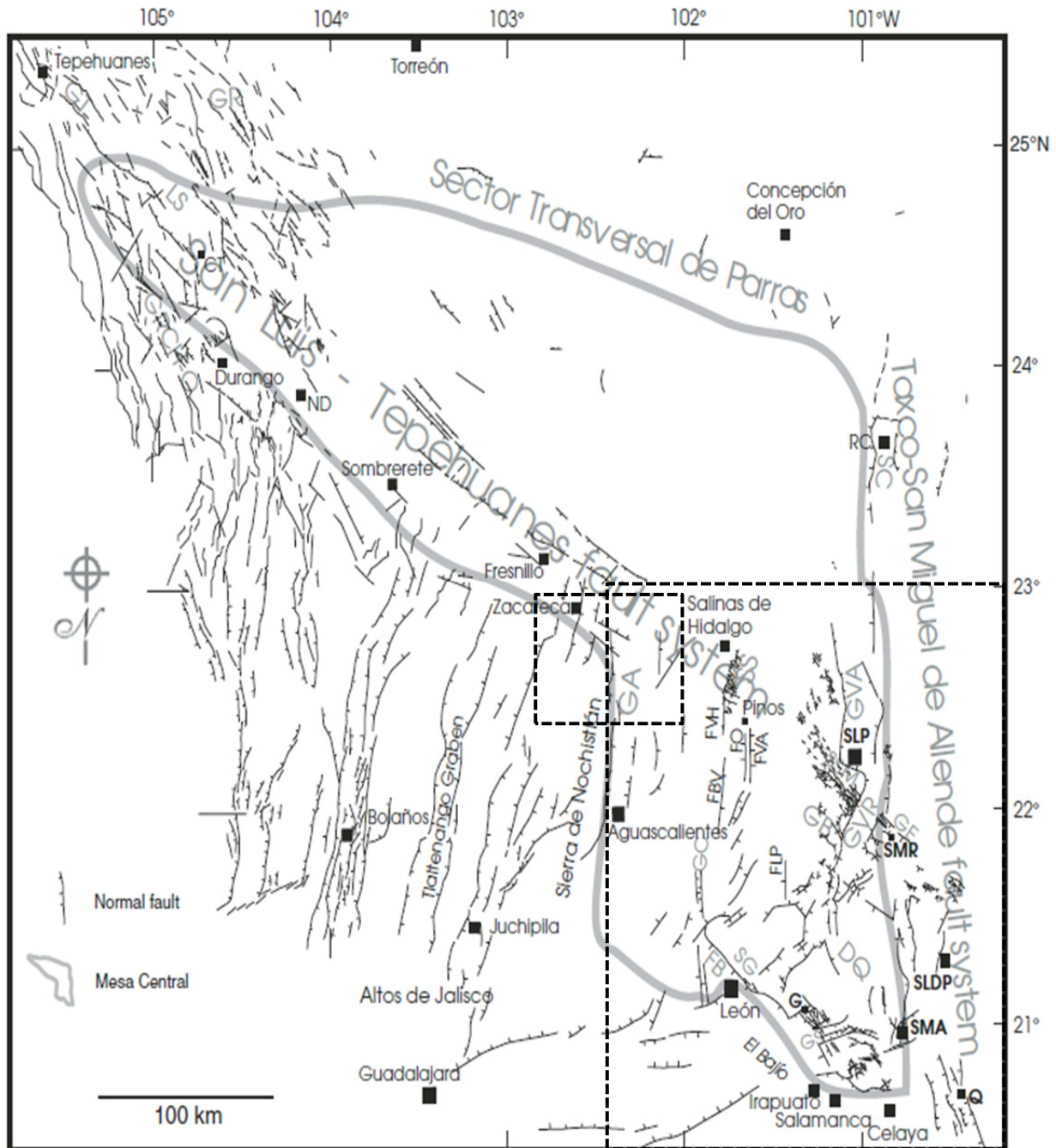


Figure 2.13 Map shows the Mesa Central, the Tepehuanes-San Luis fault system and the Taxco-San Miguel de Allende fault system. Taken from Nieto-Samaniego *et al.*, (2005). Small dotted box corresponds to the study area of Loza-Aguirre *et al.*, (2005) shown in figure 13. Big dotted box correspond to the study area of Nieto-Samaniego *et al.*, (1999) and Xu *et al.*, (2008) shown in figure 14.

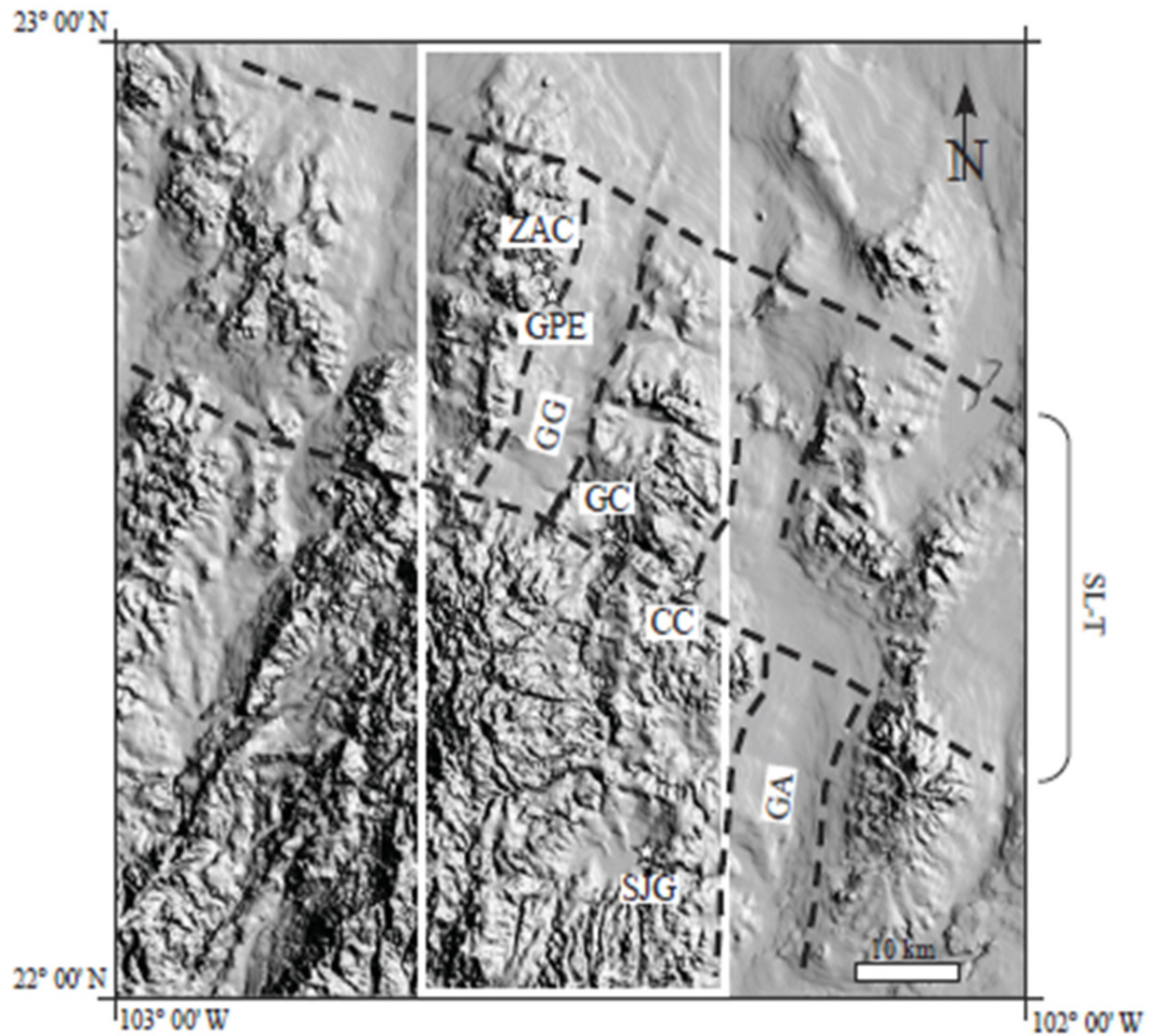


Figure 2.14 Digital elevation model showing the area where the TSL cuts and displace the Aguascalientes Graben (GA). Guadalupe Graben to the northwest (GG) is included between the TSL fault and the Guadalupe Fault. SL-T is considered as a wide shear zone by the authors. White square represents the area mapped by Loza-Aguirre *et al.*, (2005). Taken from Loza-Aguirre *et al.*, (2005).

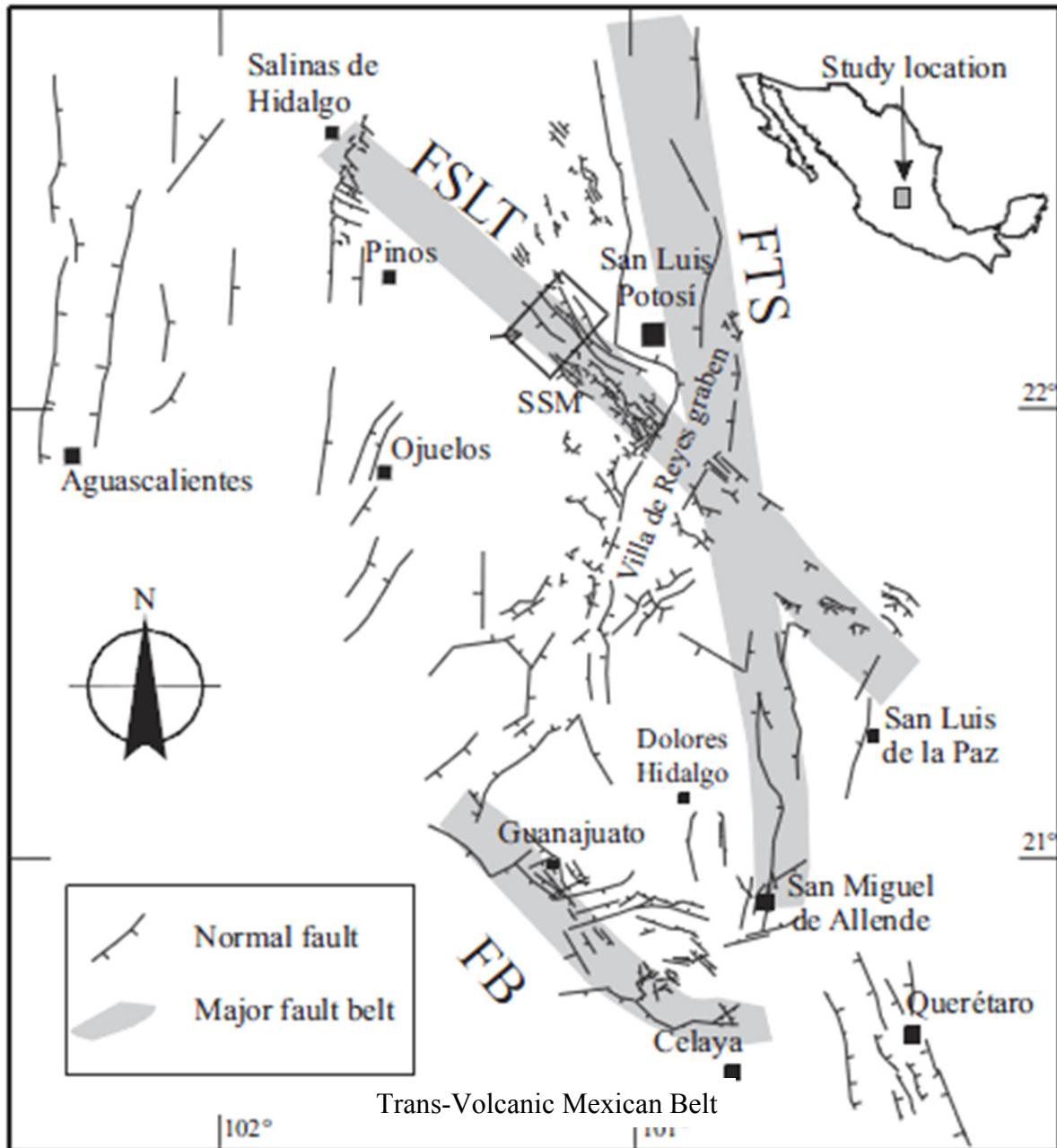


Figure 2.15 Map of Central Mexico showing the Trans-Volcanic Mexican Belt; El Bajío Fault (FB), the Villa de Reyes Graben and the intersection between the Tepehuanes fault (FSLT) and the Taxco-San Miguel de Allende fault system. (FTS). Modified from Xu *et al.*, (2008)

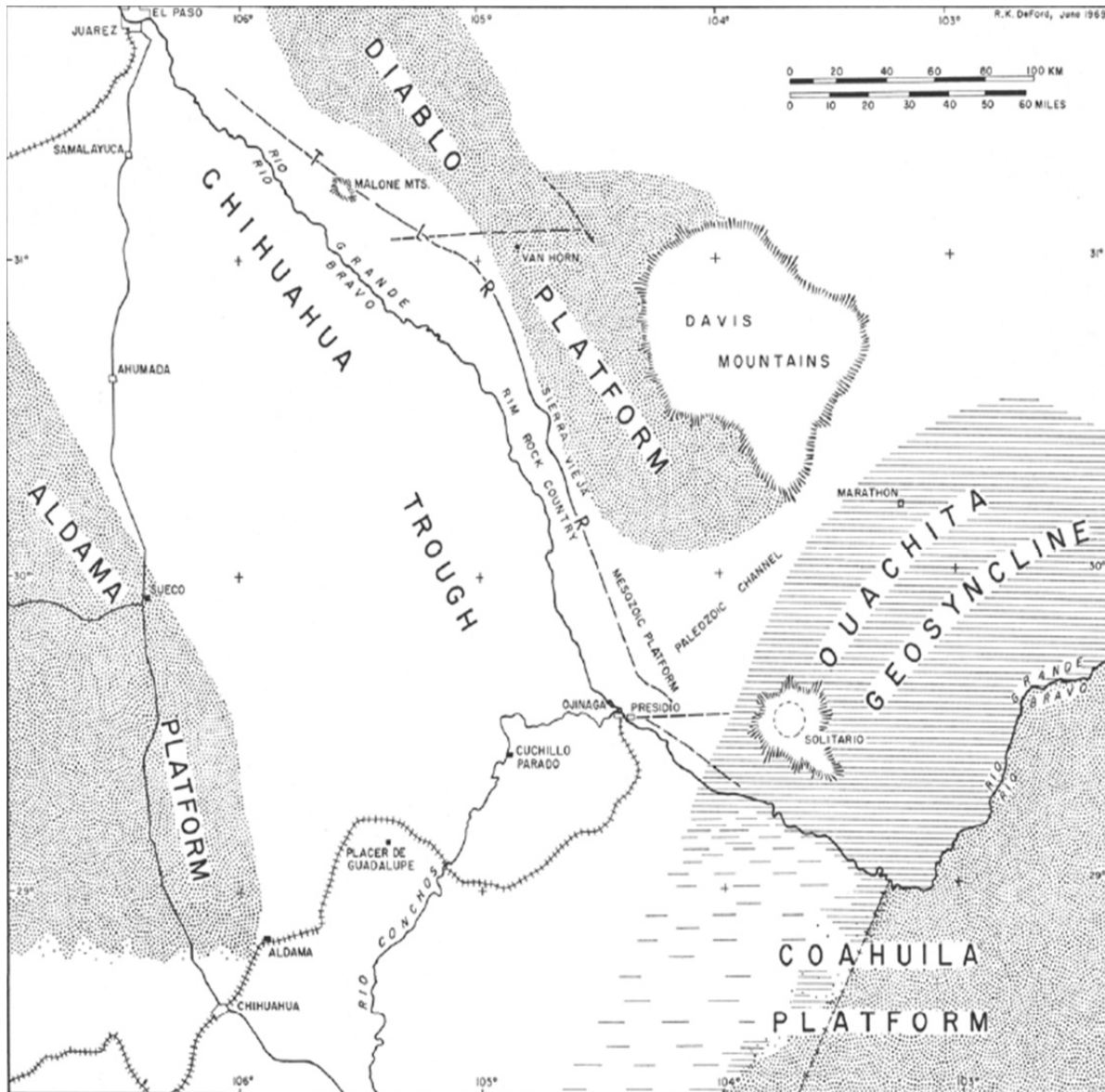


Figure 2.16 Map shows the Texas Lineament between the Rio Grande and the Diablo Platform. Taken from DeFord (1969)

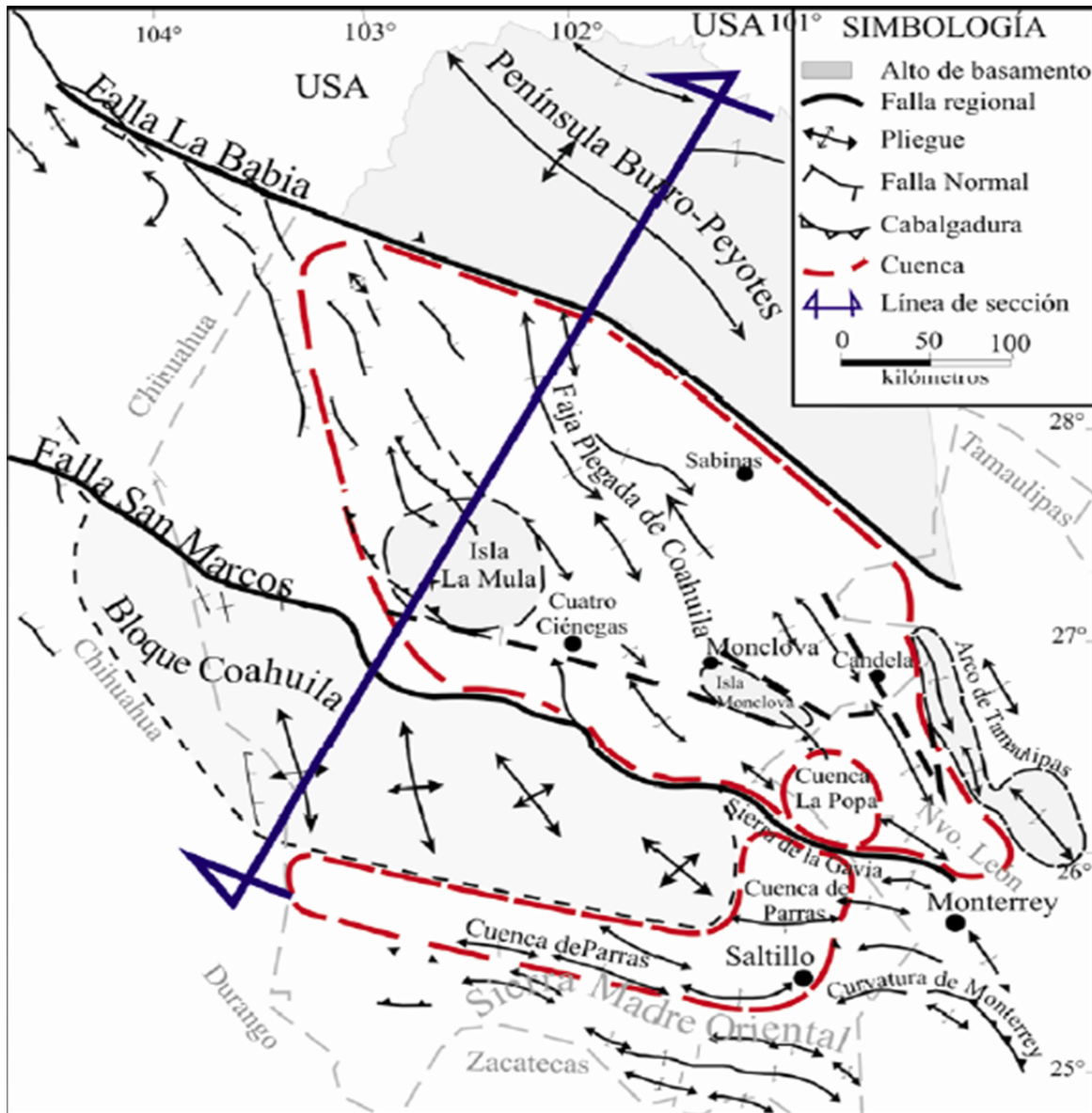


Figure 2.17 Map of La Bafia & San Marcos fault systems. Strike of the axes of the folds shows a left-lateral motion. At the bottom, faults and faults are parallel to the Sierra Madre Oriental. Taken from González-Sánchez (2008)

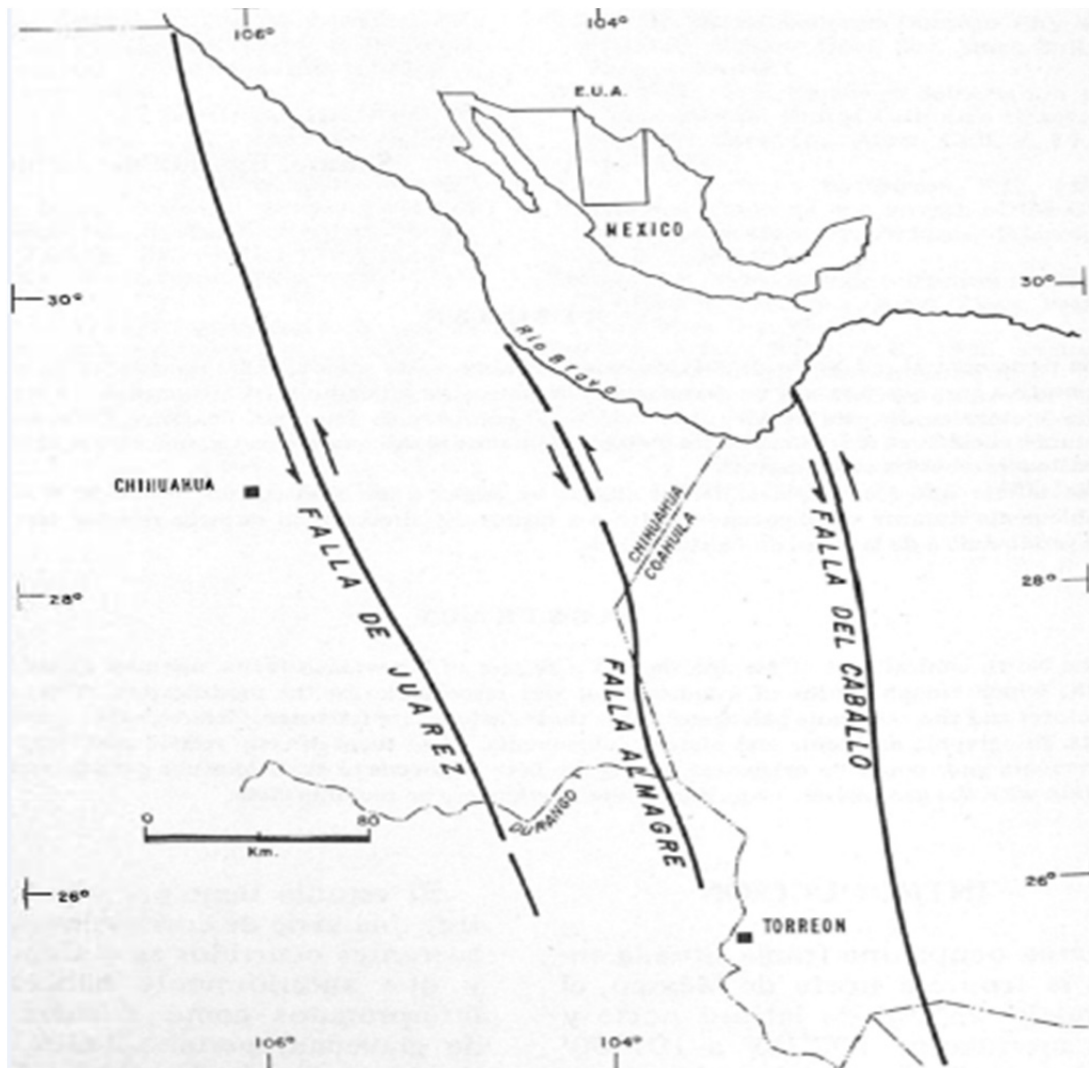


Figure 2.18 Map of El Caballo, Almagre and Juarez fault systems. The one in the middle is a right-lateral strike-slip fault according to the manuscript, while the others are left-lateral strike slip faults. Taken from de Antuñano (1984)

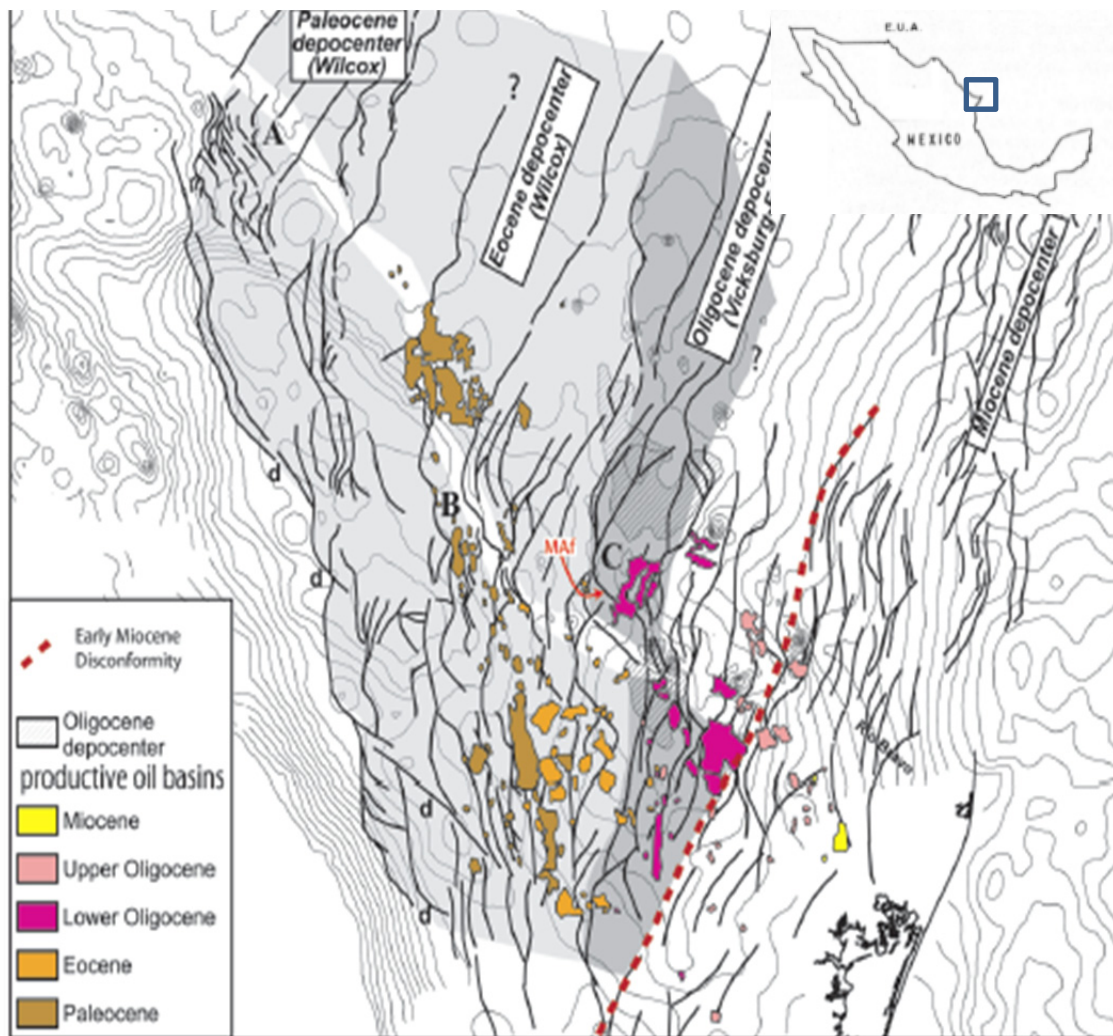


Figure 2.19 Map shows the Vicksburg-Frio Oligocene depocenter displacement by a left-lateral strike-slip fault (not shown). Location in upper right corner. Taken from Flotté *et al.*, (2008)



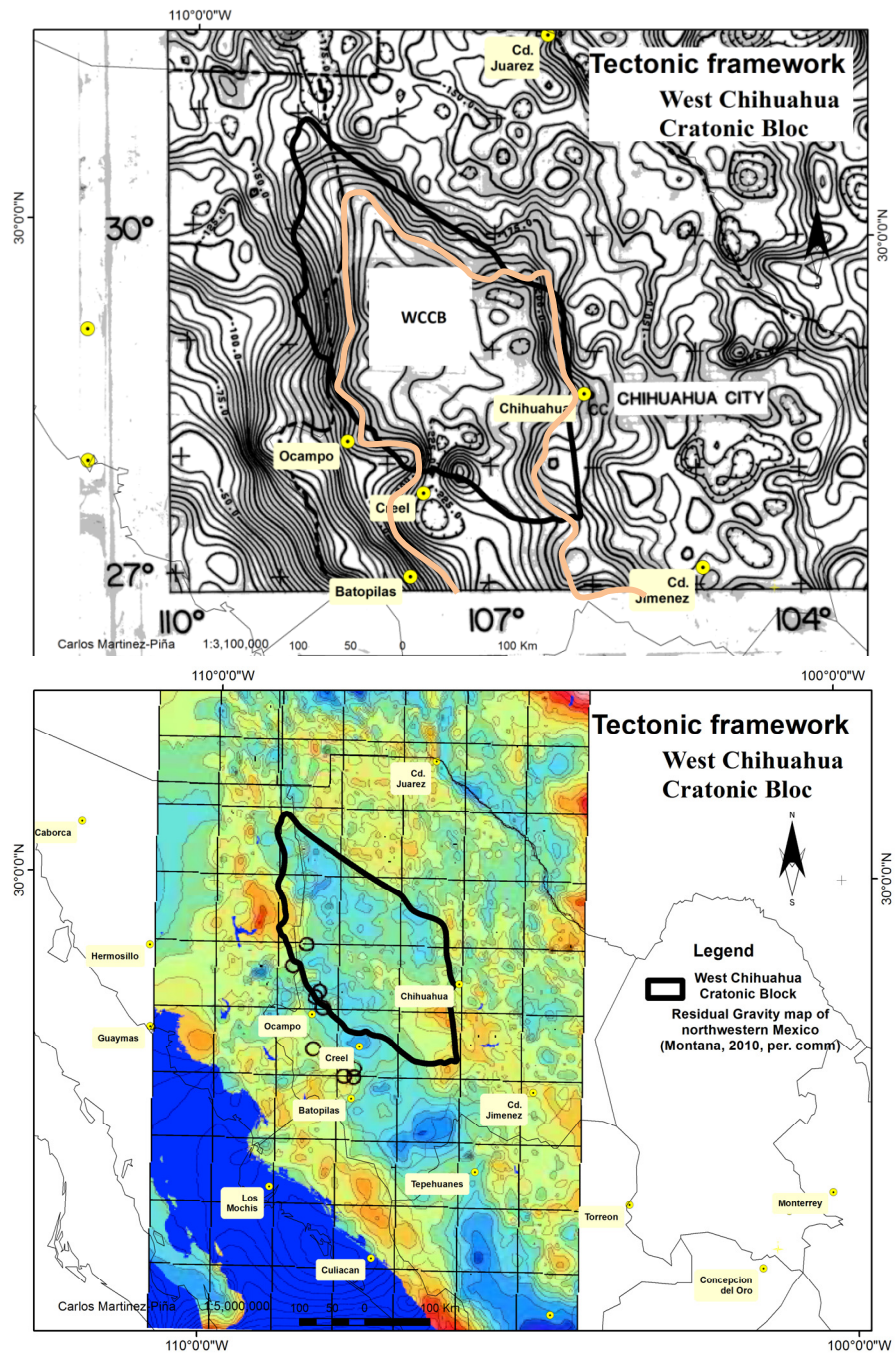


Figure 2.21a and 2.21b shows the Bouguer map and the residual map of northern Chihuahua. Upper figure (21a) shows the contrast with adjacent regions and orange line depicts the -190 miligal contour used to define the WCCB. Black line is the geomorphological outline of the Block. Below figure (21b) shows a residual gravity map by Montana (2010, pers. comm.) Outline of the block could either stretch south of Creel, or a small block should be considered

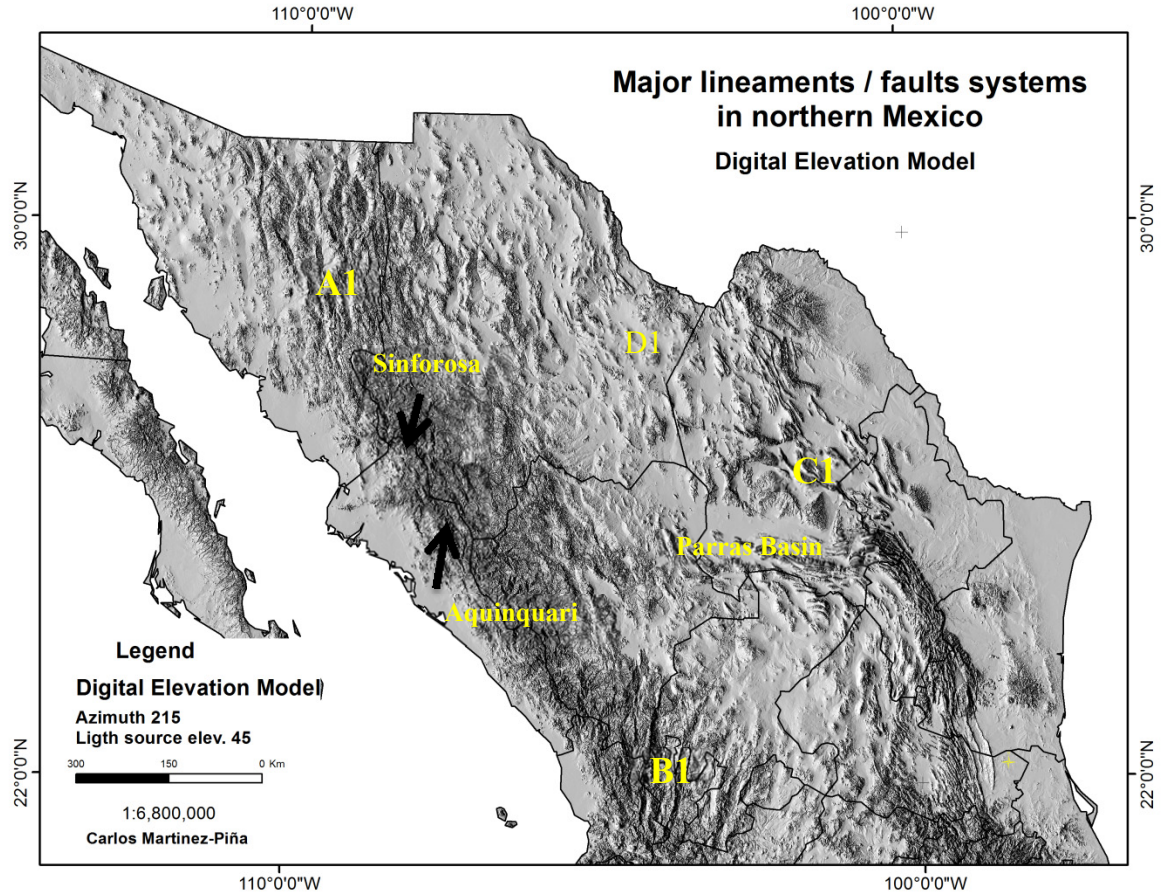


Figure 2.22 Digital elevation model: azimuth  $150^{\circ}$  and light source at  $30^{\circ}$  above the horizon line. showing the Sinforosa and Aquinquari lineaments. Both crosscut the SMO and are parallel. Lineaments in A1 strike NNW, while in B1 lineaments strike NNE. Between A1 and B1, a third ENE system is present. C1 depicts the Coahuila cratonic block. Below C1 the Parras Basin. D1 shows the NE Alamos fault and NNW faulting. Due to the change in azimuth and elevation of light source, details not seen in one model outstand in the other.

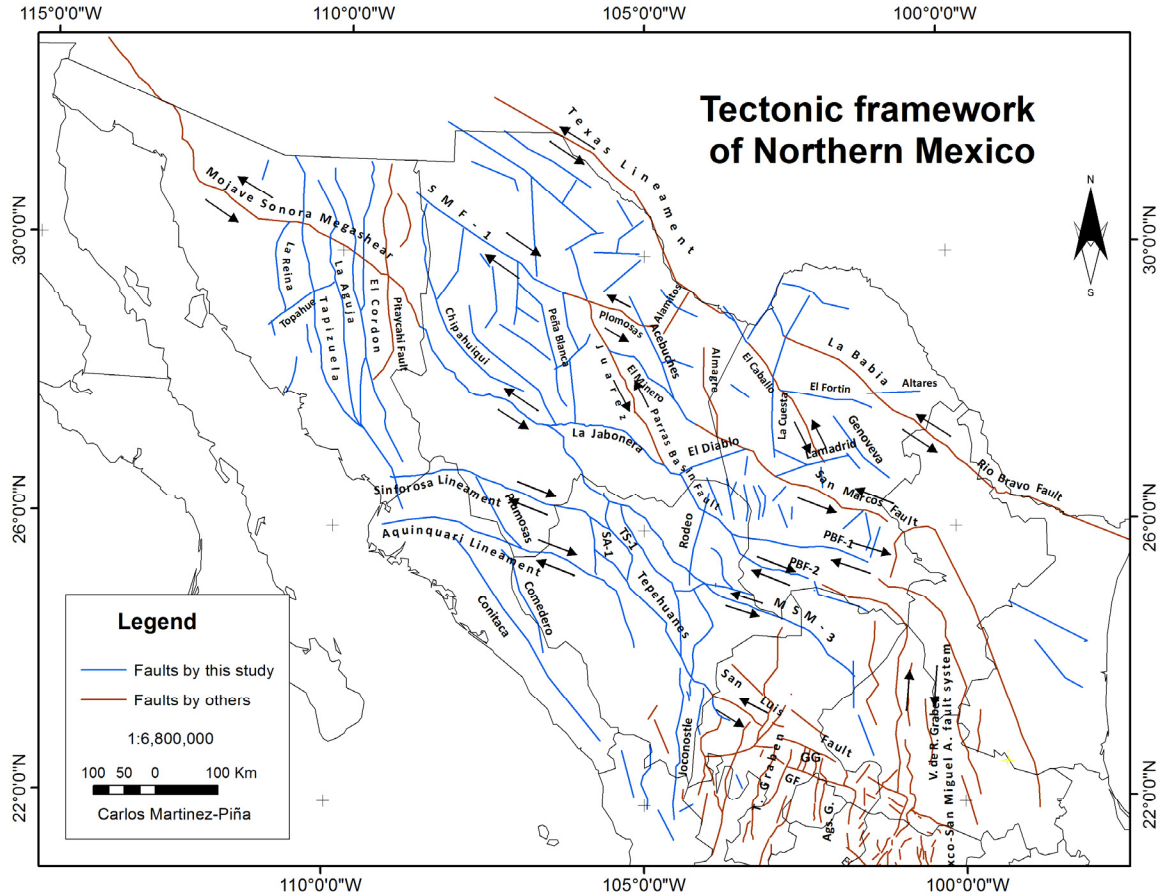


Figure 2.23 Tectonic framework map of northern Mexico showing known lineaments/fault systems and proposed lineaments, and connections. Mojave-Sonora-Megashear, San Marcos, La Babia, Rio Bravo, Texas Lineament and Tepehuanes fault system constitute the TeMeBa system. Proposed lineaments: Sinforosa, Aquinuari; MSM-3, PBF-1, and PBF-2 are proposed alternatives to the southeastern MSM trace, by ordinal order of importance. Parras Basin Fault proposed as part of the Juarez Fault, with either PBF 1 or 2 as the southeastern extension. TS-1 is a proposed connecting segment between the Tepehuanes-San Luis fault system and MSM-3. La Jabonera is a proposed connection segment between MSM and PBF. Las Plomosas is the prime proposed connecting segment between the SMF and SMF-1. El Minero and Juarez segments are proposed alternate connecting segments between the SMF and SMF-1. La Plumosa is a proposed connection between Sinforosa and Aquinuari lineaments. Comedero fault segment between Aquinuari and Conitaca Lineaments. Aguascalientes=A; Caborca=Co; Cd. Juarez=Cj; Cd. Jimenez=J; Culiacan=Cl; Concepcion del Oro=Cdo; Durango=D; Fresnillo=F; Guadalajara=G; Guaymas=Gy; Guanajuato=Gt; Hermosillo=H; Los Mochis=Lm; Mazatlan=Mz; Monterrey=Mt; Ocampo=Oc; San Luis Potosi=Slp; San Blas=Sb; Saltillo=S; Sombrerete=Sm; Tepic=Tc; Tepehuanes=Tp; Torreon=To; Zacatecas=Z



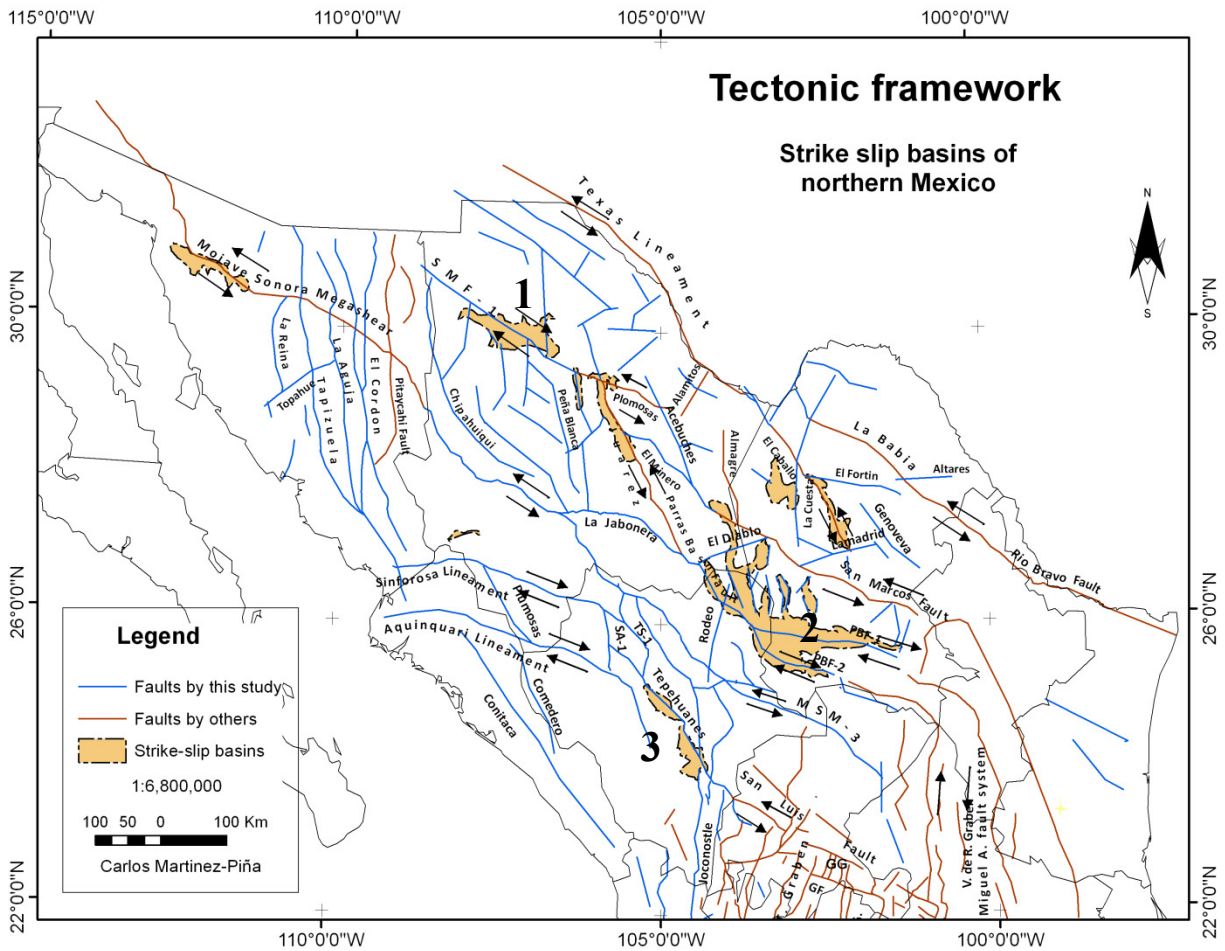


Figure 2.25 Map shows the strike slip basins 1) Marcos Basin- 2) Parras Basin 3) Durango Basin, defined by Martínez-Piña and Goodell aligned along 2-NW and S-1 from figure 24, related to low-strength shear zones.

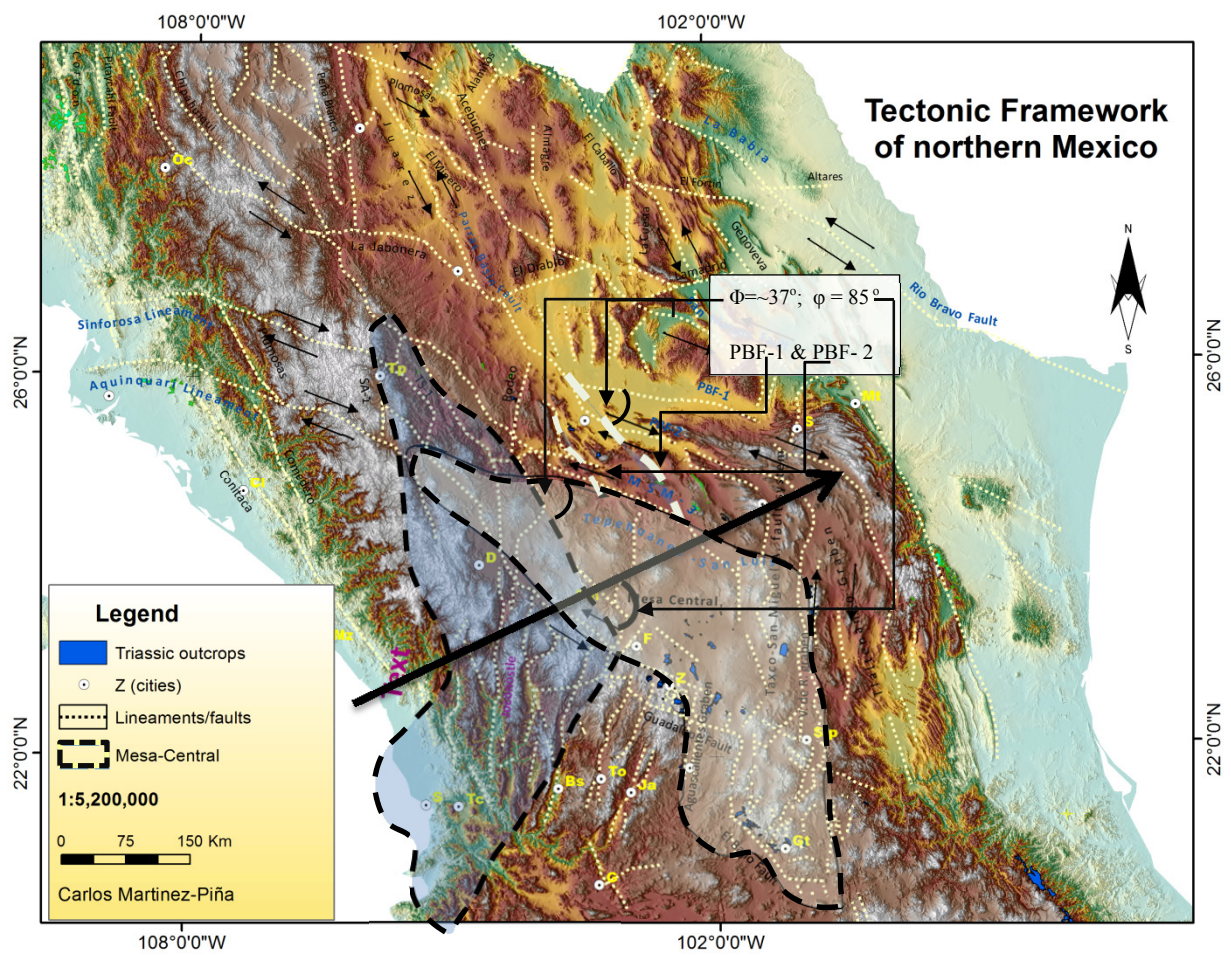


Figure 2.26 Shaded relief shows palinspastic restoration of PBF-1, PBF-2 (white dashed lines) and Mesa Central (blue). Angle of rotation is  $\sim 37^\circ$ . Black arrow represents the regional tectonic transportation vector almost orthogonal to the northern boundary of the restored MC. Angle between the north boundary of the MC and the compressive stress axis is  $85^\circ$ .

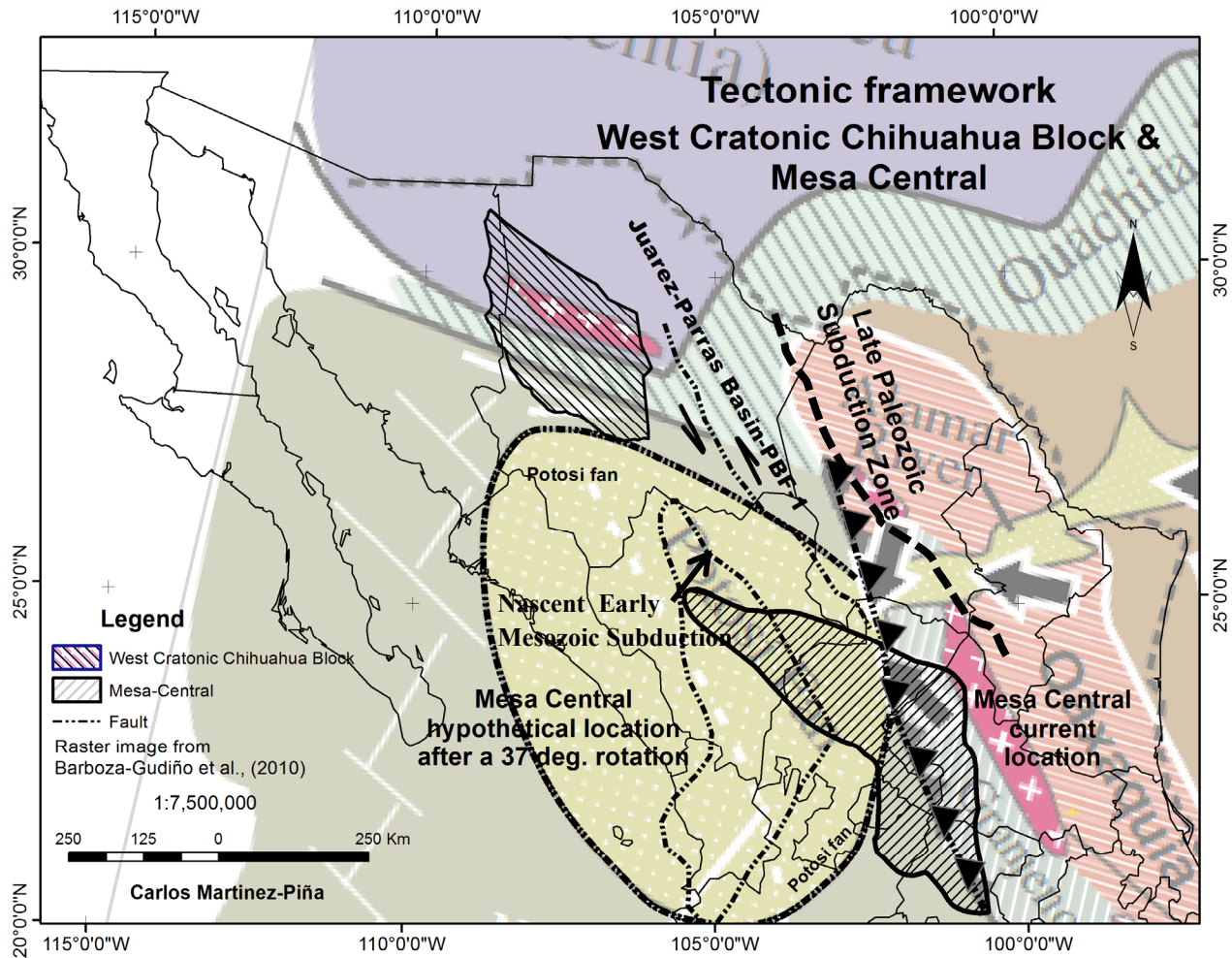


Figure 2.27 Composite map shows the location of the Potosi Fan, Mesa Central and the West Cratonic Chihuahua Block. It also depicts the hypothetical location of the Juarez-Parras Basin-PBF 1 and 2, and the Mesa Central (MC) after a 37 degree rotation that places it directly under the Potosi Fan. The Late Paleozoic subduction zone is to the north of MC while a Early Mesozoic subduction is to the south. South boundary of the WCCB and north boundary of the MC are in line. Map based on Barboza-Gudiño *et al.*, (2010)

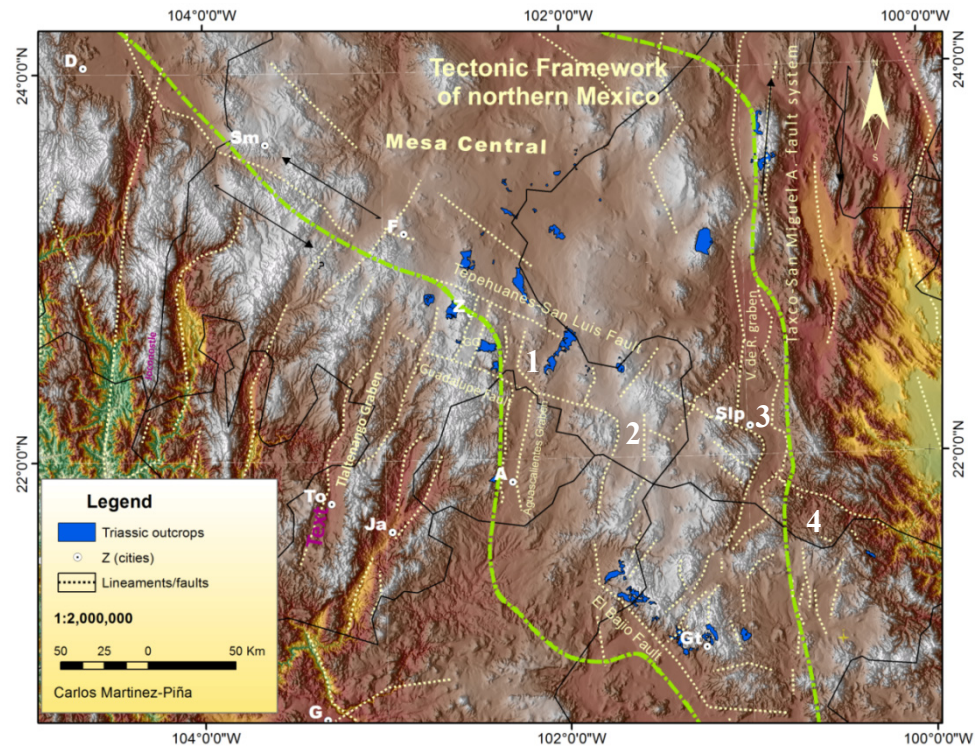
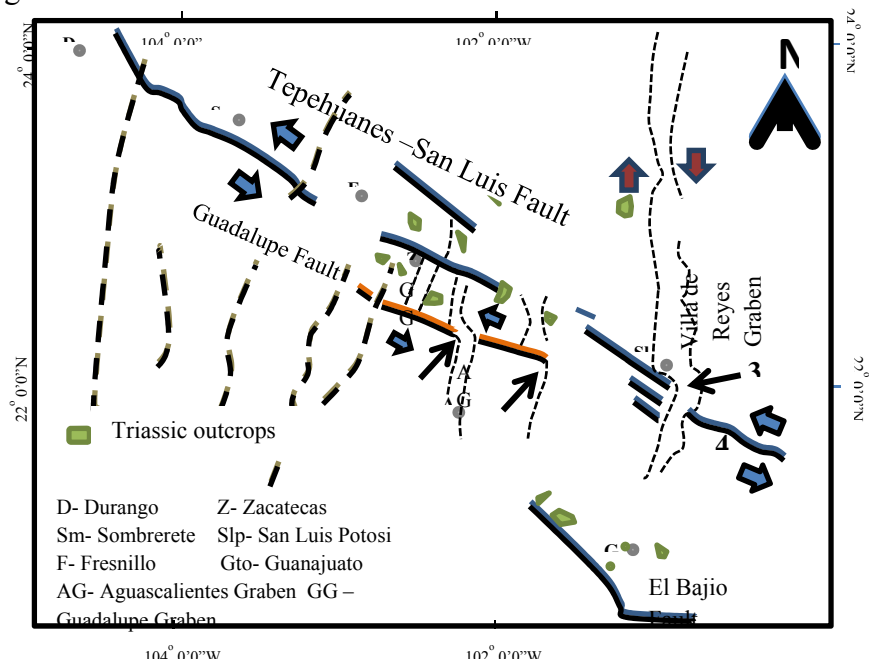


Figure 2.28 Shaded relief shows the Tepehuanes-San Luis and the Guadalupe faults. Numbers depicts the Aguascalientes Graben (1), the Villa de Reyes Graben (3). Both grabens are parallel and displaced by left lateral strike-slip faults toward the SE. In between these two, there is another graben with the same tectonic characteristics. In site 4, the TSL was displaced south by the right lateral strike slip Taxco-San Miguel de Allende fault.



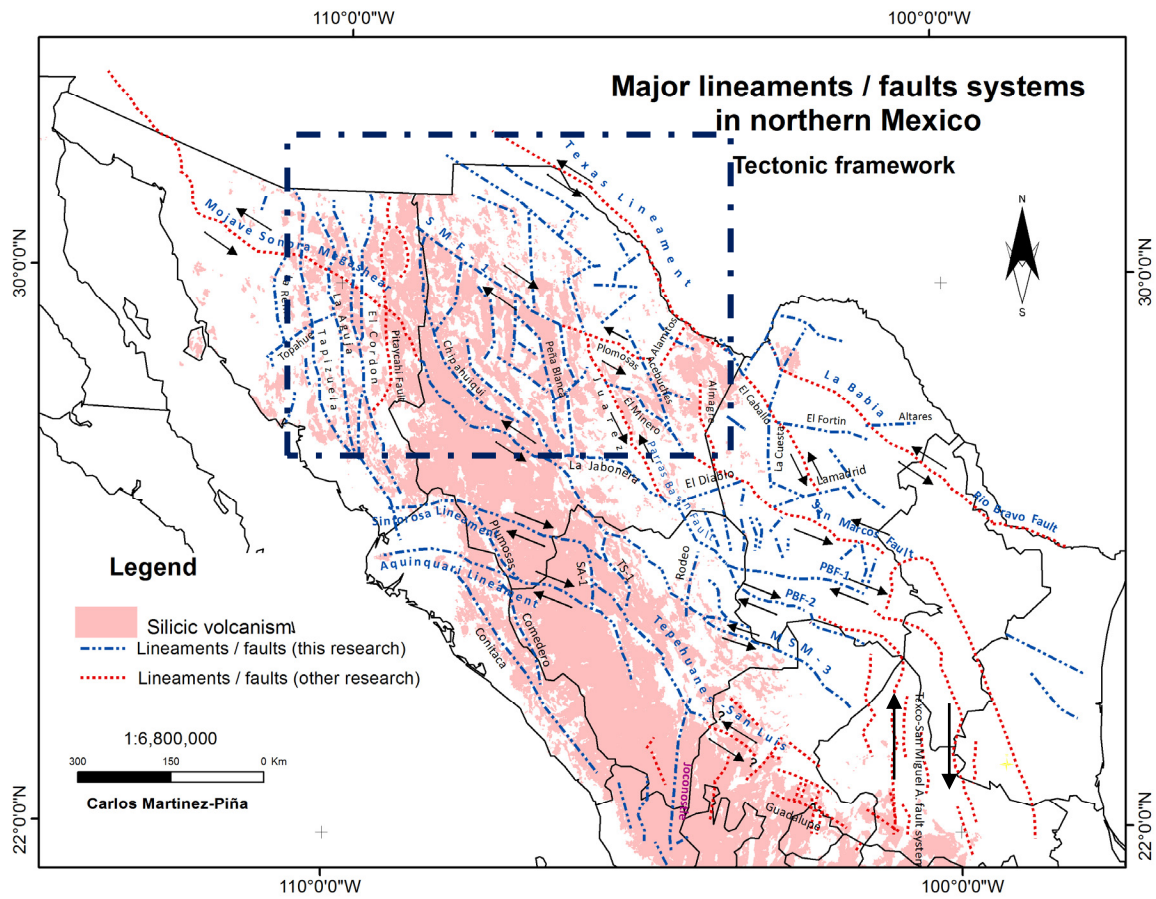


Figure 2.29 Shows the solid body of the silicic province of SMO and the severe dispersion of blocks within the inset. SMF-1 marks a strong change in slope towards the north; scattered low ranges of rhyolites. Reactivation of parallel strike-slip faults

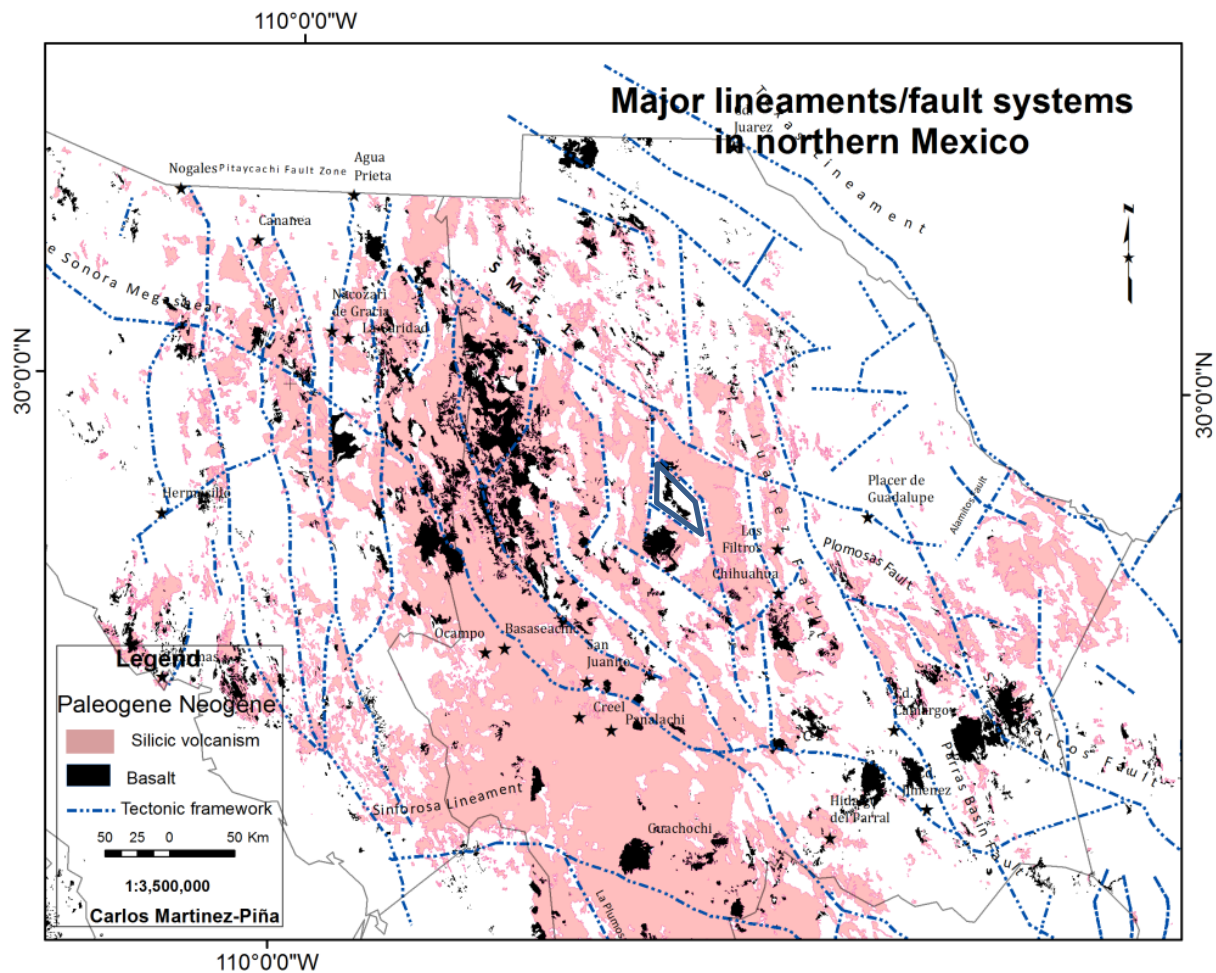
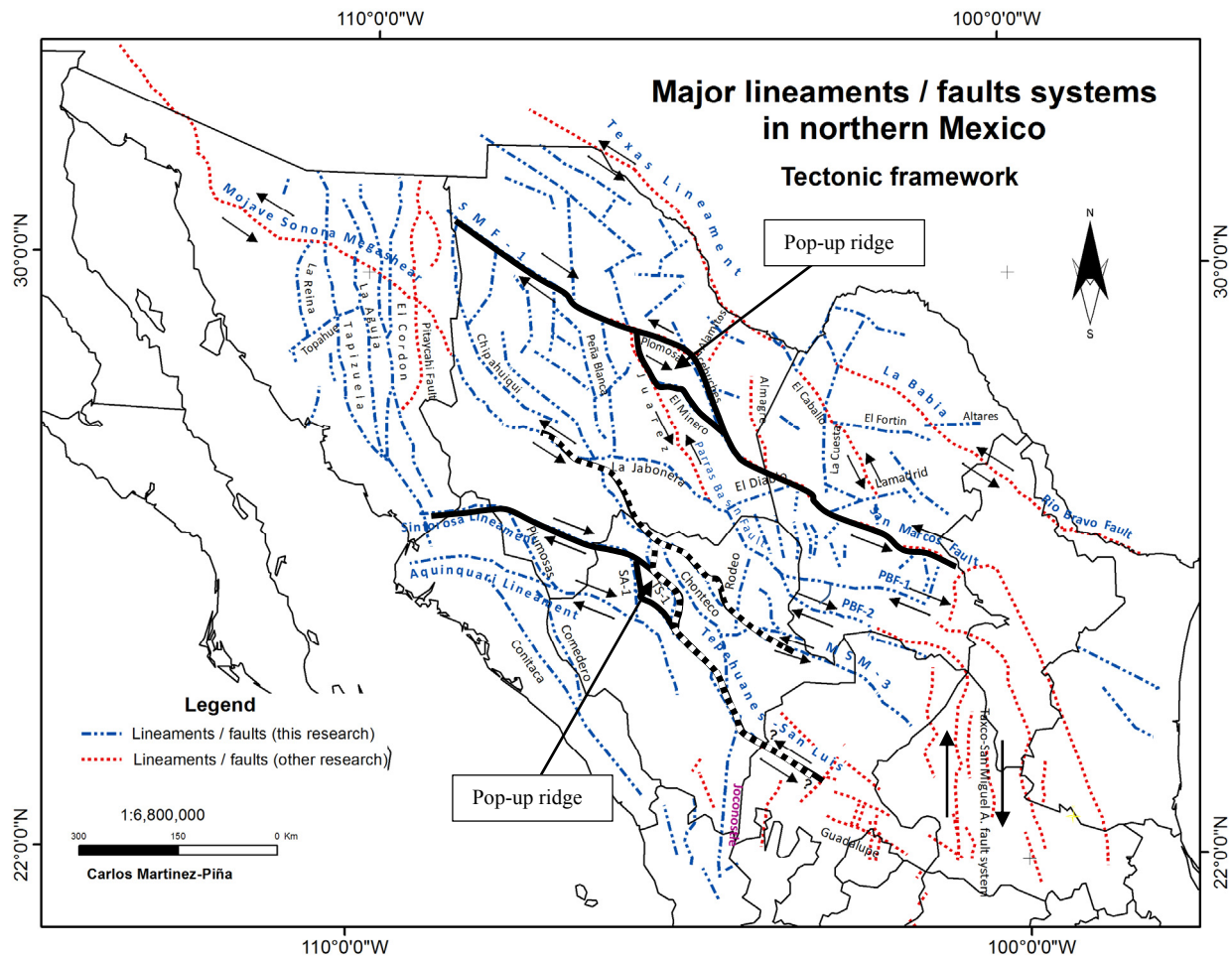
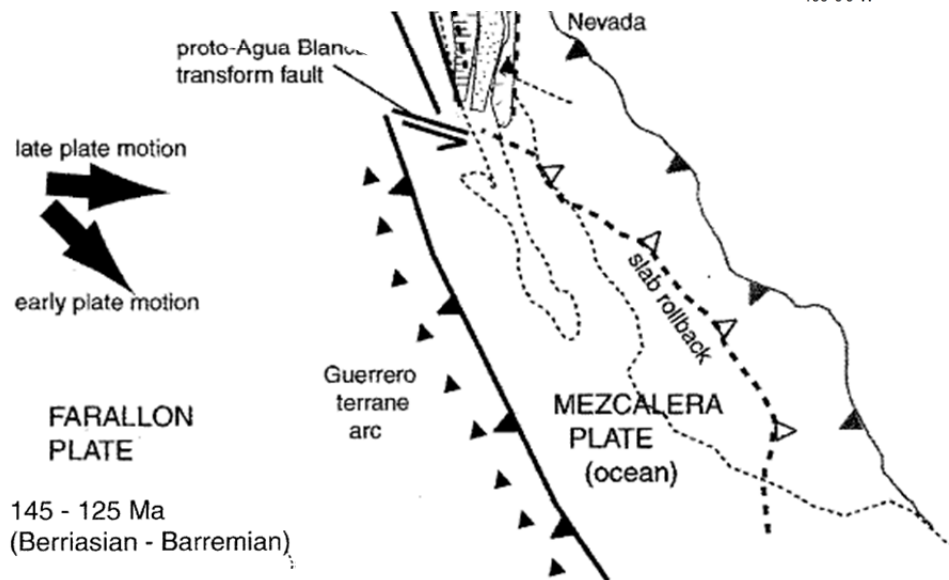
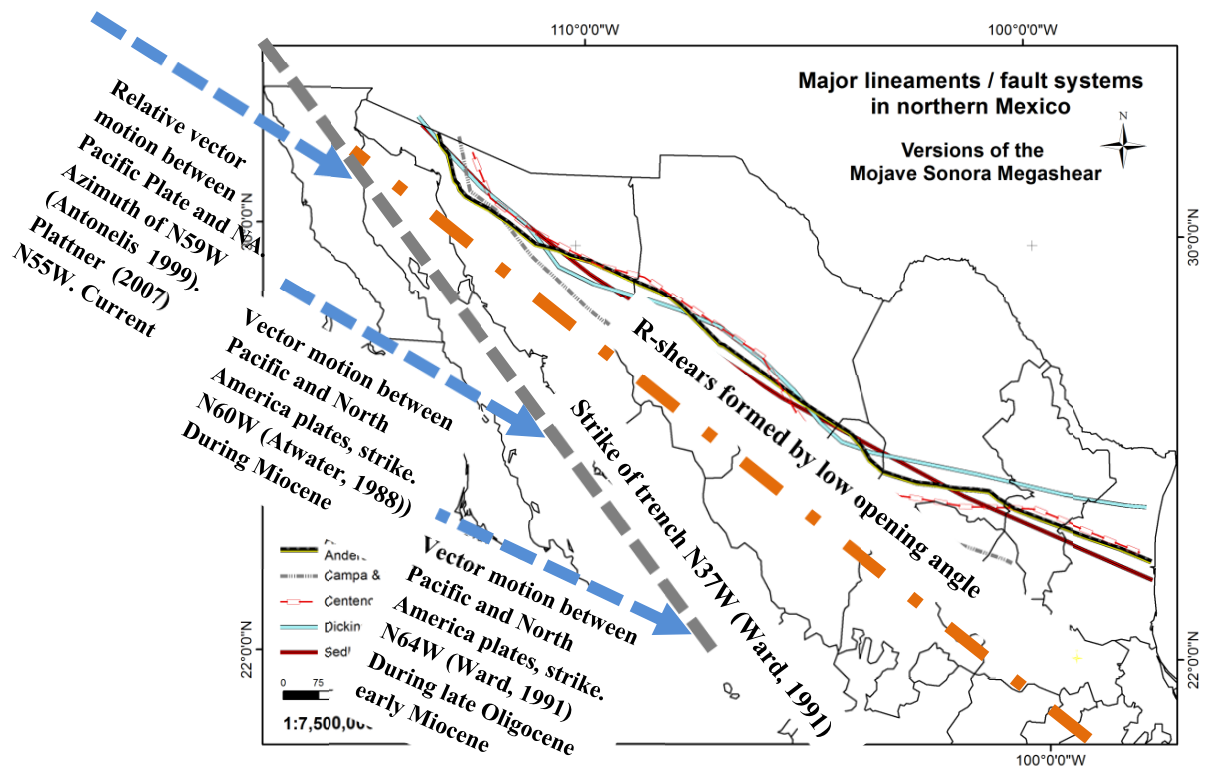


Figure 2.30 Enlargement of inset in figure 23, shows basalt outcrops along faults evidencing the extension regime described in figure 28. Pull-apart basin shown in blue lines in center of map, is prior to extension.





## **Chapter 3 Do stable blocks and mobile belts exist in the southwestern North American Proterozoic craton?**

### **3.1 Abstract**

Stable blocks and mobile belts characterize the well exposed Precambrian regions of the world. These features are superimposed upon and sometimes concordant with Precambrian age provinces. In the southwestern portion of the North American Proterozoic craton the age provinces are well documented, but the stable block versus mobile belt idea has not been put forth or emphasized. The present study combines data of several types to evaluate this behavior in southwestern North America.

It is proposed that a Proterozoic cratonic block is present in west central Chihuahua state, here named the Western Chihuahua (Proterozoic) Cratonic Block (WCCB). Bouguer gravity anomalies are effective for identifying regional cratonic blocks, and negative anomalies near -200 milligals are strongly suggestive of a cratonic block; the spatial extent of an anomaly is useful information, and difficult to provide otherwise. A granitic, cratonic character of the WCCB is suggested by elevated initial strontium ratios. Sedimentological, structural, and geochronologic data are used to test the presence of the WCCB. The presence of the WCCB is consistent with a wide variety of data.

The recognition of a new block, WCCB, requires verification from regions adjacent to the block, the mobile belts. Such regions surround the block on three sides. Data begins at 1.4 Ga, and an interplay of sedimentological, structural, and igneous activities is documented over time. Negative, depositional areas have variously been called basins, troughs, and aulacogens, and they may contain thousands of meters of sediments or evaporates, and they may have different names for each geologic era. Igneous activity may be bimodal volcanism dominated by

mafic rocks, and A type granites on the rift shoulder, and metamorphic core complexes. The spatial distribution of these features and others, defines the locations of the mobile belts. Over the geologic time of several Wilson cycles, mobile belts may participate in compression (subduction), extension (rifting), and transform (lateral) faulting. The WCCB most logically was derived from closely adjacent, North American Proterozoic craton to the northeast, by mobile belt action.

The recognition of the new cratonic block, the WCCB, aids in the definition of the mobile belts of the southwestern North American Proterozoic craton. The application of these ideas provides a better understanding of the geological evolution of the region, and in the location of resources.

### **3.2. Introduction**

Cratonic geology identifies two major types of geological features, stable blocks and mobile belts. This is best illustrated in Africa and Canada, where large regions of Precambrian granitic gneisses and intrusions form older, thicker, more stable blocks. Adjacent regions form bands or belts around the stable blocks, and they contain thick metasedimentary and volcanic sequences, may contain greenstone belt sequences of ancient oceanic crust, multiple island arcs, and represent multiple periods of deformation; these are the mobile belts. They represent the result of multiple Wilson cycles.

Throughout most of the US, Precambrian rocks are buried under vast thicknesses of younger rocks. The southwestern USA has a modest, but significant amount of Precambrian outcrop, and they have been well studied, as summarized in Karlstrom *et al.*, 2004. From southeastern California to west Texas several provinces have been identified and geochronology

studies show that they are younger to the southeast. They trend to the northeast, and have transitions with each other and subprovinces.

The physiographic/geologic overview of the area of interest is the following, and a location map is given in Figure 1. From the east to the west, the area of interest extends from the Great Plains of west Texas to the Basin and Range Province of West Texas and Chihuahua, to the northern Sierra Madre Occidental igneous province in Chihuahua, and on to the Basin and Range of Sonora. To the north of the Basin and Range of New Mexico and AZ is the Colorado Plateau. The geologic history of the area is variable, and will constitute some of the subsequent discussion. A large portion of the region is covered by young sedimentary or volcanic rocks. Documentation of the geologic record begins with the sparse Precambrian rocks in some areas, with the Mesozoic and Cenozoic exposures being progressively more abundant. PEMEX drilled 29 petroleum tests in Chihuahua during the period 1965 - 1980, and those results are integrated into data and ideas presented here.

The present study proposes the application of the “stable block/mobile belt” model to northern Mexico and the southwestern US, in order to better understand and define the North American craton and its history. The location and geologic history of the southwestern boundary of the North American craton is a subject of considerable controversy and interest. The Colorado Plateau is an example of a stable, cratonic, block in the region.

### **3.2.1 Hypothesis**

In the present study the hypothesis to be tested is that a relatively stable cratonic block is present under western Chihuahua, the Western Chihuahua Cratonic Block (WCCB), and that it is surrounded at least on 3 sides by mobile belts. The northern Sierra Madre Occidental (SMO), a

siliceous large igneous province (SLIP) (Busby *et al.*, 2004) is superimposed on the WCCB. The presence of the WCCB is supported most convincingly by gravity studies; with its large, negative gravity anomaly. After a brief geological overview of the region, details of the gravity studies will be presented and discussed. Subsequently, the petrology, structural setting, geochemistry, and geochronology of all, although few and minor Precambrian occurrences in the region will be discussed, and other relevant regional geological features will be presented. The prominence of repeated basinal features is documented on tables and figures.

### **3.4. Regional Precambrian Provinces**

The distribution of Precambrian provinces within the southwestern portion of the North American Proterozoic craton (Laurentia) remains a matter of debate, although there is also a broad agreement on certain aspects. Some features of those studies are relevant here, Figure 2 (Karlstrom *et al.*, 2004). Within SW Laurentia, Precambrian age-provinces strike northeast, and are progressively younger from the W (Mojave Province, SE California) to the E (Yavapai Province). From S AZ and NM and into W TX, Precambrian rocks are of the Mazatzal Province, 1.7-1.6 Ga, but in W TX, they are overthrust by rocks of the Grenville Province, 1.3-1.0 Ga, from the SE. Each major province is made up multiple accreted island arc complexes along with occasional batholithic masses, and separated by major sutures. Wilson cycles involved continental rifting, leaving the third arm of triple junctions as aulocogens into the cratonic interior. These zones of weakness have repeated activity, with extensional, A type igneous activity on the rift shoulders, and later, compressional tectonism over time. Regions evolved from active accretionary margins, to crustal assembly and underplating, to a tectonically active continental, cratonic, interior, after 1.45Ga.

Features of interest here are of 3 types (Fig 6). 1) Mafic magmatism can be indicative of rifting, 2) A- type felsic magmatism occurs on rift shoulders, and 3) the sedimentological assemblage of sandstone, arkose, form within rift basins. Mixtures of 1 and 2 produces bimodal character. Figures 2 and 6 show a significant concentration of the features within certain zones during the Precambrian.

For data type 2, at 1.4 Ga and again at 1.1 Ga, Laurentia experienced widespread granite/rhyolite magmatism, anorogenic or A type granites, often associated with extension (Anderson, L. J.,1983; Bickford *et al.*,2000, Stewart 2001). The 1.4Ga event represented the first major tectonic event to affect the newly assembled Proterozoic lithosphere. Subdivisions of these regions can be made (Van Schmus *et al.*, 1996; Barnes *et al.*,. 1999). Activity was focused along preexisting lithosphere boundaries or zones of weakness. In Figure 2 they can be found from SE CA in the AZ Transition Zone-TX Lineament SE to El Paso, TX, and then N in a narrow zone to north central CO. At 1.1 Ga these features were more focused. The Lake Superior rift (1.1 Ga) became the Mid Continent (MC) rift which was mapped in the subsurface southwest to Kansas, where it is still striking roughly southwest. That general strike would continue towards El Paso, TX. From subsurface studies, widespread granite/rhyolite regions take over from the MC rift, or hide it, to the southwest. The 1.4 and 1.1 Ga igneous activity has exposures from W TX N to Wyoming, and N60W to SE CA. The Franklin Mts., TX, and Pikes Peak, CO, were part of this younger activity (Karlstrom *et al.*,2004).

For data type 3, the widespread presence of a quartzite-arkose-bimodal volcanic association in S NM at Pajarito Mt (Kelley, 1968) and central AZ , Apache Group, (Karlstrom *et al.*,2004) and west Texas ( Castner, Mundy basalt breccias, and Lanoria quartzites), with ages of 1.7, 1.4, and 1.1 Ga, defines a NW trending zone of extension. A compilation by Hammond

(1984) of the ages and locations of Middle Proterozoic basaltic rocks of North America reveals a relatively tight space and time group, trending NNW across AZ between 1.15 and 1.04 Ga. These are indicated in Figure 6. The Precambrian processes which produced widespread felsic igneous regions have global analogues such as the Pan African geological event at 0.6 Ga.

The discussion above concerns the nature of the Proterozoic cratonic provinces in the southwestern USA. This information cannot reliably be carried across the international border into Mexico, except maybe in northwestern Sonora. Very few Precambrian rocks are known in Mexico, but this has not hindered widespread speculation.

### **3.5 Coherence of crustal material**

Within the Precambrian age provinces there exist dramatic variations in the coherence and thickness of the North American craton. Crustal coherence is high and the crust is thick under the Colorado Plateau and the Great Plains east of Socorro, New Mexico where there are gravity values of -220 milligals and a cratonic thickness of 50 km. The Colorado Plateau has -225 milligals and an average crustal thickness of 50 km. To the south and southwest of the Transition Zone in Arizona the crust has been disrupted, such that the Moho has a depth of only 25 km at Tucson, and decreasing to 20 km northwest to the border with California (Howell et al 1985). Southeast from Tucson along this trend of disrupted crust into southwestern New Mexico and into northern Chihuahua, the crust is thin. The Moho is at 22 km under Villa Ahumada, 125 km S of El Paso, TX. A geophysically and geochemically distinct cratonic fragment underlies the Diablo Plateau-Perdenal Uplift.

Howell et.al 1983 reported on a continental scale crustal cross section (Corridor C-3) through a part of the region. Zones are distinguished as continental, cratonic crust, such as the

Great Plains east of Socorro NM., with a gravity values of -220 milligals, versus an extended crust, such as in the Basin and Range. The corridor of study did not cross the Colorado Plateau, and the report documents extended crust throughout its trace across Arizona.

### **3.6 Gravity**

Gravity is a data type that enables identification of a distinctive feature, and its lateral dimensions. It is referred to here because it is optimal in its widespread coverage, and it is successful in identifying a large negative gravity anomaly. Other data types will then be used in an attempt to explain the anomaly. The data presented here was processed as a part of earlier studies (Goodell *et al.*, 1986; Handschy *et al.*, 2005), but some details of that processing are given here. The Bouguer gravity map of northern Chihuahua and adjacent regions is given in Figure 3.

The gravity data used here is a subset of a gravity data base resulting from the contributions of many individuals and organizations. Gravity readings are tied to a common gravity Datum (IGSN-71; Morelli, 1976), the elevation Datum for the gravity stations is sea level, and a density of 2.67 g/cm<sup>3</sup> was used in the Bouguer corrections.

The gravity data base consists of 16,873 readings, after purging the original data to produce a minimum spatial separation of 6 km. A grid with a grid interval was then constructed from the data by a program that uses a minimum curvature technique to interpolate values for each grid node (Briggs, 1974). This grid was then smoothed and contoured by the Surface II Graphics System (Sampson, 1978). Smoothing of the grid is accomplished by an arithmetic averaging of a central grid node value with surrounding grid node values over the adjacent two rows and columns. The surrounding grid node values are given an inverse distance squared

weight. Smoothing of the contour lines is done by piecewise Bessel interpolation within the grid cell and does not affect the grid node values. The polynomial surface and residual gravity maps were constructed by using a least square polynomial surface program (Lance, 1982). This program filters a grid to produce a polynomial surface approximation. These grids were then smoothed and contoured. The resulting map is shown in Figure 3.

Tectonic features in Figure 3 of familiar regions of West Texas have readily identifiable gravity signatures, and several features are labeled, including the Diablo Plateau (gravity low), several west Texas oil & gas basins, and the Paleozoic Ouachita orogenic belt.

To the west in Chihuahua, elliptical shaped areas of linear trends of highs and lows gravity values delineate the Basin and Range Province/Rio Grande rift of northeastern Chihuahua. These linear features have a N-S trend south of 30°N (El Sueco), and a NW trend north of 30°N. This region becomes the Basin & Range (B&R) of SW New Mexico and continues NW across central Arizona, south of the Transition zone and the Colorado Plateau (CP). Northwest of El Paso is the Mogollon-Datil volcanic plateau, which has a broad, uniform, negative anomaly of -225 milligals. The CP is expressed as a broad, relatively uniform, negative gravity of -200 milligals.

To the west of the B&R of eastern Chihuahua and to the south of the B&R of northern Chihuahua, is a contrasting region consisting of much more uniform and negative values. This large area has distinctive gravity responses, with values less than -200 milligals. This area has a negative gravity anomaly comparable to those of the Datil/Mogollon, Colorado Plateau, and the North American Interior Craton. This region is identified as the Western Chihuahua Cratonic

Block (WCCB). The -200 milligal contour will be lifted from this diagram for use elsewhere as the dimensions of the WCCB.

The eastern boundary of the WCCB is well defined. From Chihuahua City it trends north, extending 150 km north to nearly El Sueco at 30°N, from where it extends NW. Part of this N-S distance is along the Encinillas Graben within which Highway 45 is present. Topographic highlands form the Sierra del Nido to the west and the high plateau continues west to the main mass of the SMO, approximately 200 km to the west. The eastern boundary can be seen in the east-west cross section (figure 15, Aiken *et al.*, 1981,) as a steep transition towards a gravity deficiency to the west. Gravity values vary from -150 on the east to -225 milligals across the boundary on the west. The NE boundary of the WCCB is the NW striking zone of large gravity gradient trending NW from the north end of the Encinillas graben, south of El Sueco. This WCCB boundary trends northwest towards the border with Sonora, along a recognized geomorphic boundary. The NW terminus of the WCCB occurs over an area near the Chihuahua-Sonora border, approximately 150 km south of the SW New Mexico panhandle or bootheel.

The western boundary of the WCCB is indicated in Figure 3 as a prominent zone trending to the south with gravity values monotonically increasing to the west and southwest from values of -200 milligals in the WCCB. The data processing techniques correct for topographic expression. This western boundary is also the region with the lowest density of gravity stations, resulting in less knowledge of the details of the geophysical behavior. The regional behavior however is thoroughly constrained by the data set, and this western boundary of the WCCB is a reliable geophysical feature. West of the northern portion of the WCCB is the B&R of Sonora and further west is the Caborca Block. West of the SW portion of the WCCB is the coast of the Gulf of California (Sea of Cortes) and sea floor spreading which opened the

Gulf. Figure 4 is a vertical profile of gravity values from Creel, Chih, SW to Batopilas, Chih., showing the increase in gravity from -200 at Creel to -125 milligals. Continuing westward from this profile 150 km., to the Sea of Cortez, gravity values increase to zero

To the south of Chihuahua City the -200 milligal gravity contour continues for 100 km before taking a distinct trend to the southwest. At approximately 28°N, the -150 gravity contours of the east and west boundaries of the WCCB bend strongly towards each other. South of 28°N the dimensions and uniformity of the WCCB negative anomaly diminishes, and the remaining anomaly takes a southeasterly strike. The southern boundary of the WCCB is most reasonably within this zone at 28°N, but will not be a further consideration in this study. Over the WCCB itself, gravity contours are smooth; they change only a little over large areas. In contrast, the surrounding Basin and Ranges has repeated rapid spatial changes of gravity resulting from the bedrock mountains and loose sedimentary basins.

Gravity characteristics which help define the WCCB are 1) large negative values (-200 milligals), 2) uniformity (smoothness) of values, 3) contrast with adjacent regions. The -200 milligal contour was chosen to define by gravity the boundary of the WCCB.

Prior gravity studies of this region agree with the data presented here. In Aiken et al 1985,, on the map of the whole of Mexico, the region under consideration N of 30 N shows a broad, uniform, negative region W and NW of Chihuahua City. Crustal thickness studies document significant crustal attenuation.

#### **4. Geologic Character of the WCCB and adjacent regions**

Surficial geology of the WCCB will be reviewed, beginning with the youngest and most widespread geological units, and continuing to the older and more obscure units. The

Precambrian will be dealt with separately. Descriptive geological character such as field and structural relations, petrology, sedimentary basins, will be emphasized, and comprises part of the data against which the hypothesis is to be tested. The present geological character of the region is extension, as a part of the southern extent of the Rio Grande Rift. Earlier, more widespread extension was associated with the Basin and Range.

Large areas are covered with young basalts, and many closed drainage basin exist. The contrast is with the regions of volcanic uplands, known as silicic large igneous provinces (SLIPs). SLIPs include the 1) Datil-Mogollon Igneous Province in southern NM (Chapin, 2004), 2) West Texas Igneous Province (Henry *et al.*, 2008), and the 3) the Sierra Madre Occidental of northern Mexico (Henry, 2010; Busby, 2008).

The Datil-Mogollon Volcanic Field (DMVF) (Chapin, 2004) has 8 calderas, and is thought to overlie the SE extension of the Colorado Plateau, residing on Mazatzal province crust (Karlstrom *et al.*, 2004). The West Texas Igneous Province (Trans Pecos Igneous Province) (TPIP) has 8 calderas (Henry, *et al.*, 2008), and resides on an enriched silicic cratonic fragment.

The WCCB (Western Chihuahua Cratonic Block) north of Chihuahua City extends westward from Highway 45 at 32°N 200km west to the border with Sonora. The border strikes NW to nearly the Sonora border. The S border is not clearly defined yet. The WCCB block is topographically elevated. The eastern portion of the block is a high volcanic plateau, with large flat surfaces and isolated ranges. West of a north-south line, the main mass of the northern Sierra Madre Occidental occupies the WCCB. The Sierra Madre is an elevated volcanic plateau made of rolling hills of largely unwelded ash flow tuffs. On the western side of the range the western,

Pacific drainage has incised deep canyons into the western border of the volcanic piles, and thick ignimbrite cliffs are oftentimes exposed.

Middle Tertiary felsic volcanic rocks of the Upper Volcanic Series (UVS) form the largest portion of exposed bedrock on the WCCB, constituting the ignimbrite flare-up, comparable to the western US (Chapin, 2004, 2008). Caldera derived volcanic and volcanoclastics constitute the UVS, and numerous calderas have been identified (McDowell and Mauger, 1991), but the WCCB contains vast, monotonous sequences of unwelded tuffs.

On top of the WCCB, in addition to the UVS, there are minor young basalts (5%), young sedimentary basins/lakes (5% or more), and windows into Cretaceous limestones (5%). These are underlain in general by the Lower Volcanic Series (LVS), a group derived from subduction related processes off of the west coast of Mexico during the Mesozoic (90-80Ma), and Eocene (60-50Ma). These relations are best exposed on the western slopes of the Sierra Madre, although they are also present in Majalca Canyon north of Chihuahua City (Mauger, 1984).

Structurally, the WCCB is relatively stable. The widespread outflow facies of the calderas remain nearly horizontal, as seen dramatically west of Highway 45 north of Chihuahua City, at the eastern boundary of the WCCB, and many other places. The NW striking northern boundary of the block has several N-S trending faults and/or graben basins extending southward into the block, sometimes associated with young mafic flows.

Windows into underlying Cretaceous (carbonate) rocks are present on the block, and the margins of the block frequently give way in the surrounding ranges of the Basin and Range to thick exposures of Cretaceous rocks. Prior stratigraphic studies of the Mesozoic rocks of central Chihuahua region indicate the Aldama Platform to the west of a series of N-S trending

Cenomanian reefs, with deep water of the Chihuahua Trough to the east. These reefs formed at the eastern edge of the WCCB. Today, they outcrop in the Sierra del Cuervo, one range east of the WCCB. The Sierra del Cuervo is believed to have been derived from the eastern side of the WCCB by listric faulting in the last 30 Ma. Outcrops of Paleozoic and Precambrian rock are not known on the WCCB, but are found in several places surrounding the WCCB, as will be discussed subsequently. The Chihuahua Trough is a long term Mesozoic depo feature comprising much of eastern Chihuahua, and it represents extension related to the opening of the Gulf of Mexico. This same negative feature extends northwest into southern AZ, across to the CA border. The Rara Formation (Tovar, 1982) is a thick upper Paleozoic dark shale/sandstone formation found in several places in Chihuahua. It is interpreted to be a deep water fan deposit. These rocks are reported near Parral, to the south, just NE of Chihuahua City, and to the northwest near Ascension. Near Chihuahua City they have been studied in detail (Hanshey, 1986). Sedimentological studies suggested a source to the west (Fitzpatrick, 1986 ).

#### **4.1. Precambrian rocks near the WCCB**

Two occurrences of Precambrian rocks are present just basinward of the eastern WCCB boundary, that at Sierra La Mojina to the northeast, and at Los Filtros to the east. Neither represent bedrock in place, but they do give clues to the character of the WCCB block, adjacent. These will be described more thoroughly.

##### **4.1.2 Sierra La Mojina.**

Sierra La Mojina is 40 km west of El Sueco at 30°N, and basal conglomerates of Mesozoic age include pebbles to boulders of rhyolite, which has been dated as Precambrian. Isotopic studies on mineral separates from these boulders suggest a Rb/Sr age of 695+<sub>-</sub>10Ma, a

minimum age. K/Ar ages on the same samples showed they had been reset between 233 and 266 Ma (Denison 1970). Field relations suggest deposition from coalescing fans although no transport directions of these clastic rocks have not been made. This site lies 20 km northeast of the -200 milligal contour of the WCCB, Figure 3. It is interpreted that Precambrian rhyolites, perhaps similar to those found in the Franklin Mts. and dated at 1.1 Ga (Karlstrom *et al.*, 2004), are present in the NE corner of the WCCB and served as sources for the Precambrian rhyolite boulders at Sierra La Mojina.

#### **4.1.3 Los Filtros.**

At Los Filtros, 30 km northeast of Chihuahua City, (figure 6), amphibolite dikes and granites are found intruding older gneiss, and the granites have been dated by K/Ar as 1.03 Ga and .97 Ga (Blount, 1982, Mauger *et al.*, 1983). One mafic phase has a high F content of 2300 ppm, and a composition similar to the average continental rift alkali basalt of Condie (1979). An associated felsic phase was high in Y and Zr, a decidedly bimodal igneous event.

The Precambrian rocks are themselves allochthonous fragments contained within the Rara Formation (Blount, 1982). The Rara is a turbidite, deep sea fan sequence (Fitzpatrick, 1986) with paleocurrent measurements indicating a source from the west (figure 6). Hansch (1985) determined from detailed structural analysis that these granitic fragments, some kilometers in size, were tectonically emplaced towards the east, into the Rara. Los Filtros is located 15 km east of the very strong gravity anomaly which defines the eastern boundary of the WCCB (Aiken *et al.*, 1981). Another structural property of the Los Filtros site is its presence in the north-south trending structural block known as Sierra del Cuervo in the south and Sierra Pena Blanca in the north. This block is separated from the eastern part of the WCCB by a large listric fault, under

the Highway 45 graben. The El Cuervo/Pena Blanca block can be restored back to its pre 30 Ma position, pre-rifting, when it forms the eastern margin of the WCCB, moving Los Filtros to less than 10 km from the WCCB boundary.. This EC/PB structural block was derived from the east side of the WCCB by listric faulting since 30 Ma, concurrent with the formation of the Encinillas Graben. The Rara Formation is then a deep water fan off of the east boundary of the WCCB. The formation of the Ancestral Rocky Mountains was an orogenic event widespread in the southwestern USA consisting of the uplift of numerous tectonic blocks, and the formation of adjacent depocenters. The origin of the Ancestral Rockies is attributed to the Ouachita collisional orogeny. Foreland uplift structural style such as typically found in the Ancestral Rockies during the Ouachita orogeny would explain the Los Filtros data.

PEMEX (Petroleos Mexicanos) drilled 29 petroleum tests in Chihuahua between 1965 and 1981. Three of these wells are known to have reached Precambrian rocks, all near the US border. The Moyotes #1 well southwest of Ciudad Juarez reached granite gneiss dated at  $890 \pm 32$  by K-Ar methods (Denison, 1972). This is interpreted as part the northwest trending Burro Mts./Florida Mts./Moyotes 'uplift'(BFM, Thompson, *et.al.*, 1978), felsic Precambrian block , now recognized to be 1.1 Ga (Karlstrom *et al.*, 2004). The Chinos #1 well is further west and encountered granitic gneiss dated at  $1327 \pm 42$  Ma (Thompson *et al.*, 1978). These dates were also K-Ar. These results demonstrate a slight extension of Mazatzal rocks onto northern Chihuahua in the subsurface (see discussion below).

## **5. Initial Sr isotope ratios**

Initial Sr isotopic ratios are values calculated from data determined for Rb/Sr age dating. Ratios below 0.706 are considered to be oceanic in geologic character, whereas values greater than 0.706 are considered as contamination by continental crust. In the area of interest, such

isotopic studies are summarized below and in Figure 5. Cameron *et al.*, 1983 reported values ranging from .7075 to .7055 from Tertiary igneous rocks near Creel, west of Chihuahua City. For both felsic and mafic rocks, they found that the most radiogenic (continental) of their transect of northern Mexico were from the region immediately west of Chihuahua City. Duex (1983) compares phenocryst and whole rock initial Sr ratios from Tertiary rhyolites for samples taken from two areas, 1) the Cuahtemoc-La Junta area on the WCCB with 2) the Durango-Mazatlan transect (McDowell & Claybaugh, 1979). For the area on the WCCB, “Four rhyolites from this group have initial Sr 87/86 ratios (0.7169-0.7614) that are significantly higher than the other seven rhyolites from the same area (0.7083-.7045). The high initial Sr ratios (>0.7169) and “ the variations in initial ratios can be explained by the incorporation of up to 40% crustal material similar to a gneissic xenoliths of 0.7196 initial ratio. Initial Sr isotopic ratios are supportive of a cratonic WCCB block.

## **6. Linear Boundaries**

### **6.1. Texas Lineament:**

In far west TX there exists a long recognized geological feature (Albritton & Smith, 1972; Muehlberger, 1980) known as the Texas Lineament (TL). It has been enigmatic, although numerous significant geological changes are recognized to have taken place across this lineament. Muehlburger (1980) suggested it as a continental boundary. Indeed, this is a reasonable interpretation. Some of these characteristics will be revealed in subsequent discussion. In the present study, the TL is taken to be the boundary between the North American craton (Laurentia) to the northeast and a mobile belt to the SW. The NA craton here would most likely be Mazatzal Province rocks overridden by Grenvillian rocks, with some granite-rhyolite province, (Karlestrom et al. 2004). The TL strikes approximately N35W, and is recognized for a

length of 250 km. Its SE end may terminate along the southern border of Laurencia which lies under the Grenvillian overthrust. This may join the La Babia fault zone in Mexico. The TL extends NW to El Paso, TX where it encounters 1.4 and 1.1 Ga bimodal granite-rhyolite provinces, with the Red Bluff granite being the younger. At El Paso, the strike changes to N 60 W, and the TL is projected across SW NM (Chapin, 2004). This is in agreement with various data. This is also the area of comparison of the Mogollon-Datil Volcanic Field (MDVF) to the north of this zone and the Boot Heel Volcanic Field ( BHVF) to the south (Chapin et al, 2004). In Arizona, this trend becomes the Transition Zone.

## **6.2. Transition Zone, AZ**

The Colorado Plateau is succeeded southward by the Transition Zone, characterized by progressive disruption of fragments of the CP. A recent interpretation (Hilgendorf,2005) places the Phoenix fault here, an unseen but necessary feature. South of the Transition Zone is the Basin and Range, which extends NW across Arizona.

## **6.3. East and West boundaries of the WCCB**

The East and West boundaries of the WCCB are prominent features as indicated by several data types. They are topographic, and gravity, anomalies of the first order, and have lesser order sedimentological and structural consequences. Topographic and gravity changes on the east boundary of WCCB with the B&R of central Chihuahua are approximately 700m and an increase in gravity of 75 to 100 milligals (Aiken *et al.*,1981). The western boundary is more dramatic. At the latitude of Hermosillo, elevation decreases by (8,000-1000 feet) 2000m and gravity by (-200-100) increasing 100 mg. From the SW portion of the WCCB, SW into the Sea of Cortez changes are most extensive. Figure 4 is a vertical crustal profile and is a documentation

of important properties from within the WCCB, right, towards the Sea of Cortes, left, an oceanic spreading center. The section location is guided by the location of samples with strontium isotopic information. The section begins at Tomochic and extends south to Creel. Both locations are on the high volcanic plateau of the UVS. The section then extends towards the south and SW into Sinaloa and the coast and the Sea of Cortes spreading center. The length of this section is 150. Elevation changes from 9000 feet to zero at the coast and several thousand feet negative at ocean depths. Gravity varies from -200 milligal to zero, or slightly positive. Initial Sr ratios vary from over 0.71x on the high volcanic plateau to .705 at Batopilas.

## **7. Basins/ mobile belts**

The stable blocks of the region, CP, MDVF, West TX enriched cratonic fragment, and the WCCB, stand in contrast to the basins, or mobile belts. The WCCB is of greatest focus here, because it is new to recognition. The basins surrounding the WCCB are also of special attention. These will be discussed by region, beginning to the east of the WCCB, and then, those basins/features north and northwest of the WCCB will be discussed, and finally, those to the west of the block. These features are listed in Table 1, which documents basinal/mobile belt features by geologic time, and are illustrated in Figures 6 – 9, from the oldest to the youngest..

### **7.1 Precambrian**

Craton assembly proceeded in Laurentia from an Archean core of 2.5 Ga, and with the collision and accretion of multiple island arcs and granite bodies to form provinces, which joined with the earlier formed areas, and for them to form larger masses. Other processes, such as underplating, continued the process of cratonization. A global phenomena in this process was the occurrence of felsic igneous activity over large specific areas, producing regions labeled granite-rhyolite province. This activity was global and periodic; 1.4, 1.1, and 0.6 Ga are known

episodes; in Africa this latter is known as the Pan African Event (ref). In North America, the 1.4 and 1.1 Ga events are widespread. Their distribution in SW Laurentia is given in Fig 6, (Stewart 2001, Bickford, Barnes, Anderson, 2000). Portions of these areas are also bimodal; there are mafic rocks such as basalts in addition to the felsic granite/rhyolite. And in some areas the chemistry of the felsic rocks is such that they are 'A' type granites, or anorogenic. Were there changes between 1.4 and 1.1 in SW Laurentia? In the area under discussion, Figure 2, they both occur along the same trend zones from SE California southeast to El Paso, TX, and north to the WY-CO border. Data for this knowledge comes from study of the limited surface outcrop. Do these A granites extend eastward under the Great Plains and we just cannot see them, or under the Colorado Plateau? Studies suggest not. Volcanic rifted margins shows that A type magmatic processes occur on rift shoulders, that is , the thermally uplifted portion of the craton immediately adjacent to the faults of the rift, and then to the rift valley itself. The A type magmas produce caldera volcanism at the surface; such eruptions may be triggered by mafic intrusions. These environments are bimodal and extensional. Felsic volcanic ashes may be widespread. Rift shoulders may 100-150 km wide, and may parallel active rifts extensively. In the rift itself, there may be mafic dikes and extrusives, along with arkose, sandstone, evaporites, and continual tectonic readjustments. In the area under discussion, several such rift basin deposits are present, as indicated in Figures 2, and 6. They occur during the time period between 1.4 and 1.1 Ga.

Basinal features are only sometimes explicitly defined. Eastern basins have two boundaries which have been previously recognized as significant and repeatedly present, and those are the Texas Lineament, as an eastern boundary to basins, and the eastern boundary of the WCCB along the Encinillas Graben.

## 8.2 Paleozoic

Prolific petroleum production from the Permian basin east of the area of study encouraged multiple petroleum tests in far west Tx, SW NM, and SE AZ, and Chihuahua. Less than 10% of the area has outcrops of Paleozoic rocks, and some of them have been well studied.

Many of these results are confirmed and elaborated from study of the stratigraphy of the 29 petroleum tests in Chihuahua state made by Pemex. In the Paleozoic in N Chihuahua, the Proto-Pedregosa basin preceded the widespread Pedregosa basin, shown on Figure 8. The Pedregosa basin contains up to 15,000 feet of Paleozoic sediments in long narrow trench striking NW (Fig 8). At least 600 km long, extending from eastern Chihuahua northwest through SW NM and SE AZ, at least 1/3 of the distance across AZ. To the east of the Pedregosa basin were several other Paleozoic basins, the Delaware and the Midland, known collectively as the Permian Basin, which has been prolific in petroleum production. With the ocean to the south, these basins extended into Laurentia.

The Late Paleozoic was the time of the next major geologic event, the collision of Laurentia with Gondawana, coming from the SE. Locally, this is the Ouachita Orogenic Belt in west Texas (Figure 8); regionally it is a southwestern tail of the Appalachian Orogenic Belt which extends up the east coast of North America. This collision initiated widespread block uplift and enhanced basinal deposition, an event known as the 'Ancestral Rocky Mts.' The Pedernal block in NM was uplifted, adjacent to the downdropped Orogrande basin (Greenwood, 1977) The WCCB was present with the Rara Formation as a fan deposit off the east side of the WCCB. Foreland basin response uplifted the WCCB at this time, resulting in 1) structural emplacement of Precambrian rocks at Los Filtros into the Paleozoic Rara fan deposits, (Handschy, 1986; Mauger, 1983; Blount, 1986), 2) erosion of Precambrian rhyolite boulders off

the NE boundary of WCCB and their deposition in the rocks at La Mojina. The Mennonite well, drilled near Villa Ahumada, was still in the Permian Rara Formation, a deep water fan deposit, at 6,000 m, with a collar elevation of 1000m.

Beginning in Escabrosa time, a NW striking linear trough developed in SE AZ, NE Sonora, and adjacent NM and Chihuahua., best documented in AZ (Fig 8). This was the initiation of the Tobosa basin, also known as the Proto-Pedregosa. The evaporites in the Permian were synchronous with those in the Delaware basin to the east, where up to 3000m of salts were deposited in a long narrow north striking trough.

In Sonora, Paleozoic shelf marine sediments are present in northern Sonora, and near Hermosillo, to the south, they are replaced by deep water marine sediments, along an E-W continental (cratonic) boundary, between eu- and miogeosynclinal sedimentary deposits (Poole *et al.*, 1997; Valencia-Moreno *et al.*, 2007). Correlation of Sonora Paleozoic rocks with SW AZ cannot be made with confidence.

A different idea is to be emphasized here; that is, during the Paleozoic a N-S striking depositional basin was present along the Chihuahua-Sonora border from about 29°N to 32°N, in SE AZ (Fig 8). Such a feature is suggested by the following observations. The E-W cratonic boundary mentioned above has an inflection to the north at approximately \_\_\_W, suggesting an embayment. Palomares (1985) extended the study of Thompson (1983) to Sonora. Data was limited, however he does indicate N-S trending sedimentological basins near the Chihuahua-Sonora border during 5 of the 7 Paleozoic time periods. The duration of the zone is remarkable; exact locations need to be better defined. Palomares (1985) also recognized the Sonora platform

or peninsula to the west of the Sonora-Chihuahua border. This platform is a subset of the Caborca block and the long north-south basin west of the WCCB is a suspected aulacogen.

### **8.3. Mesozoic**

The Mesozoic in North America was a time of great activity. Triassic rifting zippered open the Atlantic Ocean, generally southeast of the earlier suture along the Appalachian Mt-Ouachita Mt., Africa to the S and Europe to the N separated from N AM. Triassic redbeds are known in eastern Sonora, and elsewhere in Mexico. Cretaceous rifting opened the Gulf of Mexico; Yucatan moved southeast from the TX Gulf Coast region to its present position. The eastern portion of the area of interest, and further to the east, during the Mesozoic is a history of passive margin formation and evolution. The western portion of the area of interest, in contrast, is subjected to multiple compressional and transtensional events, specifically during the Jurassic, early and late Cretaceous. Such events strongly influenced the history of the WCCB and adjoining regions.

The Chihuahua Trough is the Mesozoic manifestation of basin development east of the WCCB. The origin of the Chihuahua Trough is related to the opening of the Gulf of Mexico (Bilideux, 1982; Salvador 1992), and a series of interconnected basins extended from the Chihuahua Trough southeast to the Gulf of Mexico. Figure 9 (line #2) shows three stages of the development of this feature. During the Late Jurassic and Early Cretaceous, a large asymmetrical basin formed in eastern Chih, and over 3000 m of evaporates and clastics were deposited ( line #6, Figure 9). This was concurrent with the thick salt sequences in the Gulf, which are currently target for sub-salt resources. Younger Chihuahua Trough sediments are more extensive. The abrupt eastern margin of the trough is along the SW edge of the Diablo Plateau and the TX Lineament zone. The western boundary of the trough is marked in part by reef complexes

(Stege *et al.*, 1981) in the Sierra del Cuervo-Pena Blanca. To the west are the long recognized sedimentary facies of the Cretaceous Aldama Platform. This feature has been recognized by some (Dickenson 2001) but not by others. The Aldama Platform is a Mesozoic manifestation of the WCCB. The Chihuahua Trough extended east, north, and northwest of the WCCB, and into SE AZ and NE Sonora, where it is known as the Bisbee Basin. Figure 9 shows three stages of the development of this feature. More recently, Lawton & McMillan (1999) define the Mexican Borderlands rift (line #5, Figure 9). This feature (Lawton and McMillan, 1999) includes the Chihuahua Trough of northern Chihuahua, and trends NW to include the Bisbee basin of SE AZ. It continues NW to the McCoy basin on the AZ-CA border. The McCoy basin consists of 7500 m of sediments of early Cretaceous age in a deep linear trough trending ESE, (N 120°E), and it is correlated with the Bisbee Group of the northwestern Chihuahua trough.

From Late Triassic through Early Jurassic a N-S trending basin of redbeds and even coal bearing beds occurred in eastern Sonora near to and parallel with the Chihuahua border (Salavdor, 1988) as the Barranca Formation. Shelf carbonates lie to the west of this basin.

A Jurassic magmatic arc dominated SW AZ & Sonora formed by subduction off the west coast; this is also called the Mogollon Highlands (MH), (not to be confused with the Mogollon-Datil Volcanic Field). This Cordilleran chain produced many mineral deposits in long narrow belts, trending southeast across central AZ, where the trend turns south into Sonora (Fig9). Earlier depictions of this arc showed it over a broad area, however more recent studies (Stuade *et al.*, 2003) show the Jurassic arc as a narrow zone (Fig 9) trending south just west of the Sonora-Chihuahua border. Episodes of transtensional faulting also produced more silica and potassic magmatism (Tosdal *et al.*, 1989). Northeast of the MH vast quantities of sediment were received onto what is now the Colorado Plateau (CP) (line #1, fig9). Early to Middle Jurassic arc

volcanism was succeeded by the Late Jurassic to middle Cretaceous bimodal volcanism associated with back-arc rifting and transtensional faulting associated with the Mexico Borderland rift (Dickenson and Lawton, 1999; Lawton & McMillan, 2003).

Simultaneous with the formation of the Bisbee Basin to the north, in eastern Sonora, “the Bisbee flank basin lies west of the Aldama platform and separates it from the Lampazos shelf to the west”. This has been referred to as the ‘Sonora basin’ (Gonzales L& Jacques-Ayala, 1990) and Gonzalez-Leon 1994). Aptian-Albian strata at Lampazos (Dickens, 2001) is 1775m thick, in comparison to 1150m in the adjacent Bisbee Basin, and 2800m in the Chihuahua Trough.

Tectonization of these basins by forceful accretions off the west coast of Mexico took place twice, approximately 90 and 50 Ma. Transtensional and extensional movements accompanied. This is the Laramide orogeny, and it occurred up and down western North America. The spaces between them have been partially filled with sediment, which are the basins which have been discussed. Now, lateral forces occur which shove the blocks together. The softer sediments are squeezed up and out, and occur as thrust faults out of the basins and onto the more rigid blocks. In the Sierra de Juarez across from El Paso, TX., three layers of thrusting have piled up on top of each other against the buttress of the Precambrian crustal block beneath the Franklin Mts (Drewes et al,1981). At many places near the TX Lineament, basinal Cretaceous sediments are thrust northeast onto the Diablo cratonic block, vergent NE (Figure 9). In the northern part of the Pena Blanca range, 51 and 53 Ma ignimbrites with late Chihuahua Trough sediments and conglomerates, are thrust to the west, and overlain by 44 Ma ignimbrites Goodell, et al,1986). This vergence is suggestive evidence for the presence of the WCCB (figure 9). Near the northern boundary of the WCCB, SW vergent thrusts are present (Brown, 1985). These structural vergences are shown in Fig9, and point toward the stable block.

#### 8.4.Cenozoic

- 1) Metamorphic core complexes (MCC), 2) Basin & Range, 3) Rio Grande Rift (RGR).

Laramide compression was ending at approx 50 Ma., and the rise of multiple metamorphic core complexes occurred at this time. The genesis of metamorphic core complexes (MCCs) is not a topic likely to engender widespread agreement among their enthusiasts, however, a few fundamentals are generally agreed upon for those found in western North America (Armstrong, 1982; other refs). The idea to be utilized here is that MCCs are not located within stable cratonic masses; they lie in extended crust, mobile belts, adjacent to or outboard from coherent, not extended, North American craton. They form by some sort of *décollement* process above rapidly rising cratonic material, which had been entrained to great depths. They surfaced relatively quickly from depths of 30 km or greater, and they have a directional fabric, a foliation or lineation. Is this foliation directed away from a nearby stable craton? Could the presence of documented MCCs, conversely suggest the presence of a nearby stable craton, or cratonic fragment? In Arizona several MCCs have been identified south of the CP, in zones of extreme extension. Several MCCs have been recognized in Sonora; they are Sierra Mazatan, and Puerto del Sol (Valencia-Moreno, 2005). They are located on Figure 10, and lie 100 km west of the -190 milligal contour of the WCCB block. Andersen et al. 1980, describe these areas as MCCs with essentially synchronous ages of  $58 \pm 3$  Ma and  $50 \pm 3$  Ma by Pb/U isotopic studies on zircons. They note the development of these MCCs in the apparent absence of coherent Precambrian basement. In addition, Sierra Mazatan has low-dipping foliation, which is reported to have a NE-SW direction. The Sonora MCCs are evidence of the presence of a region of extended crust, compatible with a N-S trending belt near the Sonora-Chihuahua border.

Tectonic relaxation took place, and by 35 or 30 Ma relaxation turned into crustal extension, and asthenospheric magmas reached the surface in many localities. This behavior is widespread; it produces regions known as Basin & Range provinces, common in the western northern MX and US. Extension of crustal blocks over relatively thinned crust, and enhanced thermal gradients, were accommodated by large listric faults. The Great Basin of Nevada and western Utah are part of the B&R province, which then moves south into southern CA and then east across AZ and around the southern border of the Colorado Plateau. From SE AZ one branch trends south across Sonora, with young faulting and mafic extrusives (fig 10). Another branch trends southeast into SW NM and northern and eastern Chihuahua, and further SE. In NE Chihuahua, the B&R merges into the southern part of another extensional feature, known as the Rio Grande Rift, which initiated approx 12 Ma . The presence of the RGR means that Cenozoic extensional forces almost completely circum navigated the stable block, the Colorado Plateau. In a similar manner with the WCCB, the B&R in eastern Sonora continuing into SE AZ and SW NM and northern Chihuahua, continuing to eastern Chihuahua, almost completely circum navigate the WCCB. ” The Sierra Madre Occidental is an unextended block surrounded by areas of major extension.” has been recognized repeatedly.

East of the WCCB the B&R formed in the Cenozoic, beginning about 30 Ma, and sometimes associated with bimodal volcanism. The structural blocks had decidedly N and NW trends, extending from northern Chihuahua into AZ. At 12 Ma a more northerly direction became dominant as the Rio Grande Rift north into NM became dominant. The RGR merges into the B&R in northern Chihuahua. The eastern boundary of the B&R in Chihuahua is the TX Lineament zone in west TX. To the east is the Trans-Pecos Volcanic Field, also called the West Texas Volcanic Field (WTVF). The WTVF is located on the rift shoulder of the RGR.

Distribution of young mafic volcanic fields with respect to the WCCB is extensive, with many fields located around and on the block. These are found at Buenaventura, at the boundaries are fields at Yecora and Guachochi, Moctezuma and Geronimo, and the Portrillo Volcanic field, and up the Rio Grande rift. Geronimo Volcanic Field, SE AZ (3.5-9.0Ma)(Kempton et al., 1987) is hosted in San Bernardino Valley, several hundred km long, NS. The most recent activity, 1887, resulted in a high-angle fault scarp 76 km in length along the southern extension of the valley (Herd and McMasters, 1982), where another young mafic volcanic pile known as the Moctezuma Volcanic Field, Sonora, is located (Paz Moreno, 1985, Lynch, 1989). These features are indicated in Figure 9? and Table \_\_. They substantiate the western boundary of the WCCB.

In another study, Chapin *et al.*, 2004, compared the chemistry of Cenozoic volcanic rocks of the Mogollon-Datil Volcanic Field (MDVF) in southwest-central NM with those of the Boot Heel Volcanic Field (BHVF) in far southwest NM. The MDVF lies on suspected Colorado Plateau cratonic crust, whereas the BHVF is not. Data suggest that the MDVF developed on lithosphere that had not experienced significant volcanism since about 1.4 Ga (Karlstrom et al., 2004). In marked contrast, the BHVF to the south across the Transition Zone was preceded by 1.3-1.0 Ga Grenville/ rift-related magmatism, Jurassic-lower Cretaceous magmatism of the Mexican borderlands), and Laramide arc magmatism. Interpretation according to the present point of view puts the MDVF on the stable block of the Colorado Plateau, and the BHVF in the mobile belt.

A measure of present day properties of the WCCB are shown in Fig 11. Topographic features show structural/incision embayments into the uplifted WCCB. Several of these are present trending south into the NW striking WCCB boundary, and young mafic regions are

indicated. The piratization of extensive eastern drainage by the westward flowing Papigochic river, through a probably fault controlled notch in the WCCB, is an important data source. Certain versions of the location of the Mojave-Sonora Megashear project to this site.

## **8. Terrane Tectonics**

Summaries and versions of Terrane Tectonic studies of Mexico have been extensive (Coney & Campa (1983), Sedlock *et al.*, (1993) . The northern part of Chihuahua is often considered to be ‘unmoved North American craton’ (Ward, 1999). The region considered here has been at the margin of most terrane studies, and often the least understood.

The stable block/mobile belt concept introduced here for northern Chihuahua and adjacent areas need not clash with the accretionary tectonics of these prior studies. Some terranes will have cratonic cores and their boundaries will be in the mobile belts. Other terranes may be large areas without cratonic cores.

### **8.1 Caborca Block (CB)**

The Caborca block is recognized by numerous authors of versions of terrane tectonics ( )and it is usually a non-controversial item. It is a relatively stable block with Precambrian rocks of the Yavapai Province exposed on the north. To the W and SW the block terminates near the Gulf of CA, and prior to 12 Ma this W boundary was up against the N Peninsular Ranges of N Baja. The S boundary of the Caborca block has been established sedimentologically (Poole *et al.*, 2005) by the transition from miogeosynclinal rocks to the north versus eugeosynclinal rocks to the S, of an EW line. Isotopic studies of igneous rocks across the boundary substantiate this conclusion. The eastern boundary of the Caborca block is unknown, and several versions exist. The N and E boundaries become one because the NE boundary is the hypothetical MSM. The

CB is thought to have been moved into place by left lateral movement along the MSM during the Jurassic, and there is a zone to which it is believed to correlate. In the present study awareness of the behavior of the Caborca Block has been keen, because of the question of what lies west of the WCCB.

## **8.2 Mojave-Sonora Megashear (MSM)**

Results of the present study are neutral with respect to the MSM. Most projections of the MSM pass to the SW of the WCCB as defined (specified) here. Several exceptions are mentioned elsewhere. The objective here is more to establish and justify a methodology and conclusions with respect to the WCCB and mobile belts.

## **9. Discussion**

The stable block/mobile belt concept which has proved so successful in the Precambrian of Africa and Canada, can successfully be applied to the SW portion of the N American craton. A new cratonic block is identified here, the WCCB (Western Chihuahua Cratonic Block).

So, where did the WCCB come from? Is it local, or did it sail in from afar?

If we accept that the WCCB is a cratonic fragment, a small stable block, separated from the main mass of the North American craton by mobile belts manifested today as the Basin and Range and Rio Grande Rift, it is logical and most reasonable that the WCCB was derived from the adjacent North American craton from somewhere along the Texas Lineament region. The multiple extensional events probably served to separate the WCCB from the craton in multiple steps.

The presence of the WCCB presents a new element within the evolution of the SW boundary of the N American craton. The presence of the WCCB has implications with respect to the idea of the Sonora-Mojave Megashear.

## **10.1 Conclusions**

Cratonic blocks having significantly greater long term stability than adjacent areas can be identified within Precambrian provinces. These are cored by Precambrian rocks. A new such block is identified here located in western Chihuahua, the WCCB. Bouguer gravity, geochronology, and initial Sr isotope ratios are the most convincing evidence. Structure, stratigraphy, petrology, and geochemistry, provide supportive evidence.

Mobile belts are zones of thinner crust, and they have been repeatedly tectonized by transtensional and extensional events. Today these zones of mobility are expressed as the Basin and Range and Rio Grande Rift, and study over geologic time shows they are zones of long-term mobility. The WCCB discussed above is surrounded on at least 3 sides by mobile belts with over 1 Ga duration.

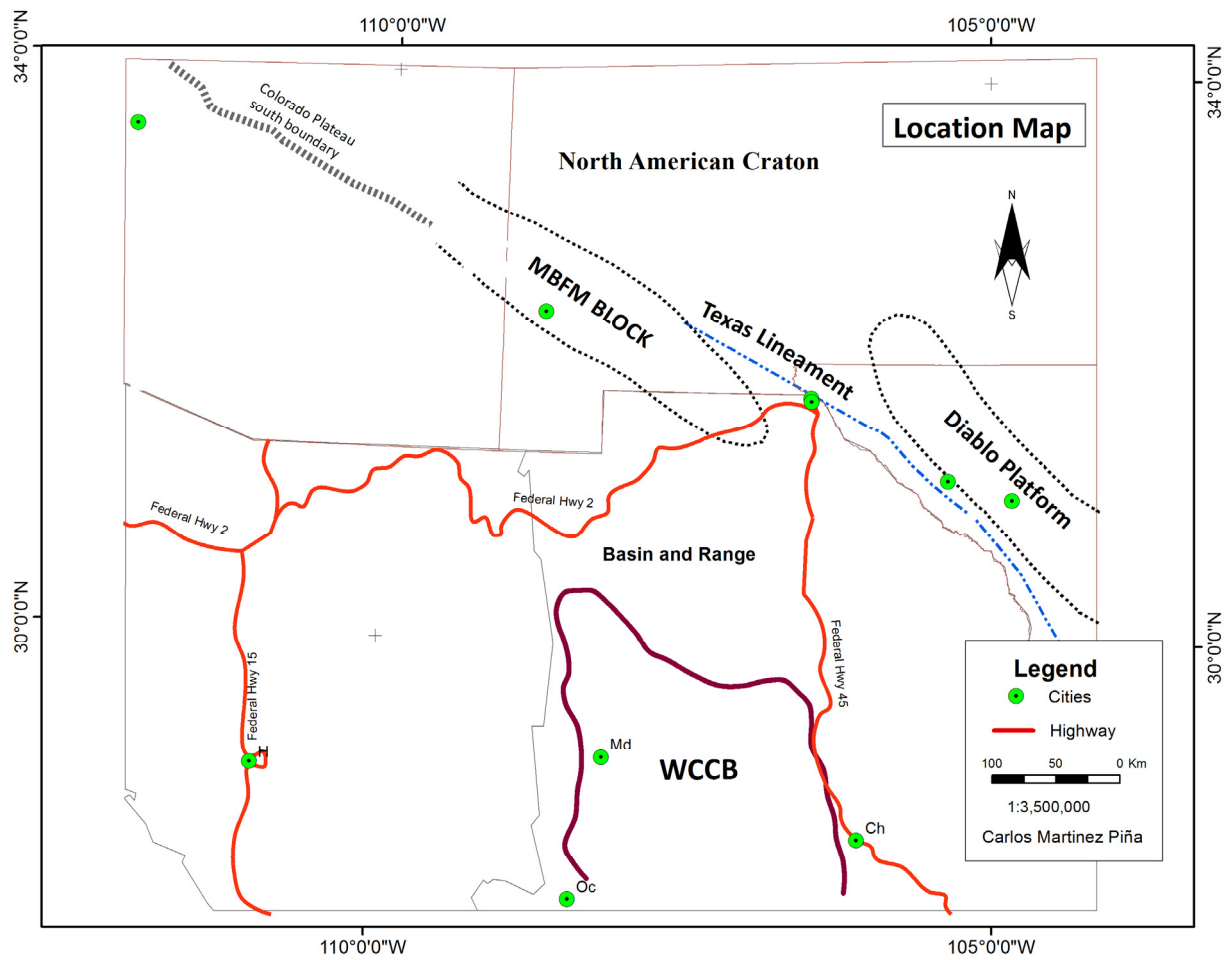


Figure 3.3 Location map of the area of interest showing relevant political boundaries, physiographic features, and sites referred to in the text.

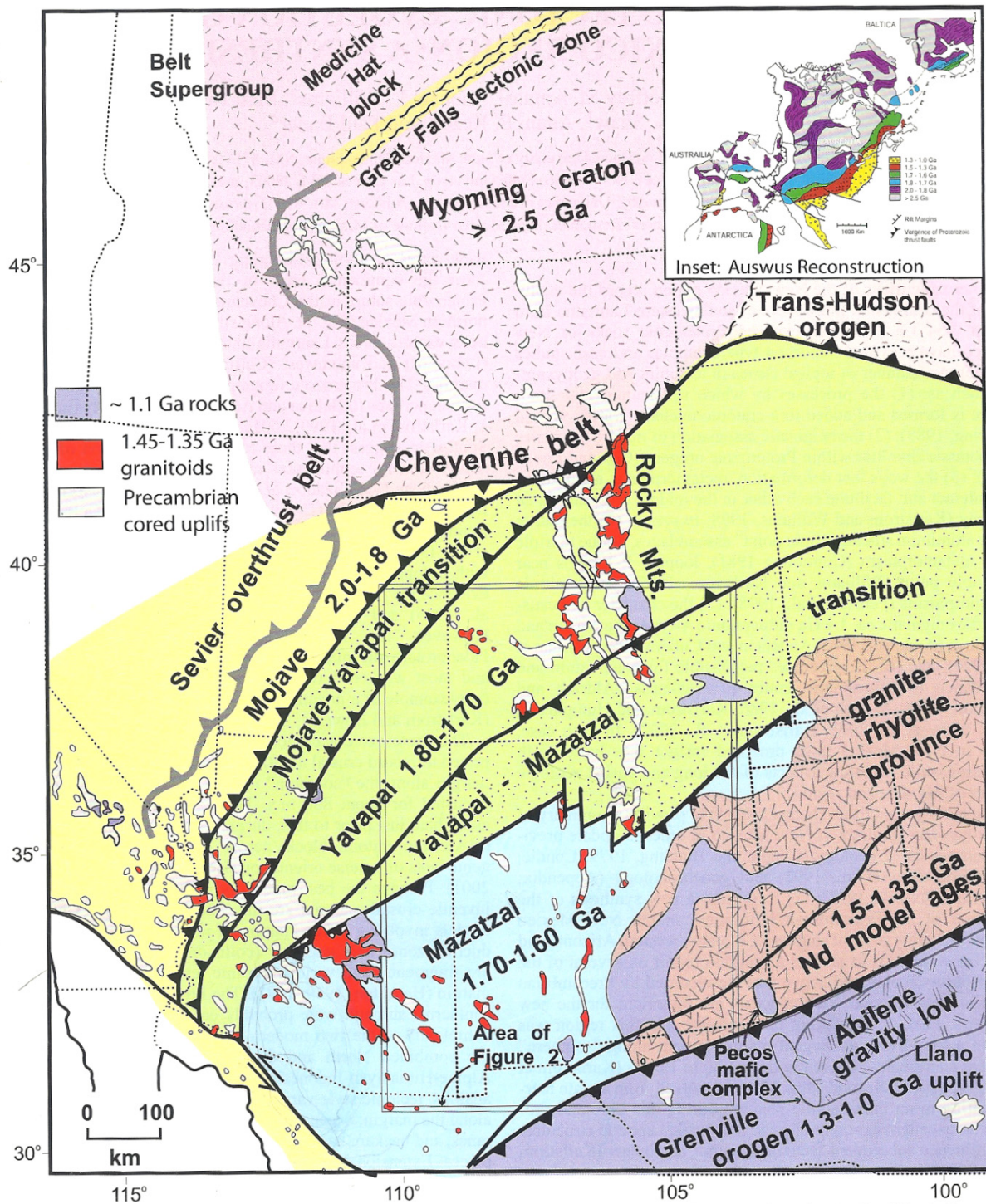


Figure 3.4 Precambrian Provinces in southwestern Laurentia showing major outcrop areas of Proterozoic rocks. Taken from Kalstrom *et al.*, (2004)

Figure 5.3 Bouguer gravity map of area, with locations of relevant features. See text for details; from Keller et al, 1985.

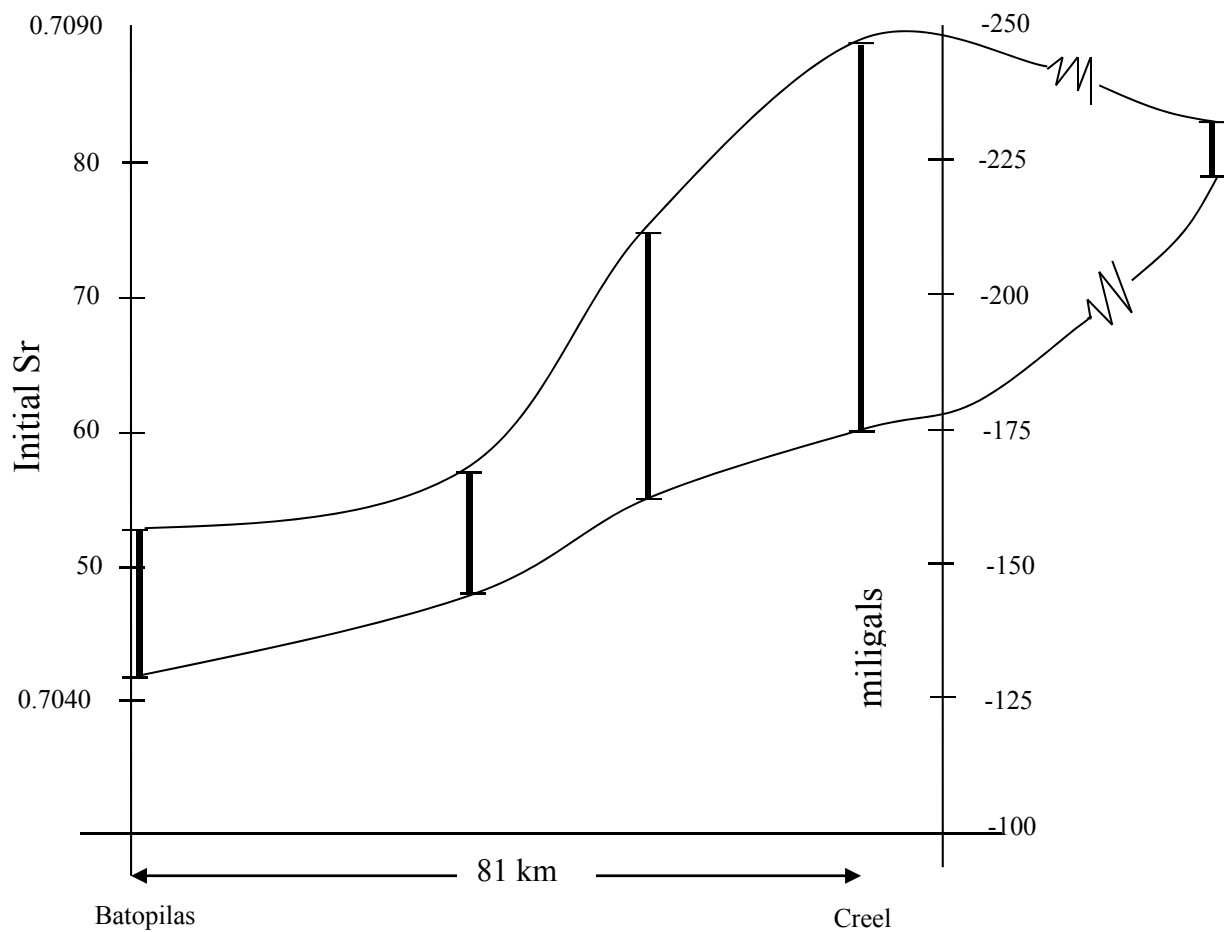


Figure 3.4 Detailed vertical profile across the southwest boundary of the WCCB giving initial Sr ratios and gravity in milligals versus distance. Initial Sr ratios from Cameron and Cameron, 1986.

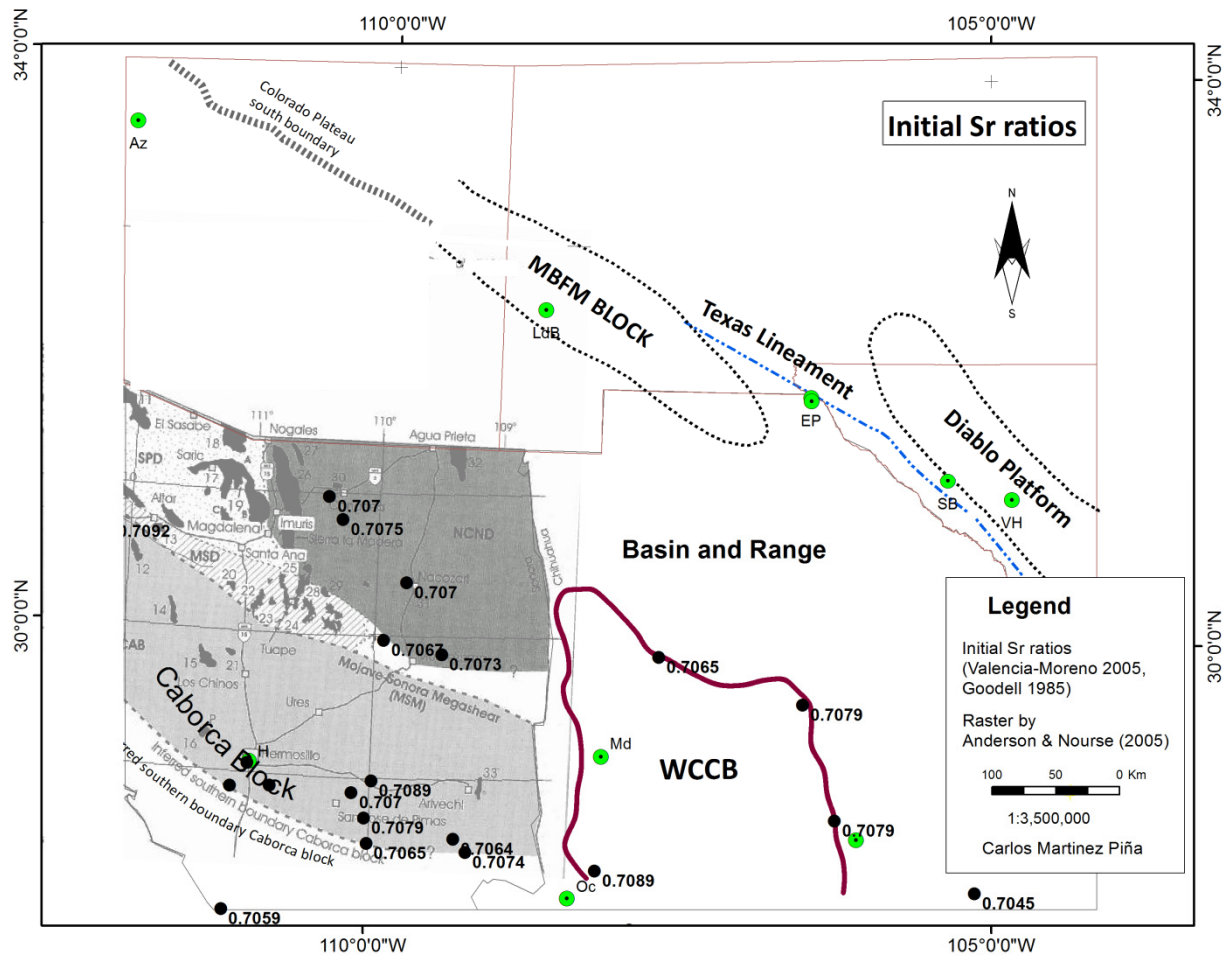


Figure 3.5 Western Chihuahua Cratonic Block (WCCB) designated as within the -190 milligal gravity contour; initial Sr isotopic ratios are given next to their locations.

J



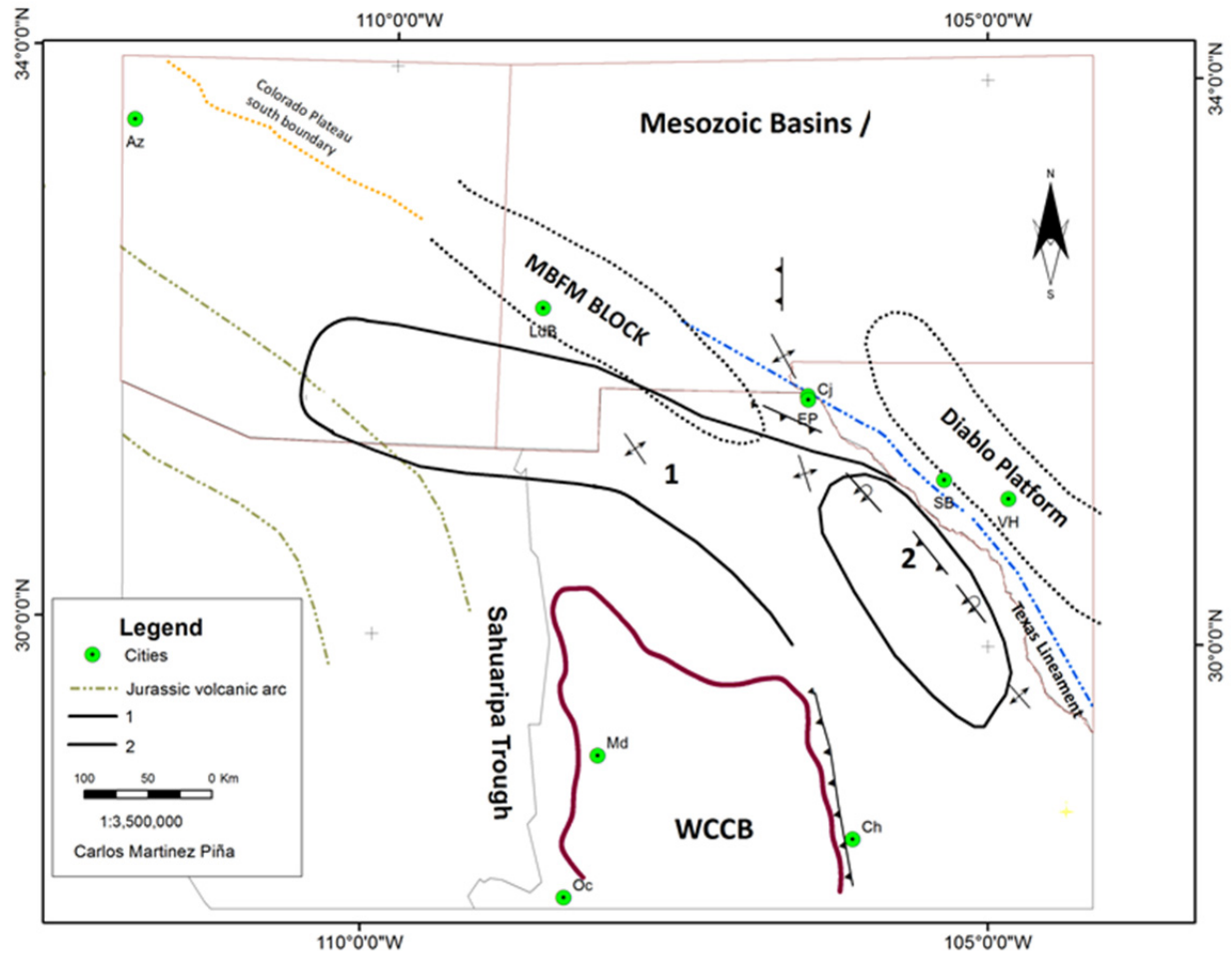


Figure. 3.8 Mesozoic positive (blocks) and negative (basins) region, and the WCCB. 1 = Chihuahua Trough and 2 = Jurassic salt, (Haenggi, 2001,2002). 3 = Structural features and thrust vergences (Dickenson and Lawton, 2001).



**Colorado  
Plateau**

**North  
American  
Craton**

**Mobile Belts**

Figure 3.10 Summary diagram

## References

- Ahlgren, S. (2001). The nucleation and evolution of Riedel shear zones as deformation bands in porous sandstone. *Journal of Structural Geology* 23 , 1203-1214.
- Alaniz-Álvarez, S., & Nieto-Samaniego, A. (2005). El sistema de fallas Taxco-San Miguel de Allende y la Faja Volcánica Transmexicana, dos fronteras tectónicas del centro de México activas durante el Cenozoico. *Boletín de la Sociedad Geológica Mexicana, Volumen Conmemorativo del Centenario de Grandes Fronteras Tectónicas de México, Tomo LVII, num, 1*, 65-82.
- Albritton, C.C., Smith, J.F., 1965, Geology of the Sierra Blanca area, Hudspeth Co., TX: *United States Geological Survey professional paper* 479, p. 131
- Anderson, P. (1989). Proterozoic plate tectonic evolution of Arizona, in Jenney J.P., and Reynolds, S.J., 1989, Geologic Evolution of Arizona: Tucson, Arizona Geological Society. *Geological Society of Arizona Digest* 17, 17-55.
- Anderson, T. H., & Silver, L. (2005). The Mojave-Sonora Megashear – Field and analytical studies leading to the conception and evolution of the hypothesis, in Anderson, T.H., Nourse, J.A. McKee, J.W., and Steiner M.B., eds., The Mojave-Sonora Megashear hypothesis: Development assessment. *and alternatives: Geological Society of America Special Paper* 393, 509-521.
- Anderson, T. H., Rodríguez-Castañeda, J. L., & Silver, L. T. (2005). Jurassic rocks in Sonora Mexico; Relations to the Mojave-Sonora megashear and its inferred northwest ward extension in Anderson, T.H., Nourse, J.A. McKee, J.W., and Steiner M.B., eds., The Mojave-Sonora Megashear hypothesis: Development, assessment and. *alternatives. Geological Society of America Special Paper* 393, 51-95.
- Anderson, T., & Nourse, J. (2005). Pull apart basins at releasing bends of sinistral Late Mojave-Sonora fault system. *in* Anderson, T.H., Nourse, J.A. McKee, J.W., and Steiner M.B., eds., The Mojave-Sonora Megashear hypothesis: Development, assessment and alternatives: *Geological Society of America Special Paper* 393, 509-521.
- Antonelis, K., Johnson, D. J., & Meghan M., M. (1999). GPS determination of current Pacific–North American plate motion. *Geology; April 1999; v. 27; no. 4; p. 299-302; DOI: 10.1130/0091-7613(1999)027<0299:GDOCPN>2.3.CO;2* *Geology; April 1999; v. 27; no. 4; p. 299-302; Geology; April 1999; v. 27; no. 4; , 299-302.*

- Aranda- Gomez, J., Housh, T., Luhr, J., Henry, C., & Chavez-Cabello, G. (2005). Reactivation of the San Marcos fault during mid-to-late Tertiary extension, Chihuahua, Mexico in Anderson, T.H., Nourse, J.A. McKee, J.W., and Steiner M.B., eds., The Mojave-Sonora Megashear hypothesis: Development, assessment and alternatives. *Geological Society of America Special Paper 393*, 509-521.
- Aranda- Gomez, J., Housh, T., Luhr, J., Henry, C., & Chavez-Cabello, G. (2005). Reactivation of the San Marcos fault during mid-to-late Tertiary extension, Chihuahua, Mexico in Anderson, T.H., Nourse, J.A. McKee, J.W., and Steiner M.B., eds., The Mojave-Sonora Megashear hypothesis: Development, assessment and alternatives. *Geological Society of America Special Paper 393*, 509-521.
- Aranda-Gómez, J. J., Aranda-Gómez, J. M., & Nieto-Samaniego, A. F. (1989). Consideraciones acerca de la evolución tectónica durante el Cenozoico de la Sierra de Guanajuato y la parte meridional de la Mesa central. *Universidad Nacional Autónoma de México, Instituto de Geología*, 33-46.
- Armin, R.A., 1987, Sedimentology and tectonic significance of Wolfcampian (lower Permian) conglomerates in the Pedrogosa basin; SE AZ, SW NM, and N Mexico: *Geological Society of America Bulletin*, 99, 42-65.
- Atmaoui, N. (2005). Development of pull-apart basins and associated structures by the Riedel shear mechanism: insight from scaled clay analogue models. *Der Fakultät für Geowissenschaften der Ruhr-Universität Bochum*, 1-94.
- Atmaoui, N., Kukowski, N., Stockhert, B., & Koing, D. (2006). Initiation and development of pull-apart basins with Riedel shear mechanism: insights from scaled clay experiments. *Int J Earth Sci (Geol Rundsch)* (2006) 95, 225-238.
- Barboza-Gudino, J. R., Orozco-Esquivel, M. T., Gomez-Anguiano, M., & Zavala-Monsivais, A. (2008). The Early Mesozoic volcanic arc of western North America in northeastern Mexico. *Journal of South American Earth Sciences* 25, 49-63.
- Barnes, M.A., Rohs, C.R., Anthony, E.Y., Van Schmus, W.R., Denison, R.E.; 1999; Isotopic and elemental chemistry of subsurface Precambrian igneous rocks, west Texas and eastern New Mexico: *Rocky Mountain Geology*, v.34, p.245-262.
- Bickford, M.E., Soegaard, K., Nielsen, K.C., McLelland, J.M., 2000, Geology and geochronology of Grenville-age rocks in the Van Horn and Franklin Mts. area, west Texas: Implications for the tectonic evolution of Laurentia during the Grenville: *Geological Society of America Bulletin*, v.112, p.1134-1148.
- Bird, D., & Burke, K. (2006). Pangea breakup: Mexico, Gulf of Mexico, and Central Atlantic Ocean. *SEG Expanded Abstracts/ Volume 25 / 1013* (2006); doi 10.1190/1.2369685.

- Blount, J.G., 1993, The geochemistry, petrogenesis and geochronology of the Precambrian meta-igneous rocks of the Sierra Del Cuervo and Cerro El Carrizalillo, Chihuahua, Mexico: PhD. Dissertation, Univ of Texas @ Austin, 242 p.
- Bryan, S., Riley, T., Jerram, D., Stephens, C., & Leat, P. (2002). Silicic volcanism: An undervalued component of large igneous provinces and volcanic rifted margins, in Menzies, M.A., Klemperer, S.L., Ebinger, C.J., and Baker, J., eds., *Volcanic Rifted Margins: Boulder, Colorado*, *Geological Society of America Special Paper 362*, 99-120.
- Busby, C. J., & Bassett, K. N. (2007). Volcanic facies architecture of an intra-arc strike-slip basin, Santa Rita Mountains, Southern Arizona. *Bulletin of Volcanology* (2007) 70:85–103, DOI 10.1007/s00445-007-0122-9, 85-104.
- Busby, C., Bassett, K., Steiner, M., & Riggs, N. (2005). Climatic and tectonic controls on Jurassic intra-arc basins related to northward drift of North America, in Anderson, T.H., Nourse, J.A., McKee, J.W., and Steiner, M.B., eds., *The Mojave-Sonora megashear hypothesis: Development, assessment, and alternatives*, *Geological Society of America Special Paper 393*, 359-376.
- Campa, F. M., & Coney, P. J. (1983). Tectono-stratigraphic terranes and mineral resource distributions in Mexico. *Canadian Journal of Earth Sciences*, Vol. 20, Number 6, June 1983 ISSN 1480-3313, 1040-1051.
- Centeno-Garcia, E., & Silva-Romo, G. (1997). Petrogenesis and tectonic evolution of central Mexico during Triassic-Jurassic time. *Revista Mexicana de Ciencias Geológicas*, volumen 14, numero 2, 244-260.
- Centeno-Garcia, E., Guerrero-Suastegui, M., & Talavera-Mendoza, O. (2008). The Guerrero Composite Terrane of western Mexico: Collision and subsequent rifting in a supra subduction zone. in Draut, A., Clift, P.D., and Scholl, D.W., eds., *Formation and Applications of the Sedimentary Record in Arc Collision Zones: The Geological Society of America, Special Paper 436*, 279-308.
- Charleston, S. (1981). A Summary of the Structural Geology and Tectonics of the State of Coahuila, Mexico. IN: *Lower Cretaceous Stratigraphy and Structure, Northern Mexico. West Texas Geological Society Field Trip Guidebook, Publication 81-74*, 28-36.
- Chávez-Cabello, G., Aranda-Gómez, J., Molina-Garza, R., Cossío-Torres, T., Arvizu-Gutiérrez, I., & González-Naranjo, G. (2005). La falla San Marcos: una estructura jurásica de basamento multirreactivada del noreste de México. *Boletín De La Sociedad Geológica Mexicana Volumen Conmemorativo Del Centenario Grandes Fronteras Tectónicas De México Tomo LVII, Num 1*, 27-52.

- Christie-Blick, N., & Biddle, K. T. (1985). Deformation and basin formation along strike slip faults. *The Society of Economic Paleontologists and Mineralogists*, 1-34.
- Clark, K. F., Goodell, P. C., & Hoffer, J. M. (1988). Stratigraphy, tectonics and resources of parts of Sierra Madre Occidental Province, Mexico. *El Paso Geological Society Guidebook*.
- Coehlo, S., Passchier, C., & Marques, F. (2006). Riedel-shear control on the development of pennant veins: Field example and analogue modelling. *Journal of Structural Geology* 28, 1658-1669.
- Coney, P. J., & Campa, M. F. (1984). Terrenos sospechosos de aloctonia y acrecion del occidente y sur del continente americano. *801. Depto. Geol. Uni-Son. Vol I No. I*, 1-24.
- Cunningham, W. D., & Mann, P. (2007). Tectonics of strike-slip restraining and releasing bends. *Geological Society, London, Special Publications 2007; v. 290;*, 1-12.
- Dávila Alcocer, V. M., Centeno García, E., Valencia, V., & Fitz D., E. (2009). Una nueva interpretación de la estratigrafía de la Región de Tolimán, Estado de Querétaro. *Boletín de la Sociedad Geológica Mexicana, volumen 61, num. 3*, 491-497.
- de Cserna, Z. (1989). An Outline of the geology of Mexico. *The Geology of North America Vol. A, The Geology of North America - An overview*, The Geological Society of America, 233-264.
- de Cserna, Z. (1989). An outline of the geology of México. The geology of North America. *Geological Society of America Vol. A*.
- DeFord, R. K. (1964). History of geologic exploration in Chihuahua, in Geology of Mina Plomosas-Placer de Guadalupe area, Chihuahua, Mexico;. *Field trip guidebook: West Texas Geological Society, Publication, núm. 64-50*, 116-129.
- DeFord, R. K. (1969). Some keys to the geology of Northern Chihuahua. *New Mexico Geological Society, Guide book, Twentieth Field Conference, The Border Region*, 68-79.
- Dickinson, W. R. (2002). The Basin and Range Province as a Composite Extensional Domain. *International Geology Review, Vol. 44*, 1-38.
- Dickinson, W., & Lawton, T. (2001). Carboniferous to Cretaceous assembly and fragmentation of Mexico. *GSA Bulletin; September 2001; v. 113; no. 9*, 1142-1160;.
- Dickinson, W., & Lawton, T. (2001). Carboniferous to Cretaceous assembly and fragmentation of Mexico. *GSA Bulletin; September 2001; v. 113; no. 9*, 1142-1160;

- Eguiluz de Antuñano, S. (1984). Tectonica Cenozoica del norte de Mexico. *Bol. Asoc. Mex. Geologos Petroleros, Vol. XXXVI, num 1.*
- Eguiluz de Antuñano, S., Aranda G., M., & Randall, M. (2000). Tectonica de la Sierra Madre Oriental. *Boletin de la Sociedad Geologica Mexicana v LIII, (2000), 1-26.*
- Estes, J. E., & Star, J. L. (1993). Remote sensing and GIS integrations: towards a prioritized research agenda. *25th International Symposium, Remote Sensing Environment Change.* Graz, Austria: Remote Sensing Journal.
- Ferrari, L., Valencia-Moreno, M., & Bryan, S. (2005). Magmatismo y tectónica en la Sierra Madre Occidental y su relación con la evolución de la margen occidental de Norteamérica. *Boletín de la Sociedad Geológica Mexicana, Volumen Conmemorativo del Centenario, Temas Selectos de la Geología Mexicana, Tomo LVII, num.3, 343-378.*
- Flotte, N., Martinez-Reyes, J., Rangin, C., Le Pichon, X., Husson, L., & Tardy, T. (2008). The Rio Bravo fault, a major late Oligocene left-lateral shear zone. *Bull. Soc. géol. Fr., 2008, t. 179, no 2, 147-160.*
- Flotte, N., Martinez-Reyes, J., Rangin, C., Le Pichon, X., Husson, L., & Tardy, T. (2008). The Rio Bravo fault, a major late Oligocene left-lateral shear zone. *Bull. Soc. géol. Fr., 2008, t. 179, no 2, 147-160.*
- Goetz, L. K., & Wood D., P. (1985). A Paleozoic transorm margin in Arizona, New Mexico, west Texas and northern Mexico. *Marathon-Marfa Region of west Texas, Simposium and Guidebook, Permian Basin Section, Society od Paleontologists and Mineralogy, Eds., Patricia Wood Dickerson and William Muehlberger 85-81, 173-184.*
- Gonzalez S., F. (2008). *Caracterización y génesis de los yacimientos minerales estratoligados de celestina, barita, fluorita y plomo-zinc del noreste de México.* Mexico: Universidad Nacional Autonoma de Mexico, Tesis Doctorado.
- Goodell, P. C. (1986). La Tectonica de Chihuahua. *Sociedad Geologica Mexicana, Delegacion Chihuahua (invited speaker).*
- Goodell, P. C., Handschy, J. W., Deaterage, S. J., Hoover, J. D., Dyer, J. R., & Keller, G. R. (1985). Iniciacion y reactivacion del aulacogeno Proterozoico de Mexico septentrional. *Presentacion a la Sociedad Geologica Mexicana, Delegacion Chihuahua.*
- Goodell, P. C., Keller, G. R., & Dyer, J. R. (1986). El Bloque tectonico Sierra del Nido: un cratoncito recién conocido en el norte de Mexico. *Sociedad Geologica Mexicana, UACH, Excursion Geologia, Libreto Guia.*
- Goodell, P.C., 1986, La tectonica de Chihuahua: Soc. Geol. Mexicana, Deleg. Chihuahua, Mexico (invited speaker).

Excursion Geologica, Libreto Guia.

Goodell, P.C., J.R. Dyer and G.R. Keller, 1985, Initiation and reactivation of Proterozoic aulacogen, northern Mexico: *Amer. Assoc. Petrol. Geol. Ann. Mtg.*, Abst. w/Prog., v. 69, p. 258.

Goodell, P.C., J.R. Dyer and G.R. Keller, 1985, Initiation and reactivation of Proterozoic aulacogen, northern Mexico: *Amer. Assoc. Petrol. Geol. Ann. Mtg.*, Abst. w/Prog., v. 69, p. 258.

Goodell, P.C., J.W. Handschy, S.J. Deatherage, J.D. Hoover, J.R. Dyer, and G.R. Keller, (1985), Iniciacion y reactivation del aulacogeno Proterozoico de Mexico Septentrional: Presentacion a la *Soc. Geol. Mexicana*, Deleg. Chihuahua,

Grajales-Nishimura, J. L., Terrell, D. J., & Damon, P. E. (1992). Evidencias de la prolongacion del arco magmatico cordillerano del Triasico Tardio-Jurasico en Chihuahua, Durango y Coahuila. *Bol. AMPG*, vol. XLII, num. 2 , 1-18.

Greenwood,E., Kottowski,F.E., Thompson, S., (1977), Petroleum potential and stratigraphy of Pedrogosa basin; comparison with Permian and Orogrande basins: *American Association of Petroleum Geologists Bulletin*, v. 61, p. 1448-1469.

Haenggi, W. T. (2001). Tectonic history of the Chihuahua trough, Mexico and adjacent USA, Part I: the pre-Mesozoic setting. *Boletin de la Sociedad Geologica Mexicana*, Tomo LIV, 2001, 28-66.

Haenggi, W. T. (2002). Tectonic history of the Chihuahua trough, Mexico and adjacent USA, Part II: Mesozoic and Cenozoic. *Bol. Soc. Geol. Mex.*, LV (1), 38-94.

Henry,C.D., Aranda G.,J.J., (1992), The real southern Basin and Range:Mid-to late Cenozoic extension in Mexico: *Geology*,v.20,p.701-704. Hoffman,P.F., 1988, United plates of America; the birth of a craton; early Proterozoic assembly and growth of Laurentia: *Annual Review of Earth and Planetary Sciences*, v.16,p.543-603.

Hildebrand, R. S. (2009). Did westward subduction cause the Cretaceous-Tertiary orogeny in the North American Cordillera? *Geological Society of America Special Paper* 457, 457-471.

Holohan, E., van Wyk de Vries, B., & Troll, V. (2007). Analogue models of caldera collapse in strike-slip tectonic regimes. *Bull Volcanol* (2008) 70:773–796, 773-796.

King, G. P. (1978). Geological faults: fracture, crie, strain. *Phil. Trans. R. Soc. London. A*. 288, 197-212.

- Longoria, J. M. (1994). Recognition and characteristics of a strike-slip fault system in Mexico and its Mesozoic transpressional regime: implications in plate tectonics and paleogeographic reconstruction. *Bol. Depto. Geol. Uni-Son, 1994, Vol. 11 no. 1*, 77-104.
- Lopez-Ramos, E. (1981). Paleogeografía y Tectónica de México. *Univ. Nal. Auton. Mexico, Instituto de Geología, Revista, vol. 5, num 2 (1981)*, 158-177.
- Lowman Jr., P. D., & Tiedemann, H. A. (1971). Terrain photography from Gemini spacecraft: Final geologic report. *Goodard Space Fligh Center, Greenbelt Maryland, X-644-71-15*, 81.
- Loza-Aguirre, I., Nieto-Samaniego, A., Alaniz-Álvarez, S., & Iriondo, A. (2008). Relaciones estratigráficas co-estructurales en la intersección del sistema de fallas San Luis-Teprehuanes y el graben de Aguascalientes, México central. *Revista Mexicana de Ciencias Geológicas*, v. 25, núm. 3., 533-548.
- Mann, P., Hempton, M. R., Bradley, D. C., & Burke, D. (1983). Development of Pull-Apart Basins. *The Journal of Geology Vol. 91, No. 5 (Sep., 1983)*, 529-554 .
- Marrett, R., & Peacock, D. C. (1999). Strain and stress. *Journal of Structural Geology 21, Elsevier Science Ltd.*, 1057-1063.
- Martínez M., C., Luca, F., Chavez-Cabello, G., & Thierry, C. (2004). La Deformación Laramide en México: una evolución geológica no resuelta. *La Orogenia Laramide en México: edad y cinemática de la deformación y magmatismo asociado. GEOS, Vol. 24, No. 2, Noviembre, 2004*.
- Martínez-Piña, C., & Goodell, P. (In progress). The definition of the kinematics of strike-slip faults by analyzing releasing bends, restraining bends and compressional zones, using shear mechanism diagrams and models from analogue materials research and Integrated Geographic Information Systems.
- McClay, K., & Bonora, M. (2001). Analog models of restraining stepovers in strike-slip fault systems. *AAPG BULLETIN*, v. 85, NO.2 (February 2001), *The American Association of Petroleum Geologists*, 233-260.
- McKee, J. W., & Jones, N. W. (1979). A large Mesozoic fault in Coahuila, Mexico. *Geological Society of America Abstracts with Programs*, v. 11, p. 476, 476.
- McKee, J. W., & Jones, N. W. (1984). History of recurrent activity along a major fault in northeastern Mexico. *Geology*, v. 12., 103-107.
- McKee, J. W., Jones, N. W., & Anderson, T. H. (1999). Late Paleozoic and early Mesozoic history of the Las Delicias terrane, Coahuila, Mexico. *in Bartolini, C., Wilson, J.L., and*

- Lawton, T.F., eds., *Mesozoic Sedimentary and Tectonic History of North Central Mexico: Boulder, Colorado, Geological Society of America Special Paper 340*, 161-189.
- Molina-Garza, R. S., Chávez-Cabello, G., Iriondo, A., Porras-Vázquez, M. A., & Terrazas-Calderón, G. D. (2008). Paleomagnetism, structure and  $^{40}\text{Ar}/^{39}\text{Ar}$  geochronology of the Cerro Mercado pluton, Coahuila: Implications for the timing of the Laramide orogeny in northern Mexico. *Revista Mexicana de Ciencias Geológicas*, v. 25, núm. 2, 284-301.
- Molina-Garza, R., & Iriondo, A. (2005). La Megacizalla Mojave-Sonora: la hipótesis, la controversia y el estado actual del conocimiento. *Boletín de la Sociedad Geológica Mexicana, Volumen Conmemorativo del Centenario, Grandes Fronteras Tectónicas de México, Tomo LVII, núm. 1*, 1-26.
- Muehlberger, W. (1965). Late Paleozoic movement along the Texas Lineament. *New York Academy of Sciences Transactions, series II*, 27, 385-392.
- Muehlberger, W. R. (1980). Texas lineament revisited. In: Trans-Pecos Region. *New Mexico Geol. Soc., 31st Field Conference Guidebook*, 113-121.
- Nieto-Samaniego, A. F., Alaniz-Alvarez, S. A., & Labarthe-Hernandez, G. (1997). La deformación Cenozoica poslaramídica en la parte meridional de la Mesa Central, México. *Revista Mexicana de Ciencias Geológicas, volumen 14, número 1*, 13-35.
- Nieto-Samaniego, A., Alaniz-Alvarez, S., & Camprubí, A. (2007). Mesa Central of México: Stratigraphy, structure, and Cenozoic tectonic evolution in Alaniz-Álvarez, S.A., and Nieto-Samaniego, Á.F., eds., *Geology of México: Celebrating the Centenary of the Geological Society of México. Geological Society of America Special Paper 422*, 41-70.
- Nieto-Samaniego, A., Ferrari, L., Alaniz-Alvarez, S., Labarthe-Hernandez, G., & Rosas-Elguera, J. (2007). Mesa Central of México: Stratigraphy, structure, and Cenozoic tectonic evolution in Alaniz-Álvarez, S.A., and Nieto-Samaniego, Á.F., eds., *Geology of México: Celebrating the Centenary of the Geological Society of México, Geological Society of America Special Paper 422*.
- Nieto-Samaniego, A., Ferrari, L., Alaniz-Alvarez, S. A., Labarthe-Hernández, G., & Rosas-Elguera, J. (1999). Variation of Cenozoic extension and volcanism across the southern Sierra Madre Occidental volcanic province, Mexico. *GSA Bulletin; March 1999; v. 111; no. 3*, 347-363.
- Nourse, J.A., McKee, J.W., and Steiner, M.B., eds., The Mojave-Sonora megashear hypothesis: Development, assessment, and alternatives, *Geological Society of America Special Paper 393*, 359-376.

- O' Leary, D. W., Friedman, J. D., & Pohn, H. A. (1976). Lineament, linear, lineation: Some proposed new standards for old terms. *Geological Society of America Bulletin*, v. 87, 1463-1469.
- Oviedo P., E. G. (2008). T ctonica de la Sierra Cuesta de Infierno Chihuahua y su relaci n con el levantamiento de Plomosas. *Centro de Geociencias; Posgrado en Ciencias de la Tierra, UNAM*, 1-177.
- Plattner, C., Malservisi, R., Dixon, T. H., LaFemina, P., Sella, G. F., Fletcher, J., y otros. (2007). New constraints on relative motion between the Pacific Plate and Baja California microplate (Mexico) from GPS measurements. *Geophys. J. Int.* doi: 10.1111/j.1365-246X.2007.03494.x.
- Richards, J. (2000). Lineaments Revisited. *Soc. Economic Geologists Newsletter*, No. 42, p. 1, 14-20.
- Rodr guez-Castaneda, J. L. (1997). Gravity-sliding structures in Cretaceous-early tertiary rocks in north-central Sonora, Mexico-regional significance. *Revista Mexicana de Ciencias Geol gicas, volumen 14, numero 1, Universidad Nacional Aut noma de Mexico, Instituto de Geologia, Mexico,D.F.*, 1-12.
- Salas, G. P. (1975). *Carta y Provincias Metalogen ticas de la Rep blica Mexicana*. Mexico, D.F.: Consejo de Recursos Minerales, Publicaci n 21 E .
- Scanvic, J. L. (1997). *Areospatial Remote Sensing in Geology*. Orleans, France: Editions BRGM iSBN 90-5410-725-I.
- Shunshan, X., Nieto-Samaniego, A. F., Alaniz- lvarez, S. A., & Grajales-Nishimura, J. M. (2008). Evolution of the geometry of normal faults in the Oligocene volcanic field of the Mesa Central, Mexico. *Bolet n de la Sociedad Geol gica Mexicana, Volumen 60, N m 1*, 71-82.
- Suter, M., & Contreras, J. (2002). Active tectonics of northeast Sonora, Mexico (southern Basin and Range Province) and the 3 May 1887 Mw earthquake. *Bulletin of the Seismological Society of America, Vol. 92, No. 2*, 581-589.
- Tardy, M. L., Bourdie, H., Coulon, J., Ortiz-Hern ndez, C., & Yta, M. L. (1992). Intraoceanic Setting of the Western Mexico Guerrero Terrane-Implications for the Pacific-Tethys Geodynamic relationships during the Cretaceous. *Universidad Aut noma de M xico, Insituto de Geologia, Revista, vol. 10, n mero 2*, 118-128.
- ten Brink, U. S., Katzman, R., & Lin, J. (1996). Three-dimensional models of deformation near strike-slip faults. *Journal of Geophysical Research, Vol. 101, No. B7, July 10, 1996*, 16205-16220.

- Thorton, J. C., & Arik, A. (2004). *Ocampo deposit mineral resources, technical report sibmitted to Gamon Lake Resources Inc.* Tucson, Arizona: Mintec Inc.
- Torres, R., Ruiz P., J., Patchett, P. J., & Grajales, J. M. (1999). Permo-Triassic continental arc in eastern Mexico: tectonic implications for reconstructions of southern North America. *Geological Society of America, Special Paper 340*, 191-196.
- Turner, G. L. (1962). The Deming axis, southeastern Arizona, New Mexico and Trans-Pecos Texas. *New Mexico Geological Society Fall Field Conference Guidebook - 13 Mogollon Rim Region, East-Central Arizona Robert H. Weber and H. Wesley Peirce, eds.,* 59-71.
- Twiss, R. J., & Moores, E. M. (2007). *Structural Geology, Second Edition*. New York: W.H. Freeman and Company.
- Umhoefer, P. (2003). A model on the North America Cordillera in the early Cretaceous: Tectonic escape related to arc collision of the Guerrero terrane and a change in the North America plate motion, in Johnson, S.E., Paterson, S.R., Fletcher, J.M. Girty, G.H.,. Kimbrough, D.L. and Martin-Barajas, A., eds. *Tectonic evolution of northwestern Mexico and the southwestern USA, Boulder, Colorado, Geological Society of America, Special Paper 374*, 117-134.
- Walper, J. L., 1977, Paleozoic tectonics of the southern margin of North America: Gulf Coast *Association of Geological Societies Transactions*, v. 27, p. 230–241. 7
- Ward, P. L. (1999). Subduction cycles under western North America during the Mesozoic and Cenozoic eras in Miller, D. M., and Busby, C., Jurassic i Magmatism and Tectonics of the North American Cordillera: Boulder, Colorado. *Geological Society of America Special Paper 299*.
- Warrior, S. (2008). Paleomagnetic investigation of the Mojave-Sonora Megashear Hypothesis in North Central and Northeastern Mexico. *Master of Sciene Thesis, Department of Geological Sciences, University of Texas at El Paso Texas*.
- Wood D., P. (1981). Evidence for Late Cretaceous-Early Tertiary transpression in Trans-Pecos Texas and adjacent Mexico. *Marathon-Marfa Region of West Texas: Simposium and Guidebook, Permian Basin Section, Society of Economic Paleontologists and Mineralogists, Eds., Patricia Wood Dickerson & William Muelhberger Publication 85-81*, 189-194
- Xie, X., & Heller, P. L. (2009). Plate tectonics and basin subsidence history. *GSA Bulletin; January/February 2009; v. 121; no. 1/2, doi: 10.1130/B26398.1*, 55-64.

### **Vita**

Carlos M. Martinez Piña was born on March 26 in Ciudad Juárez, Chihuahua, México. The oldest of two children of Carlos Martinez Villarreal and Consuelo P. de Martinez, he graduated from Preparatoria Federal No. 1 in June 1964. He entered the Instituto Politécnico Nacional, in México D.F. and received his B.S. in Geological Engineering in September 1969. In September 2004, he entered the Universidad Autónoma de Ciudad Juárez and received his M.S degree in Environmental Engineering in June 2006, and started a Ph.D. in August.